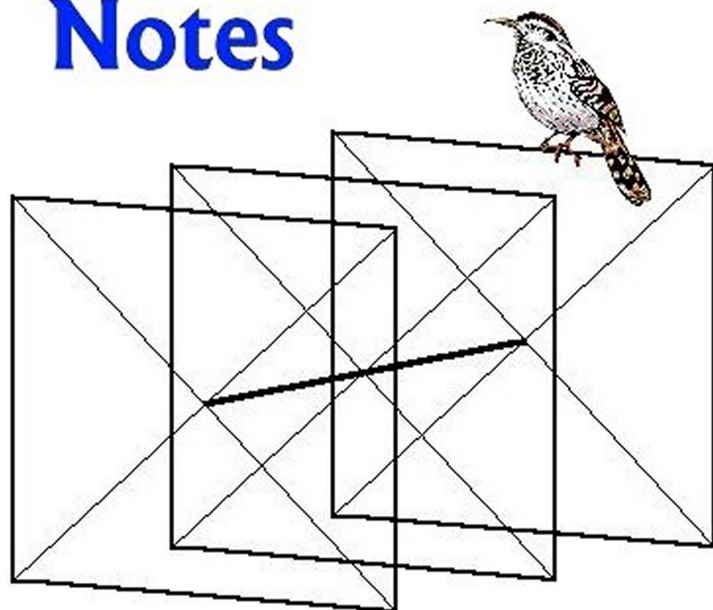


Cubical Quad Notes



Volume 1
A Review of Existing Designs

L. B. Cebik, W4RNL

Cubical Quad Notes

Volume 1 A Review of Existing Designs

L. B. Cebik, W4RNL

***Published by
antenneX Online Magazine***

<http://www.antennex.com/>

POB 72022

Corpus Christi, Texas 78472 USA

Copyright © 2000 by **L. B. Cebik** jointly with ***antenneX Online Magazine***. All rights reserved. No part of this book may be reproduced or transmitted in any form, by any means (electronic, photocopying, recording, or otherwise) without the prior written permission of the author and publisher jointly.

ISBN: 1-877992-01-1

Dedication

This 2-volume study of cubical quads is dedicated to my wife, my friend, my supporter, and my colleague, all of whom are Jean. Her patience, understanding, and assistance gave me the confidence to retire early from academic life to undertake full-time the continued development of my website <http://www.cebik.com> which is devoted to providing as best I can information of use to radio amateurs and others—both beginning and experienced—on various antenna and related topics. These volumes are an outgrowth of that work—and hence, of Jean's help at every step.

About the author

L. B. Cebik, W4RNL, has published over a dozen books, with works on antennas for both the beginner and the advanced student. Among his books are a basic tutorial in the use of NEC antenna modeling software and compilations of his many shorter pieces. His articles have appeared in virtually every amateur radio publication, with translations of some into several languages. A regular columnist for *antenneX*, *10-10 News*, *Low Down*, and others, LB also maintains a web site as a service to radio amateurs and others interested in antennas at <http://www.cebik.com>. Retired from academic life at the University of Tennessee, Knoxville, LB devotes himself to continuing education at his web site, in print, and as both Technical and Educational Advisor to the ARRL.

Table of Contents

Preface	6
Chapter 1. Introduction	8
Chapter 2. Full-Size 2-Element Quads	16
Chapter 3. Variations and Comparisons Among 2-Element Quads	29
Chapter 4. Shrunken 2-Element Quads	51
Chapter 5. Multi-Band 2-Element Quad Beams	71
Chapter 6. Alternative Common Feed Systems for Multi-Band 2-Element Quad Beams	94
Chapter 7. Stacking 2-Element, 5-Band Quads	106
Chapter 8. Separately Feeding Multi-Band Quads	121
Chapter 9. Monoband Quads of More Than 2 Elements	131
Chapter 10. Special Notes on 3-Element Quads	151
Chapter 11. Larger Multi-Band Quads	163
Chapter 12. Where Do We Go From Here?	186
Other Publications	188

Preface to Volume 1

A Review of Existing Quad Designs

Over a period of several years, I received many requests to make available some of the models of quad arrays in my collection of models. These requests led me to a systematic review of those models, the data from which appear in this small collection of quad notes. The resulting study has three purposes:

1. To investigate the properties and performance potential of existing quad designs—or at least a fair sampling of those designs. To that end, the following chapters are filled with tables and graphs that summarize the data in the most usable forms.
2. To provide modelers with information that will make the modeling of quads a more reliable activity. Therefore, most chapters will contain model descriptions as well as tables of dimensions so that the modeler can replicate the model itself using his or her preferred software.
3. To develop a set of tentative conclusions about the trends in quad properties and potentials. Since so little information directly related to quad arrays for amateur use is systematic, it seemed useful to see if I might discover some of the directions that might be eventually taken for further quad studies. Some of those directions will appear in Volume 2 of this set.

The history of amateur quad design is composed of essentially spot designs, that is, individual quad array designs with no essential connection to the fundamentals of quad loop operation, let alone parasitic relations among quad loops. The most published so-called formulas for cutting the loops of a quad array make no reference to element diameter and thus are suspect. As well, most quad arrays using more than 2 elements strive for a short boom (with a few exceptions), and element spacing is boiled down to a few standard separations. The results have been some very useful arrays, but little understanding of how their limitations may relate to some of the fundamental properties of quads.

This volume attempts to explore at least some of the quad array designs that already exist in order to see what they can and cannot do. As well, we shall keep our eyes open for anything that provides clues to what underlies the performance curves we obtain. The key tool for the investigation will be NEC-4 antenna modeling software, although NEC-2 will suffice to accurately model quad arrays. The basic procedure will include the development of performance curves for entire amateur bands—with 10 meters and 20 meters featured mostly. So much data that we encounter record only the peak performance information so that we are left in the dark on matters like the operating bandwidth of an array. If we are to understand and appreciate quad arrays fully, we must see their performance across the operating passbands that we ordinarily register in terms of the bandwidth of a major ham band.

Along the way, we shall encounter a number of questions deserving special attention. Perhaps the most asked question concerns how to feed effectively a multi-band multi-element quad array. We shall examine a number of options. As well, hams often ask about stacking multi-band quads, and we shall address that inquiry in due course. Still, the fundamental question will be how quads perform the way they do, and what modeling can add to our understanding of these intriguing antennas.

Some of the antennas that we shall study may well be worth building. This recommendation is, of course, highly conditional. A design is worth building only if it meets—better than competing designs—all or most of the operating goals and needs of a particular station. Along the path of these studies, I have built a few of the antennas to confirm the modeling data—and the data hold up quite well indeed.

These books should be required reading for anyone interested in quads:

- William Orr, W6SAI, and Stuart Cowan, W2LX. *Cubical Quad Antennas*, 3rd Ed., Lakewood, NJ: Radio Amateur Callbook, 1993
- Bob Haviland, W4MB. *The Quad Antenna*. Hicksville, NY: CQ Communications, 1993
- John Koszeghy, K2OB. *High Performance Cubical Quad Antennas*, 2nd Ed. (Self-published)

1. Introduction

The cubical quad antenna likely got its name from the appearance of early 2-element versions of the array. As **Fig. 1-1** suggests, the arrangement of the elements makes a sort of visual, if not a geometrically pure, cube.

The history of the quad is succinctly told in the Orr and Cowan book on *Cubical Quad Antennas* (pp. 5-9) and needs little repetition here, except to note the pioneering work of Clarence C. Moore, W9LZX. His antenna, once patented, has grown into a large collection of arrays, all using the full-wavelength loop as the fundamental element or elements. Commercial and homebrew versions are widely used, although they are far less numerous than the Yagi-Uda array.

The 2-Element
"Cubical" Quad
Antenna

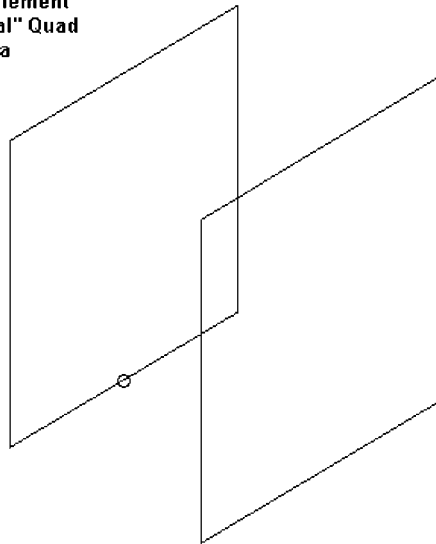
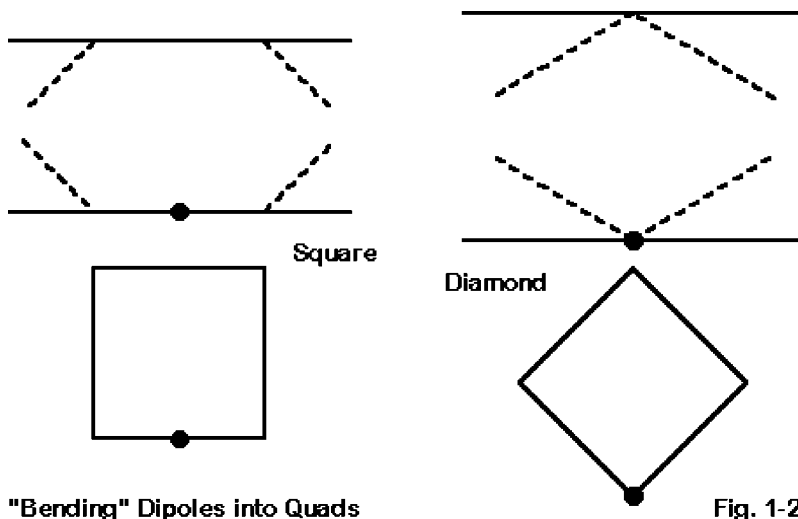


Fig. 1-1

One key to understanding the operation of a quad array lies in the simple quad loop, a 1λ square loop of wire. Such a loop radiates broadside to the plane of the wire. If we enlarge the loop to a 2λ circumference, the radiation tends to be off the edges. Similarly, if we shrink the loop to less than 0.5λ circumference, radiation is also off the edges.

One convenient way to think about a simple quad loop is to view it as shown in **Fig. 1-2**, as two dipoles spaced about $1/4\lambda$ apart, with their ends bent and drawn together. For a square loop, the analysis works quite well. For the diamond form of the loop, we must think of the antenna as two $1/2\lambda$ Veeps drawn together. We may use a single feedpoint owing to the direct

connection of the dipole ends: the two $1/2 \lambda$ sections will be in phase—less a little wire resistance loss.



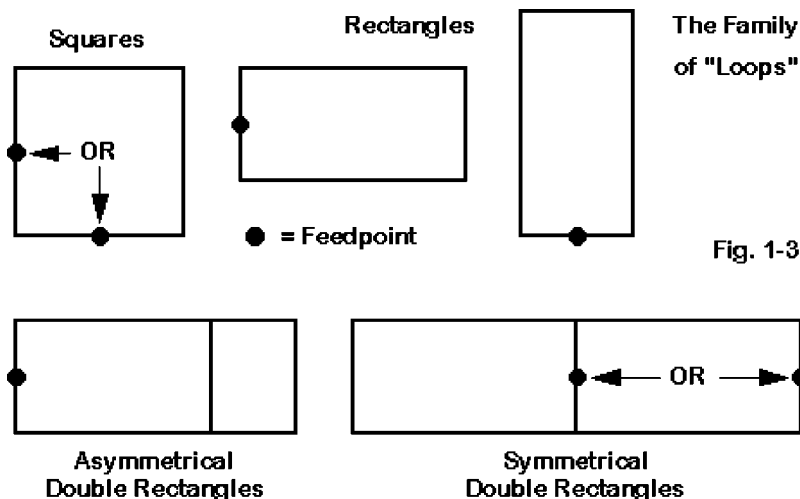
Since the spacing between the loops is relatively small— 0.25λ or its equivalent with the diamond—the “stacking” gain of the two dipoles fed in phase will be far less than theoretically possible at wider spaces that approach $5/8 \lambda$. However, the gain of a single HF wire square or diamond quad loop will be about 1.2 dB over a dipole at a similar height.

Something About the Family of Loops

The square and diamond quad loops with 4 equal sides are simply members of a much larger family of loops. **Fig. 1-3** provides us with some other members of the family.

The square is a special form of a rectangle. Rectangular antennas are commonplace in the literature. For example, with the rectangle vertical, but the feedpoint placed on one of the horizontal wires, we can adjust the shape to lower the feedpoint impedance relative to the square, dropping it from a value well above 100Ω down to some very low values. Ordinarily, we select a rectangular shape that provides us with a direct match for $50\text{-}\Omega$ coaxial cable. In the process, we may discover an increase in loop gain. In fact, as we increase the loop height and decrease the width, the gain can easily double that of a dipole. When turned on its side, the rectangle provides vertically polarized radiation at very low angles, an especially attractive feature for the

lower HF bands. Since the side-fed rectangle is a closed loop, it requires no radial system to complete it and comprises one member of the family of SCVs (self-complete, vertically polarized loop antennas).



Loops need not be single. Dan Handelsman, N2DT, has conducted—and continues to conduct—the most exhaustive studies of asymmetrical and symmetrical double rectangles (ADRs and SDRs). The simple symmetrical double rectangle has been used as a vertically polarized low-band array. The ADR is perhaps best known in its vertical form as the "hennenna," which shows additional gain over a rectangle. When fed at the center wire, the array can easily be matched to 50- Ω coaxial cable.

The chief advantage of using the square, then, has nothing to do with its feedpoint impedance—which is well above 100 Ω at resonance—or its gain—which is modest compared to other family members. Instead, the square and diamond quad loops derive their popularity from two other factors. First, the squared loop is easiest among all loops to support. Ordinarily, four arms composed of non-conductive material extend from a hub to the corners, supporting a wire element. The hub may then be connected to a boom or to the mast.

Second, the squared loop is easiest among all shapes to arrange into a parasitic array. The inter-element coupling has so far been easiest to control when the loops are squared. Since two loops having slightly different sizes (for example, a driven element and a larger reflector element) can be ar-

ranged concentrically, but on separate arms to obtain parasitic spacing, symmetrical quad arrays are far simpler to design and model than arrays of rectangles.

Because the “stacked” dipoles that compose a quad loop are bent, the current magnitude at the quad loop corners is higher than at corresponding points along a linear dipole element. The vertical portions of the elements have some radiation. Hence, the total pattern for a quad array shows a vertically polarized component, even in free-space patterns that are not affected by ground reflections. **Fig. 1-4** shows the free-space azimuth patterns of a 2-element quad and a short-boom 3-element Yagi, both with gain figures between 7.1 and 7.2 dBi. The linear elements of the Yagi show no trace of a vertical component to the radiation. However, the quad beam shows a small but distinct vertical component such that the front-to-side ratio is less than that of the Yagi.

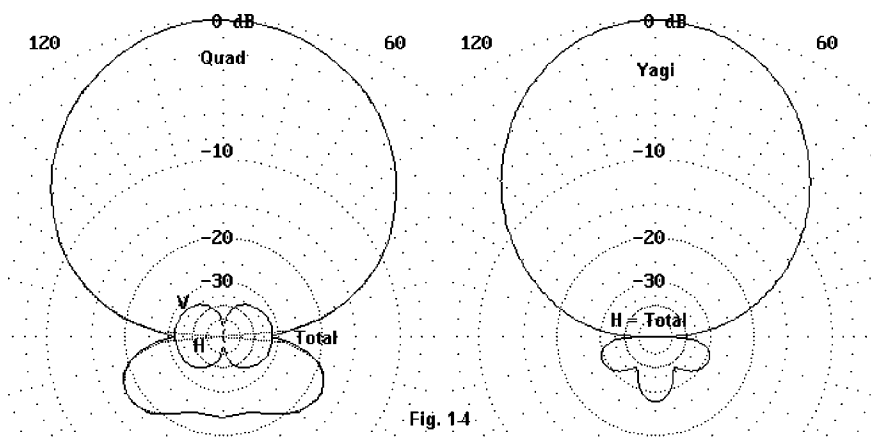


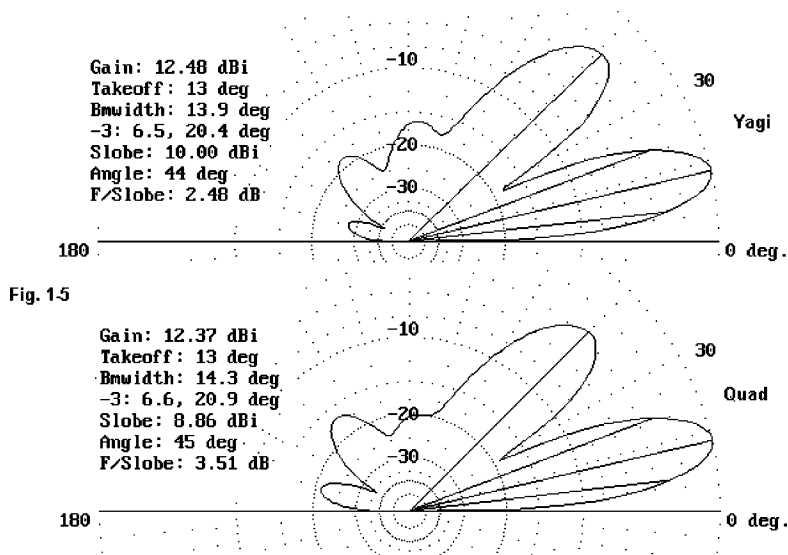
Fig. 1-4

While we are briefly comparing Yagis and quads, let us take the two antennas a step further to eliminate a myth about quads—namely, that they have a lower take-off angle (or elevation angle of maximum radiation) than Yagis at the same height. The two antennas whose free-space azimuth patterns appear in **Fig. 1-4** can be placed at comparable heights above ground and directly compared with respect to elevation patterns.

The elevation pattern for a quad is a composite of the patterns for the upper and lower elements, just as with any stacked array. What the upper element provides by way of a lower take-off angle, the lower element takes away by having a higher take-off angle. Essentially, the take-off angle of a quad is equivalent to that of a Yagi of similar gain mounted between 5/8 and

2/3 the way up from the quad bottom to top wires. Hence, if we take a 10-meter quad and place its hub at 35' up, the corresponding Yagi height for the same take-off angle will be about 36-37'.

Fig. 1-5 provides elevation patterns for the short-boom 3-element Yagi at 36' and the 2-element quad with its hub at 35'. Any differences in pattern shape are too small to be operationally noticeable.



There are other mysteries and myths surrounding quads that we cannot resolve in the present context of study. For example, operators claim that a quad will open and close the upper HF DX bands. Whatever phenomena may (or may not) be at work for these operators, it cannot be analyzed adequately with the chief analytical tool at my disposal—the antenna modeling program. While the available programs are quite adequate to predict and analyze antenna performance, they are not designed to deal with the interaction of radiated signals with the ionosphere. As a results, while modeling studies are very apt in clarifying many of the properties of the quad—and arrays based on the quad loop—some questions must go unanswered.

Something About Modeling Quad Loops

Although there are no disks of model files accompanying this volume, there will be numerous descriptions of models from which any modeler can construct his or her own models in whatever software is preferred. So that

one may study the models in conjunction with the data that emerge from them, model descriptions appear within the chapters in which they are discussed. Ultimately, the experienced modeler will not need many descriptions, because virtually all models are constructed in the same manner. Initially, all models begin in a free space environment. Each loop is centered on a 0, 0 X (or Y) and Z axis. The loop corners are then defined as shown in **Fig. 1-6**.

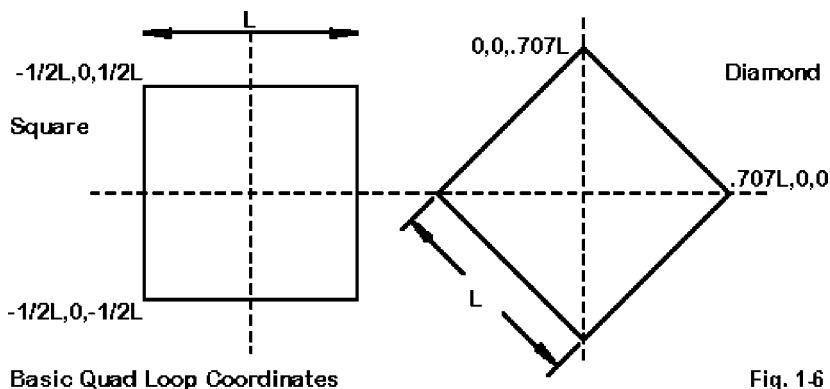


Fig. 1-6

For square loops with bottom wires parallel to the ground, a coordinate set consists of two entries, each one-half the side dimension, with + or - signs as dictated by the particular corner of the loop. Hence, the upper left corner of a loop with 9' sides will use -4.5, 0, 4.5 as X, Y, and Z coordinates.

Diamond loops require that one multiply one-half the length of a side by 1.414 (or the full side length L by 0.707) to arrive at the peak, which will then be at either the X (or Y) or the Z coordinate when the other is zero. The same loop as above, but turned 45° to a diamond configuration, would use for the top coordinates 0, 0, 6.36.

The "unused" coordinate (X or Y, according to one's modeling conventions), of course, receives the spacing dimension between elements. Simple monoband quads can set any element to zero and count from that point. Multi-band spider-hub quads often use a zero-center point to best advantage. Once you have one element complete and correct, you may then use an appropriate copy mechanism to replicate the element, changing coordinate numbers (or letters, if symbolic entry is used) to account for dimensional differences.

Once the loops have been constructed in a free space environment, ad-

justment for height above ground is a simple matter of changing all Z-coordinates by the same amount. Of course, the amount will be the height above ground if the height represents the loop center. Other adjustments may be needed if the height represents the bottom of the lowest wire.

Despite occasional remnant protestations from a few quad designers, antenna modeling programs have proven very effective and accurate for designing and analyzing quads. All computer simulation programs have some limitations, so let's note the most important ones.

MININEC 3.13, the core of such programs as ELNEC, AO, and NEC4WIN, has a problem with corner-clipping as segment centers tend to give the effect of linking and ignoring the small increment to the actual corner junction or pulse. The standard method for reducing this effect to negligible amounts is length tapering. Length tapering can be manually or automatically implemented, and the automatic systems can be visible or invisible to the user who does not look at the post-run wire tables for the antenna. It is a process of reducing the length of segments gradually as corners are approached so that two conditions are met. First, the segments closest to the corner are very short without exceeding the minimum segment length, either absolutely or relative to wire diameter. Second, the changes in length from one segment to the next are within the boundaries set for accurate output from the core. Expert MININEC, a more recent proprietary development from the originators of MININEC, uses an algorithm that overcomes the "corner" limitation of public domain MININEC.

NEC (-2 or -4) (as found in programs like NECWires, EZNEC, and NEC-Win Plus) does not require length-tapering at corners, since the currents are taken from the entire segment. However, NEC has two limitations to note. First, angular junctions of wires having different diameters tend to yield inaccurate results. This is no problem for the standard wire quad loop. Nonetheless, some quad designs for VHF especially use large diameter tubular horizontal members and thinner vertical wires to connect them. NEC has a problem with this configuration. Second, NEC requires that the source be placed on a segment, which presents problems to corner feed points, such as might occur on a diamond shaped quad. We shall look at the alternatives for handling this situation as we proceed through the models. Among the alternatives are the use of a dual source on the segments immediately adjacent to the fed corner and the construction of a short 3-segment feed (source) wire at the element corner.

The initial monoband quads in this study will all be for 10 meters. In most

instances, I shall not express dimensions in terms of equations of the order “ $L = 1234/f$.” The required length of a quad loop will vary with the wire diameter on any band, and such classic formulas take no account of this fact. The fatter the wire, the larger the quad loop must be for the same resonant frequency. Therefore, unless one adjusts the wire size as well as the quad loop length, scaling will be imperfect. Since the initial models will use #14 AWG copper wire (0.064" diameter”), direct diameter scaling makes for unlikely assemblies (for example, #10 AWG on 20 meters based on the use of #14 AWG on 10 meters).

In the end, modeling issues are secondary to the prime purpose at hand: to analyze quad antennas in order to discover what their practical properties are. Modeling issues and techniques will arise from time to time for two reasons. First, some readers may wish to replicate (and go beyond) the modeling done for these notes. Second, any study must reveal its techniques to allow for evaluation and verification of the work. Since modeling—mixed with some building and testing to confirm some results—is the key tool of analysis for the investigation, its use should be transparent throughout.

Note that the purpose of this work is one of discovery. My aim is not to judge the quad. If the work is reasonably done, judgments will be self-forming relative to the adequacy of a quad—or more accurately, a particular quad design—for certain types of jobs. Since the final evaluation of whether to use a quad requires a clear set of operational requirements, only the potential user can make such a judgment. At most, these notes may contribute to such judgments and evaluations—and hopefully to better quad designs in the future.

Every step toward future best begins with a clear view of the past. To that end, this first volume is devoted to existing quad designs.

2. Full-Size 2-Element Quads

Models of full size 2-element quad beams are not difficult to make or to optimize for some desired set of maximum performance figures at a design frequency. Almost all 2-element quads use the driver-reflector configuration to maximize the operating bandwidth (relative to driver-director parasitic beams). Since the quad offers a bit of extra gain and a very good front-to-back ratio relative to a 2-element driver-reflector Yagi with the same element spacing, operating bandwidth is the next parameter on the normal list of specifications, and we shall be very interested in this parameter as we proceed.

There are three dimensions to any quad. As **Fig. 2-1** demonstrates, the first dimension is the wire length or loop size of each element. We can specify this dimension as the length of a side, since most quads employ a square configuration for ease of mechanical construction. Hence, the circumference of the loop is simply 4 times the length of a side. As noted in the introduction, the length of half the side can be important in setting up coordinates for a model.

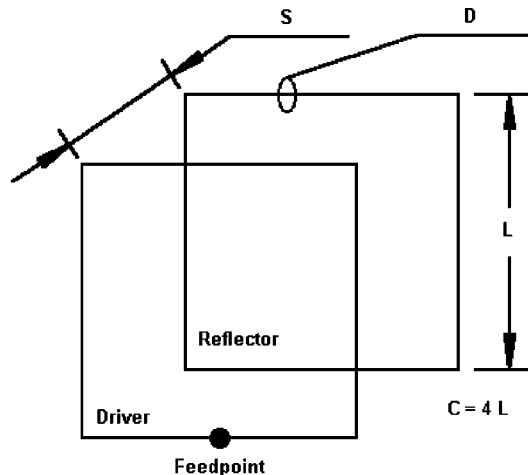


Fig. 2-1

Basic Quad Dimensions

As our first exercise below will demonstrate, element spacing will be extremely important to 2-element quad design models. The closer the spacing, the smaller the requisite loops sizes and the lower the source impedance. Since the 2-element quad has a relatively high (compared to 50 Ohms) source impedance, some designers favor close spacing in the attempt to bring the source impedance into a close match with coax. Whether this is wise we shall see.

The third dimension of a quad is the wire size or diameter. For a given loop resonant frequency, the fatter the wire, the larger the required loop circumference. This factor is directly opposed to what we encounter with linear elements. It applies not only to completely closed geometries, like the quad loop, but to many other nearly closed geometries, where normally linear free element ends are brought into close proximity to other normally free element ends.

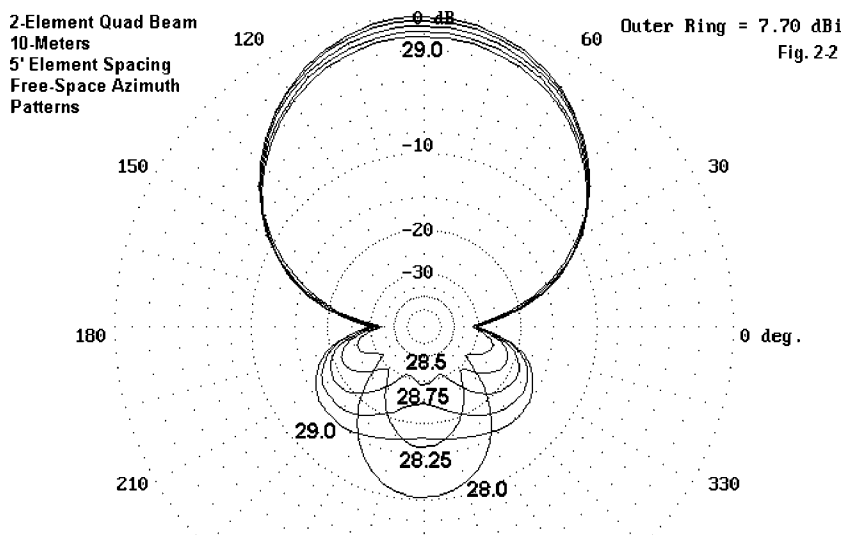
Unless otherwise specified, all of the quad models that we shall examine in this chapter will use #14 AWG copper wire. Also, except as noted, the models will be designed for a center frequency of 28.5 MHz. The design center frequency can mean many things, since it does not itself say what parameter or parameters are maximized at this frequency. In general, for 2-element design work, setting the resonant frequency of the driver and the approximate maximum front-to-back ratio for the design frequency is a satisfactory starting point. In any 2-element driver-reflector parasitic array, the gain will describe a descending curve from well below the design center to well above it. Peak gain occurs at a point of virtually useless front-to-back ratio and is designed into a quad only for special purposes. The 180E front-to-back ratio for any design tends to show a peak that is a useful reference mark. Adjustments may be required if the slope of performance away from the peak is not symmetrical.

Likewise, it is usually harmless to begin with the assumption that the VSWR curve relative to the resonant impedance of the antenna will be roughly symmetrical. Hence, setting the resonant point of the antenna under design to the same frequency as the peak in front-to-back performance is a safe start unless previous analyses indicate otherwise. Adjustments in the driver frequency can usually be made later to compensate for any lack of symmetry in the VSWR curve without unduly upsetting the overall antenna performance. (This is not always true of 2-element Yagis, but is generally true of 2-element quads.)

Remember that the basic quad beam is essentially a 4-element array, although we commonly call it a 2-element beam. Each loop is 1λ long, consisting of two dipoles joined at their ends and spaced, relative to their high current regions, about $1/4 \lambda$ apart. Since the spacing is not optimal for achieving maximum gain from two dipoles, we tend to consider the loop to be a single element with about 1.2 to 1.4 dB (maximum) gain over the dipole.

Remember also that peak performance figures can be misleading. Very often, the only extended frequency information given about an antenna de-

sign is the 2:1 VSWR curve. However, every major performance parameter deserves attention.



The azimuth patterns in **Fig. 2-2** show significant elements of the performance potential of a monoband quad for 10 meters across the first MHz of the band. If we looked only at the pattern for 28.5 MHz, the design center frequency for this model, we might misunderstand the actual performance. The near-maximum front-to-back pattern might not make clear how that parameter varies across the band. For this model, the low-end front-to-back figure barely exceed 10 dB. Above 28.25 MHz, the front-to-rear performance is at least 15 dB below the maximum forward gain. Only in the vicinity of mid-band is the front-to-rear performance everywhere at least 18 dB below maximum forward gain.

The collection of patterns also reveals that there is a significant variation in the forward gain across the band--something over 1 dB between 28 and 29 MHz, with the lowest gain at the highest frequency. The decrease in gain with an increase in frequency is a characteristic typical of parasitic 2-element driver-reflector designs, whether Yagi or quad. Parasitic designs having a director typical show an increase in gain as the frequency increases.

Quad Performance as a Function of Element Spacing

Let's examine the modeled performance potential of a series of 10-meter 2-element quads that differ chiefly in the spacing between the elements. Each

quad was set for near resonance (+/- about 2 Ohms reactance) at 28.5 MHz. In addition, the maximum front-to-back ratio was positioned as near a practicable to this same frequency. Using these two criteria as design specifications, the maximum forward gain of the array was allowed to set itself. In fact, in nearly all cases, the maximum forward gain achievable from the quad falls outside the lower end of the band, that is, below 28 MHz.

As the spacing increases, placing resonance and the maximum front-to-back ratio at mid-band requires larger loops for each of the 2 elements. **Table 2-1** shows the essential dimensions for #14 AWG bare copper wire models in this series. "L" means side length and "C" means loop circumference.

Table 2-1. 2-Element Quad Model Dimensions

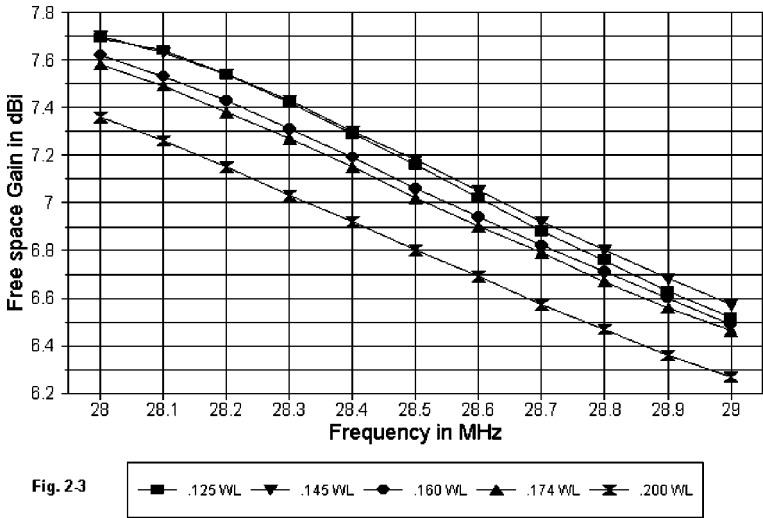
Spacing λ	Spacing feet	L Driver feet	C Driver feet	L Reflector feet	C Reflector feet
0.125	4.31	8.66	34.64	9.16	36.64
0.145	5.02	8.70	34.80	9.19	36.77
0.160	5.50	8.72	34.88	9.23	36.92
0.174	6.00	8.77	35.06	9.25	37.00
0.200	6.90	8.82	35.28	9.30	37.20

We can get the best idea of the trends in performance potential by looking at a series of graphs across the first MHz of 10 meters.

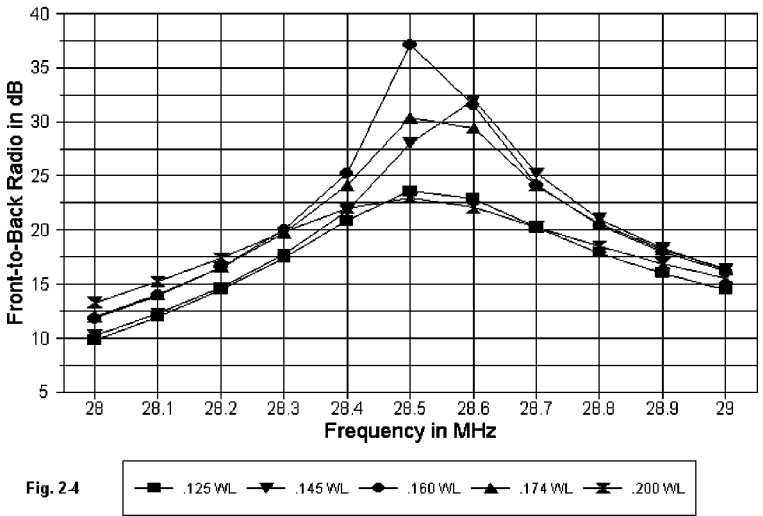
In **Fig. 2-3**, we get a good view of the gain curves associated with each of the spacings used. Clearly, the widest spacing yields the lowest gain across the band (although gain is not the only consideration in selecting a design). The gain increases as spacing narrows through to the 5' (0.145 λ). However, as the spacing narrows to 1/8 λ (4.31'), the overall gain curve shows a slight decrease--beginning on a par with the 0.145 λ curve, but decreasing more rapidly as the frequency increases.

Note that the average gain difference between the highest and lowest curves is about 0.4 dB. Operationally, this might be no great loss, but it might be considered to remain above the threshold of significance. In contrast, the differential between any two adjacent curves in the overall plot is truly insignificant. Despite the lack of operational significance, the collection of curves does show the trends in gain--given the design criteria used in constructing the models.

Full-Size 2-Element Quads
Gain vs. Element Spacing



Full-Size 2-Element Quads
F-B Ratio vs. Element Spacing



In all cases, as shown in **Fig. 2-4**, the maximum 180-degree front-to-back value occurs between 28.5 and 28.6 MHz. Interestingly, both the closest element spacing (0.125λ) and the widest spacing (0.2λ) show the lowest peak value. In a curve of this sort, where the checked frequencies are 0.1 MHz apart, it is not possible to say with assurance whether there is no sharp peak or whether it is too sharp to appear.

Nonetheless, it is not the peak, but the overall performance curve that is most important. All of the antennas show a maximum front-to-back ratio well above 20 dB, but equally, all dip well below the 20 dB mark at the band edges. The widest spacings show the best low end performance, while there is no significant difference in performance at the upper band edge.

In general, the quad tends to show a 20 dB 180-degree front-to-back ratio for 500 kHz or less. From the pattern tendencies shown in **Fig. 2-2**, the overall front-to-rear performance will be a bit less. Hence, unless one intends to operate over only a very small portion of the band relative to its full span, the deep null that one can obtain at some specific frequency turns out not to indicate accurately the antenna's actual performance potential.

Full-Size 2-Element Quads VSWR vs. Element Spacing

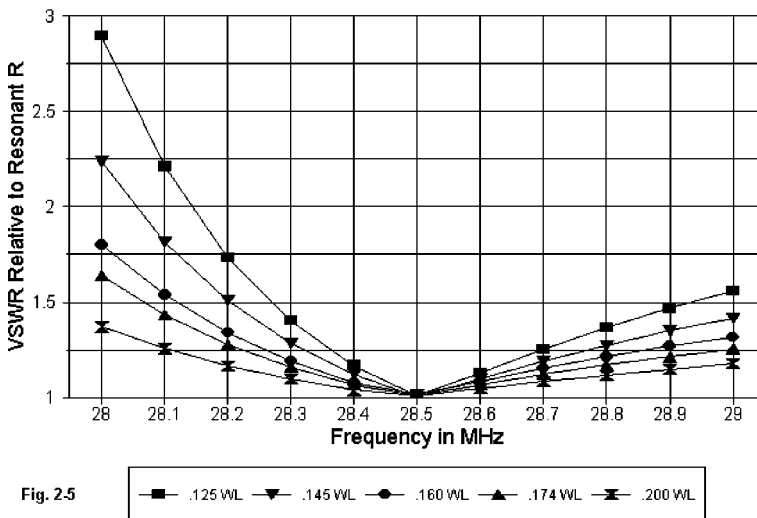


Fig. 2-5

Fig. 2-5 reveals that the closer the element spacing, the steeper the VSWR curve--and vice versa. Also revealed is the fact that, at any spacing in the

range of the models, the curve is much steeper below the resonant frequency than above it.

What the curves do not reveal is the actual antenna impedance at or near resonance. **Table 2-2** provides modeled performance figures at 28.5 MHz for the five models as a reference against which to read the graphs.

Table 2-2. Modeled Performance Figures

Spacing λ /feet	Free Space Gain dBi	Front-to-Back Ratio dB	Feedpoint Impedance R +/- jX Ohms
0.125/4.31	7.16	23.6	102 - j 1
0.145/5.02	7.18	28.0	118 - j 0
0.160/5.50	7.07	40.1	135 - j 2
0.174/6.00	7.02	30.4	146 _ j 2
0.200/6.90	6.81	23.8	166 - j 2

The three widest spacings show SWR values under 2:1 across the first MHz of 10 meters, relative to their resonant impedances. However, over any of the spacings surveyed in these models, the quad shows a very slow rise in SWR above the resonant frequency. We can use this fact to slightly redesign any of the models for a more even SWR performance. We simply reduce the frequency of resonance by enlarging the driven element. **Table 2-3** shows the changes that we would need to make to arrive at the new resonant frequency.

Table 2-3. Revised 2-Element Quad Dimensions

Spacing λ	Spacing feet	L Driver feet	C Driver feet	L Reflector feet	C Reflector feet
Original					
0.145	5.02	8.70	34.80	9.19	36.77
Modified					
0.145	5.02	8.76	35.04	9.19	36.77

The change of about 1" per side is sufficient to lower the resonant frequency by about 0.15 MHz. No change is made to the reflector. Let's examine what happens to performance.

The change of gain, shown in **Fig. 2-6**, is wholly without significance.

Likewise, as **Fig. 2-7** reveals, there is no change in the front-to-back ratio performance with the modification of the driven element.

Full-Size 2-Element Quads
Gain vs. Resonant Frequency

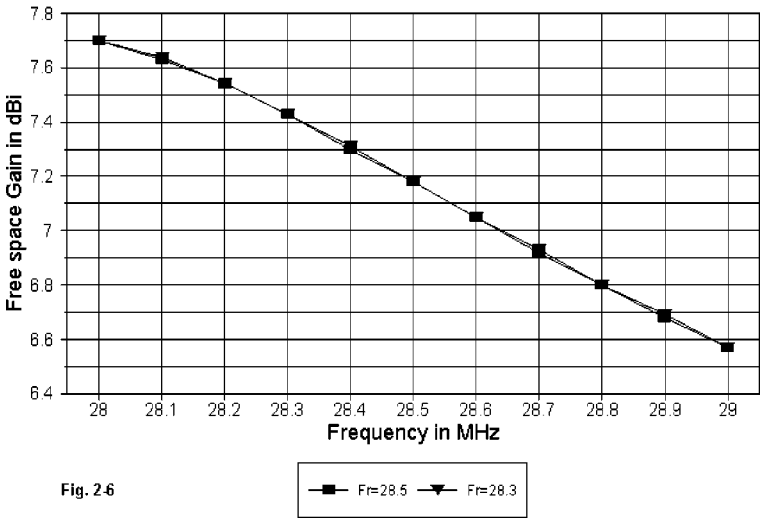


Fig. 2.6

Full-Size 2-Element Quads
F-B Ratio vs. Resonant Frequency

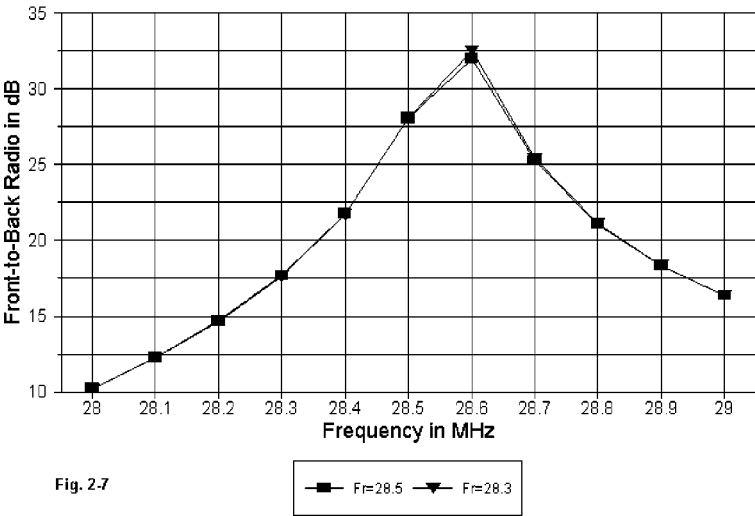


Fig. 2.7

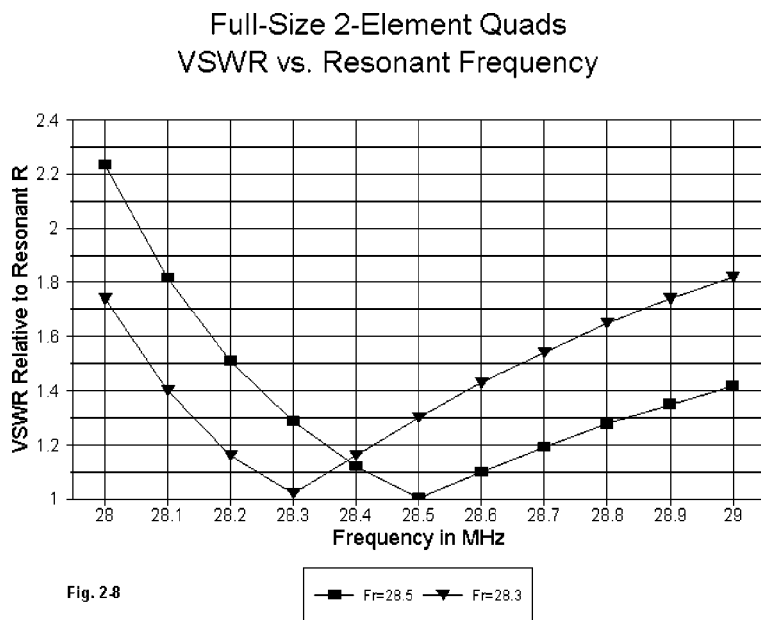


Fig. 2-8 shows the new SWR curve relative to the old one. The SWR across the first MHz of 10 is now well below 2:1. Changing the resonant frequency to about 28.3 MHz has evened out the values to produce a curve more equal at the ends--without otherwise disturbing the antenna's potential performance.

The exercise shows more than our ability to adjust the SWR curve. It demonstrates the relative immunity of the reflector to moderate changes in the length of the driven element. Hence, the designer has some freedom to place the front-to-back curve and the SWR curve anywhere along the operating band that yields a set of desired operating characteristics.

The models used in this comparative study have used a variable number of segments, range from 7 per side to 21 per side. However, the common 2-element quad converges in NEC with only about 5 segments per side, so differences in gain, front-to-back ratio, and source impedance reports will be minimal.

Let's look at one of the quad models to see how it may translate from one program to another. The following EZNEC model description of the modified quad with 0.145λ element spacing is typical of all of the 2-element quad

models whose dimensions have been shown in this chapter.

```
2 el quad 10m 5' sp #14                      Frequency = 28.35  MHz.

Wire Loss: Copper -- Resistivity = 1.74E-08 ohm-m, Rel. Perm. = 1

----- WIRES -----

Wire Conn.--- End 1 (x,y,z : ft)  Conn.--- End 2 (x,y,z : ft)  Dia(in) Segs

1  W4E2  -4.380,  0.000, -4.380  W2E1   4.380,  0.000, -4.380  # 14  21
2  W1E2   4.380,  0.000, -4.380  W3E1   4.380,  0.000,  4.380  # 14  21
3  W2E2   4.380,  0.000,  4.380  W4E1  -4.380,  0.000,  4.380  # 14  21
4  W3E2  -4.380,  0.000,  4.380  W1E1  -4.380,  0.000, -4.380  # 14  21
5  W8E2  -4.596, -5.018, -4.596  W6E1   4.596, -5.018, -4.596  # 14  21
6  W5E2   4.596, -5.018, -4.596  W7E1   4.596, -5.018,  4.596  # 14  21
7  W6E2   4.596, -5.018,  4.596  W8E1  -4.596, -5.018,  4.596  # 14  21
8  W7E2  -4.596, -5.018,  4.596  W5E1  -4.596, -5.018, -4.596  # 14  21

----- SOURCES -----

Source      Wire      Wire #/Pct From End 1      Ampl.(V, A)  Phase(Deg.)  Type
      Seg.      Actual          (Specified)

1          11      1 / 50.00  ( 1 / 50.00)      1.000        0.000        V

No loads specified
No transmission lines specified
Ground type is Free Space
```

In programs having provision for symbolic coordinate entry, three variables would suffice for a full free space description of the model: a value for the driver corners, a value for the reflector corners, and a value for the element spacing. An example, using the AO format is shown below. The axes used for the elements are Y and Z, with the driver coordinate designated “de” and the reflector coordinate “ref.” The relative positions of the driver and reflector along the X axis are shown as “dep” and “rep.” Otherwise, the model is identical to the EZNEC description shown above.

```
2-Element Quad
Free Space Symmetric
28.3 MHz
8 copper wires, feet
ref = 4.596
de = 4.38
rp = -5.018
dep = 0
1  dep -de -de  dep de  -de #14
1  dep -de -de  dep -de  de #14
1  dep -de de   dep de  de  #14
1  dep de  de   dep de  -de #14
1  rp  -ref -ref  rp  ref  -ref #14
1  rp  -ref -ref  rp  -ref  ref #14
```

```

1      rp  -ref ref      rp  ref  ref  #14
1      rp  ref  ref      rp  ref  -ref #14
1 Source
Wire 1, center

```

A more general format is the .NEC ASCII file used by NEC-Win Pro and other NEC-2/-4 programs. The same antenna model (with elements in the X and Z axes) in this format appears in the NEC-Win file:

```

CM 2 el quad 5' sp #14 cu
CE
GW 1 21 -4.38 0 -4.38 4.38 0 -4.38 2.67060367454068E-03
GW 2 21 4.38 0 -4.38 4.38 0 4.38 2.67060367454068E-03
GW 3 21 4.38 0 4.38 -4.38 0 4.38 2.67060367454068E-03
GW 4 21 -4.38 0 4.38 -4.38 0 -4.38 2.67060367454068E-03
GW 5 21 -4.596 -5.018 -4.596 4.596 -5.018 -4.596 2.67060367454068E-03
GW 6 21 4.596 -5.018 -4.596 4.596 -5.018 4.596 2.67060367454068E-03
GW 7 21 4.596 -5.018 4.596 -4.596 -5.018 4.596 2.67060367454068E-03
GW 8 21 -4.596 -5.018 4.596 -4.596 -5.018 -4.596 2.67060367454068E-03
GS 0 0 .3048
GE 0
EX 0 1 11 0 1 0
LD 5 1 1 21 5.8001E7
LD 5 2 1 21 5.8001E7
LD 5 3 1 21 5.8001E7
LD 5 4 1 21 5.8001E7
LD 5 5 1 21 5.8001E7
LD 5 6 1 21 5.8001E7
LD 5 7 1 21 5.8001E7
LD 5 8 1 21 5.8001E7
FR 0 11 0 0 28 .1
RP 0 1 360 1000 90 0 1 1
EN

```

The wire size (radius) and the material specification (copper) are shown in numerical terms in this file, in the GW and LD lines, respectively. The FR line specified a frequency sweep from 28 to 29 MHz in 0.1 MHz steps.

Both the AO and the .NEC file are usable. Simply type the file and save it as an ASCII file. Use the .ANT extension for the AO file and the .NEC extension for the NEC-Win file. These files may then be modified to create other quad configurations.

Any modeler should know not to expect precisely the same results from different programs. At the outset, input and output rounding conventions will alter numeric values very slightly. The selected values for material resistivity may vary slightly from one program to the next. NEC-2 occurs in 16- and

32-bit versions, with very slightly different outputs. The sum of these variations can yield slight numeric differences while using ostensibly the same core.

MININEC differs from NEC in placing pulses at segment junctions. This procedure requires a degree of length tapering in the approach to an angular junction to prevent corner clipping. Depending on the degree of length tapering, MININEC may show a lesser or greater departure from NEC values in the direction that suggests a slightly shorter or higher frequency antenna.

To illustrate the difference, **Table 2-4** lists results from NEC-Win (NEC-2), EZNEC (NEC-2), and AO (MININEC) for a single model--the 5' spaced antenna modified for resonance near 28.3 MHz. The values for free space forward gain, 180-degree front-to-back ratio, and source impedance are shown for 28, 28.5, and 29 MHz in an X/Y/Z format (except for source impedance).

Table 2-4. Performance Reports from 3 Programs

Parameter	NEC-Win	EZNEC	AO
Gain in dBi	7.71/7.18/6.58	7.70/7.18/6.57	7.73/7.29/6.68
F-B in dB	10.3/28.4/16.3	10.2/28.2/16.4	8.9/23.2/18.0
Impedance			
28.0	69.4 - j 35.4	69.2 - j 42.5	62.5 - j 45.1
28.5	120.6 + j 19.6	120.2 + j 12.4	111.0 + j 14.0
29.0	162.0 + j 45.5	161.5 + j 38.2	154.0 + j 43.0

Operationally--which here would include constructing a 2-element quad of the given design--the differences in these programs are insignificant. The two NEC-2 programs are very close, but not exact. Compared to both NEC-2 result sets, the MININEC output is a bit generous with gain and stingy with front-to-back ratio, with a systematically lower source impedance. However, the variables of construction will in virtually all cases exceed any differences among the numbers in the reports.

If we hold the wire size constant (#14 AWG copper), then the quad does not directly scale to other frequencies without some adjustment of side lengths for both the driver and the reflector. **Table 2-5** provides 2-element quad model dimensions for 10 meters through 20 meters for similar performance. To discover the amount of adjustment needed, relative to the original 10-meter model, you may take the ratio of the new frequency to 28.5 MHz and determine the scaled length of the sides to compare with the dimensions used in the actual model. All models use an element spacing of 0.125 λ .

Table 2-5. #14 AWG Copper Wire 2-Element Quads for 20-10 Meters

Frequency MHz	Spacing feet	L Driver feet	C Driver feet	L Refl. feet	C Refl. feet	Segments per side
28.5	4.31	8.66	34.64	9.16	36.64	7
24.94	4.93	9.91	39.62	10.47	41.86	9
21.22	5.79	11.64	46.56	12.26	49.04	11
18.12	6.79	13.62	54.48	14.35	57.40	13
14.17	8.68	17.42	69.68	18.30	73.20	15

The selection of segmentation for each model was determined by my eventual goal of combining all of the individual quads into a single 5-band quad model--a topic which we shall address in a future chapter. By taking $1/2$ the length of a side, one can get the requisite value for the coordinates for the drivers and the reflectors. The remainder of the model construction is routine.

The modeled performance of the resultant monoband quads is tabulated in **Table 2-6**.

Table 2-6. Modeled Performance of 2-Element Quads

Frequency MHz	Free Space Gain dBi	Front-to-Back Ratio dB	Feedpoint Impedance R +/- jX Ohms
28.5	7.16	23.6	102 - j 1
24.95	7.11	23.9	105 + j 1
21.22	7.18	23.2	99 + j 2
18.12	7.14	23.7	101 - j 1
14.17	7.15	23.2	99 + j 0

Despite having the narrowest operating bandwidth of the range of element spacings we have surveyed, all of these $1/8 \lambda$ spaced models are amenable to the use of a simple $1/4 \lambda$ section of 75-Ohm coax as a matching section for a 50-Ohm main transmission line. However, if the characteristics of one of the wider-spaced 10-meter models is desired, proportional enlargement of the spacing and the side lengths will put one very close to the desired model.

This collection of models should put one well on to the road of quad modeling throughout the upper HF region. However, it does not exhaust the modeling possibilities for simple, full-size 2-element monoband quads. In the next chapter, let's look at a few variations on these models and at some questions of comparison.

3. Variations and Comparisons Among 2-Element Quads

Rarely is the modeling of a quad beam just an exercise. The modeling activity generally precedes some decision-making about building or purchasing an actual antenna. Hence, we cannot proceed without encountering various kinds of controversies. In this chapter, we shall consider three such unsettled matters.

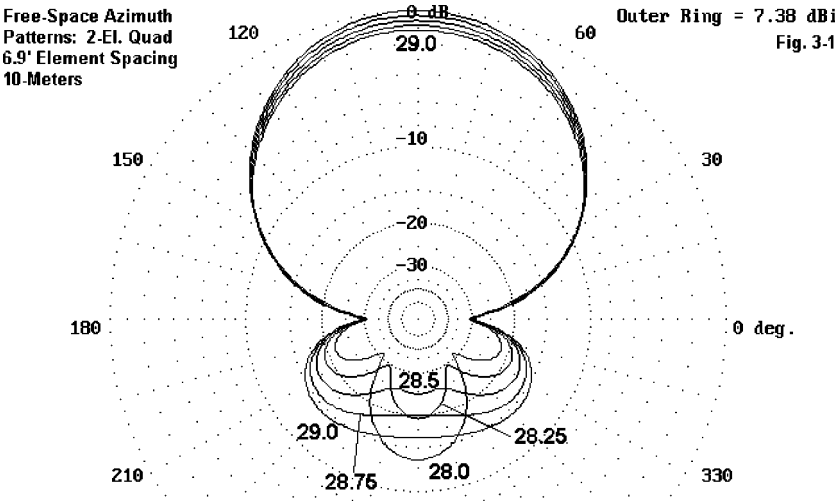
Element Spacing and Flexibility

One of the possible conflicts lies wholly within the realm of quads and concerns the best element spacing for quads. Both MININEC and NEC consistently show that more closely spaced 2-element quads to exhibit higher gain than more widely spaced models. The contrasting spacings are those close to 0.125λ on one side and those closer to 0.2λ on the other. Some have claimed that closely spaced quads do not perform in reality as models predict and that widely spaced quads are superior in gain.

Unfortunately, this contention is not universally supported. Some builders of closely-spaced quads claim that they obtain the performance predicted by calculations, models, and other quad users. Hence, we have an open question based on the disparity of experiences.

One important advantage of more widely spaced quads can be demonstrated by examining the azimuth patterns across a ham band, in this case, the first MHz of 10 meters.

In **Fig. 3-1**, we have patterns every 250 kHz across the lower end of 10 meters for the most widely-spaced quad in our collection, the one with 0.2λ element spacing. This azimuth pattern exercise can be compared with **Fig. 2-2** in the preceding episode. The rear quadrants of the patterns in **Fig. 3-1** show far less variation than those of the more closely spaced (0.145λ) version in **Fig. 2-2**. The lesser variation indicates that minor variations of structure--whether loop length or spacing--create smaller performance changes when the elements are more widely spaced.



Another way to approach the same point is to examine the source impedance of various quad designs across the operating passband. **Table 3-1** lists source impedances for three models: the most closely spaced version (0.125λ), a middling version (0.16λ) and a widely paced version (0.2λ). Only three checkpoints are given: 28.0, 28.5, and 29.0 MHz.

Table 3-1. Source Impedance: R +/- j X Ohms

Frequency	0.125λ	0.16λ	0.2λ
28.0	$52.6 - j 64.9$	$86.0 - j 47.3$	$127.4 - j 29.7$
28.5	$101.7 - j 0.9$	$134.7 - j 2.1$	$165.7 + j 3.3$
29.0	$147.4 + j 30.4$	$167.5 + j 20.3$	$184.2 + j 17.5$
Delta R	94.9 Ohms	81.5 Ohms	56.8 Ohms
Delta X	95.3 Ohms	67.6 Ohms	47.2 Ohms

Compared to the values for the narrowest spacing, the resistance range for the widest spacing is 40% smaller and the reactance range 50% smaller. Since none of the values obtained for the feedpoint impedance of the 2-element quad is a direct match for the usual 50-Ohm coax feedline, some sort of matching system will be required. Not only will the lesser resistance and reactance excursions make it easier to provide a band-edge-to-band-edge match within a 2:1 SWR range, but as well they will in most systems improve efficiency (or, to say the same thing, reduce losses).

Replicating the performance of a model with an actual antenna requires more than just obtaining an SWR curve that is similar to that predicted by a model. The parameters of gain and front-to-back ratio must also be repli-

cated by adjustment of the antenna dimensions. Normally, the front-to-back ratio is easier to determine than gain. A helper station or a signal source at least 10λ distant from the antenna is usually sufficient to find the frequency at which signals from the antenna rear are minimum.

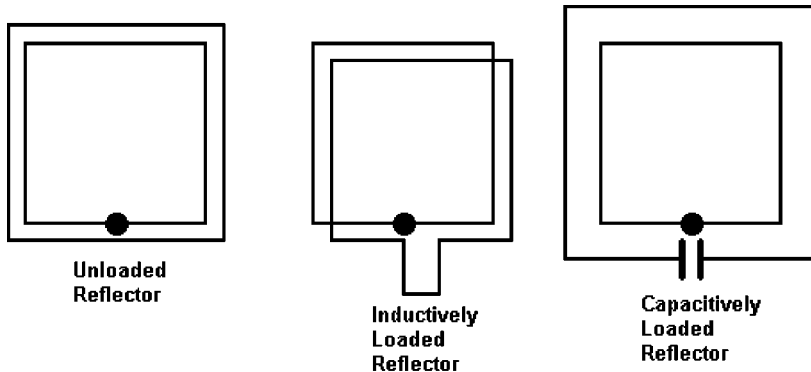


Fig. 3-2

Adjustment of a full-size reflector requires alteration of the wire length of a loop that is often already soldered closed. However, two alternative schemes often permit reflector adjustment.

As shown in **Fig. 3-2**, we may use either inductive or capacitive loading on the reflector. In many past designs, inductive loading has been used because it permits the reflector to be the same size as the driven loop--about 5% shorter than a full size reflector at the closest spacing. The inductive reactance required to electrically lengthen the reflector to full size can be provided by either an inductor or a length of shorted transmission line. If we choose to use capacitive loading, we must enlarge the reflector and electrically shorten it with capacitive reactance. Ordinarily, a variable capacitor is used to find the correct value and then is replaced by a fixed capacitor.

Apart from the matter of loop size, we can wonder if one loading system has an advantage over the other. Here modeling can suggest some answers. I created three alternative models to the 0.125λ element spacing version of the full size quad. There are two inductively loaded quads with identical loops sizes, one using an inductor with a Q of 300 and the other using a shorted transmission line. Since the inductively loaded models shortened the reflector loop length by 5%, the reflector loop for the capacitively loaded model increases in length by a like amount. **Table 3-2** shows the dimensions of the 4 antennas, each of which uses a 4.31' (0.125λ) spacing between elements at 28.5 MHz.

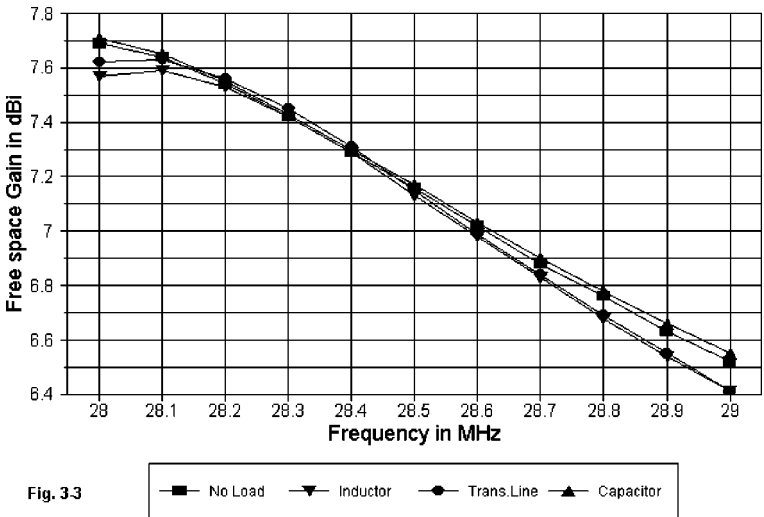
Table 3-2. Dimensions of 4 Sample Quads

Load Type	L Driver feet	C Driver feet	Refl. feet	C Refl. feet	Refl. React. Ohms
None	8.66	34.64	9.16	36.64	---
Coil	8.66	34.64	8.66	34.64	140
TL	8.66	34.64	8.66	34.64	140
Capac.	8.66	34.64	9.68	38.72	150

A coil with a Q of 300 and a reactance of 140 Ohms will have at the design frequency of 28.5 MHz a series resistance of about 0.47 Ohms and an inductance of 0.78 microH. To achieve the same reactance with a 600-Ohm, velocity factor 1.0 transmission line requires a shorted section about 1.26' long. A capacitive reactance of 150 Ohms at 28.5 MHz requires about 37.3 pF.

All of these values can be modeled in NEC and all but the transmission line can be modeled in MININEC using the facilities for mathematical loads. Since the loads are installed at the center point of the reflector lower element, the likelihood of error due to a differential between a mathematical load and a physically modeled load is minimized. Comparing the performance reports across the first MHz of 10 meters for all four models provides some interesting results.

Full-Size 2-Element Quads
Gain vs. Reflector Loading



Operationally, the gain of the 4 quad models is insignificantly different, as shown in **Fig. 3-3**. However, some emergent trends are apparent. Both forms of inductive loading narrow the pass band of the gain curve so that the gain peak is no longer lower in frequency than 28 MHz. There is a noticeably more rapid decrease in gain at the high end of the pass band as well. The gain curve for the capacitively loaded model is insufficiently different from that of the unloaded model to suggest that capacitive loading provides a shallower curve of gain decrease across the band. However, the hint of difference may lead some modelers to experiment with even larger reflectors and heavier capacitive-reactance loading.

Full-Size 2-Element Quads
F-B Ratio vs. Reflector Loading

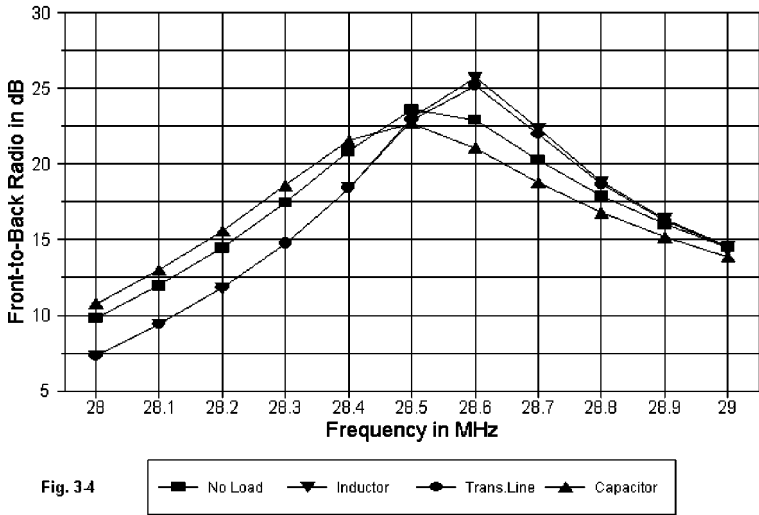
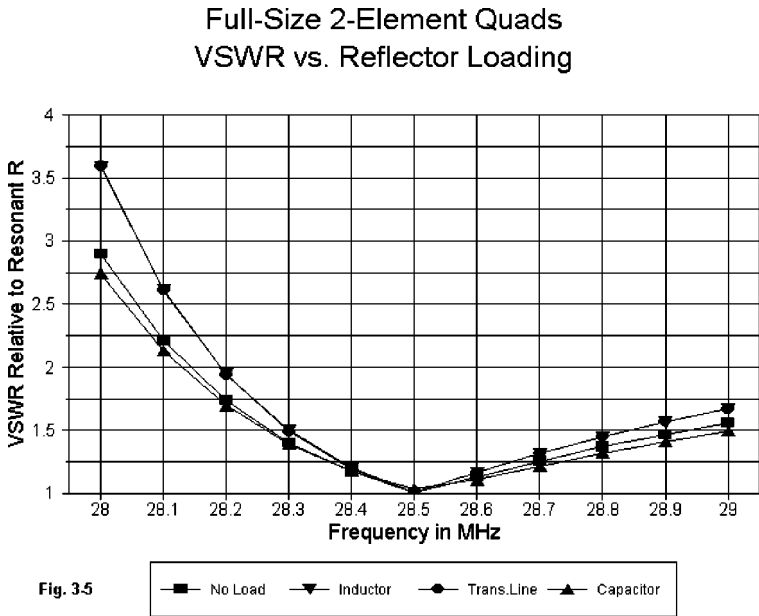


Fig. 3-4

In contrast to their gain curve, the inductively loaded models provide a higher peak front-to-back ratio than either the unloaded or the capacitively loaded model, as revealed in **Fig. 3-4**. The curve for the capacitively loaded model is distinctly shallower than even that of the unloaded model. All of the models show about the same front-to-back ratio at the upper end of the pass band, which makes evident the reduced front-to-back ratio at the lower end of the band provided by the two inductively loaded models. As with gain, the inductively loaded models show a narrower passband for a given performance level, while the larger, capacitively loaded reflector shows a wider pass band for a given level of performance.



The SWR (relative to the impedance at resonance) performance of the models appears in **Fig. 3-5**. Note that the 600-Ohm shorted stub provides an SWR curve that is indistinguishable from that for a coil with a Q of 300. Both curves are significantly sharper than the curves for the unloaded model and the capacitively loaded model. Consistent with the results for gain and for the front-to-back ratio, the capacitively loaded model shows the broadest curve.

The SWR curves for all four models can be brought within a 2:1 SWR range by lowering the driver resonant frequency. However, the drivers for the inductively loaded models will have to be resonated at a noticeably lower frequency than those of the unloaded and capacitively loaded models in order to achieve a 2:1 SWR operating bandwidth

For reference, **Table 3-3** lists the reported performance figures for the design center frequency (28.5 MHz) for the four models.

Table 3-3. Performance Figures for 4 Quad Designs

Load	Free Space	Front-to-Back	Feedpoint Impedance
Type	Gain dBi	Ratio dB	R +/- jX Ohms
None	7.16	23.6	102 - j 1
Coil	7.13	23.1	96 + j 0
Trans. Line	7.15	22.9	96 + j 1
Capacitor	7.17	22.7	106 - j 4

Both the capacitively loaded and the transmission-line stub loaded models invoke no losses in the modeled load. Hence, their gains are about the same as the unloaded model. The reflector coil has a finite Q (300) and hence shows the effect of the loss. Inductive loading, with its smaller reflector loop size, also lowers the resonant impedance of the model. In contrast, capacitive loading and the larger reflector loop increase the resonant impedance of the array. The variance from the impedance of the unloaded full-size quad is not great, but it indicates another trend to be cataloged for possible later use.

Reflector loading provides a convenient method of optimizing the front-to-back performance of the quad beam. Of the two inductive methods, there is little to choose between using a coil and using a shorted transmission line stub. However, capacitive loading provides greater advantages than either form of adding inductive reactance, but at the cost of a physically larger reflector loop. Whether or not the larger loop is mechanically feasible in given situations, modeling cannot say.

External Comparisons

Besides providing data that are useful in deciding how one might design a 2-element quad beam, modeling can also make a contribution to the decision of whether to construct a quad or some competitive antenna type, such as a 2-element or 3-element Yagi-Uda array. What modeling can contribute are projections of performance potential.

However, modeling cannot provide a definitive answer to the typical quad vs. Yagi dispute. Whether there are factors beyond gain, front-to-back ratio, and SWR bandwidth that give one or the other antenna type the edge exceeds the ability of models to determine. Hence, we shall confine modeling analysis to what it can do.

Fig. 3-6 shows the outlines of a short-boom 3-element Yagi, a typical driver-reflector 2-element Yagi, and one of the 2-element quad models--the version using 5' spacing and a driver resonated at about 28.35 MHz to bring the SWR curve within 2:1 limits across the first MHz of 10 meters. The dimensions of the three antennas appear in **Table 3-4**.

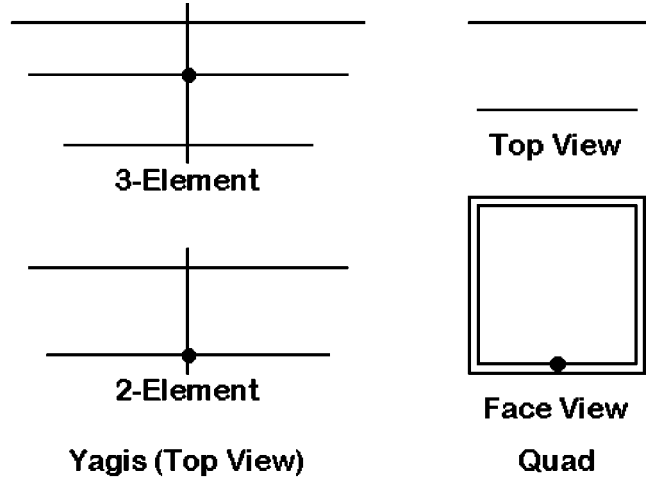


Fig. 3-6

Table 3-4. Dimensions of Compared Yagis and Quads

Quad:	Spacing λ	Spacing feet	L Driver feet	C Driver feet	L Reflector feet	C Reflector feet
	0.145	5.02	8.76	35.04	9.19	36.77
2-El. Yagi:	Spacing λ	Spacing feet	L Driver feet	L Reflector feet		
	0.125	4.33	16.06	17.33		
3-El. Yagi:	Ref-DE Sp-feet	DE-Dir Sp-feet	Total feet	L Refl. feet	L Driver feet	L Dir. feet
	2.5	5.0	7.5	17.66	16.63	15.44

The footprints of these 3 antenna models are clear in **Fig. 3-6**. However, the “footprint” figure of speech also reminds us that while the Yagis are flat sandals, the quad is a boot with as much height as width.

For reference, here are EZNEC model descriptions of the two Yagis used for this set of comparisons. The models are so simple that translation into any other program format should be easy.

```
2-el Yagi 1/8 wl sp 10m                                Frequency = 28.4  MHz.

Wire Loss: Aluminum -- Resistivity = 4E-08 ohm-m, Rel. Perm. = 1

----- WIRES -----

Wire Conn.--- End 1 (x,y,z : ft)  Conn.--- End 2 (x,y,z : ft)  Dia(in) Segs
1          -8.667,  0.000,  0.000          8.667,  0.000,  0.000 5.00E-01 31
2          -8.033,  4.333,  0.000          8.033,  4.333,  0.000 5.00E-01 31

----- SOURCES -----

Source      Wire      Wire #/Pct From End 1      Ampl.(V, A)  Phase(Deg.)  Type
            Seg.      Actual      (Specified)
1           16       2 / 50.00   ( 2 / 50.00)      1.000        0.000        I

Ground type is Free Space
.....
```

```
3-el Yagi short-boom 10m                                Frequency = 28.5  MHz.

Wire Loss: Aluminum -- Resistivity = 4E-08 ohm-m, Rel. Perm. = 1

----- WIRES -----

Wire Conn.--- End 1 (x,y,z : ft)  Conn.--- End 2 (x,y,z : ft)  Dia(in) Segs
1          -8.828,  0.000,  0.000          8.828,  0.000,  0.000 5.00E-01 31
2          -8.317,  3.000,  0.000          8.317,  3.000,  0.000 5.00E-01 31
3          -7.721,  7.500,  0.000          7.721,  7.500,  0.000 5.00E-01 31

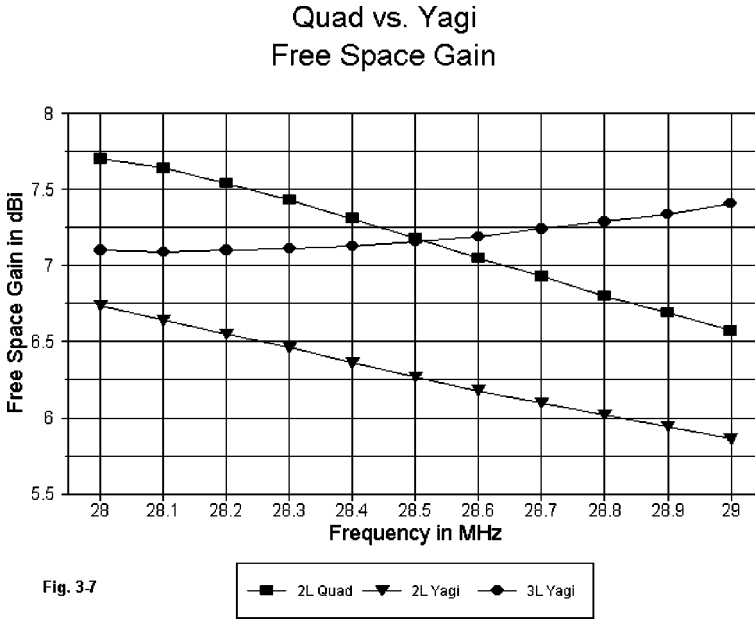
----- SOURCES -----

Source      Wire      Wire #/Pct From End 1      Ampl.(V, A)  Phase(Deg.)  Type
            Seg.      Actual      (Specified)
1           16       2 / 50.00   ( 2 / 50.00)      1.000        0.000        I

Ground type is Free Space
```

Since the Yagis are for study purposes only, their elements are a uniform 0.5" diameter and are aluminum. Slightly longer elements lengths would be required for actual Yagis using an element diameter tapering schedule. The quad remains #14 AWG copper wire. The 3-element Yagi is adapted from an N6BV design in the ARRL *Antenna Book* YO collection. I have intentionally used a short boom version that is competitive in gain with the 2-element quad. 3-element Yagis with booms in the vicinity of 11.5 to 12 feet on 10 meters would show about an additional 1 dB forward gain.

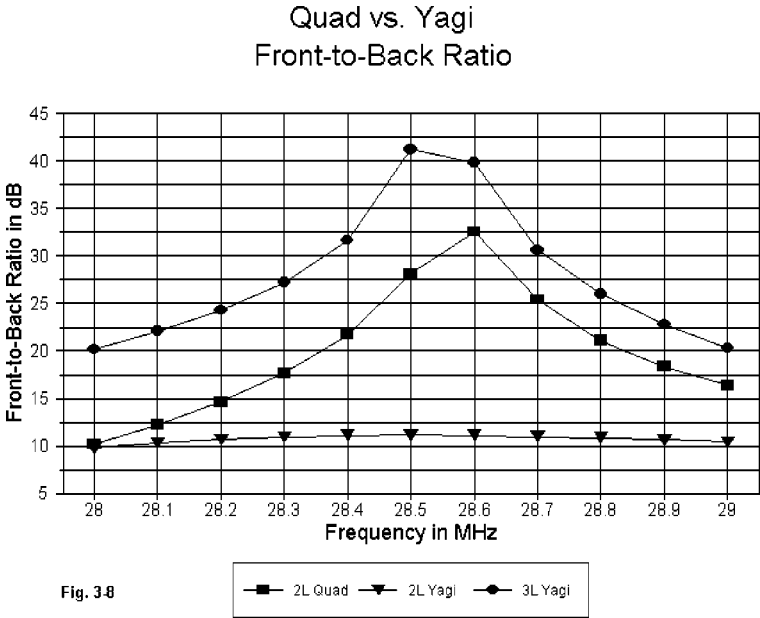
It is possible to make parallel frequency sweeps with the three designs and compare the performance potential of the three antennas.



The free-space forward gain of all three antennas appears in **Fig. 3-7**. At the design center frequency (28.5 MHz), the 3-element Yagi and the 2-element quad have almost identical gain figures. However, the gain vs. frequency characteristics of the quad and the larger Yagi are opposing, so that as the gain of one increases, the gain of the other decreases. The 3-element Yagi shows a rather small gain change across the pass band, while the change for the quad is about 0.8 dB.

The gain of the 2-element Yagi is significantly lower than that of the 2-element quad--almost a full dB across the band. Because the quad and the 2-element Yagi are both driver-reflector designs, their gain curves parallel. A driver-director 2-element Yagi gain curve would parallel that of the 3-element Yagi, but the operating bandwidth would be much narrower.

It may be useful to notice one more property displayed by the gain curves. By judicious selection of data points, one can develop some misleading claims about antennas. For example, if we focus only on the gain at 28 MHz, then the gain differential between the 2-element and 3-element Yagis is only about a third of a dB--hardly a sufficient reason to add the third element. At 29 MHz, the differential is about 1.6 dB, making the 2-element Yagi seem hardly worthwhile in the comparison. As always, the message is the same: do not be satisfied with data points. Instead, demand full passband curves.



If there is one place where the 2-element driver-reflector Yagi suffers, it is in the category of the front-to-back ratio, as **Fig. 3-8** reveals. The flat curve between 10 and 11 dB would be reflected in any defined front-to-rear performance evaluation. This curve does not mean that the 2-element Yagi is not useful. In fact, it can be an advantage to some types of net and contest operations where total rejection of signals from the rear quadrants is not a useful property. Again, a 2-element driver-director design would show a higher front-to-back ratio, but would be usable only over a much narrower bandwidth.

However, both the quad and the 3-element Yagi show superior overall front-to-back performance. The curves are remarkably parallel to each other. At the lower end of the band, the Yagi shows almost 10 dB greater rear rejection, with a lesser advantage in the upper part of the pass band. All-in-all, the quad is clearly intermediate to the Yagis in front-to-back performance.

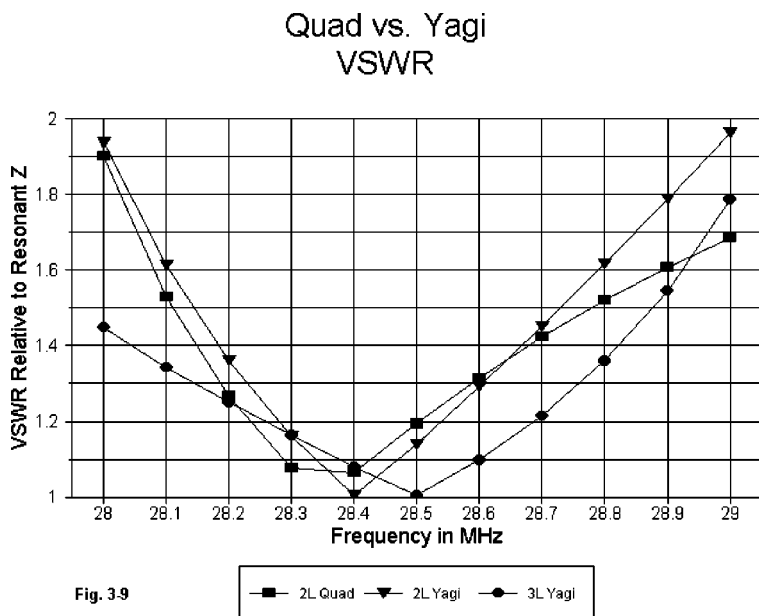


Fig. 3-9 shows that all three antennas, relative to their resonant impedances, are capable of a 2:1 SWR across the pass band of concern here. Of more interest are contrasting patterns of the SWR curves. The steep quad curve below resonance (28.35 MHz in the example) becomes a very shallow curve above resonance. The 2-element Yagi--resonated at 28.4 MHz to achieve the 2:1 SWR fit--reflects the low-end steep curve of the quad, but is no where near as shallow above resonance. In sharpest contrast stands the 3-element Yagi curve: shallower below resonance and steeper above resonance. Built into these curves are some lessons about the effects of directors on Yagi design.

The true business at hand is placing the performance potential of the 2-element full-size quad beam among its normal design competitors. As expected, it comes out somewhere in the middle.

However, the competitors on this modeling comparison are full-size monoband Yagis. Monoband quads in amateur use are rarely the norm. Where they are used, the operator often wants minimal size and sometimes resorts to techniques of shrinking the full-size quad. Therefore we shall have to look at shrunk quads and their potential performance. Keeping the Yagi figures and the full-size quad figures in mind will be useful in evaluating the performance potential of scrunched and squashed quads.

The other major use of 2-element quads is in multi-band version covering 3 to 5 amateur bands. We shall also have to examine some models of these types of antennas. But first, a small digression.

Diamonds, Squares, and Rectangles

Some quad makers prefer the square shape. It occupies the smallest vertical and horizontal dimensions. Other quad builders prefer the diamond shape. They find it more resistant to the rigors of ice and snow than the square shape. Both of these preferences involve factors to which modeling cannot speak.

With respect to performance, neither shape has an edge. In my collection of quad models, I have found no difference in the performance figures for either shape. To illustrate this assertion, let's look at the model description for the diamond equivalent of the 0.125 λ spaced 2-element quad. The model is simple enough not to require replication in other formats.

```
2el quad dia. 6.12/6.48/4.31sp                      Frequency = 28.5  MHz.

Wire Loss: Copper -- Resistivity = 1.74E-08 ohm-m, Rel. Perm. = 1

----- WIRES -----

Wire Conn.--- End 1 (x,y,z : ft)  Conn.--- End 2 (x,y,z : ft)  Dia(in) Segs

1   W4E2   6.123,  0.000,  0.000  W2E1   0.000,  0.000,  6.123  # 14   7
2   W1E2   0.000,  0.000,  6.123  W3E1  -6.123,  0.000,  0.000  # 14   7
3   W2E2  -6.123,  0.000,  0.000  W4E1   0.000,  0.000, -6.123  # 14   7
4   W3E2   0.000,  0.000, -6.123  W1E1   6.123,  0.000,  0.000  # 14   7
5   W8E2   6.476, -4.310,  0.000  W6E1   0.000, -4.310,  6.476  # 14   7
6   W5E2   0.000, -4.310,  6.476  W7E1  -6.476, -4.310,  0.000  # 14   7
7   W6E2  -6.476, -4.310,  0.000  W8E1   0.000, -4.310, -6.476  # 14   7
8   W7E2   0.000, -4.310, -6.476  W5E1   6.476, -4.310,  0.000  # 14   7

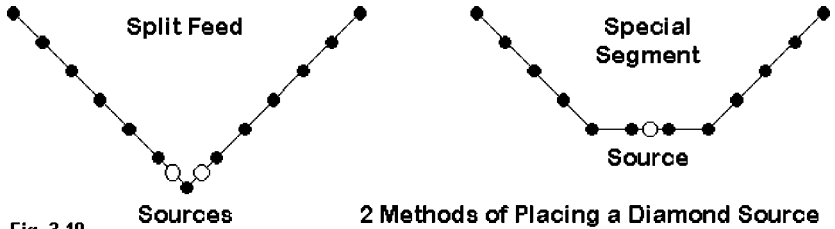
----- SOURCES -----

Source      Wire      Wire #/Pct From End 1      Ampl.(V, A)  Phase(Deg.)  Type
      Seg.      Actual      (Specified)

1          7      3 /100.00  ( 3 /100.00)      1.000      0.000      SV

Ground type is Free Space
```

The model is fed in one of the two most commonly used ways--with a split feed, one source being placed on each of the segments adjacent to the lowest corner.



As shown in **Fig. 3-10**, one can also create a special wire of at least 3 segments having equal length with the single source placed on the center segment. This feed method tends to shorten the overall loop size by a tiny amount—enough to show up in the performance report decimal columns, but not enough to affect building plans or performance curves.

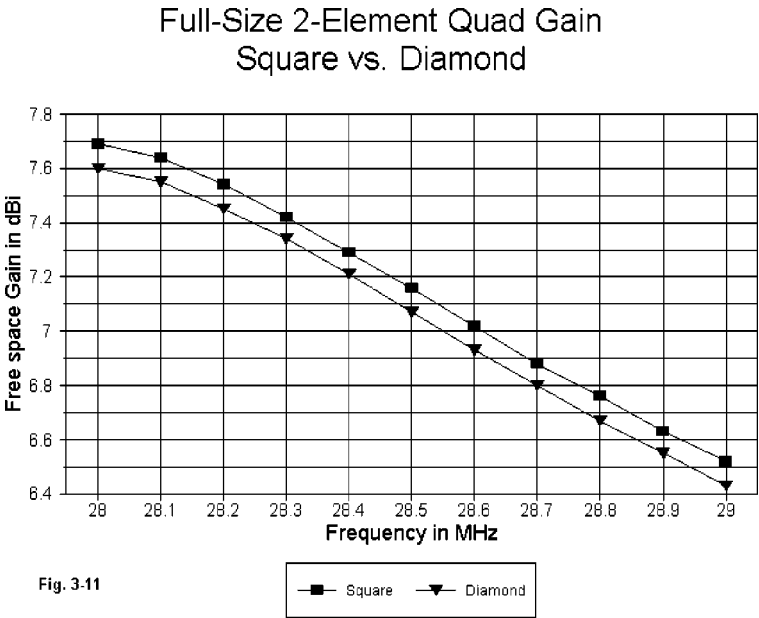
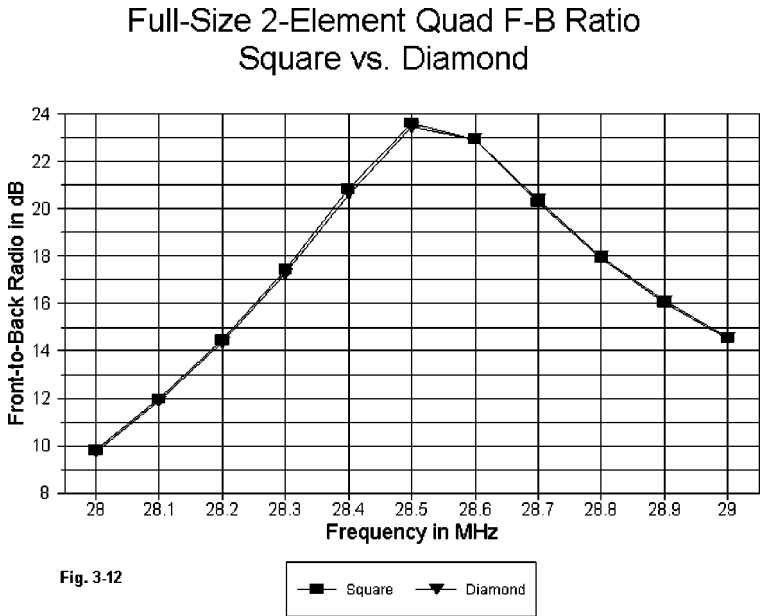


Fig. 3-11 shows that the gain is systematically within 0.09 dB between the two shapes for the entire first MHz of 10 meters.

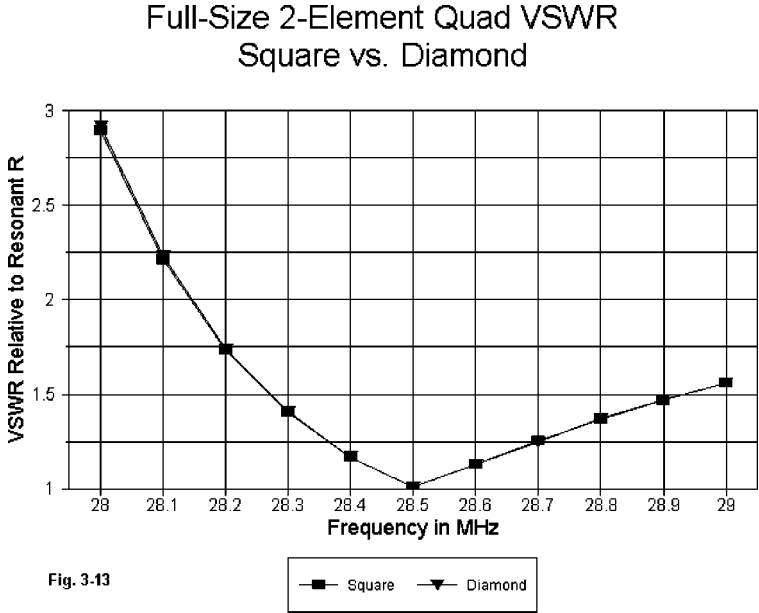
The front-to-back ratio for the two models is even closer, as most of the reference markers obscure each other in **Fig. 3-12**.



Although the diamond shaped quad shows a resonant impedance about 4 Ohms higher than the square version, **Fig. 3-13** shows that the two SWR curves overlap each other almost perfectly. One might view the graphing of this set of overlapping curves as excessive exposition. However, given the degree to which I have urged the showing of full passband curves to verify modeling claims about performance, this graph collection is simply a matter of practicing what I preach.

More importantly, the conclusion supported by the graphs is this: there is no significant difference in performance between square and diamond quad configurations, if the loop circumferences and element spacing are the same.

With the square-diamond comparison complete, we may now turn to another variation: the rectangle. However arranged, the square is not the quad form capable of the highest gain. A vertical rectangle can increase gain significantly.



Consider 2-element monoband quads with the dimensions listed in **Table 3-5**. A “length” (L) entry of the order 6.9/11 means that the rectangle is 6.9’ horizontally and 11’ vertically. The circumference shows the relationship of the rectangular models to the square model used as a comparator. All three models happen to use #12 AWG copper wire, since they occurred as part of a separate modeling experiment. (Note: as a reminder, the 10-meter models used throughout this study use #14 AWG copper wire unless otherwise noted.)

Table 3-5. Dimensions of Rectangular and Square Quads					
Spacing λ	Spacing feet	L Driver feet	C Driver feet	L Reflector feet	C Reflector feet
Rectangular					
0.200	6.91	6.8/11.0	35.60	7.4/11.0	36.80
0.160	5.50	6.9/11.0	35.80	7.3/11.0	36.60
Square					
0.200	6.91	8.86	35.44	9.32	37.28

For reference, here is an EZNEC model description of the wide-spaced rectangular 2-element quad array.

2-el. rect. quad

Frequency = 28.5 MHz.

Wire Loss: Copper -- Resistivity = 1.74E-08 ohm-m, Rel. Perm. = 1

----- WIRES -----

Wire Conn.--- End 1 (x,y,z : ft) Conn.--- End 2 (x,y,z : ft) Dia(in) Segs

1

W4E2

-3.400,

0.000,

-5.500

W2E1

3.400,

0.000,

-5.500

12

11

2

W1E2

3.400,

0.000,

-5.500

W3E1

3.400,

0.000,

5.500

12

15

3

W2E2

3.400,

0.000,

5.500

W4E1

-3.400,

0.000,

5.500

12

11

4

W3E2

-3.400,

0.000,

5.500

W1E1

-3.400,

0.000,

-5.500

12

15

5

W8E2

-3.700,

-6.900,

-5.500

W6E1

3.700,

-6.900,

-5.500

12

11

6

W5E2

3.700,

-6.900,

-5.500

W7E1

3.700,

-6.900,

5.500

12

15

7

W6E2

3.700,

-6.900,

5.500

W8E1

-3.700,

-6.900,

5.500

12

11

8

W7E2

-3.700,

-6.900,

5.500

W5E1

-3.700,

-6.900,

-5.500

12

15

----- SOURCES -----

Source Wire Wire #/Pct From End 1 Ampl.(V, A) Phase(Deg.) Type

Seg. Actual (Specified)

1 6 1 / 50.00 (1 / 50.00) 1.000 0.000 I

Fig. 3-14 provides a sketch of the rectangular quad outline. The rectangles in the models shown here have not been shape-optimized for maximum gain, so further improvements might well be made to the mid-band performance shown in **Table 3-6** for reference.

Fig. 3-14

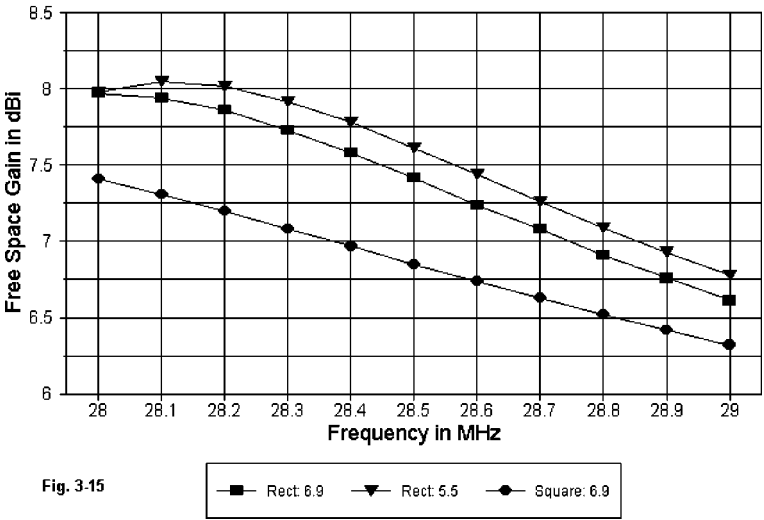
Chapter 3 ~ Variations and Comparisons Among 2-Element Quads

Table 3-6. Mid-Band Performance Figures for 3 Quads

Antenna	Free Space Gain dBi	Front-to-Back Ratio dB	Feedpoint Impedance R +/- jX Ohms
Rect: wide space	7.42	26.7	109 - j 3
Rect: close space	7.61	19.8	94 + j39
Square	6.85	24.0	167 + j 8

Both the close-spaced rectangle and the square were resonated lower in the band (28.3 to 28.35 MHz) to establish an SWR curve with close to equal values at the band edges. (Note: for comparison with the #12 square quad in the table above, the #14 copper version of the square quad, shown in the preceding chapter, had a free space gain of 6.81 dBi, a front-to-back ratio of 23.8 dB, and a source impedance of 166 Ohms.)

Rectangular vs. Square 2-El. Quads
Free Space Gain



The gain curves for the three models, shown in **Fig. 3-15**, demonstrate the higher gain possible with a 2-element parasitic rectangular beam. At midband, the wide-spaced rectangle shows a 0.5 dB advantage over the square model, and further improvement might be possible by optimizing the rectangle's shape for maximum gain. The ratio of horizontal to vertical dimension will vary with frequency, so optimization would be required for each band on which such a scheme might be used.

Although the rectangles provide higher gain than the square quad, the rectangles yield lower front-to-back ratios on average than the square model, as revealed in **Fig. 3-16**. Despite the peak in the wide spaced rectangular model, the overall performance is less satisfactory than the square, with the lower end of the band suffering most. Some improvement can likely be effected by sliding the front-to-back maximum lower in frequency.

There are in fact a number of design variables for rectangular quads that one might alter in an effort to improve performance in one or another category. The alignment of the rectangles is one factor. Another is the relative shapes of the driver and reflector: should one keep the side-to-side dimension constant, or keep the vertical dimension constant, or make the two rectangles truly concentric? These notes, obviously, are only a first sample of potentials.

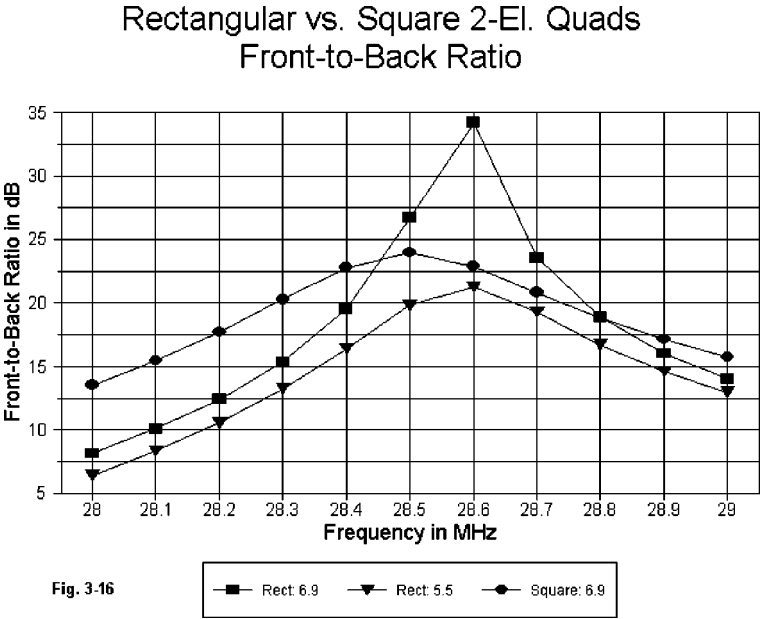
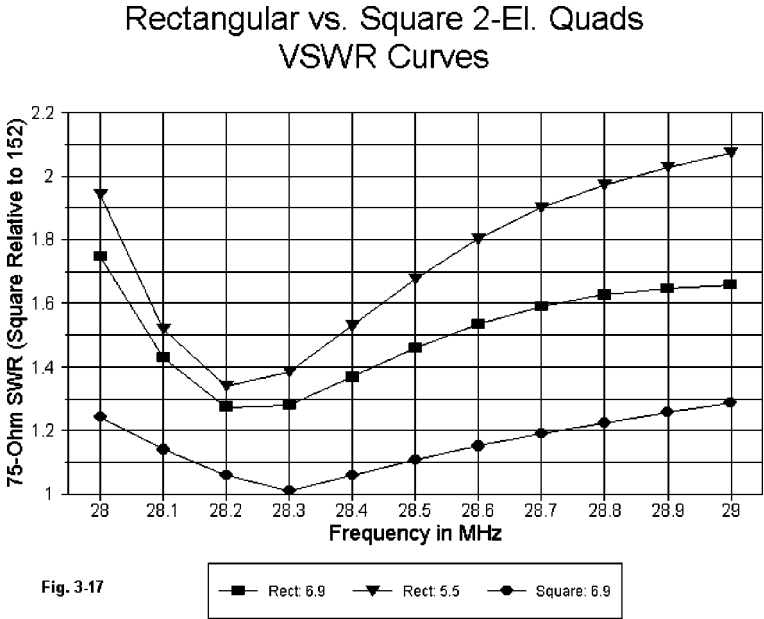
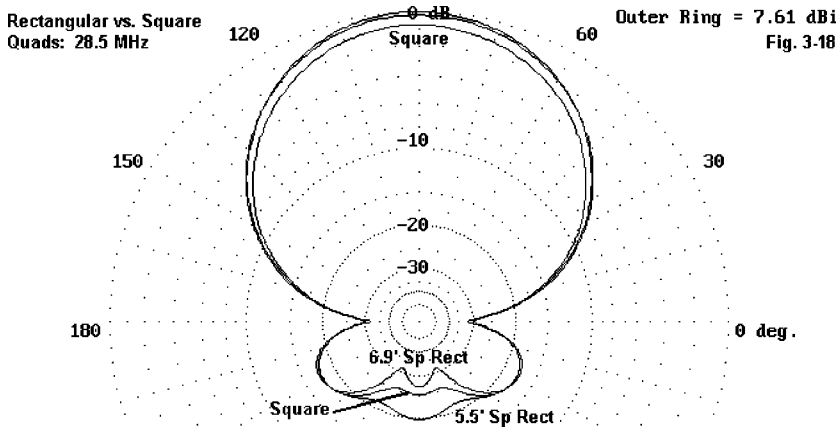


Fig. 3-17 provides some SWR curves for the three models. The curve for the square is referenced to the resonant impedance of the antenna (about 166 Ohms) simply to show the flatness of the curve. Without provision for matching, the two rectangular quads both achieve usable 75-Ohm SWR curves, with the wide-spaced model slightly better. As one makes a horizontally polarized loop more vertically rectangular, the source impedance decreases. The decrease in source impedance for a single rectangular loop also shows up in the source impedance for multi-element rectangular quad arrays.



Comparative mid-band (28.5 MHz) free space azimuth patterns appear in **Fig. 3-18**. The increased gain and decreased front-to-back ratio are quite clear on the pattern overlays.



The point of this particular modeling exercise is to demonstrate that the square quad is simply not the ultimate in quad gain, no matter the spacing or loop size. The rectangular quad is capable of significantly higher gain. Of course, the square has some structural advantages which may override use of a higher-gain configuration. But, then, almost every antenna represents a compromise among all of the factors and specifications that go into their design and construction. The quad is no exception.

A square quad has a side-to-side dimension of about $1/4 \lambda$, with a similar vertical dimension. Spacing between elements of a 2-element quad beam range from about 0.125λ to 0.2λ in most of the published designs. For 10-meters, the resultant 9' side dimensions are easily supported with standard fiberglass arm construction. However, a 20-meter 2-element quad requires 13' arms to support the 18' side dimensions. Structurally, most quad support arms taper from the hub end to the tip, thus leaving the thinnest portion of the arm to support the heaviest lengths of wire in the elements.

Although these mechanical features can be worked out to yield a strong assembly, the quad has acquired something of a reputation for collapsing under the weight of accumulated snow and ice during the winter. There are many solutions to this problem, ranging from heating the elements to prevent

icy build-up, to building stronger support assemblies, to resignation from the quad field and a return to Yagi-Uda arrays. Some quad aficionados simply plan on rebuilding their antennas as soon as the spring thaw permits.

These structural matters lie beyond the frontier of any contribution to be made by this study. However, they do serve as a background for our next chapter. One direction in which quad builders have gone is to try to shrink the quad by various loading schemes. A smaller quad structure is an inherently stronger structure for any given wire size and support arm diameter. The question that remains from these efforts to reduce the overall size of the quad is this: what performance sacrifices might be dictated by reducing the size of the quad loop circumference.

4. Shrunk 2-Element Quads

The art of creating a miniature quad--that is, any quad significantly smaller than full size--has been around almost as long as the quad itself. There are many techniques for achieving a smaller size quad. Most fundamental--and perhaps the lossiest--is adding either center or corner inductors to each quad loop.

My own collection of models has focused on a technique that may owe to Paul Carr, N4PC, and which appears in Lew McCoy's book *On Antennas* from CQ Communications. It consists of inseting the loop wires at the low current, high voltage points at the loop sides. Paul reasoned that this form of "linear loading" would have the least impact on gain and front-to-back ratio. I studied variations of the technique, including building some trial versions, for a piece in *Communications Quarterly* a few years back. The models discussed here will be a selection from the large number accumulated during that study. Like the full-size models we have already examined, all use #14 AWG copper wire. All models will be in free space for consistency with the previous models.

Because the techniques for shortening quad loops are many and varied, this collection of models will necessarily be incomplete. However, the progression of models may provide some background for evaluating other types of miniature quads that you decide to model.

The 78% Square

At about 78% full size, one reaches a limit for providing single insets on each side of a square quad loop. If the size is further reduced, the insets will overlap at the loop center. Some flexibility remains, since the insets can be made wider or narrower, as well as longer or shorter, in order to fit the building technique.

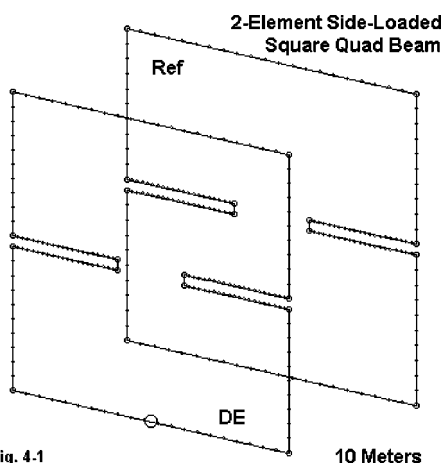


Fig. 4.1

Fig. 4-1 shows the outlines of a single inset square quad beam. The models that we shall look at have 6.96' sides on the driven element. Two versions will be compared, one with 4.31' spacing (0.125λ), the other with 5' spacing (0.145λ). The reflector sides are 7.24' and 7.40', respectively.

For those who wish to replicate the models, the following extracts from EZNEC model description files provide the coordinates.

```
2L 3.46/3.62/4.31 linear load                                Frequency = 28.5  MHz.

Wire Loss: Copper -- Resistivity = 1.74E-08 ohm-m, Rel. Perm. = 1

----- WIRES -----

Wire Conn.--- End 1 (x,y,z : ft)  Conn.--- End 2 (x,y,z : ft)  Dia(in) Segs

1  W12E2  -3.460,  0.000, -3.460  W2E1   3.460,  0.000, -3.460  # 14  21
2  W1E2   3.460,  0.000, -3.460  W3E1   3.460,  0.000, -0.125  # 14  10
3  W2E2   3.460,  0.000, -0.125  W4E1   0.825,  0.000, -0.125  # 14  21
4  W3E2   0.825,  0.000, -0.125  W5E1   0.825,  0.000,  0.125  # 14   1
5  W4E2   0.825,  0.000,  0.125  W6E1   3.460,  0.000,  0.125  # 14  21
6  W5E2   3.460,  0.000,  0.125  W7E1   3.460,  0.000,  3.460  # 14  10
7  W6E2   3.460,  0.000,  3.460  W8E1  -3.460,  0.000,  3.460  # 14  21
8  W7E2  -3.460,  0.000,  3.460  W9E1  -3.460,  0.000,  0.125  # 14  10
9  W8E2  -3.460,  0.000,  0.125  W10E1 -0.825,  0.000,  0.125  # 14  21
10 W9E2  -0.825,  0.000,  0.125  W11E1 -0.825,  0.000, -0.125  # 14   1
11 W10E2 -0.825,  0.000, -0.125  W12E1 -3.460,  0.000, -0.125  # 14  21
12 W11E2 -3.460,  0.000, -0.125  W1E1  -3.460,  0.000, -3.460  # 14  10
13 W24E2 -3.620, -4.310, -3.620  W14E1  3.620, -4.310, -3.620  # 14  21
14 W13E2  3.620, -4.310, -3.620  W15E1  3.620, -4.310, -0.125  # 14  10
15 W14E2  3.620, -4.310, -0.125  W16E1  0.930, -4.310, -0.125  # 14  21
16 W15E2  0.930, -4.310, -0.125  W17E1  0.930, -4.310,  0.125  # 14   1
17 W16E2  0.930, -4.310,  0.125  W18E1  3.620, -4.310,  0.125  # 14  21
18 W17E2  3.620, -4.310,  0.125  W19E1  3.620, -4.310,  3.620  # 14  10
19 W18E2  3.620, -4.310,  3.620  W20E1 -3.620, -4.310,  3.620  # 14  21
20 W19E2 -3.620, -4.310,  3.620  W21E1 -3.620, -4.310,  0.125  # 14  10
21 W20E2 -3.620, -4.310,  0.125  W22E1 -0.930, -4.310,  0.125  # 14  21
22 W21E2 -0.930, -4.310,  0.125  W23E1 -0.930, -4.310, -0.125  # 14   1
23 W22E2 -0.930, -4.310, -0.125  W24E1 -3.620, -4.310, -0.125  # 14  21
24 W23E2 -3.620, -4.310, -0.125  W13E1 -3.620, -4.310, -3.620  # 14  10

----- SOURCES -----

Source   Wire      Wire #/Pct From End 1   Ampl.(V, A)  Phase(Deg.)  Type
        Seg.      Actual          (Specified)

1         11       1 / 50.00   ( 1 / 50.00)       1.000        0.000        I

.....
```

2L 3.46/3.7/5 linear load

Frequency = 28.5 MHz.

Wire Loss: Copper -- Resistivity = 1.74E-08 ohm-m, Rel. Perm. = 1

----- WIRES -----

Wire Conn.---	End 1 (x,y,z : ft)	Conn.---	End 2 (x,y,z : ft)	Dia(in)	Segs
1	W12E2 -3.460, 0.000, -3.460	W2E1	3.460, 0.000, -3.460	# 14	21
2	W1E2 3.460, 0.000, -3.460	W3E1	3.460, 0.000, -0.125	# 14	10
3	W2E2 3.460, 0.000, -0.125	W4E1	0.740, 0.000, -0.125	# 14	21
4	W3E2 0.740, 0.000, -0.125	W5E1	0.740, 0.000, 0.125	# 14	1
5	W4E2 0.740, 0.000, 0.125	W6E1	3.460, 0.000, 0.125	# 14	21
6	W5E2 3.460, 0.000, 0.125	W7E1	3.460, 0.000, 3.460	# 14	10
7	W6E2 3.460, 0.000, 3.460	W8E1	-3.460, 0.000, 3.460	# 14	21
8	W7E2 -3.460, 0.000, 3.460	W9E1	-3.460, 0.000, 0.125	# 14	10
9	W8E2 -3.460, 0.000, 0.125	W10E1	-0.740, 0.000, 0.125	# 14	21
10	W9E2 -0.740, 0.000, 0.125	W11E1	-0.740, 0.000, -0.125	# 14	1
11	W10E2 -0.740, 0.000, -0.125	W12E1	-3.460, 0.000, -0.125	# 14	21
12	W11E2 -3.460, 0.000, -0.125	W1E1	-3.460, 0.000, -3.460	# 14	10
13	W24E2 -3.700, -5.000, -3.700	W14E1	3.700, -5.000, -3.700	# 14	21
14	W13E2 3.700, -5.000, -3.700	W15E1	3.700, -5.000, -0.125	# 14	10
15	W14E2 3.700, -5.000, -0.125	W16E1	1.140, -5.000, -0.125	# 14	21
16	W15E2 1.140, -5.000, -0.125	W17E1	1.140, -5.000, 0.125	# 14	1
17	W16E2 1.140, -5.000, 0.125	W18E1	3.700, -5.000, 0.125	# 14	21
18	W17E2 3.700, -5.000, 0.125	W19E1	3.700, -5.000, 3.700	# 14	10
19	W18E2 3.700, -5.000, 3.700	W20E1	-3.700, -5.000, 3.700	# 14	21
20	W19E2 -3.700, -5.000, 3.700	W21E1	-3.700, -5.000, 0.125	# 14	10
21	W20E2 -3.700, -5.000, 0.125	W22E1	-1.140, -5.000, 0.125	# 14	21
22	W21E2 -1.140, -5.000, 0.125	W23E1	-1.140, -5.000, -0.125	# 14	1
23	W22E2 -1.140, -5.000, -0.125	W24E1	-3.700, -5.000, -0.125	# 14	21
24	W23E2 -3.700, -5.000, -0.125	W13E1	-3.700, -5.000, -3.700	# 14	10

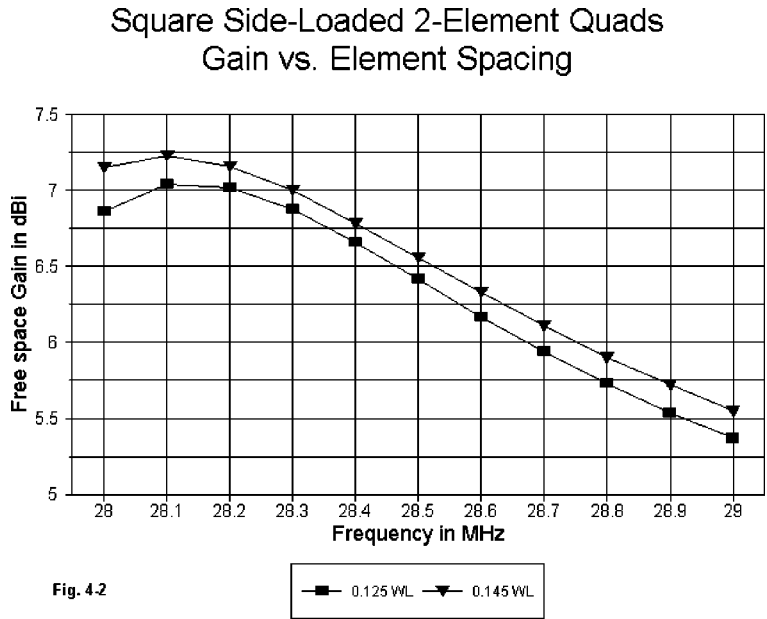
----- SOURCES -----

Source	Wire Seg.	Wire #/Pct Actual	From End 1 (Specified)	Ampl.(V, A)	Phase(Deg.)	Type
1	11	1 / 50.00	(1 / 50.00)	1.000	0.000	I

The length and width of the inset wires can be derived from simple exercises in subtraction. In making the models, I juggled the inset size and reflector loop length for something approaching best performance, although further tweaking of any of the models is certainly possible.

There is a tendency in shrinking quads to shrink the spacing between elements. However, better performance can be obtained with somewhat wider spacing. In these models, 0.125λ and 0.145λ spacing are compared. As with past models, 28.5 MHz is the design center frequency for resonance and for maximum 180-degree front-to-back ratio. As we shall see, there are opportunities for sliding either or both of these characteristic to other points within the passband.

Fig. 4-2 shows a clear gain advantage for the wider-spaced version of the single-inset square, although the actual amount may not be operationally significant. More notable than this gain differential is the fact that with the shrinking of the quad size, the gain curve is steeper, and the gain peak now falls within the passband (28 to 29 MHz) rather than below it. At the design center frequency, gain is about 0.5 dB below that of comparable full-size 2-element quad beams.



Where the added spacing between elements shows up most graphically is in the front-to-back ratio, as **Fig. 4-3** demonstrates. The wider spaced version not only peaks at a higher value (by about 4 dB), but as well is better across the entire passband.

For reference, **Table 4-1** provides the modeled performance figures for the two antennas at the design frequency.

Table 4-1. Performance Figures for 2 78% Shrunk Quads			
Antenna Version	Free Space Gain dBi	Front-to-Back Ratio dB	Feedpoint Impedance R +/- jX Ohms
0.125 λ	6.42	13.4	76 - j 1
0.145 λ	6.56	17.3	78 - j 0

Square Side-Loaded 2-Element Quads
F-B Ratio vs. Element Spacing

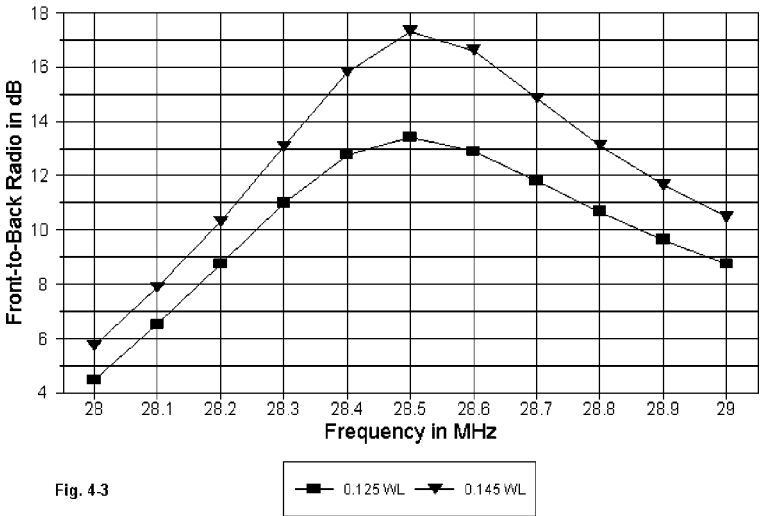


Fig. 4.3

Square Side-Loaded 2-Element Quads
VSWR vs. Element Spacing

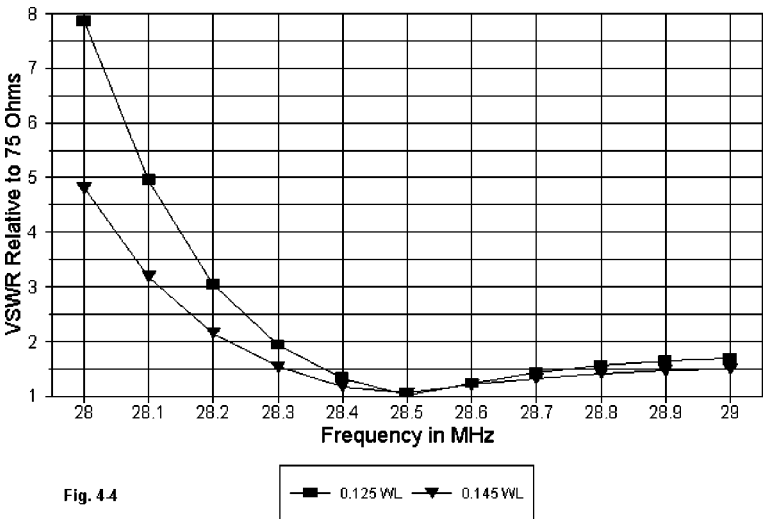


Fig. 4.4

As shown in **Fig. 4-4**, wider element spacing also makes the 75-Ohm VSWR curve shallower, especially at the lower end of the band. One aspect

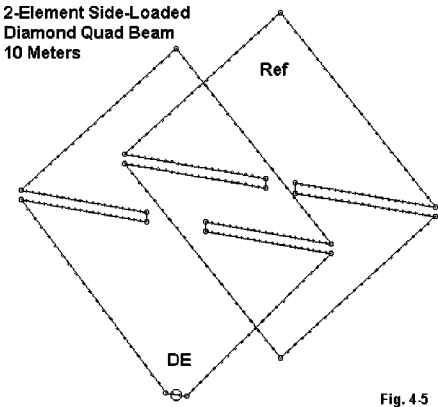
of shrinking quads is the fact that it is possible to obtain a low SWR not only at the upper limit of the passband (29 MHz), but well beyond that point. However, some caution must be used when changing the design frequency to fit the SWR curve: the downward curves of both the gain and the front-to-back ratios quickly reduce the antenna performance to just above dipole level.

One can judiciously slide the resonant point of the antenna lower in the passband by lengthening the driver loop or its insets. Equally judicious sliding of the front-to-back peak by similar adjustments to the reflector is also possible. The latter changes can equalize the front-to-back ratio at the passband limits. Unlike a full size quad, where the adjustments are fairly (although not completely) independent, changes to one element of the shrunk quad tend to affect the properties normally associated with the other element. Hence, even when modeling, care should be used to make adjustments in small amounts.

The 72% Diamond

The single inset square is the largest of this collection of shrunk quad models. If we turn the square into a diamond, we obtain additional room for longer insets. This move permits a smaller loop size.

Fig. 4-5 shows the general scheme of the diamond version of the shrunk quad. The sides are about 6.36' long. For this antenna, the loop dimensions for both the driver and the reflector were held equal, with all adjustments made to the insets. The following model descriptions provide the coordinates for both 0.125 λ and 0.145 λ versions of the antenna design.



2L dia 6.36'/side 4.31 sp linear load Frequency = 28.5 MHz.

Wire Loss: Copper -- Resistivity = 1.74E-08 ohm-m, Rel. Perm. = 1

----- WIRES -----

Wire Conn.---		End 1 (x,y,z : ft)			Conn.---		End 2 (x,y,z : ft)			Dia(in)		Segs	
1	W1E2	0.300,	0.000,	-4.500	W2E1	4.500,	0.000,	-0.125		# 14		21	
2	W1E2	4.500,	0.000,	-0.125	W3E1	0.860,	0.000,	-0.125		# 14		21	

3	W2E2	0.860,	0.000,	-0.125	W4E1	0.860,	0.000,	0.125	# 14	1
4	W3E2	0.860,	0.000,	0.125	W5E1	4.500,	0.000,	0.125	# 14	21
5	W4E2	4.500,	0.000,	0.125	W6E1	0.000,	0.000,	4.500	# 14	21
6	W5E2	0.000,	0.000,	4.500	W7E1	-4.500,	0.000,	0.125	# 14	21
7	W6E2	-4.500,	0.000,	0.125	W8E1	-0.860,	0.000,	0.125	# 14	21
8	W7E2	-0.860,	0.000,	0.125	W9E1	-0.860,	0.000,	-0.125	# 14	1
9	W8E2	-0.860,	0.000,	-0.125	W10E1	-4.500,	0.000,	-0.125	# 14	21
10	W9E2	-4.500,	0.000,	-0.125	W11E1	-0.300,	0.000,	-4.500	# 14	21
11	W10E2	-0.300,	0.000,	-4.500	W1E1	0.300,	0.000,	-4.500	# 14	3
12	W21E2	0.000,	-4.310,	-4.500	W13E1	4.500,	-4.310,	-0.125	# 14	21
13	W12E2	4.500,	-4.310,	-0.125	W14E1	0.430,	-4.310,	-0.125	# 14	21
14	W13E2	0.430,	-4.310,	-0.125	W15E1	0.430,	-4.310,	0.125	# 14	1
15	W14E2	0.430,	-4.310,	0.125	W16E1	4.500,	-4.310,	0.125	# 14	21
16	W15E2	4.500,	-4.310,	0.125	W17E1	0.000,	-4.310,	4.500	# 14	21
17	W16E2	0.000,	-4.310,	4.500	W18E1	-4.500,	-4.310,	0.125	# 14	21
18	W17E2	-4.500,	-4.310,	0.125	W19E1	-0.430,	-4.310,	0.125	# 14	21
19	W18E2	-0.430,	-4.310,	0.125	W20E1	-0.430,	-4.310,	-0.125	# 14	1
20	W19E2	-0.430,	-4.310,	-0.125	W21E1	-4.500,	-4.310,	-0.125	# 14	21
21	W20E2	-4.500,	-4.310,	-0.125	W12E1	0.000,	-4.310,	-4.500	# 14	21

----- SOURCES -----

Source	Wire Seg.	Wire #/Pct Actual	From End 1 (Specified)	Ampl.(V, A)	Phase(Deg.)	Type
1	2	11 / 50.00	(11 / 50.00)	1.000	0.000	I

.....

2L dia 6.36/side 5.0 sp linear load Frequency = 28.5 MHz.

Wire Loss: Copper -- Resistivity = 1.74E-08 ohm-m, Rel. Perm. = 1

----- WIRES -----

Wire	Conn.---	End 1 (x,y,z : ft)	Conn.---	End 2 (x,y,z : ft)	Dia(in)	Segs
1	W11E2	0.300, 0.000, -4.500	W2E1	4.500, 0.000, -0.125	# 14	21
2	W1E2	4.500, 0.000, -0.125	W3E1	0.770, 0.000, -0.125	# 14	21
3	W2E2	0.770, 0.000, -0.125	W4E1	0.770, 0.000, 0.125	# 14	1
4	W3E2	0.770, 0.000, 0.125	W5E1	4.500, 0.000, 0.125	# 14	21
5	W4E2	4.500, 0.000, 0.125	W6E1	0.000, 0.000, 4.500	# 14	21
6	W5E2	0.000, 0.000, 4.500	W7E1	-4.500, 0.000, 0.125	# 14	21
7	W6E2	-4.500, 0.000, 0.125	W8E1	-0.770, 0.000, 0.125	# 14	21
8	W7E2	-0.770, 0.000, 0.125	W9E1	-0.770, 0.000, -0.125	# 14	1
9	W8E2	-0.770, 0.000, -0.125	W10E1	-4.500, 0.000, -0.125	# 14	21
10	W9E2	-4.500, 0.000, -0.125	W11E1	-0.300, 0.000, -4.500	# 14	21
11	W10E2	-0.300, 0.000, -4.500	W1E1	0.300, 0.000, -4.500	# 14	3
12	W21E2	0.000, -5.000, -4.500	W13E1	4.500, -5.000, -0.125	# 14	21
13	W12E2	4.500, -5.000, -0.125	W14E1	0.400, -5.000, -0.125	# 14	21
14	W13E2	0.400, -5.000, -0.125	W15E1	0.400, -5.000, 0.125	# 14	1
15	W14E2	0.400, -5.000, 0.125	W16E1	4.500, -5.000, 0.125	# 14	21
16	W15E2	4.500, -5.000, 0.125	W17E1	0.000, -5.000, 4.500	# 14	21
17	W16E2	0.000, -5.000, 4.500	W18E1	-4.500, -5.000, 0.125	# 14	21
18	W17E2	-4.500, -5.000, 0.125	W19E1	-0.400, -5.000, 0.125	# 14	21
19	W18E2	-0.400, -5.000, 0.125	W20E1	-0.400, -5.000, -0.125	# 14	1
20	W19E2	-0.400, -5.000, -0.125	W21E1	-4.500, -5.000, -0.125	# 14	21
21	W20E2	-4.500, -5.000, -0.125	W12E1	0.000, -5.000, -4.500	# 14	21

----- SOURCES -----

Chapter 4 ~ Shrunk 2-Element Quads

Source	Wire Seg.	Wire #/Pct Actual	From End 1 (Specified)	Ampl.(V, A)	Phase(Deg.)	Type
1	2	11 / 50.00	(11 / 50.00)	1.000	0.000	I

For both models, the source is placed on a special wire on the center of its three segments. For reference, **Table 4-2** gives the design frequency performance figures for the two models:

Table 4-2. Performance Figures for 2 72% Shrunkn Quads

Antenna Version	Free Space Gain dBi	Front-to-Back Ratio dB	Feedpoint Impedance R +/- jX Ohms
0.125 λ	6.14	12.6	82 + j 0
0.145 λ	6.24	16.6	86 - j 3

In accord with our natural expectations, the additional shrinkage (6%) of the diamond relative to the square results in a further reduction in gain—all relative to the full-size 2-element quads that we explored in the preceding chapters. How operationally significant the gain reduction is must be measured by potential users against the total package of operational criteria. This note, of course, applies to the evaluation of performance figures for any antenna whatsoever.

Diamond Side-Loaded 2-Element Quads
Gain vs. Element Spacing

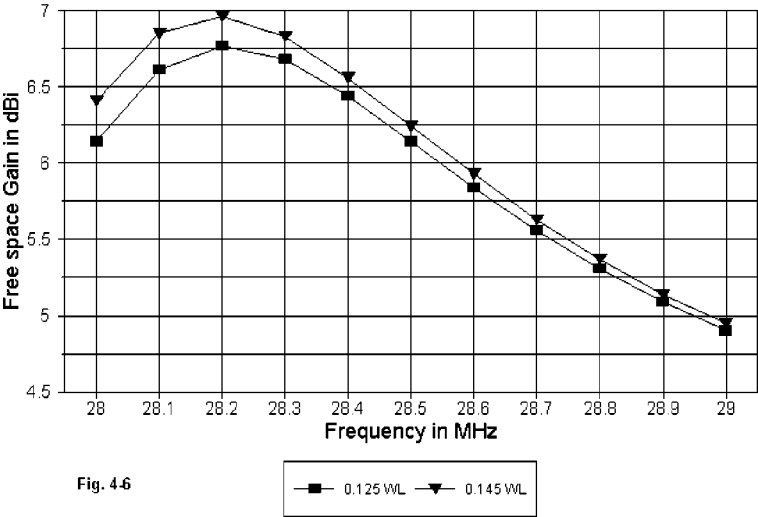


Fig. 4-6

As **Fig. 4-6** shows, the wide spaced version shows a bit more gain than the narrower spaced version. More notable is the fact that the further shrinkage of the design has moved the gain peak farther into the passband. The lower band edge gain is now significantly lower than the peak gain. Compare **Fig. 4-6** to **Fig. 4-2**.

Diamond Side-Loaded 2-Element Quads
F-B Ratio vs. Element Spacing

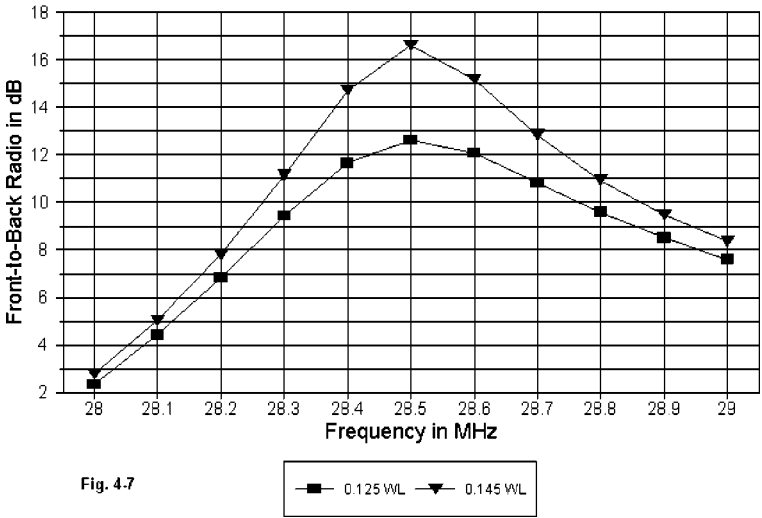


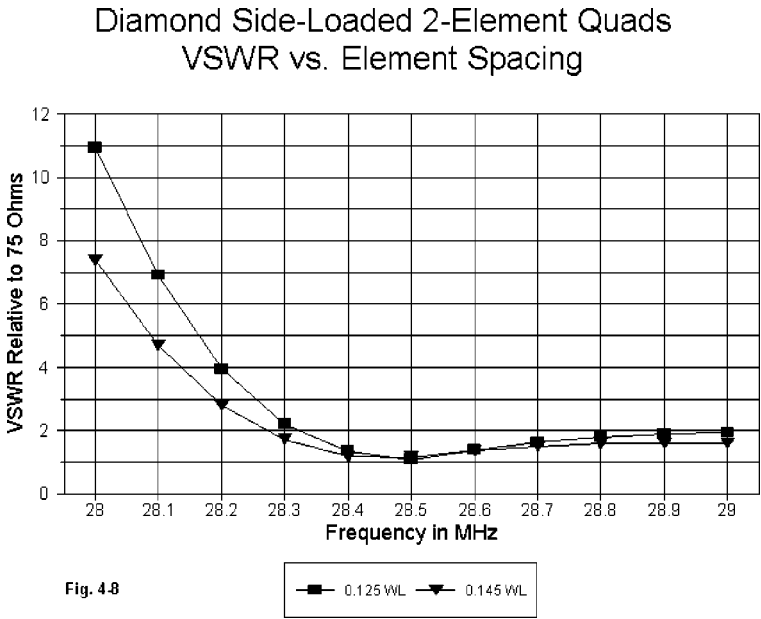
Fig. 4-7

The front-to-back curves for the 72% diamond, shown in **Fig. 4-7**, reveal about the same differential between versions as those for the 78% square. (Remember to compare these curves with comparable spaced full-size 2-element quads featured in the two preceding chapters.) However, the rate of fall-off from the peak front-to-back value is much faster. Although the values given are for the 180E front-to-back ratio, they are indicative of overall rear quadrant performance. As the size of the quad continues to shrink, it becomes more important to move the peak front-to-back ratio down the band. Indeed, it is true for any reduced-size array that, as the operating bandwidth narrows, tailoring the performance to the portion of the band most needed becomes a necessary part of the design process.

As one might expect, the SWR curves in **Fig. 4-8** are much steeper below the resonant frequency than for the square. Once more, judicious movement of resonance to a point lower in the band can provide a wider operating

bandwidth using the usual 2:1 SWR ratio as a guide.

Indeed, by appropriate tweaking, one can so position the resonant point and the front-to-back peak to increase the peak front-to-back value significantly. However, that move must be balanced against the front-to-back performance across the passband. A sharper peak may not always result in higher values at the passband edges.



The diamond configuration offers some structural advantages over the square. Perhaps the key benefit of using the diamond is that the insets can be run along the horizontal support arms. With the judicious use of spacers attached to the arm, the insets can be set in a very stable position, thus reducing motion in the wind and consequential detuning of the array.

Whatever the construction method used, it is usually wise to anchor the insets to the boom or the hub with strong non-conductive cording. Of course, observe the usual precautions of using materials that are UV-resistant or UV-protected. As well, use materials that resist stretching after a rain shower.

8	W7E2	0.580,	0.000,	0.125	W9E1	0.580,	0.000,	0.375	# 14	1
9	W8E2	0.580,	0.000,	0.375	W10E1	3.000,	0.000,	0.375	# 14	19
10	W9E2	3.000,	0.000,	0.375	W11E1	3.000,	0.000,	3.000	# 14	10
11	W10E2	3.000,	0.000,	3.000	W12E1	-3.000,	0.000,	3.000	# 14	21
12	W11E2	-3.000,	0.000,	3.000	W13E1	-3.000,	0.000,	0.375	# 14	10
13	W12E2	-3.000,	0.000,	0.375	W14E1	-0.580,	0.000,	0.375	# 14	19
14	W13E2	-0.580,	0.000,	0.375	W15E1	-0.580,	0.000,	0.125	# 14	1
15	W14E2	-0.580,	0.000,	0.125	W16E1	-3.000,	0.000,	0.125	# 14	19
16	W15E2	-3.000,	0.000,	0.125	W17E1	-3.000,	0.000,	-0.125	# 14	1
17	W16E2	-3.000,	0.000,	-0.125	W18E1	-0.580,	0.000,	-0.125	# 14	19
18	W17E2	-0.580,	0.000,	-0.125	W19E1	-0.580,	0.000,	-0.375	# 14	1
19	W18E2	-0.580,	0.000,	-0.375	W20E1	-3.000,	0.000,	-0.375	# 14	19
20	W19E2	-3.000,	0.000,	-0.375	W1E1	-3.000,	0.000,	-3.000	# 14	10
21	W40E2	-3.000,	-4.310,	-3.000	W22E1	3.000,	-4.310,	-3.000	# 14	21
22	W21E2	3.000,	-4.310,	-3.000	W23E1	3.000,	-4.310,	-0.375	# 14	10
23	W22E2	3.000,	-4.310,	-0.375	W24E1	0.425,	-4.310,	-0.375	# 14	19
24	W23E2	0.425,	-4.310,	-0.375	W25E1	0.425,	-4.310,	-0.125	# 14	1
25	W24E2	0.425,	-4.310,	-0.125	W26E1	3.000,	-4.310,	-0.125	# 14	19
26	W25E2	3.000,	-4.310,	-0.125	W27E1	3.000,	-4.310,	0.125	# 14	1
27	W26E2	3.000,	-4.310,	0.125	W28E1	0.425,	-4.310,	0.125	# 14	19
28	W27E2	0.425,	-4.310,	0.125	W29E1	0.425,	-4.310,	0.375	# 14	1
29	W28E2	0.425,	-4.310,	0.375	W30E1	3.000,	-4.310,	0.375	# 14	19
30	W29E2	3.000,	-4.310,	0.375	W31E1	3.000,	-4.310,	3.000	# 14	10
31	W30E2	3.000,	-4.310,	3.000	W32E1	-3.000,	-4.310,	3.000	# 14	21
32	W31E2	-3.000,	-4.310,	3.000	W33E1	-3.000,	-4.310,	0.375	# 14	10
33	W32E2	-3.000,	-4.310,	0.375	W34E1	-0.425,	-4.310,	0.375	# 14	19
34	W33E2	-0.425,	-4.310,	0.375	W35E1	-0.425,	-4.310,	0.125	# 14	1
35	W34E2	-0.425,	-4.310,	0.125	W36E1	-3.000,	-4.310,	0.125	# 14	19
36	W35E2	-3.000,	-4.310,	0.125	W37E1	-3.000,	-4.310,	-0.125	# 14	1
37	W36E2	-3.000,	-4.310,	-0.125	W38E1	-0.425,	-4.310,	-0.125	# 14	19
38	W37E2	-0.425,	-4.310,	-0.125	W39E1	-0.425,	-4.310,	-0.375	# 14	1
39	W38E2	-0.425,	-4.310,	-0.375	W40E1	-3.000,	-4.310,	-0.375	# 14	19
40	W39E2	-3.000,	-4.310,	-0.375	W21E1	-3.000,	-4.310,	-3.000	# 14	10

----- SOURCES -----

Source	Wire Seg.	Wire #/Pct Actual	From End 1 (Specified)	Ampl.(V, A)	Phase(Deg.)	Type
1	11	1 / 50.00	(1 / 50.00)	1.000	0.000	I

The more numerous the insets, the higher the number of wires in a model. For those used to modeling antennas with simple geometries, the model size in terms of both wires and segments may seem high. The relatively thin wire (#14 AWG) allows the use of short segment lengths. For NEC models, the segment junctions should align as closely as possible wherever there are closely spaced wires. This is especially important in the insets.

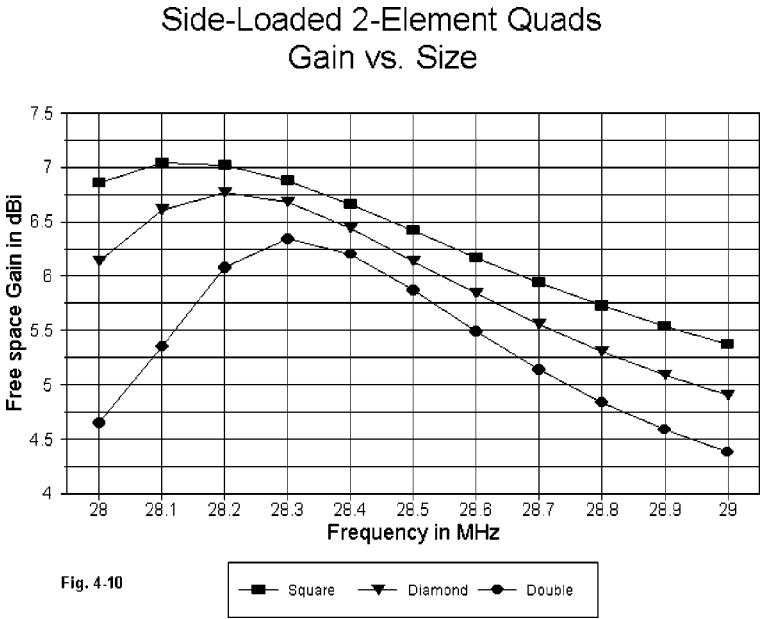
Table 4-3 provides the performance figures at the design frequency for the 68% double-inset square for an element spacing of 0.125λ . Also in the table are comparative figures for the single-inset diamond and square, using the same element spacing. The progression of the figures can provide a general set of expectations for shrinkage of performance with shrinkage of antenna size. However, it is well to remember that these figures are for the

design frequency and represent peak performance values. They give no clue to the operating bandwidth of the antenna.

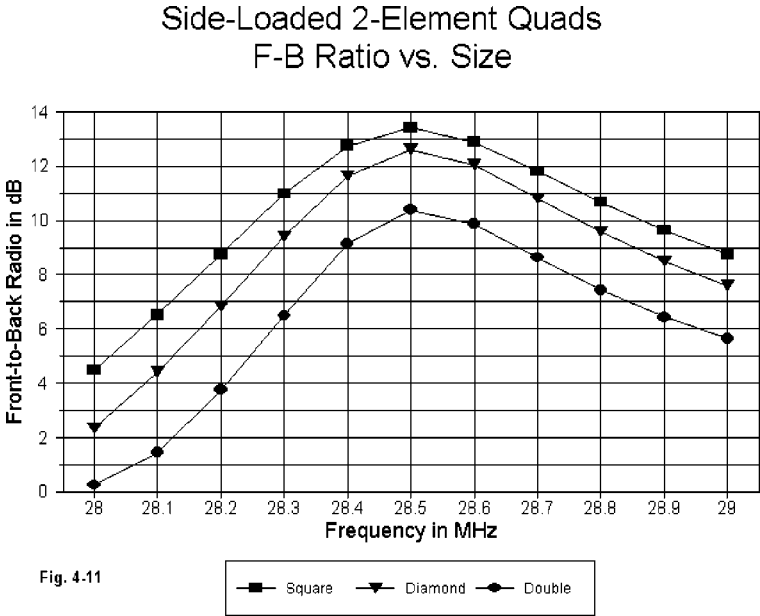
Table 4-3. Comparative Peak Performance of 3 Shrunk Quad Models

Antenna Version	Free Space Gain dBi	Front-to-Back Ratio dB	Feedpoint Impedance R +/- jX Ohms
68% square	5.87	10.4	58 - j 0
72% diamond	6.14	12.6	82 + j 0
78% square	6.42	13.4	76 - j 1

The following graphs will provide similar comparisons across the pass-band.



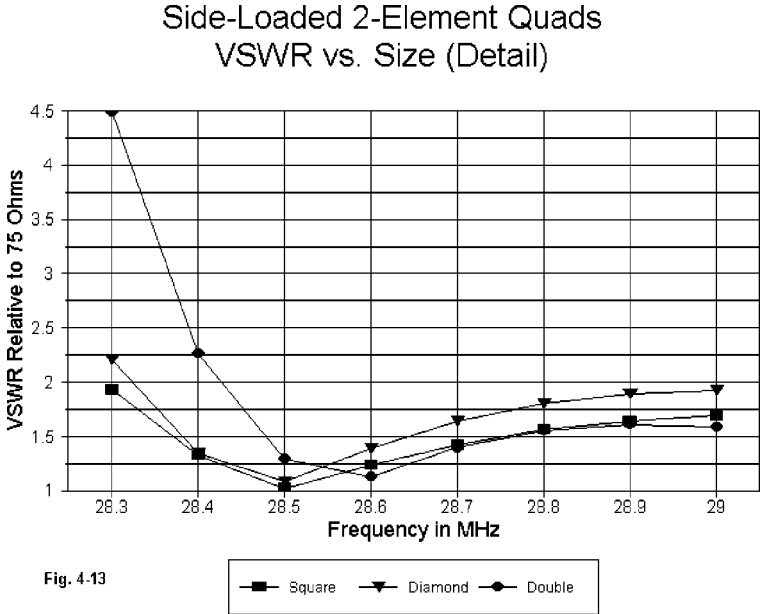
The gain curves in **Fig. 4-10** show how the gain peak moves more radically toward the design frequency with each reduction in antenna size. Also worth noting is the steeper rate of gain fall-off in the smaller quads in this collection of models.



When antenna resonance and peak front-to-back ratio are designed for the same frequency, the curves for all three models are exceptionally congruent, as shown in **Fig. 4-11**. Note that the front-to-back ratio is almost non-existent at the lower end of the band for the smallest model.

Fig. 4-12 shows the 75-Ohm SWR curve for the three antennas across the entire first MHz of 10 meters. Besides showing how steep the low end curve is for the 68% square, the graphic actually obscures some interesting properties of the antenna. Therefore, let's eliminate the highest values of SWR.

In **Fig. 4-13**, we obtain a clearer picture of the impedance behavior of the smallest quad, relative to its larger single-inset brethren. The lowest SWR occurs close to 28.6 MHz because the resonant impedance of the antenna is below 60 Ohms. However, note the shape of the curve as it moves toward the upper end of the band. The SWR actually decreases by the time we reach 29 MHz. It would be very easy during antenna adjustment to deceive oneself into thinking that all is well by obtaining a relatively flat SWR curve. Looking at this curve alone can obscure the fairly narrow passband for usable gain and front-to-back ratio of this small antenna.

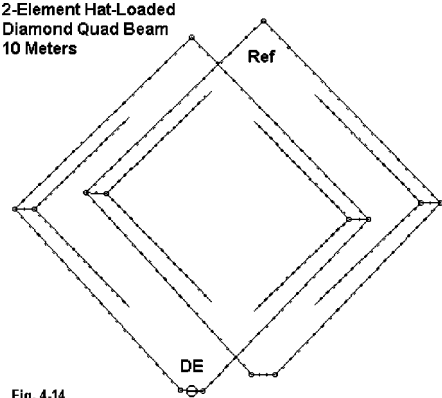


The 72% Hat-Loaded Diamond

I first ran into the hat-loaded design in *HF Antennas for All Locations* by Les Moxon, G6XN. My interest in the design was to compare the performance of a hat-loaded antenna to an inset-loaded version.

Fig. 4-14 shows the general outline of a diamond version of the hat-loaded quad beam. Square versions are also easily possible, although the diamond allows the hat wires to be somewhat longer.

A perfect hat would extend outside the loop at the side junction and have two wires exactly end-to-end for relatively perfect radiation cancellation. Placing them inside the loop makes construction easier, since they can be suspended from the normal loop wires. The exact lengths of the wires will vary with their spacing from the loop wires.



For the purposes of comparison, the hat model was made from the 72% diamond, using 5' element separation (0.145 λ). At the original inset position, the loop was closed and the hat structure added. The following model description will provide guidance for the coordinates used.

```
2L dia 6.36/side 5.0 hat load                      Frequency = 28.5  MHz.

Wire Loss: Copper -- Resistivity = 1.74E-08 ohm-m, Rel. Perm. = 1

----- WIRES -----

Wire Conn.--- End 1 (x,y,z : ft)  Conn.--- End 2 (x,y,z : ft)  Dia(in) Segs

1  W11E2  0.300,  0.000, -4.500  W2E1   4.500,  0.000,  0.000  # 14  21
2   W3E1  4.500,  0.000,  0.000  W6E1   0.000,  0.000,  4.500  # 14  21
3   W1E2  4.500,  0.000,  0.000  W4E1   4.000,  0.000,  0.000  # 14   2
4   W5E1  4.000,  0.000,  0.000          1.589,  0.000,  2.411  # 14  17
5   W3E2  4.000,  0.000,  0.000          1.589,  0.000, -2.411  # 14  17
6   W2E2  0.000,  0.000,  4.500  W7E1  -4.500,  0.000,  0.000  # 14  21
7  W10E1 -4.500,  0.000,  0.000  W8E1  -4.000,  0.000,  0.000  # 14   2
8   W9E1 -4.000,  0.000,  0.000          -1.589,  0.000,  2.411  # 14  17
9   W7E2 -4.000,  0.000,  0.000          -1.589,  0.000, -2.411  # 14  17
10  W6E2 -4.500,  0.000,  0.000 W11E1  -0.300,  0.000, -4.500  # 14  21
11 W10E2 -0.300,  0.000, -4.500 W1E1   0.300,  0.000, -4.500  # 14   3
12 W22E2  0.300, -5.000, -4.500 W13E1  4.500, -5.000,  0.000  # 14  21
13 W14E1  4.500, -5.000,  0.000 W17E1  0.000, -5.000,  4.500  # 14  21
14 W12E2  4.500, -5.000,  0.000 W15E1  4.000, -5.000,  0.000  # 14   2
15 W16E1  4.000, -5.000,  0.000          1.324, -5.000,  2.676  # 14  17
16 W14E2  4.000, -5.000,  0.000          1.324, -5.000, -2.676  # 14  17
17 W13E2  0.000, -5.000,  4.500 W18E1 -4.500, -5.000,  0.000  # 14  21
18 W21E1 -4.500, -5.000,  0.000 W19E1 -4.000, -5.000,  0.000  # 14   2
19 W20E1 -4.000, -5.000,  0.000          -1.324, -5.000,  2.676  # 14  17
20 W18E2 -4.000, -5.000,  0.000          -1.324, -5.000, -2.676  # 14  17
21 W17E2 -4.500, -5.000,  0.000 W22E1  -0.300, -5.000, -4.500  # 14  21
22 W21E2 -0.300, -5.000, -4.500 W12E1  0.300, -5.000, -4.500  # 14   3

----- SOURCES -----

Source      Wire      Wire #/Pct From End 1      Ampl.(V, A)  Phase(Deg.)  Type
            Seg.      Actual      (Specified)

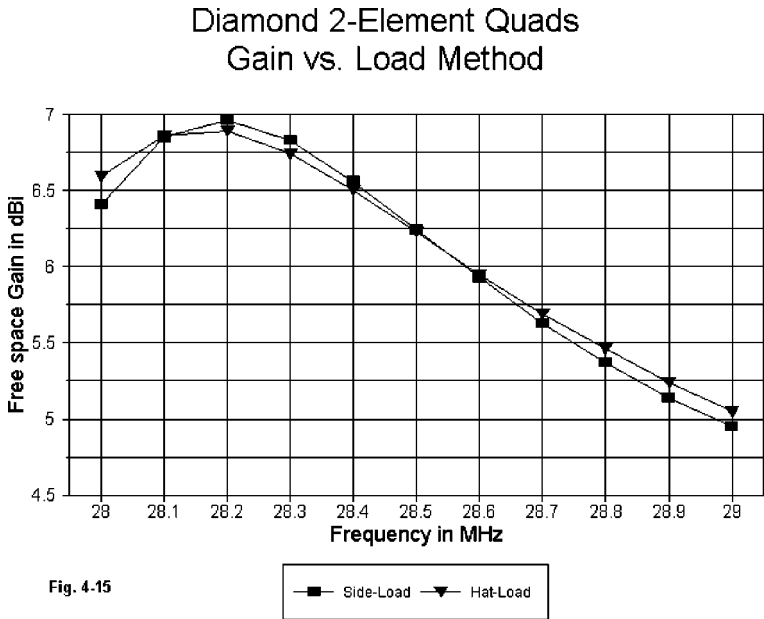
1           2       11 / 50.00    ( 11 / 50.00)      1.000        0.000        I
```

The feedpoint is the same as for the single-inset diamond model. For reference, **Table 4-4** lists the design frequency performance numbers for the two 5'-spaced models.

Table 4-4. Performance Values for 72% 2 Diamond Quads			
Antenna Version	Free Space Gain dBi	Front-to-Back Ratio dB	Feedpoint Impedance R +/- jX Ohms
diamond inset	6.24	16.6	86 - j 3
diamond hat	6.23	18.4	93 + j 0

The gain curves in **Fig. 4-15** show a remarkable coincidence, given the physical differences in the load designs. There is nothing to choose between loads in this department. Indeed, the gain curve suggests that there appears to be little to recommend one form of element end loading over another, since both essentially are ways to add sufficient wire to the element to obtain resonance without contributing significantly to the overall radiation from the antenna. However, before reaching such a conclusion, one should examine all important aspects of performance for proposed arrays.

As the subsequent front-to-back and SWR curves will show, there may be certain advantages to one geometric configuration over another. There may be variations in the peak front-to-back ratio or in the SWR curve that stem from the proximity of the “loading” wires to the main portions of the radiating element. Even though the current level on the end portions of the element is low, it does not go to zero. As a result, the positions of the end wires to the main wires—along with the relative current magnitudes and phases of currents on each of them—become in some cases significant design fac-



tors.

As shown in **Fig. 4-16**, the hat model shows about a full dB or slightly

greater advantage in average front-to-back performance (apart from the higher difference in peak value). This amount of added front-to-back ratio would scarcely be noticeable in operation. Moreover, it is not clear that the inset model might not be tweakable to obtain a similar set of values (or the hat model “de-tweaked” by intention or accident to obtain the inset curve).

Nonetheless, the hat model does appear to have an advantage in the front-to-back category of performance. However, the difference may be small enough that construction considerations might easily override it.

Diamond 2-Element Quads F-B Ratio vs. Load Method

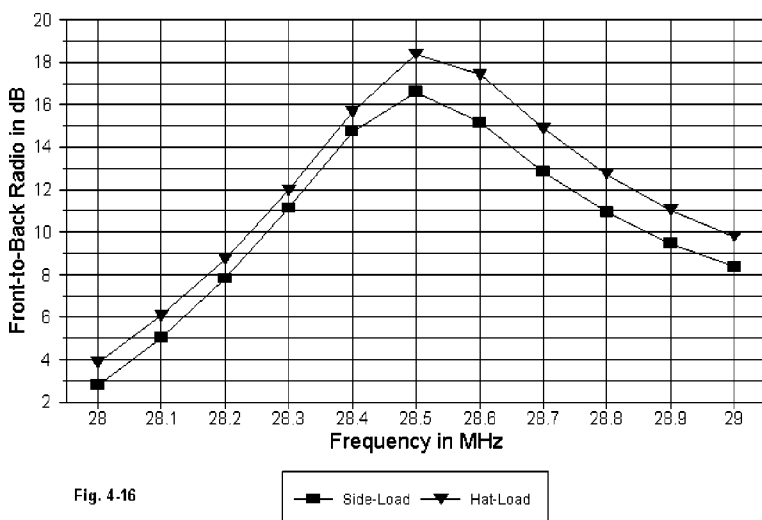


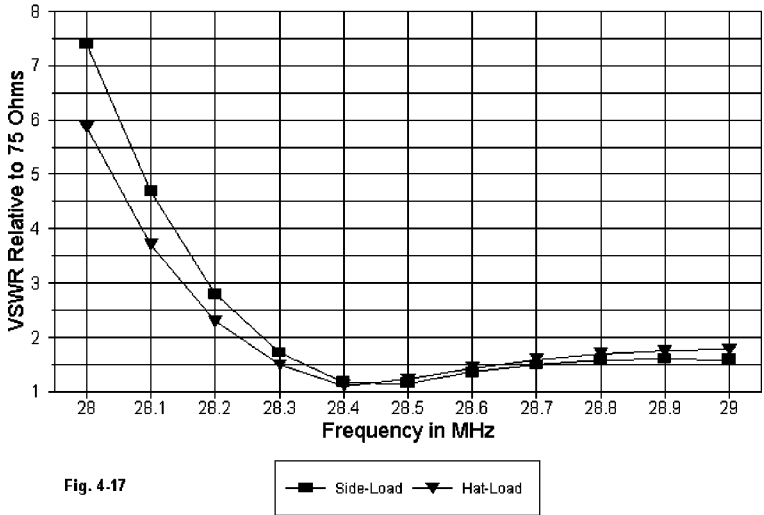
Fig. 4-16

The SWR curves in **Fig. 4-17** show differences partly as a result of the higher resonant impedance of the hat model. (The resistive portion of the source impedance for all of the antennas we have examined drops to 30 Ohms or less at the lower band edge—28 MHz.) Judicious resonance movement would yield an operating bandwidth that covered most of the first MHz of 10 meters.

As we have seen with the other models of shrunken quads, merely moving the operating point to obtain a low SWR does not itself guarantee that we shall obtain significant gain of front-to-back ratio from an array. Unless one has an antenna of known characteristics with which to compare performance, it may be difficult to assess an antenna like the shrunken quad in casual

operation. Indeed, if one is moving from a simple dipole or other doublet to the shrunken quad with its operating point set to give the widest SWR bandwidth, the apparent signal strength gain and semblance of rearward signal

Diamond 2-Element Quads
VSWR vs. Load Method

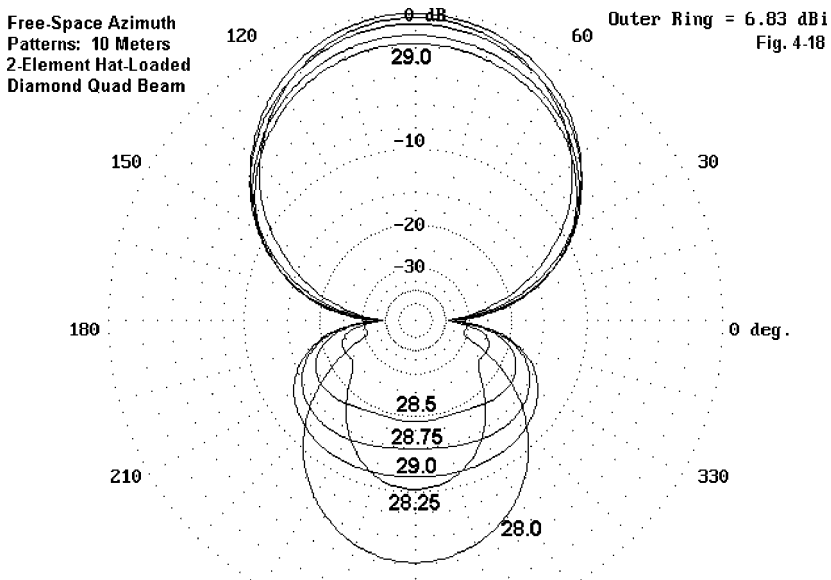


rejection may seem better than measurement would confirm.

Lest we once more fall into the lethargy that equates performance with the SWR curve, let's close with a gallery of azimuth patterns across the pass-band for the hatted model. It is an effective compromise between the large and the small square, as well as being virtually identical to the patterns of the 5' spaced inset diamond. **Fig. 4-18** summarizes the performance characteristics of the category of shrunken quads in the versions we have examined here.

Trying to cover all of the varieties of schemes used to miniaturize quad beams would be prohibitive in terms of both time and space. The models we have looked at have maintained reasonable efficiency and minimized losses in their means of shrinking the quad. The effects of both loop size and of element spacing have been sampled as a guide to further modeling (not to mention building). My own building of some of them suggests that they will perform to modeled specifications. The shrunken quad, then, provides a

useful antenna for limited space installations, especially if one does not need full performance coverage of an entire band. Adaptations of these designs



may also prove useful in the smaller non-harmonic (WARC) bands.

The one feature missing from these shrunken quads is the ability to nest antennas of this design to produce a multi-band array. Indeed, the full size 2-element quad remains the chief vehicle for this type of service. In the next chapter, we shall survey some of the multi-band 2-element quads in my files.

5. Multi-Band 2-Element Quad Beams

One of the advantages of the full-size quad is that one can nest the beam within or around others to form a multi-band HF array of very respectable performance. The total real estate involved is no larger than that required by the largest beam of the group--normally a 20 meter array for upper HF applications.

It is possible to model (or design) 5-band quads with about 400 total segments. In past years, the run time for such a model on a PC would have been fairly taxing, especially for frequency sweeps on each of the bands covered by the antenna. Computer speed has sliced the time to the barely noticeable. The major time is now spent on constructing the model.

My own collection of 2-element 5-band models is somewhat limited, containing just four different types (and a host of variations on them). However, each may be worth a separate look, since each has some distinctive features.

A Spider Quad with 0.125λ Element Spacing

Although the term “spider” is sometimes used to label any hub device that holds the supports for quad elements, its best use is to label those 8-legged hubs that hold all of the supports for a multi-band 2-element beam. One feature of quads constructed by this method is that the element spacing between the driver and the reflector is constant in terms of wavelengths. Whether this is an advantage, we shall see along the way.

The first model originated as simply a study item, designed to look at the question of whether multi-band quads should be fed in common or with separate lines for each driver and with the unused driver loops closed. Throughout these notes, I have chosen the latter option for clarity within the models.

The study began with separate 2-element quad models for each of the 5 upper HF amateur bands. To refresh our memories, I shall import a small table (**Table 5-1**) from the Chapter 2. L means side length, and C means loop circumference.

Table 5-1. Dimensions for 0.125 λ Spaced Monoband Quad Beams

Frequency MHz	Spacing feet	L Driver feet	C Driver feet	L Refl. feet	C Refl. feet	Segments per side
28.5	4.31	8.66	34.64	9.16	36.64	7
24.94	4.93	9.91	39.62	10.47	41.86	9
21.22	5.79	11.64	46.56	12.26	49.04	11
18.12	6.79	13.62	54.48	14.35	57.40	13
14.17	8.68	17.42	69.68	18.30	73.20	15

When combined, the required dimensional changes to achieve resonance and peak front-to-back performance at the design frequency for each band show up in **Table 5-2** for the 5-band quad array.

Table 5-2. Dimensions for 0.125 λ Spaced 5-Band Quad Beam

Frequency MHz	Spacing feet	L Driver feet	C Driver feet	L Refl. feet	C Refl. feet	Segments per side
28.5	4.31	8.64	34.56	9.20	36.80	7
24.94	4.93	9.90	39.60	10.20	40.80	9
21.22	5.79	11.63	46.52	12.06	48.24	11
18.12	6.79	13.66	54.64	14.06	56.24	13
14.17	8.68	17.50	70.00	18.06	72.24	15

The reason for using the indicated number of segments per side in the independent quads should be clear. In the combined quad, the segmentation was selected to have--to the degree feasible--identical segment lengths throughout and segment junctions that aligned from one loop to the next.

The element spacing of this first model is 0.125 λ, resulting in the proportions shown in **Fig. 5-1**. Each loop is full size, with no loading. As with the monoband models, the design called for resonance at each band center and, insofar as possible, the peak front-to-back ratio at the same frequency. It should be clear that there is from the start of design work some interaction among the elements when configured as a multi-band array. Although the changes to the driver elements are very small, the required revision of reflector loops is greater. Notice especially that virtually all of the loops

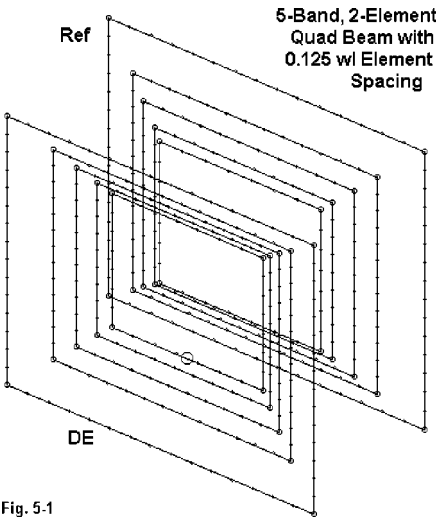


Fig. 5-1

grow larger except for the 20-meter reflector, which must be smaller relative to the monoband models. Of course, the 20-meter reflector is the only loop without a larger loop within the near field of the array.

In case someone would like to replicate the 5-band model, an EZNEC description follows. It is feasible to extract the description as an ASCII document and to modify it to fit the formats required by other programs that use input files in ASCII format. Although many format changes are required, number-entry typing errors are eliminated by this procedure. As with all antenna models, the user is invited to try as many variations as desired on the basic model presented.

5-band quad: 1/8 wl sp

Frequency = 28.5 MHz.

Wire Loss: Copper -- Resistivity = 1.74E-08 ohm-m, Rel. Perm. = 1

----- WIRES -----

Wire Conn.--- End 1 (x,y,z : ft) Conn.--- End 2 (x,y,z : ft) Dia(in) Segs

1	W4E2	-4.320,	2.155,	-4.320	W2E1	4.320,	2.155,	-4.320	# 14	7
2	W1E2	4.320,	2.155,	-4.320	W3E1	4.320,	2.155,	4.320	# 14	7
3	W2E2	4.320,	2.155,	4.320	W4E1	-4.320,	2.155,	4.320	# 14	7
4	W3E2	-4.320,	2.155,	4.320	W1E1	-4.320,	2.155,	-4.320	# 14	7
5	W8E2	-4.600,	-2.155,	-4.600	W6E1	4.600,	-2.155,	-4.600	# 14	7
6	W5E2	4.600,	-2.155,	-4.600	W7E1	4.600,	-2.155,	4.600	# 14	7
7	W6E2	4.600,	-2.155,	4.600	W8E1	-4.600,	-2.155,	4.600	# 14	7
8	W7E2	-4.600,	-2.155,	4.600	W5E1	-4.600,	-2.155,	-4.600	# 14	7
9	W12E2	-5.815,	2.897,	-5.815	W10E1	5.815,	2.897,	-5.815	# 14	11
10	W9E2	5.815,	2.897,	-5.815	W11E1	5.815,	2.897,	5.815	# 14	11
11	W10E2	5.815,	2.897,	5.815	W12E1	-5.815,	2.897,	5.815	# 14	11
12	W11E2	-5.815,	2.897,	5.815	W9E1	-5.815,	2.897,	-5.815	# 14	11
13	W16E2	-6.030,	-2.897,	-6.030	W14E1	6.030,	-2.897,	-6.030	# 14	11
14	W13E2	6.030,	-2.897,	-6.030	W15E1	6.030,	-2.897,	6.030	# 14	11
15	W14E2	6.030,	-2.897,	6.030	W16E1	-6.030,	-2.897,	6.030	# 14	11
16	W15E2	-6.030,	-2.897,	6.030	W13E1	-6.030,	-2.897,	-6.030	# 14	11
17	W20E2	-8.750,	4.334,	-8.750	W18E1	8.750,	4.334,	-8.750	# 14	15
18	W17E2	8.750,	4.334,	-8.750	W19E1	8.750,	4.334,	8.750	# 14	15
19	W18E2	8.750,	4.334,	8.750	W20E1	-8.750,	4.334,	8.750	# 14	15
20	W19E2	-8.750,	4.334,	8.750	W17E1	-8.750,	4.334,	-8.750	# 14	15
21	W24E2	-9.030,	-4.334,	-9.030	W22E1	9.030,	-4.334,	-9.030	# 14	15
22	W21E2	9.030,	-4.334,	-9.030	W23E1	9.030,	-4.334,	9.030	# 14	15
23	W22E2	9.030,	-4.334,	9.030	W24E1	-9.030,	-4.334,	9.030	# 14	15
24	W23E2	-9.030,	-4.334,	9.030	W21E1	-9.030,	-4.334,	-9.030	# 14	15
25	W28E2	-4.950,	2.465,	-4.950	W26E1	4.950,	2.465,	-4.950	# 14	9
26	W25E2	4.950,	2.465,	-4.950	W27E1	4.950,	2.465,	4.950	# 14	9
27	W26E2	4.950,	2.465,	4.950	W28E1	-4.950,	2.465,	4.950	# 14	9
28	W27E2	-4.950,	2.465,	4.950	W25E1	-4.950,	2.465,	-4.950	# 14	9
29	W32E2	-5.100,	-2.465,	-5.100	W30E1	5.100,	-2.465,	-5.100	# 14	9
30	W29E2	5.100,	-2.465,	-5.100	W31E1	5.100,	-2.465,	5.100	# 14	9
31	W30E2	5.100,	-2.465,	5.100	W32E1	-5.100,	-2.465,	5.100	# 14	9
32	W31E2	-5.100,	-2.465,	5.100	W29E1	-5.100,	-2.465,	-5.100	# 14	9
33	W36E2	-6.830,	3.393,	-6.830	W34E1	6.830,	3.393,	-6.830	# 14	13
34	W33E2	6.830,	3.393,	-6.830	W35E1	6.830,	3.393,	6.830	# 14	13

35	W34E2	6.830,	3.393,	6.830	W36E1	-6.830,	3.393,	6.830	# 14	13
36	W35E2	-6.830,	3.393,	6.830	W33E1	-6.830,	3.393,	-6.830	# 14	13
37	W40E2	-7.030,	-3.393,	-7.030	W38E1	7.030,	-3.393,	-7.030	# 14	13
38	W37E2	7.030,	-3.393,	-7.030	W39E1	7.030,	-3.393,	7.030	# 14	13
39	W38E2	7.030,	-3.393,	7.030	W40E1	-7.030,	-3.393,	7.030	# 14	13
40	W39E2	-7.030,	-3.393,	7.030	W37E1	-7.030,	-3.393,	-7.030	# 14	13

----- SOURCES -----

Source	Wire Seg.	Wire #/Pct Actual	From End 1 (Specified)	Ampl.(V, A)	Phase(Deg.)	Type
1	4	1 / 50.00	(1 / 50.00)	1.000	0.000	V

All models continue to be in free space. This particular model grew in stages, going from a monoband antenna to a tribander to a full 5-band model. Hence, the wires are grouped in series of 8 each, with the bands in order being 10, 15, 20, 12, and 17. To test the performance on any band, change the source position to the center of the following wires for each band: 20 = wire 17; 17 = wire 33; 15 = wire 9; 12 = wire 25; and 10 = wire 1.

Since 12 and 17 meters are such narrow bands, graphing performance on them is a fruitless exercise in drawing straight lines across the page. The wider bands (10, 15, and 20) were graphed by running frequency sweeps that divided each band into 10 equal parts (resulting in 11 values). Hence, the graphs record steps from the bottom of the band. Each 20-meter step is 0.035 MHz; each 15-meter step is 0.045 MHz; and each 10-meter step is 0.1 MHz.

5-Band 2-Element Quad: 0.125 WL
Gain vs. Band

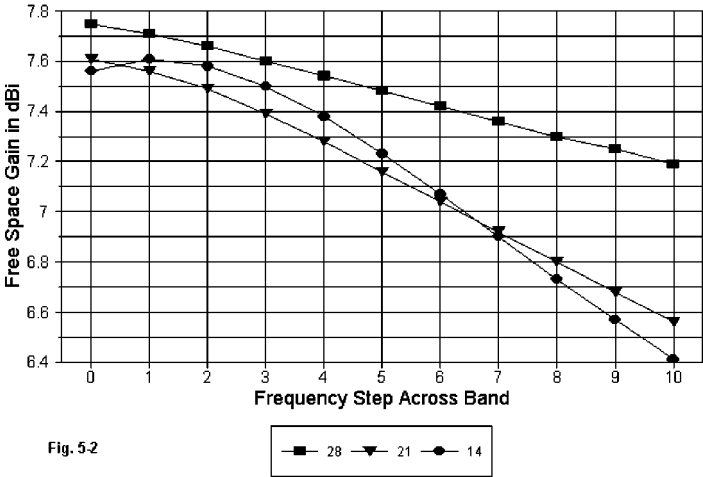


Fig. 5-2

The gain curves in **Fig. 5-2** show an interesting trend. Although the 10-meter band is wider than the other as a percentage of the center frequency, the gain holds up better on that band than on the lower bands. Indeed, the gain is higher than for the lower bands--higher even than the monoband version of the 10-meter quad.

For reference, **Table 5-3** lists the key performance figures for the independent quad beams at the center frequency for each band.

Table 5-3. Key Performance Figures for Monoband Quads

Frequency MHz	Free Space Gain dBi	Front-to-Back Ratio dB	Feedpoint Impedance R +/- jX Ohms
28.5	7.16	23.6	102 - j 1
24.95	7.11	23.9	105 + j 1
21.22	7.18	23.2	99 + j 2
18.12	7.14	23.7	101 - j 1
14.17	7.15	23.2	99 + j 0

For contrast, **Table 5-4** lists the performance of the combined beam at each band center.

Table 5-4. Key Performance Figures for the Multi-Band Quad

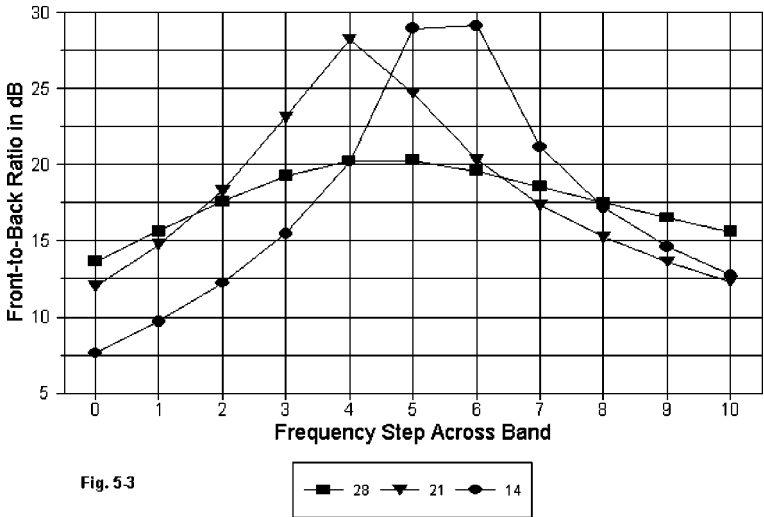
Frequency MHz	Free Space Gain dBi	Front-to-Back Ratio dB	Feedpoint Impedance R +/- jX Ohms
28.5	7.48	20.3	40 - j 0
24.95	7.16	24.7	42 + j 0
21.22	7.23	28.9	53 + j 0
18.12	7.32	25.8	61 - j 0
14.17	7.23	32.4	84 - j 0

As **Fig. 5-3** suggests, the front-to-back ratio is subject to very steep peaks on all but 10 meters. However, the band edge values resemble those of the monoband close-spaced quad beams--fairly low compared to mid-band values. In general, this close-spaced spider quad does not provide any improvement in front-to-rear performance relative to covering entire bands over monoband quads of similar spacing.

The source impedance values shown in the table are at considerable variance from those of the monoband quad beams, indicating a significant amount of interaction among elements. Those who are interested in the interactions will wish to examine the current tables for the supposedly inac-

tive elements in the quad. Even with separate feed for each band and the unused driver loops closed, there is considerable current on adjacent loops to the pair of primary concern for each band.

5-Band 2-Element Quad: 0.125 WL
Front-to-Back Ratio vs. Band



5-Band 2-Element Quad: 0.125 WL
VSWR vs. Band

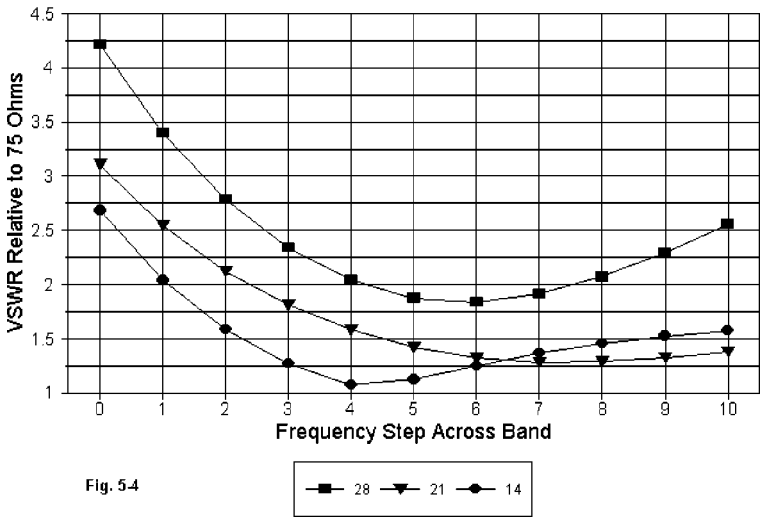


Fig. 5-4 shows the 75-Ohm SWR values for the 3 wide bands. Although this particular 5-band quad might well have been referenced to 50-Ohms, all of the others we shall examine more aptly use a 75-Ohm standard. Hence, the graph was made consistent with the others.

In fact, only the 10-meter curve is not movable to fit a 2:1 SWR bandwidth standard. Both the 15-meter and the 20-meter drivers can be adjusted to move their SWR curves. Note the leveling off of the 20-meter SWR above the band center, but also compare that phenomenon with the gain fall-off at the upper end of the band.

Although the constant spacing of the elements in terms of wavelengths seems to be an advantage in the abstract, that appearance fails to reckon with the complex interactions of the elements. The source impedance climbs from the innermost quad to the outermost, which can make matching a complex affair.

Moreover, the operating bandwidth of the close-spaced quad is somewhat narrow, suggesting that a wider spacing may be advantageous. So we may turn from this study model to something a little more versatile. For the moment, we shall stay with the spider construction that places the elements for each band a constant distance apart when measured in terms of a fraction of a wavelength.

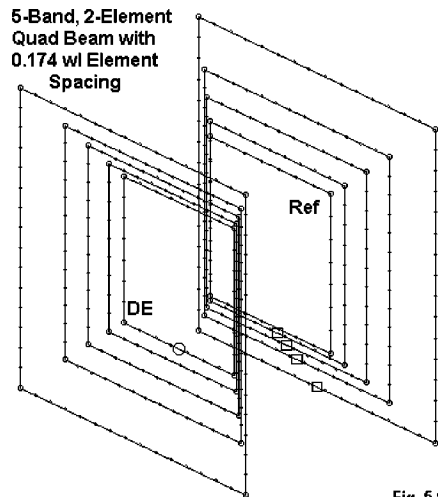


Fig. 5.5

A Spider Quad with 0.174λ Element Spacing and Capacitive Reflector Loading

One direction for overcoming some of the limitation of the close-spaced spider is to increase the spacing. One useful study model in my collection uses an element spacing pf 0.174λ , which is 6' at 10 meters (28.5 MHz).

Fig. 5-5 shows the general configuration of the model. The inward slope

of the elements toward the boom is more extreme than in the close-spaced model. The squares on the reflector elements (all except 10 meters) represent a second attempt to add flexibility: loading capacitors. The reflectors for 20 through 12 meters are made longer than normal and electrically shortened with capacitors. As we noted with monoband beams, this practice permits more precise setting of the front-to-back ratio without altering the reflector loop lengths, and it slightly widens the operating bandwidth. Because the 10-meter and 12-meter reflectors are so closely spaced to begin with, enlarging the 10-meter reflector was deemed impractical.

Table 5-5 lists the dimensions of note in the model, along with the value of the capacitor used. No losses are charged to the capacitor. In the model, it is important to use a Type 0 load that calls for an actual value of capacitance so that frequency sweeps will accurately portray the behavior of the antenna across the passband. Since the reactance of the capacitor will change as the frequency changes, the use of a type 4 complex impedance (series resistance and reactance) load will not reflect the capacitor's actual effects. In the table, the segments/side column has been omitted, since all the quad models in this collection use the same segmentation scheme as the first one.

Table 5-5. Dimensions for 0.174 λ Spaced 5-Band Quad Beam

Frequency MHz	Spacing feet	L Driver feet	C Driver feet	L Refl. feet	C Refl. feet	Reflector cap. pF
28.5	6.00	8.63	34.54	9.40	37.60	—
24.94	6.86	9.88	39.52	10.56	42.23	80
21.22	8.06	11.72	46.86	12.39	49.56	125
18.12	9.44	13.77	55.08	14.48	57.92	135
14.17	12.07	17.67	70.66	18.48	73.90	225

In replicating and improving this model, if changes are made to any of the loading capacitors, it is important to check the effects of the change on other bands. The most notable interaction is between 10 and 12 meters, since the loops are so close in length. A 10 pF change in the 12-meter loading capacitor created operationally insignificant but numerically noticeable changes in the reported values for every other band.

For anyone wishing to replicate this particular model, here is the EZNEC model description.

```
5-band quad: .174 wl sp                                Frequency = 28.5 MHz.
Wire Loss: Copper -- Resistivity = 1.74E-08 ohm-m, Rel. Perm. = 1
```

----- WIRES -----

Wire	Conn.---	End 1 (x,y,z : in)	Conn.---	End 2 (x,y,z : in)	Dia(in)	Segs
1	W4E2	-51.800, 36.000,-51.800	W2E1	51.800, 36.000,-51.800	# 14	7
2	W1E2	51.800, 36.000,-51.800	W3E1	51.800, 36.000, 51.800	# 14	7
3	W2E2	51.800, 36.000, 51.800	W4E1	-51.800, 36.000, 51.800	# 14	7
4	W3E2	-51.800, 36.000, 51.800	W1E1	-51.800, 36.000,-51.800	# 14	7
5	W8E2	-56.400,-36.000,-56.400	W6E1	56.400,-36.000,-56.400	# 14	7
6	W5E2	56.400,-36.000,-56.400	W7E1	56.400,-36.000, 56.400	# 14	7
7	W6E2	56.400,-36.000, 56.400	W8E1	-56.400,-36.000, 56.400	# 14	7
8	W7E2	-56.400,-36.000, 56.400	W5E1	-56.400,-36.000,-56.400	# 14	7
9	W12E2	-59.300, 41.138,-59.300	W10E1	59.300, 41.138,-59.300	# 14	9
10	W9E2	59.300, 41.138,-59.300	W11E1	59.300, 41.138, 59.300	# 14	9
11	W10E2	59.300, 41.138, 59.300	W12E1	-59.300, 41.138, 59.300	# 14	9
12	W11E2	-59.300, 41.138, 59.300	W9E1	-59.300, 41.138,-59.300	# 14	9
13	W16E2	-63.350,-41.138,-63.350	W14E1	63.350,-41.138,-63.350	# 14	9
14	W13E2	63.350,-41.138,-63.350	W15E1	63.350,-41.138, 63.350	# 14	9
15	W14E2	63.350,-41.138, 63.350	W16E1	-63.350,-41.138, 63.350	# 14	9
16	W15E2	-63.350,-41.138, 63.350	W13E1	-63.350,-41.138,-63.350	# 14	9
17	W20E2	-70.300, 48.350,-70.300	W18E1	70.300, 48.350,-70.300	# 14	11
18	W17E2	70.300, 48.350,-70.300	W19E1	70.300, 48.350, 70.300	# 14	11
19	W18E2	70.300, 48.350, 70.300	W20E1	-70.300, 48.350, 70.300	# 14	11
20	W19E2	-70.300, 48.350, 70.300	W17E1	-70.300, 48.350,-70.300	# 14	11
21	W24E2	-74.350,-48.350,-74.350	W22E1	74.350,-48.350,-74.350	# 14	11
22	W21E2	74.350,-48.350,-74.350	W23E1	74.350,-48.350, 74.350	# 14	11
23	W22E2	74.350,-48.350, 74.350	W24E1	-74.350,-48.350, 74.350	# 14	11
24	W23E2	-74.350,-48.350, 74.350	W21E1	-74.350,-48.350,-74.350	# 14	11
25	W28E2	-82.650, 56.623,-82.650	W26E1	82.650, 56.623,-82.650	# 14	13
26	W25E2	82.650, 56.623,-82.650	W27E1	82.650, 56.623, 82.650	# 14	13
27	W26E2	82.650, 56.623, 82.650	W28E1	-82.650, 56.623, 82.650	# 14	13
28	W27E2	-82.650, 56.623, 82.650	W25E1	-82.650, 56.623,-82.650	# 14	13
29	W32E2	-86.900,-56.623,-86.900	W30E1	86.900,-56.623,-86.900	# 14	13
30	W29E2	86.900,-56.623,-86.900	W31E1	86.900,-56.623, 86.900	# 14	13
31	W30E2	86.900,-56.623, 86.900	W32E1	-86.900,-56.623, 86.900	# 14	13
32	W31E2	-86.900,-56.623, 86.900	W29E1	-86.900,-56.623,-86.900	# 14	13
33	W36E2	-106.00, 72.408,-106.00	W34E1	106.000, 72.408,-106.00	# 14	15
34	W33E2	106.000, 72.408,-106.00	W35E1	106.000, 72.408,106.000	# 14	15
35	W34E2	106.000, 72.408,106.000	W36E1	-106.00, 72.408,106.000	# 14	15
36	W35E2	-106.00, 72.408,106.000	W33E1	-106.00, 72.408,-106.00	# 14	15
37	W40E2	-110.85,-72.408,-110.85	W38E1	110.850,-72.408,-110.85	# 14	15
38	W37E2	110.850,-72.408,-110.85	W39E1	110.850,-72.408,110.850	# 14	15
39	W38E2	110.850,-72.408,110.850	W40E1	-110.85,-72.408,110.850	# 14	15
40	W39E2	-110.85,-72.408,110.850	W37E1	-110.85,-72.408,-110.85	# 14	15

----- SOURCES -----

Source	Wire Seg.	Wire #/Pct Actual	From End 1 (Specified)	Ampl.(V, A)	Phase(Deg.)	Type
1	4	1 / 50.00	(1 / 50.00)	1.000	0.000	V

----- LOADS -----

Load	Wire Seg.	Wire #/Pct Actual	From End 1 (Specified)	Laplace Coefficients
1	5	13 / 50.00	(13 / 50.00)	Coefficients listed below
2	6	21 / 50.00	(21 / 50.00)	Coefficients listed below
3	7	29 / 50.00	(29 / 50.00)	Coefficients listed below

Chapter 5 ~ Multi-Band 2- Element Quad Beams

4	8	37 / 50.00	(37 / 50.00)	Coefficients listed below		
Load 1	s^0	s^1	s^2	s^3	s^4	s^5
Num	1.000E+00	0.000E+00	0.000E+00	0.000E+00	0.000E+00	0.000E+00
Den	0.000E+00	8.000E-11	0.000E+00	0.000E+00	0.000E+00	0.000E+00
Load 2	s^0	s^1	s^2	s^3	s^4	s^5
Num	1.000E+00	0.000E+00	0.000E+00	0.000E+00	0.000E+00	0.000E+00
Den	0.000E+00	1.250E-10	0.000E+00	0.000E+00	0.000E+00	0.000E+00
Load 3	s^0	s^1	s^2	s^3	s^4	s^5
Num	1.000E+00	0.000E+00	0.000E+00	0.000E+00	0.000E+00	0.000E+00
Den	0.000E+00	1.351E-10	0.000E+00	0.000E+00	0.000E+00	0.000E+00
Load 4	s^0	s^1	s^2	s^3	s^4	s^5
Num	1.000E+00	0.000E+00	0.000E+00	0.000E+00	0.000E+00	0.000E+00
Den	0.000E+00	2.246E-10	0.000E+00	0.000E+00	0.000E+00	0.000E+00

The dimensions of this model are listed in inches. The band-by-band source positions are as follows: 10 = wire 1; 12 = wire 9; 15 = wire 17; 17 = wire 25; and 20 = wire 33. Loads are listed by reference to Laplace transform notation, but the capacitor values can be read directly from the s^1 denominator position.

For reference, **Table 5-6** lists the performance potential reports for the band centers from 10 to 20 meters.

Table 5-6. Key Performance Figures for the 0.174 λ Spaced Quad

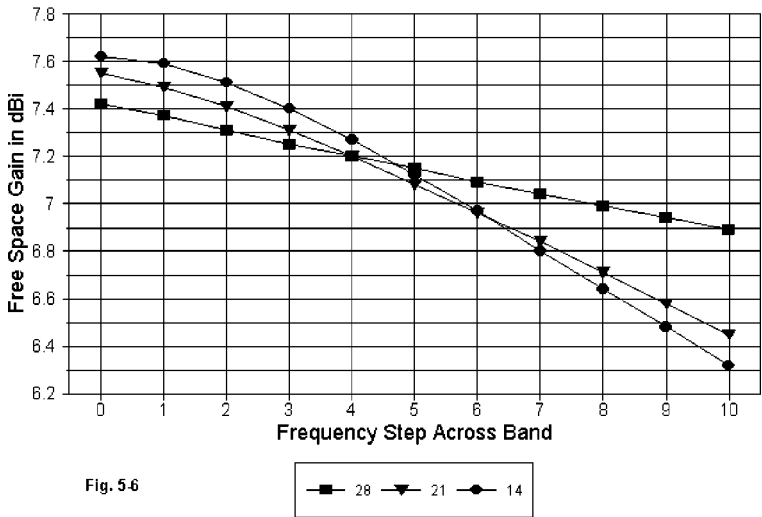
Frequency MHz	Free Space Gain dBi	Front-to-Back Ratio dB	Feedpoint Impedance R +/- jX Ohms
28.5	7.15	32.4	58 + j 16
24.95	7.05	31.0	70 + j 3
21.22	7.07	29.1	90 + j 20
18.12	7.08	25.8	94 + j 8
14.17	7.11	23.8	118 - j 3

The resonant points for 10 and 15 meters were intentionally lowered, resulting in the inductively reactive source impedances for those bands at the specified frequencies. More notable is the fact that widening the spider did not overcome the tendency of this design to show an increasing source impedance magnitude as we move from the inner loops to the outer ones. This phenomena alone suggests that matching a spider to a given feedline will present some problems.

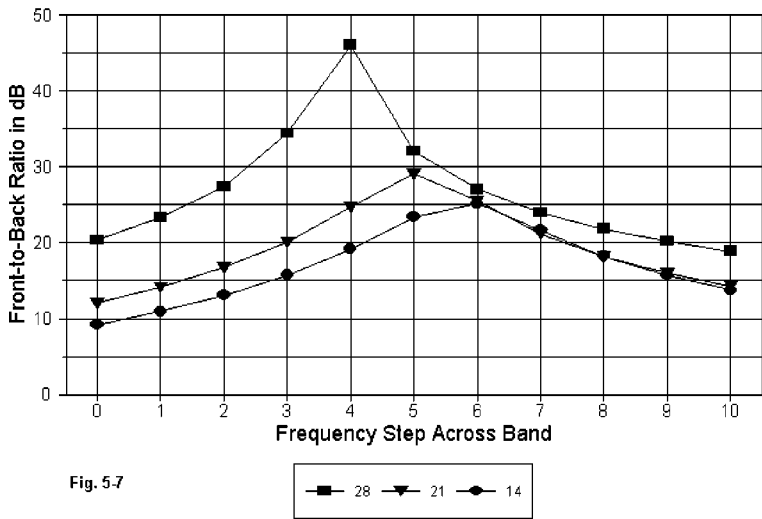
The gain curves in **Fig. 5-6** show a good correlation to those for the narrow-spaced version of the 5-band quad. The gain curve for 10 meters is overall lower because the design effort aimed to raise the front-to-back ratio. However, the gain change across 10 meters is virtually identical to that of the

narrower quad. The 20-meter gain curve is slightly steeper for this model relative to the previous one.

5-Band 2-Element Quad: 0.174 WL
Gain vs. Band



5-Band 2-Element Quad: 0.174 WL
Front-to-Back Ratio vs. Band



Whereas the previous model showed high peak values of front-to-back ratio on 15 and 20, with 10 meters showing a relatively smooth curve, the front-to-back ratio curves in **Fig. 5-7** show just the opposite. 10-meter front-to-back ratios are very good across the band. 15 and 20 show only mild peaks, but with overall performance significantly lower than on 10. The performance on 20 meters, at the low end of the band, is improved, although the high-end figure is almost identical for the two models. Except on 10 meters (and the narrow WARC bands—17 and 12 meters), attaining a 20 dB front-to-back ratio across the band with the spider design will be difficult.

5-Band 2-Element Quad: 0.174 WL
Front-to-Back Ratio vs. Band

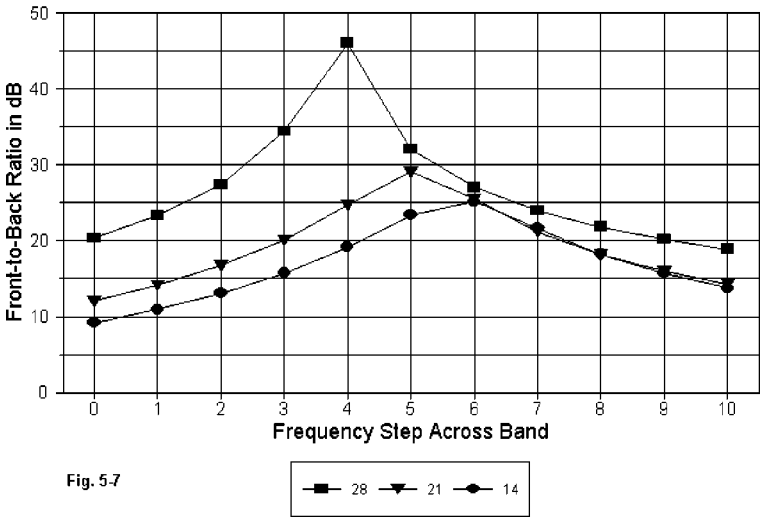


Fig. 5-7

The wider spacing of the present spider design significantly improves the 75-Ohm SWR operating bandwidth, despite the variability of source impedances from band-to-band. As shown in **Fig. 5-8**, all bands except 10 meters come in at under 2:1 SWR across the bands, and the 10-meter curve yields about 750 kHz of under 2:1 SWR operation.

Wider spacing, then, does provide superior performance over narrow spacing in spider designs. Part of the reason for the improvements involves complex interactions among the elements. The theoretically inactive elements are in practice quite active—at least to the degree necessary to shape the performance curves for the 5-band quad. Removing the loops for 12 and

17 meters would require a complete refiguring of the multi-band quad for effective 3-band operation. Some of loop size changes are small but necessary, suggesting that the multi-band quad is not the broad-banded insensitive beast that its early reputation made it out to be.

5-Band 2-Element Quad: 0.174 WL VSWR vs. Band

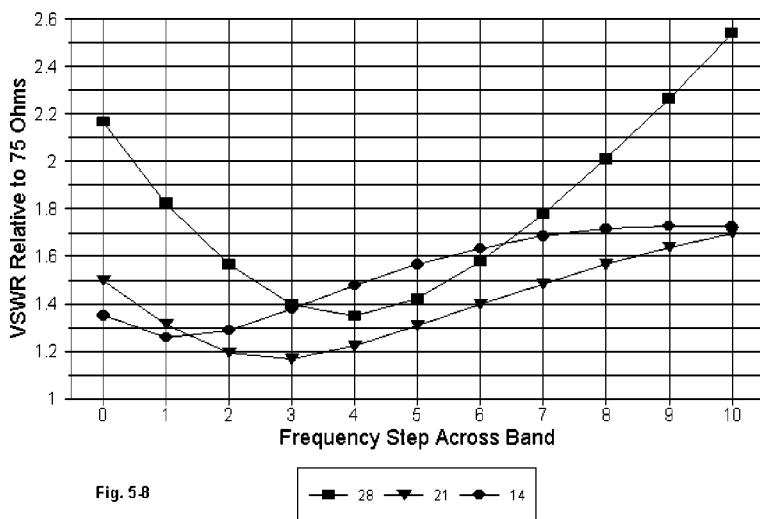


Fig. 5-8

A “Flat-Loop” (Planar) Quad with 8' Element Spacing and Capacitive Reflector Loading

In the April, 1992, edition of *QST* (p. 52), KC6T published a quad design that used flat plane loops spaced 8' apart. The 5-band design employed capacitor loading of the reflector. In addition, the designer used gamma matches on the drivers.

In my own model of this antenna, some modifications have been made for modeling convenience. The driven elements were resonated at band centers. The reflector loads were optimized for the free space model. The differences between my values and the values used in the two practical versions described in the article reaffirm the importance of determining the actual value of loading required through field adjustment. The 10-meter reflector is not loaded. **Fig. 5-9** shows the general outline of the resultant model.

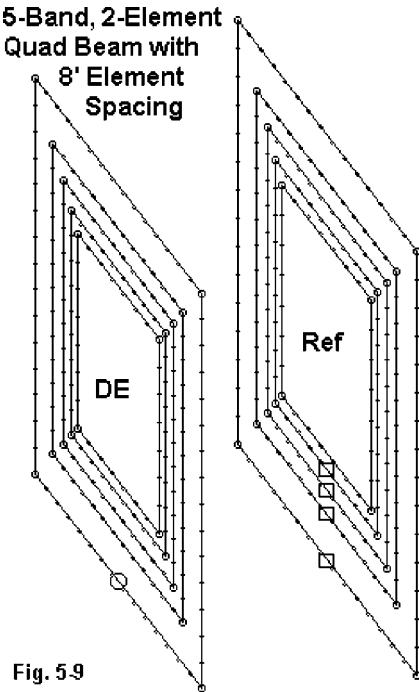


Fig. 5-9

The dimensions for the model follow in **Table 5-7**. Note especially the spacing in wavelengths for each band. The 10- and 12-meter loops are farther apart than those in the models explored so far, while 20-meter elements are closer.

Table 5-7. Dimensions for KC6T Planar 5-Band Quad Beam

Frequency MHz	Spacing λ	L Driver feet	C Driver feet	L Refl. feet	C Refl. feet	Reflector cap. pF
28.5	0.232	8.58	34.34	9.35	37.40	—
24.94	0.202	9.90	39.60	10.72	42.86	58
21.22	0.173	11.65	46.60	12.60	50.40	68
18.12	0.147	13.68	54.74	14.70	58.80	76
14.17	0.115	17.47	69.86	18.80	75.20	94

Here is the corresponding EZNEC model description of the KC6T quad.

```
2el quad KC6T QST 4-92, p 52                      Frequency = 28.5  MHz.

Wire Loss: Copper -- Resistivity = 1.74E-08 ohm-m, Rel. Perm. = 1

----- WIRES -----
```

Wire Conn.--- End 1 (x,y,z : ft) Conn.--- End 2 (x,y,z : ft) Dia(in) Segs									
1	W4E2	-4.292,	0.000,	-4.292	W2E1	4.292,	0.000,	-4.292	# 14 7
2	W1E2	4.292,	0.000,	-4.292	W3E1	4.292,	0.000,	4.292	# 14 7
3	W2E2	4.292,	0.000,	4.292	W4E1	-4.292,	0.000,	4.292	# 14 7
4	W3E2	-4.292,	0.000,	4.292	W1E1	-4.292,	0.000,	-4.292	# 14 7
5	W8E2	-4.950,	0.000,	-4.950	W6E1	4.950,	0.000,	-4.950	# 14 9
6	W5E2	4.950,	0.000,	-4.950	W7E1	4.950,	0.000,	4.950	# 14 9
7	W6E2	4.950,	0.000,	4.950	W8E1	-4.950,	0.000,	4.950	# 14 9
8	W7E2	-4.950,	0.000,	4.950	W5E1	-4.950,	0.000,	-4.950	# 14 9
9	W12E2	-5.825,	0.000,	-5.825	W10E1	5.825,	0.000,	-5.825	# 14 11
10	W9E2	5.825,	0.000,	-5.825	W11E1	5.825,	0.000,	5.825	# 14 11
11	W10E2	5.825,	0.000,	5.825	W12E1	-5.825,	0.000,	5.825	# 14 11
12	W11E2	-5.825,	0.000,	5.825	W9E1	-5.825,	0.000,	-5.825	# 14 11
13	W16E2	-6.842,	0.000,	-6.842	W14E1	6.842,	0.000,	-6.842	# 14 13
14	W13E2	6.842,	0.000,	-6.842	W15E1	6.842,	0.000,	6.842	# 14 13
15	W14E2	6.842,	0.000,	6.842	W16E1	-6.842,	0.000,	6.842	# 14 13
16	W15E2	-6.842,	0.000,	6.842	W13E1	-6.842,	0.000,	-6.842	# 14 13
17	W20E2	-8.733,	0.000,	-8.733	W18E1	8.733,	0.000,	-8.733	# 14 15
18	W17E2	8.733,	0.000,	-8.733	W19E1	8.733,	0.000,	8.733	# 14 15
19	W18E2	8.733,	0.000,	8.733	W20E1	-8.733,	0.000,	8.733	# 14 15
20	W19E2	-8.733,	0.000,	8.733	W17E1	-8.733,	0.000,	-8.733	# 14 15
21	W24E2	-4.675,	-8.000,	-4.675	W22E1	4.675,	-8.000,	-4.675	# 14 7
22	W21E2	4.675,	-8.000,	-4.675	W23E1	4.675,	-8.000,	4.675	# 14 7
23	W22E2	4.675,	-8.000,	4.675	W24E1	-4.675,	-8.000,	4.675	# 14 7
24	W23E2	-4.675,	-8.000,	4.675	W21E1	-4.675,	-8.000,	-4.675	# 14 7
25	W28E2	-5.358,	-8.000,	-5.358	W26E1	5.358,	-8.000,	-5.358	# 14 9
26	W25E2	5.358,	-8.000,	-5.358	W27E1	5.358,	-8.000,	5.358	# 14 9
27	W26E2	5.358,	-8.000,	5.358	W28E1	-5.358,	-8.000,	5.358	# 14 9
28	W27E2	-5.358,	-8.000,	5.358	W25E1	-5.358,	-8.000,	-5.358	# 14 9
29	W32E2	-6.300,	-8.000,	-6.300	W30E1	6.300,	-8.000,	-6.300	# 14 11
30	W29E2	6.300,	-8.000,	-6.300	W31E1	6.300,	-8.000,	6.300	# 14 11
31	W30E2	6.300,	-8.000,	6.300	W32E1	-6.300,	-8.000,	6.300	# 14 11
32	W31E2	-6.300,	-8.000,	6.300	W29E1	-6.300,	-8.000,	-6.300	# 14 11
33	W36E2	-7.350,	-8.000,	-7.350	W34E1	7.350,	-8.000,	-7.350	# 14 13
34	W33E2	7.350,	-8.000,	-7.350	W35E1	7.350,	-8.000,	7.350	# 14 13
35	W34E2	7.350,	-8.000,	7.350	W36E1	-7.350,	-8.000,	7.350	# 14 13
36	W35E2	-7.350,	-8.000,	7.350	W33E1	-7.350,	-8.000,	-7.350	# 14 13
37	W40E2	-9.400,	-8.000,	-9.400	W38E1	9.400,	-8.000,	-9.400	# 14 15
38	W37E2	9.400,	-8.000,	-9.400	W39E1	9.400,	-8.000,	9.400	# 14 15
39	W38E2	9.400,	-8.000,	9.400	W40E1	-9.400,	-8.000,	9.400	# 14 15
40	W39E2	-9.400,	-8.000,	9.400	W37E1	-9.400,	-8.000,	-9.400	# 14 15

----- SOURCES -----

Source	Wire Seg.	Wire #/Pct Actual	From End 1 (Specified)	Ampl.(V, A)	Phase(Deg.)	Type
1	4	1 / 50.00	(1 / 50.00)	1.000	0.000	V

----- LOADS -----

Load	Wire Seg.	Wire #/Pct Actual	From End 1 (Specified)	Laplace Coefficients
1	5	25 / 50.00	(25 / 50.00)	Coefficients listed below
2	6	29 / 50.00	(29 / 50.00)	Coefficients listed below
3	7	33 / 50.00	(33 / 50.00)	Coefficients listed below
4	8	37 / 50.00	(37 / 50.00)	Coefficients listed below

Load	1	s^0	s^1	s^2	s^3	s^4	s^5
Num	1.000E+00	0.000E+00	0.000E+00	0.000E+00	0.000E+00	0.000E+00	0.000E+00
Den	0.000E+00	5.800E-11	0.000E+00	0.000E+00	0.000E+00	0.000E+00	0.000E+00
Load	2	s^0	s^1	s^2	s^3	s^4	s^5
Num	1.000E+00	0.000E+00	0.000E+00	0.000E+00	0.000E+00	0.000E+00	0.000E+00
Den	0.000E+00	6.810E-11	0.000E+00	0.000E+00	0.000E+00	0.000E+00	0.000E+00
Load	3	s^0	s^1	s^2	s^3	s^4	s^5
Num	1.000E+00	0.000E+00	0.000E+00	0.000E+00	0.000E+00	0.000E+00	0.000E+00
Den	0.000E+00	7.640E-11	0.000E+00	0.000E+00	0.000E+00	0.000E+00	0.000E+00
Load	4	s^0	s^1	s^2	s^3	s^4	s^5
Num	1.000E+00	0.000E+00	0.000E+00	0.000E+00	0.000E+00	0.000E+00	0.000E+00
Den	0.000E+00	9.360E-11	0.000E+00	0.000E+00	0.000E+00	0.000E+00	0.000E+00

This model gives dimensions in feet, but the order of loops differs. All of the driver loops are listed, followed by all of the reflectors, each in ascending wavelength order from 10 to 20 meters. Hence the source wires are as follows: 10 = wire 1; 12 = wire 5; 15 = wire 9; 17 = wire 13; and 20 = wire 17. Anyone who believes that I should set myself a more consistent set of modeling conventions for 5-band quads would be entirely in the right.

Table 5-8. Key Performance Figures for the KC6T Planar Quad

Frequency	Free Space	Front-to-Back	Feedpoint Impedance
MHz	Gain dBi	Ratio dB	R +/- jX Ohms
28.5	7.46	22.8	75 - j 0
24.95	7.20	30.6	77 + j 0
21.22	7.28	34.4	70 + j 2
18.12	7.30	31.7	70 + j 2
14.17	7.21	24.0	77 + j 2

Table 5-8, the band-center performance potential reports, will serve as a reference for the graphs to follow.

The first thing to notice is that this model sustains the higher gain values that we found in the narrow spider quad along with the higher front-to-back ratios (except for 10 meters) of the wide spider quad. The second and very important thing to notice is the source impedances for all five bands. The band-center 75-Ohm SWR for all bands is insignificant. Hence, the use of a gamma match on the original design proves to be unnecessary. A simple 1.4:1 balun would resolve the 50-Ohm match problem and suppress common mode currents at the same time.

The gain curves (Fig. 5-10) for the KC6T design show an overlap at the lower end of the bands. The overlap results from an increase in gain for the lower two bands relative to the two spider-construction models. The 10-meter

gain variance across the band is the lowest of the three designs we have examined. The gain drop-off for any band is equal to or less than the best figures for any of our designs. Nonetheless, the drop-off does run from 1 to 1.2 dB for 15 and 10 meters. I have not yet found a design that does not have this type of curve without setting the gain around 6.5 dBi in the first place. One key to the steep gain curves is the fact that these quads use very thin elements, especially when compared to the tubular elements found in Yagi-Uda arrays.

5-Band 2-Element Quad: 8' Fixed
Gain vs. Band

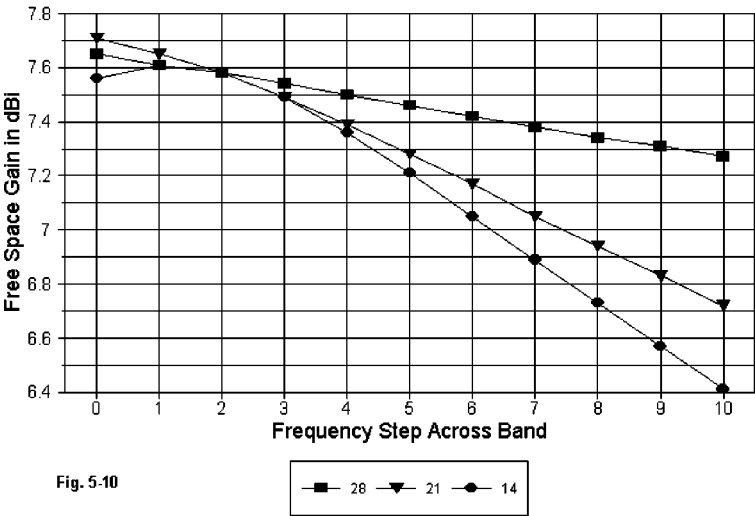


Fig. 5-10

Interestingly, the 10-meter portion of the antenna, when extracted from the overall 5-band environment, is not capable of the gain as a monoband beam relative to the gain that it shows within the larger set of loops. A free space gain of about 6.5 dBi, with a front-to-back ratio approaching 20 dB is the best I have been able to model from that part of the antenna. Moreover, the independent resonant impedance is over 170 Ohms--a far cry from the 75-Ohm impedance that 10 meters shows in the 5-band model. Just how the other loops contribute to the 10-meter gain and source impedance remains to be calculated, but an examination of the adjacent loop currents is certainly in order.

5-Band 2-Element Quad: 8' Fixed Front-to-Back Ratio vs. Band

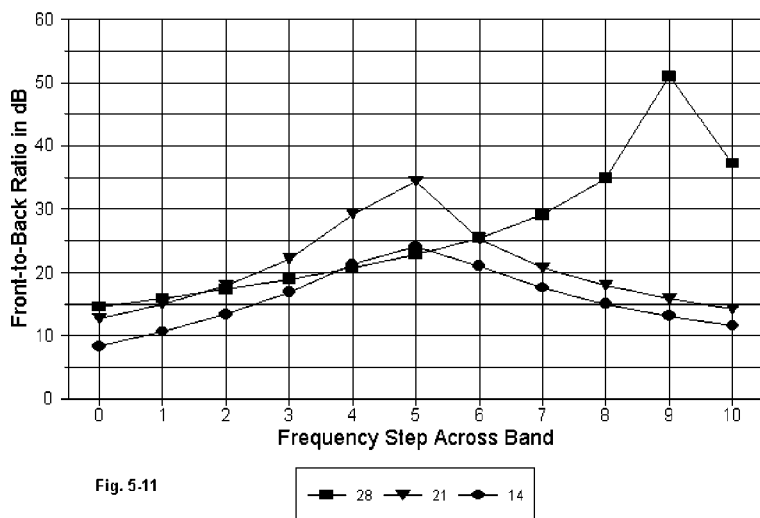


Fig. 5-11

As the model is presently structured, the front-to-back performance is somewhat deficient and requires further design work. See **Fig. 5-11**. It is uncertain whether significant improvements can be made, given the inherently narrow-band front-to-back performance that is endemic to thin-wire quads in general. 10-meter performance begins at about 15 dB and peaks at over 50 dB. 15-meter performance peaks near 35 dB, but decreases to about 15 dB at the band edges in a well balanced curve. 20-meter performance is poorest of all, with the low edge of the band below the 10 dB mark. However, the close spacing of the 20-meter elements at under $1/8 \lambda$, along with use of an element diameter that is a very small fraction of a wavelength, may prevent significant improvements. Perhaps only the addition of a 30-meter set of elements to this model will allow some improvement to the 20-meter front-to-back curve.

The 75-Ohm SWR curves for the 3 wide bands, shown in **Fig. 5-12**, suggest that the antenna has good potential for direct matching to 75-Ohm feedline. The resonant point on 20 meters needs to be moved much lower in the band--with consequent adjustments to every other loop. 10 meters provides nearly 800 kHz of 2:1 SWR bandwidth, even before line losses are used to obscure the remaining mismatch at the antenna terminals.

5-Band 2-Element Quad: 8' Fixed VSWR vs. Band

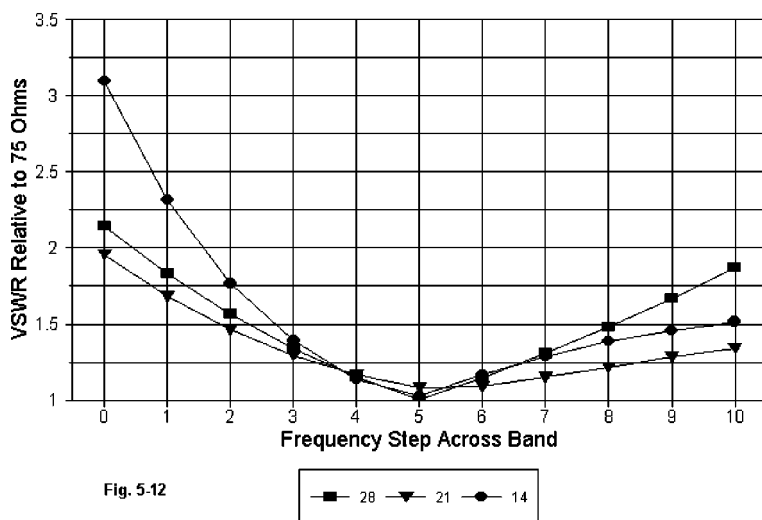


Fig. 5-12

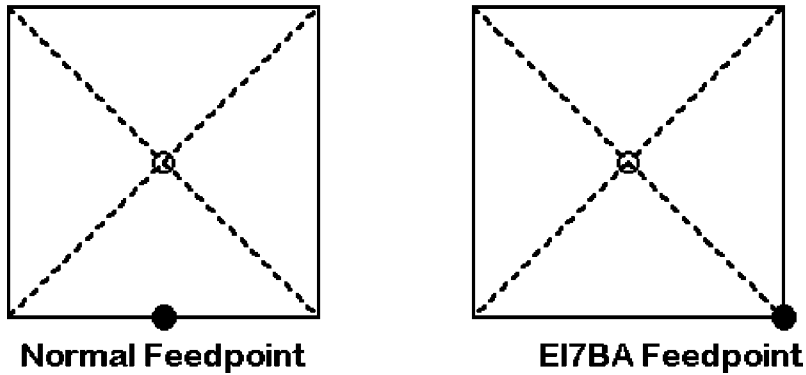
With the increasing use of CATV low-loss hardline for fixed position runs between the antenna location and the shack entry, using a 75-Ohm feed system with an antenna of this design seems quite feasible. Driver switching can be accomplished with either solid or foam core 75-Ohm cable at the antenna end of the line. A single 75:50 Ohm transformer or unun can be used at the operating position to effect a match with equipment inputs and outputs. Alternatively, for use with a low-loss 50-Ohm main feedline, a single wide-band matching device might be located in the remote switch box, with all switching done at 75 Ohms.

Although 8-legged spiders and similar designs that keep quad elements spaced the same amount in terms of wavelength have become very popular, modeling exercises may breed a new respect for older fixed spacing designs. The KC6T design forms a very good starting point for improvements--and is a good design to model in its own right.

The Square and Its Feedpoint

EI7BA has built a quad somewhat similar to the wide-spaced spider we have examined. However, he has altered the feedpoint for mechanical reasons.

Fig. 5-13



For a square quad, the normal feedpoint, especially with spider construction, leaves a long run of unsupported feedline from the hub to the center of the element, as suggested in **Fig. 5-13**. If we have a multi-band quad, then we might have 5 line lengths, the net weight of which begs for a sky-hook.

EI7BA runs his feedlines to the corner(s) of the quad square. One might use the same corner for all bands or distribute the weight each side of center. The question then arises as to the effect the change of feed position might have upon the antenna pattern.

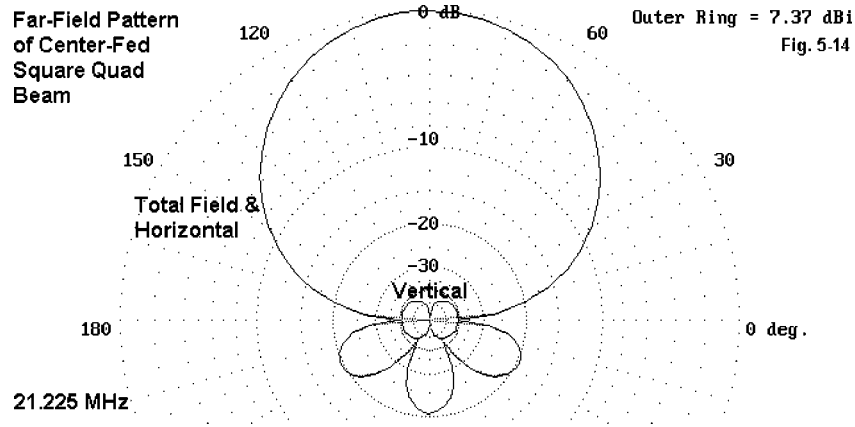
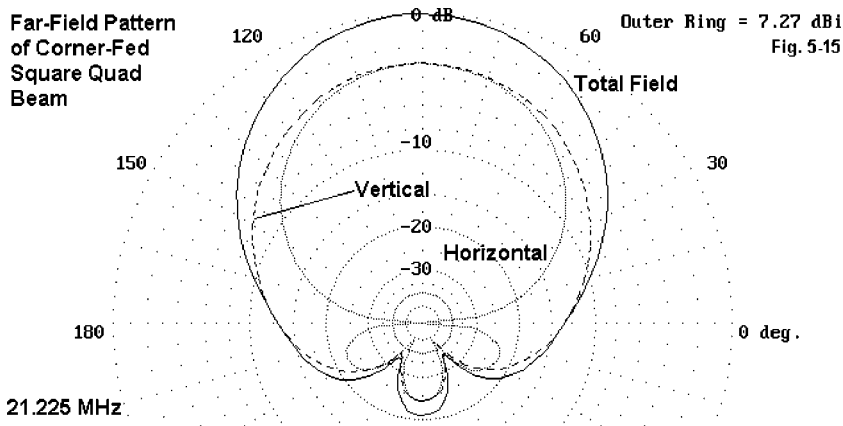


Fig. 5-14 shows the band-center pattern of the EI7BA quad on 15 meters using the normal centered feedpoint. Performance at this frequency is good with respect both to gain and front-to-back performance. As the figure shows,

the vertically polarized component of the total far field is very small--at least 40 dB down from the horizontal and total fields, which are indistinguishable in the pattern graphic.

Moving the feedpoint to one corner has some interesting effects, which are displayed in **Fig. 5-15**. First, the vertically and horizontally polarized components of the field have equal forward gain values. Together, they yield a total field that is only down by 0.1 dB relative to the center-feed result. The total field has a wider beam width and extends beyond the 90-degree points we often use to define front-to-side ratio. The normal feed system produces front-to-side values greater than 35 dB down, whereas the front-to-side ratio for the corner feed is about 13 dB.

When we set aside simple habits of expectation, it is not at all clear that one can say that one pattern is superior to the other without introducing a good bit of information about the operating goals and style of the individual user. One can develop equal numbers of scenarios favoring each total field pattern. Whether the corner feed offers any advantages or disadvantages relative to propagation, modeling itself cannot say.



The repositioning of the feedpoint to the corner does tend to raise the source impedance of the antenna by a small amount. In one example, the change was from 75 Ohms to about 85 Ohms. Such changes will have to be factored into the design itself by anyone using this alternative feed system.

When Is Enough Enough?

Hopefully, the models made available here will provide a sufficient start to

anyone interested in exploring multi-band 2-element quads. However, lest one think of these notes as in any way definitive, here is a list of some questions not tackled.

1. Does the diamond shape have any electrical effect (in contrast to obvious mechanical effects) upon a multi-band quad? Models of monoband quads suggest a negative answer, but I have not run any multi-band models to verify this suggestion.

2. What is the optimal spacing for either spider or flat plane quads? The models noted here are only samples, not exhaustive investigations. Hence, there are possibilities yet to be tapped.

3. What is the effect of using much fatter wire in the multi-band quad? Using #10 aluminum wire or other candidates for the loops has not been explored here. Some loop size changes are inevitable, but the interactions and their consequences for performance and feedpoint impedance figures remains to be figured.

4. What effect will using metal or partially metal support arms have on quad performance? Metal arms or arm segments were not a part of these models.

5. What is the effect of using a common feed point for all of the drivers in a 5-band quad? The models used here restricted themselves to feeding one driver at a time, with the unused drivers having closed loops. The common-feed question requires separate exploration.

6. How will antenna height above ground affect quad performance, especially the source impedance. All of the models we have looked at have been free space versions to make the performance figures comparable. Although quads have a reputation of relative immunity to surrounding objects, every proposed quad should be modeled at its height of intended use.

7. Can 5-band 3- and 4-element multi-band quads be modeled? In principle, the answer is a deceptively easy "yes." However, each 5-band element adds 20 wires to the model or about 200 segments. Since run times grow exponentially rather than linearly, the resultant models may require modeler patience. (The present generation of PCs has plenty of resources, so that is not a limitation.) Some programs with 500 segment limitations may not be able to handle models of large quads adequately, and reducing the segmentation per loop side in order to fit the model to the program runs the danger of

producing inaccurate results.

These are not all of the questions that remain unanswered, but they are enough to remove any sense of definitiveness to these casual notes. My intent has been simply to make available some of the models in my collection to those interested in quad modeling--and to show some of the performance potential and limitations of each of the designs considered. We have only scratched the surface of the quad question cluster.

6. Alternative Common Feed Systems for Multi-Band 2-Element Quad Beams

When we specify an interest in a 2-element 5-band quad beam, we are usually, but not always, saying more than just these facts. Ordinarily, we are also looking for an array that is compatible with a 50-Ohm (or at most a 75-Ohm) coaxial cable system. Under these circumstances, I have on a number of occasions--for reasons that shall be illustrated--recommended separate feed lines to each driver in the quad array, most often combined at a remote switch near the hub of the antenna. Over the years, a number of individuals have made some discoveries and rediscoveries that are worthy of note as alternatives to the remote switching idea. In the process of looking at these alternatives, we may also understand somewhat better a. what goes on in an array with a common feed system and b. some different ways of overcoming the less-than-optimal parts of what is going on.

The Separate-Feed Standard

In order to make some valid comparisons, let's use a single antenna throughout the exercise: the close-spaced spider array shown in the preceding chapter in **Fig. 5-1**. Although we shall modify the antenna as we proceed, we shall begin with the dimensions in **Table 6-1** and the model description.

Table 6-1. Dimensions for 0.125 λ Spaced 5-Band Quad Beam

Frequency MHz	Spacing feet	L Driver feet	C Driver feet	L Refl. feet	C Refl. feet	Segments per side
28.5	4.31	8.64	34.56	9.20	36.80	7
24.94	4.93	9.90	39.60	10.20	40.80	9
21.22	5.79	11.63	46.52	12.06	48.24	11
18.12	6.79	13.66	54.64	14.06	56.24	13
14.17	8.68	17.50	70.00	18.06	72.24	15

5-band quad: 1/8 wl sp

Frequency = 28.5 MHz.

Wire Loss: Copper -- Resistivity = 1.74E-08 ohm-m, Rel. Perm. = 1

----- WIRES -----

[illegible]

1	W4E2	-4.320,	2.155,	-4.320	W2E1	4.320,	2.155,	-4.320	# 14	7
2	W1E2	4.320,	2.155,	-4.320	W3E1	4.320,	2.155,	4.320	# 14	7

3	W2E2	4.320,	2.155,	4.320	W4E1	-4.320,	2.155,	4.320	# 14	7
4	W3E2	-4.320,	2.155,	4.320	W1E1	-4.320,	2.155,	-4.320	# 14	7
5	W8E2	-4.600,	-2.155,	-4.600	W6E1	4.600,	-2.155,	-4.600	# 14	7
6	W5E2	4.600,	-2.155,	-4.600	W7E1	4.600,	-2.155,	4.600	# 14	7
7	W6E2	4.600,	-2.155,	4.600	W8E1	-4.600,	-2.155,	4.600	# 14	7
8	W7E2	-4.600,	-2.155,	4.600	W5E1	-4.600,	-2.155,	-4.600	# 14	7
9	W12E2	-5.815,	2.897,	-5.815	W10E1	5.815,	2.897,	-5.815	# 14	11
10	W9E2	5.815,	2.897,	-5.815	W11E1	5.815,	2.897,	5.815	# 14	11
11	W10E2	5.815,	2.897,	5.815	W12E1	-5.815,	2.897,	5.815	# 14	11
12	W11E2	-5.815,	2.897,	5.815	W9E1	-5.815,	2.897,	-5.815	# 14	11
13	W16E2	-6.030,	-2.897,	-6.030	W14E1	6.030,	-2.897,	-6.030	# 14	11
14	W13E2	6.030,	-2.897,	-6.030	W15E1	6.030,	-2.897,	6.030	# 14	11
15	W14E2	6.030,	-2.897,	6.030	W16E1	-6.030,	-2.897,	6.030	# 14	11
16	W15E2	-6.030,	-2.897,	6.030	W13E1	-6.030,	-2.897,	-6.030	# 14	11
17	W20E2	-8.750,	4.334,	-8.750	W18E1	8.750,	4.334,	-8.750	# 14	15
18	W17E2	8.750,	4.334,	-8.750	W19E1	8.750,	4.334,	8.750	# 14	15
19	W18E2	8.750,	4.334,	8.750	W20E1	-8.750,	4.334,	8.750	# 14	15
20	W19E2	-8.750,	4.334,	8.750	W17E1	-8.750,	4.334,	-8.750	# 14	15
21	W24E2	-9.030,	-4.334,	-9.030	W22E1	9.030,	-4.334,	-9.030	# 14	15
22	W21E2	9.030,	-4.334,	-9.030	W23E1	9.030,	-4.334,	9.030	# 14	15
23	W22E2	9.030,	-4.334,	9.030	W24E1	-9.030,	-4.334,	9.030	# 14	15
24	W23E2	-9.030,	-4.334,	9.030	W21E1	-9.030,	-4.334,	-9.030	# 14	15
25	W28E2	-4.950,	2.465,	-4.950	W26E1	4.950,	2.465,	-4.950	# 14	9
26	W25E2	4.950,	2.465,	-4.950	W27E1	4.950,	2.465,	4.950	# 14	9
27	W26E2	4.950,	2.465,	4.950	W28E1	-4.950,	2.465,	4.950	# 14	9
28	W27E2	-4.950,	2.465,	4.950	W25E1	-4.950,	2.465,	-4.950	# 14	9
29	W32E2	-5.100,	-2.465,	-5.100	W30E1	5.100,	-2.465,	-5.100	# 14	9
30	W29E2	5.100,	-2.465,	-5.100	W31E1	5.100,	-2.465,	5.100	# 14	9
31	W30E2	5.100,	-2.465,	5.100	W32E1	-5.100,	-2.465,	5.100	# 14	9
32	W31E2	-5.100,	-2.465,	5.100	W29E1	-5.100,	-2.465,	-5.100	# 14	9
33	W36E2	-6.830,	3.393,	-6.830	W34E1	6.830,	3.393,	-6.830	# 14	13
34	W33E2	6.830,	3.393,	-6.830	W35E1	6.830,	3.393,	6.830	# 14	13
35	W34E2	6.830,	3.393,	6.830	W36E1	-6.830,	3.393,	6.830	# 14	13
36	W35E2	-6.830,	3.393,	6.830	W33E1	-6.830,	3.393,	-6.830	# 14	13
37	W40E2	-7.030,	-3.393,	-7.030	W38E1	7.030,	-3.393,	-7.030	# 14	13
38	W37E2	7.030,	-3.393,	-7.030	W39E1	7.030,	-3.393,	7.030	# 14	13
39	W38E2	7.030,	-3.393,	7.030	W40E1	-7.030,	-3.393,	7.030	# 14	13
40	W39E2	-7.030,	-3.393,	7.030	W37E1	-7.030,	-3.393,	-7.030	# 14	13

----- SOURCES -----

Source	Wire Seg.	Wire #/Pct Actual	From End 1 (Specified)	Ampl.(V, A)	Phase(Deg.)	Type
1	4	1 / 50.00	(1 / 50.00)	1.000	0.000	V

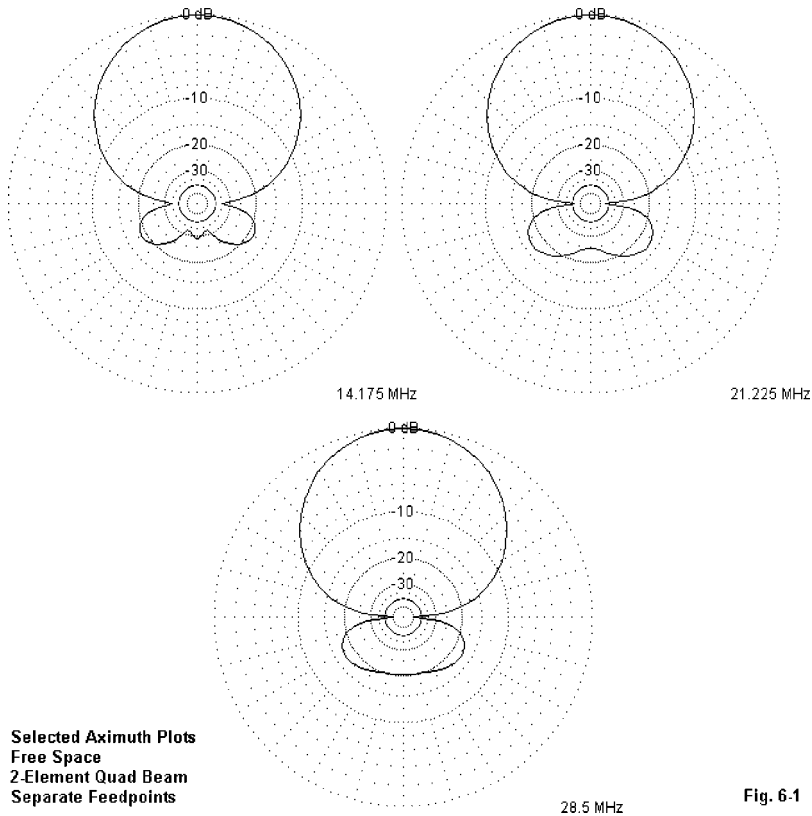
With separate feedpoints, the array produces the results in **Table 6-2** at the design frequencies for each of the 5 bands.

Table 6-2. Key Performance Figures for the Multi-Band Quad

Frequency MHz	Free Space Gain dBi	Front-to-Back Ratio dB	Feedpoint Impedance R +/- jX Ohms
28.5	7.48	20.3	40 - j 0
24.95	7.16	24.7	42 + j 0
21.22	7.23	28.9	53 + j 0
18.12	7.32	25.8	61 - j 0
14.17	7.23	32.4	84 - j 0

Graphs for the passband characteristics of the antenna appear in Chapter 5. Although these figures are very significant, for our present investigation, we shall be more interested in the general radiation patterns (far-field patterns) for the antenna. Not only do such patterns tell us a great deal about the antenna's basic behavior, they can, in addition, reveal something about the interactions among the elements—especially whether such interactions are harmful or beneficial. The patterns for the 5-band quad are based on a separate feedline to each driven elements, with all of the unused driver loops being closed or short-circuited across the feedpoint.

Fig. 6-1 shows the 20, 15, and 10 meter free-space azimuth patterns for this array. Note that each is a “well-behaved” pattern with very distinct side-nulls and a standard rear pattern for antennas of this type. Each band's pattern is virtually indistinguishable from a monoband quad beam pattern for the same frequency. In general, the free-space azimuth pattern for a horizontally polarized array is almost identical to the azimuth pattern taken at the take-off angle (elevation angle of maximum radiation) with the antenna over real ground at a specified mounting height. The only difference will be the gain figure, which will be between 5 and 6 dB higher due to ground reflections that add to the incident radiation from the antenna. The free-space gain of the 5-band quad antenna at its design frequencies is just about 7 dBi. At a height of about 1 λ on any given band, the maximum gain will be between 12 and 13 dBi.



Common Feed

Quad common feed is usually achieved in one of the three ways shown in **Fig. 6-2**. At its most simple, the system simply involves connecting the driver wires for each band together at a certain point. Alternatively, we can connect the wires together at the terminals of a balun to adjust the impedance for a match to coaxial cable. A third method is to use a transmission line section to feed the wires in phase with each other. The first two feed systems deform the drivers of some bands by introducing non-horizontal angles to the lower driver wire. The phasing line system does not.

At the suggestion of WD8JOL, who has been planning a revision to a commercial quad, I experimented with introducing a 150-Ohm phasing line to the drivers of the 0.125-wavelength spaced model above--which is similar in arrangement to one or more commercial quads. The phase line--as a physi-

cal matter--can be constructed from reasonably heavy wire and polycarbonate or similar spacers. For a model, the TL facility does all of the necessary work. Like Parker’s model, I obtained best results by connecting the main source or feedline to the 17-meter element. For planar element sets using the same system, connection to the 20-meter element is normally best. However, it is wise to be prepared to experimentally find the optimal connection point for any given design—either by modeling or field adjustment.

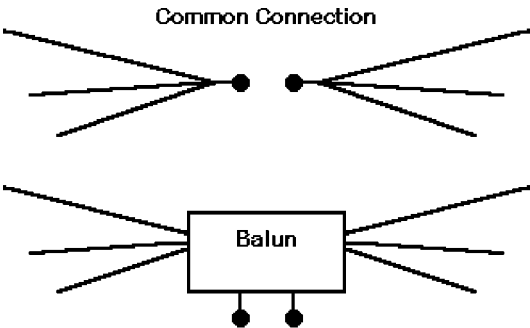
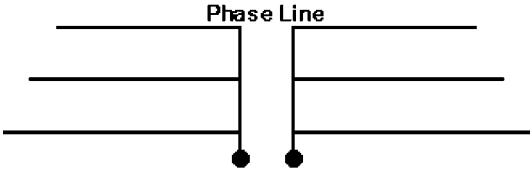


Fig. 6-2



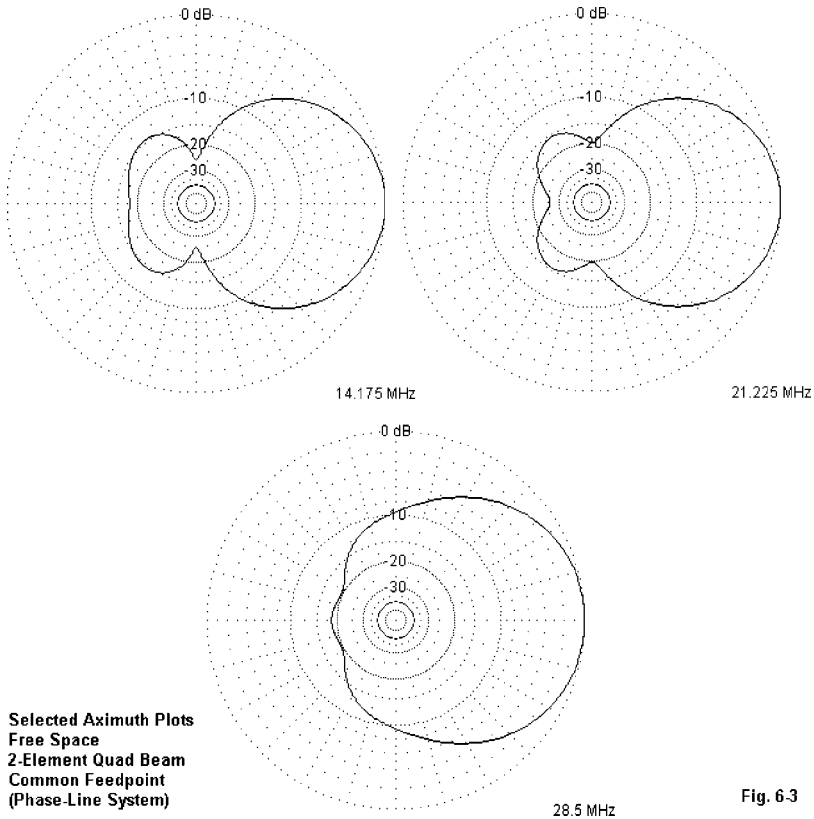
Typical Quad Common-Feed Systems

The feedpoint impedance for all bands at their design frequencies is close enough to 100 Ohms to presume that the coax line will be fed through a 2:1 balun of some sort. The modeled performance figures obtained from this arrangement are shown in **Table 6-3**.

Table 6-3. Key Performance Figures for the Phase-Line-Fed Quad

Frequency MHz	Free Space Gain dBi	Front-to-Back Ratio dB	Feedpoint Impedance R +/- jX Ohms
28.5	5.89	21.2	95 + j 36
24.95	7.26	27.1	121 + j 25
21.22	7.15	27.0	100 + j 6
18.12	7.21	24.3	97 - j 2
14.17	7.21	23.8	103 - j 20

The results will vary somewhat with the exact element dimensions. For the design used here, the low ends of the bands showed higher than acceptable SWR values. However, the most important thing to notice is the pattern shape, which is shown in free-space azimuth patterns for 20, 15, and 10 in **Fig. 6-3**.



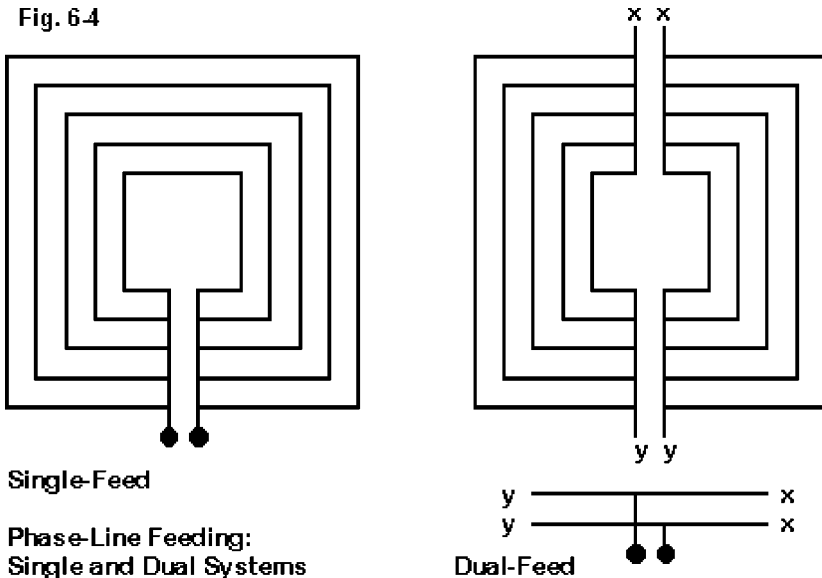
Typically, with any form of common feed, the first casualty is the front-to-side ratio. Remember that the patterns of **Fig. 6-3** are in free space, and the side nulls are reduced as the antenna is placed closer to the ground. However, on some bands, the side nulls disappear altogether with common-point quad feeding. If we begin with reduced front-to-side ratios, matters tend to become progressively worse with lower heights. The reduced front-to-side ratio is evident even at 20 meters and wholly disappears for 10 meters. The particularly poor front-to-side ratio at 10 meters results from the fact that with a

single common feed, the 20 meter element uses a significant portion of the fed 10-meter power and radiates at angles wide of the center line. The composite pattern for these two drivers (with minor affects from the 12-meter elements) gives us the 10-meter azimuth shape shown in **Fig. 6-3**, which also shows a reduction in gain relative to the separate feed system used in the initial model.

Many operators may find the pattern and lower 10-meter gain to be completely satisfactory: it is a matter of exchanging a bit of gain and pattern shape for the simplicity of a common feed system. Other operators, however, wish to pursue alternatives which avoid both the cost of a remote switch and the change of pattern shape.

Dual Phase Lines

In the search for a common feed with well-behaved patterns, we often overlook the fact that feeding a quad loop never yields perfect conditions on the top wire, that is, an element center with the same current magnitude and phase as at the center of the lower element. One way to overcome this imperfection is to feed both the top and bottom element centers. In this case, we shall use phasing lines to both sets of element centers, as shown in **Fig. 6-4**.



If the modeled loop is continuous, and modeled continuously “around the horn,” you will discover that the model calls for a half-twist in one of the feedline junction assemblies to achieve in-phase feeding. However, with dual feed, this convention of modeling--which is very useful with single-feed-point-per-loop systems--is not accurate. In reality, you must use an untwisted feed. More accurately, you should model dual-feed loops by beginning at the far left center (or far right center) and then model both upper and lower loop halves in the same direction. Then, the model will reflect reality in all details and the in-phase feeding will be straight-forward.

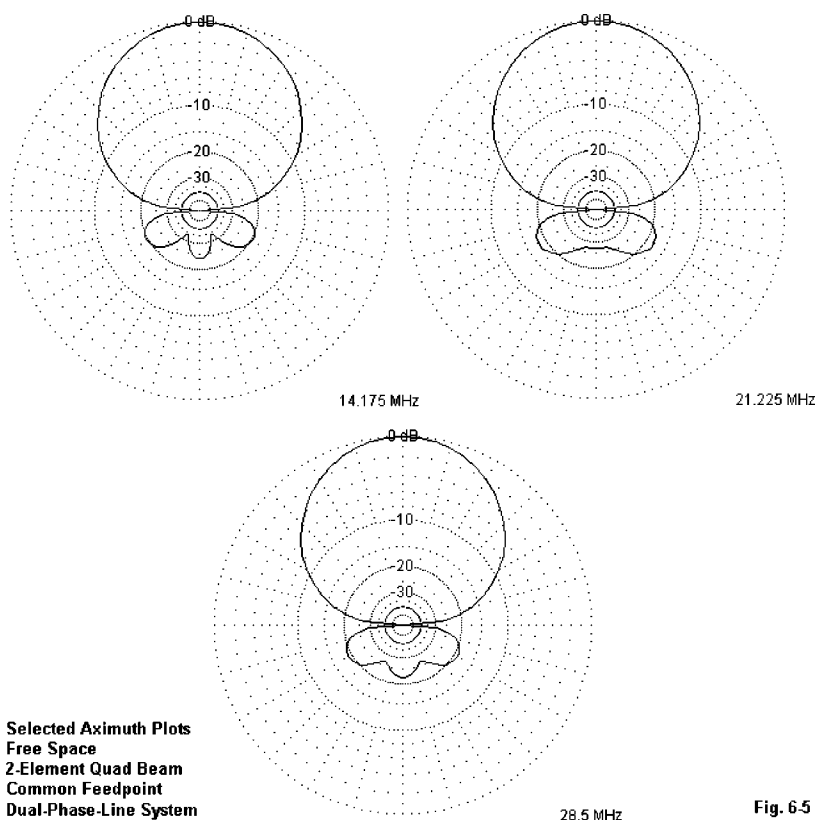
With the dual feed system, the result is an almost total absence of current on the 20 meter elements when 10-meter energy is fed to the system. As a result, we obtained the following results from the spider beam rearranged for two 150-Ohm phasing lines.

Table 6-4. Key Performance Figures for the Dual-Phase-Line-Fed Quad

Frequency MHz	Free Space Gain dBi	Front-to-Back Ratio dB	Feedpoint Impedance R +/- jX Ohms
28.5	7.77	22.1	104 + j 53
24.95	7.49	21.6	72 + j 35
21.22	7.20	27.0	57 + j 5
18.12	7.19	23.4	49 - j 14
14.17	7.27	23.5	77 + j 38

The results were obtained using 150-Ohm phase lines, with junction lines of 100 Ohms. At the design frequencies, the junction would be satisfactory for a 75-Ohm main cable for this particular exercise. However, the SWR bandwidth may not be satisfactory at the lower ends of the wider bands.

Despite these limitations, great strides have been made in the control of the patterns, as shown by the examples in **Fig. 6-5**. For all bands, the front-to-side ratios have been restored. As well, 10-meter performance has improved even beyond the level shown for independently fed drivers. However, I should add a reminder here that in none of the feed systems do we overcome the inherently narrow banded operating characteristics of a 2-element thin-wire quad, whether a monoband version or a multi-band array. The gain changes rapidly across the band, and the front-to-back ratio peaks above 20 dB only for a narrow band segment. These characteristics are inherent in the small diameter elements and the spacing used.

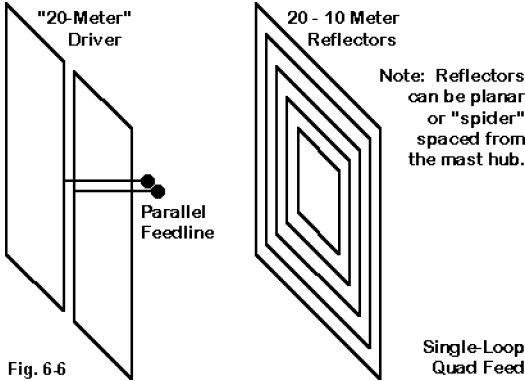


Not all versions of the dual-phase-line feed system for 2-element multi-band quad arrays will show impedances that combine for some sort of coaxial cable main feeder. However, in all cases, the system may be used with parallel feedline both as the phase-line connectors and as the main feedline. Of course, the user would need a balanced antenna tuner. Moreover, care must be taken in routing the parallel line so that it maintains an adequate distance from the tower or mast and so that it remains distant from the rotator housing as the antenna is turned throughout its cycle. These measures are not difficult to implement, but they may be initially foreign to those most used to handling coaxial feedlines.

Single-Loop Feed

If we are going to use a dual-feed system that puts the center of both the upper and the lower horizontal elements in phase--and if we are going to use

parallel feedline and a tuner in the process--than we might as well eliminate all but the 20-meter driver. With both horizontal elements fed in phase, the resonance of the driver element no longer matters. In fact, we may construct a quad array that resembles the simplified sketch in **Fig. 6-6**.



Such a system goes at least as far back as the 1969 work of DJ4VM and has been recently improved upon by Dr. Hartmut Waldner, DF6PW. Hartmut's version of the antenna--in operation--uses a diamond planar configuration. For my modeling investigations, I have applied the principle to the planar array of KC6T and to the 0.125λ -spaced spider array. In both cases, I simply removed all of the driver wires from the model except the ones for 20 meters. I then used 450-Ohm parallel line to feed the top and bottom horizontal sections of the remaining driver and took impedance readings at their junction. The exercise established that the principle may be applied with equal success to both planar and to spider arrays.

The results obtained from the spider array are in line with those from the DF6PW planar array and appear in **Table 6-5**. Note that the design-frequency performance values indicate that there is interaction among the reflector elements. The aim of the feed method is to obtain acceptable performance, but not to replicate the performance of the initial spider array.

Table 6-5. Key Performance Figures for the Single-Loop-Fed Quad

Frequency MHz	Free Space Gain dBi	Front-to-Back Ratio dB	Feedpoint Impedance R +/- jX Ohms
28.5	8.47	14.7	11 + j 51
24.95	8.40	15.0	14 - j 43
21.22	8.02	18.6	33 - j 180
18.12	7.72	20.1	187 - j 544
14.17	7.21	25.2	61 + j 270

Immediately apparent is the higher gain of the system as the frequency is increased. The cost of the higher gain is a loss of some front-to-back ratio from 15 through 10 meters. Only an individual operational goal analysis will

tell a prospective builder whether the trade-off is a reasonable one.

The patterns are well controlled on all bands, as shown in **Fig. 6-7**. Of course, the table makes clear that to obtain these values, the feed system must be based on parallel feedline and a balanced ATU. Indeed, Harmut reports that he has relieved his shack of considerable RF by rebuilding a network tuner into a balanced link-coupled tuner. The lines used in the model tests were 450-Ohm transmission lines. However, any parallel line should work about as well.

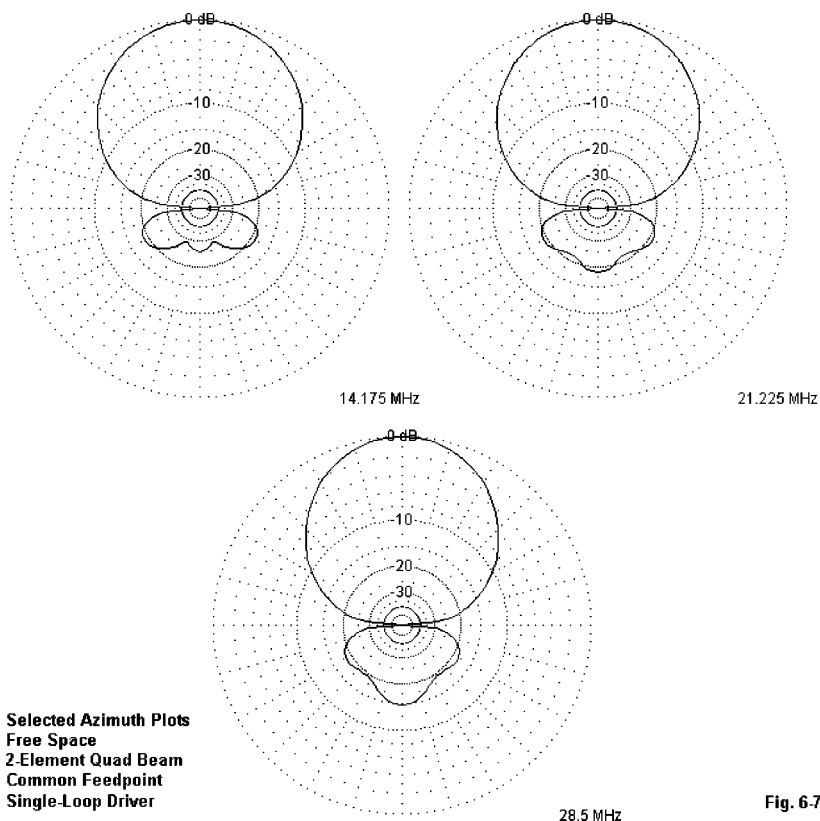


Fig. 6-7

Overcoming the upper band pattern distortion of a common-feed multi-band quad array, then, has more than one route to solution. For those wedded to coaxial cable feed techniques, the separately fed driver system will continue to be the most attractive. However, dual feed of the driver or drivers holds an equal potential for returning the quad patterns to good be-

havior on all bands. To sustain the desired peak front-to-back ratios, the dual phase lines to a full array of feeders may be the best route. For added upper band gain at the cost of some of the front-to-back ratio, the single loop driver can be attractive--especially since it does away with 4 ice-gathering wire loops in the array.

In none of the exercises did I make any modifications to the dimensions of any of the loops in the 0.125-wavelength spider array. I simply added phase lines and/or removed unneeded elements from one feed system to the next. Hence, I cannot say that the optimum performance has been achieved. It appears from initial modeling tests that closer-spaced arrays attain higher peak gains than more widely spaced arrays achieve from the single-driver system. Compared to planar arrays, there might be a slight greater advantage in using single-loop feed systems with the spider version, especially in terms of improving the operating bandwidth. However, the system is equally applicable to both types of designs.

Of course, for many operating purposes, the simpler system of combining feedlines in the most traditional ways may prove satisfactory. In antenna matters, there are always alternatives. Which system is superior requires careful measurement against operating goals and local circumstances by the potential user. These notes are simply a vehicle of making builders aware that there are alternative methods for achieving a combined feed for a multi-band 2-element quad array. Each alternative presents a set of challenges as well as a set of advantages.

7. Stacking 2-Element, 5-Band Quads

Because there appears to be interest in the stacking potential of quads, especially 2-element, 5-band quads, I decided to stack a pair of models and see what they would do. I used 24' spacing between array centers. I first ran the single array in free space, followed by the pair in free space, for a check on the relative gain and other performance properties. I then placed the lower quad 50' up and the higher 24' above that to see if ground would create any unusual or undesirable effects. Details of the dimensions of the quads used in this preliminary exploration of stacking appear in Chapter 5.

The KC6T Planar 5-Band Quad

The quads used in this initial run are models in NEC-4 of the KC6T quad in April, 1992 *QST* (p.52), one of the finest planar quad designs I have found with a constant 8' spacing, as shown in **Fig. 7-1**. It uses loading capacitance in the reflector to set the operating frequency. The loading capacitance is modeled throughout as a value of C rather than as a reactance so that the model will provide a more accurate view of the quad's operating bandwidth. The model drivers are self-resonant at the design frequency. The models have been set for the most desirable combination of gain, F-B, and impedance at mid-band to reveal the rate of change of these parameters both above and below the design frequency.

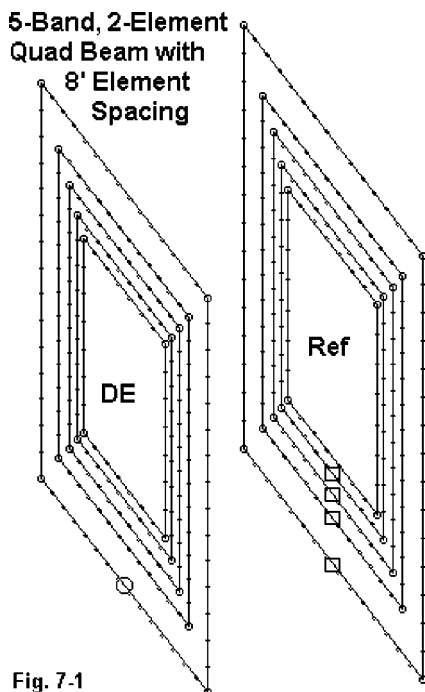


Fig. 7-1

Stack of 2 5-Band
2-Element Quads
24' Center-to-Center

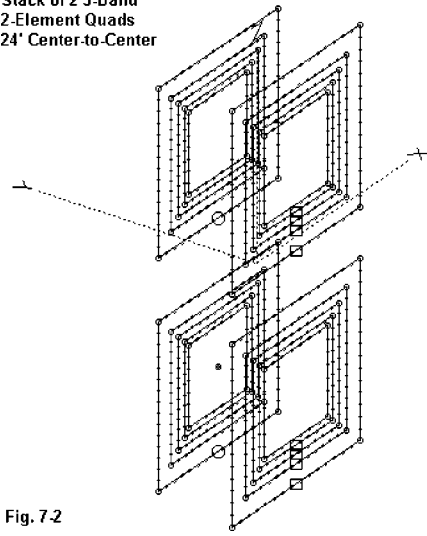


Fig. 7-2

Fig. 7-2 shows an outline of the stacked pair of planar quads.

The tabulated data consist of the gain in dBi, the take-off angle (where relevant), the front-to-back ratio in dB, the half-power (or -3 dB) beamwidth, the feedpoint impedances (as $R + jX$ Ohms), and the 75-Ohm SWR (for which the original array had been set). The data are for the band-edge and mid-band frequencies of the wider ham bands (20, 15, and 10 meters) and for the mid-point of the narrower bands (17 and 12 meters). Together, these data provide a fairly inclusive view of the performance of the antenna array when it consists of either a single beam or a pair of them in a stack.

Table 7-1. A Single KC6T Quad in Free Space

Frequency Mhz	Free-Space Gain dBi	Front-to-Back Ratio dB	Beamwidth Degrees	Feed Z $R + jX$	75-Ohm SWR
14.0	7.6	8.3	69	$34.7-j45.6$	3.10
14.175	7.2	24.0	73	$76.6+j 1.6$	1.03
14.35	6.4	11.6	76	$112.2+j 9.4$	1.52
18.118	7.3	31.7	74	$69.5+j 1.7$	1.08
21.0	7.7	12.6	72	$47.3-j30.0$	1.96
21.225	7.3	34.4	75	$69.5+j 1.7$	1.08
21.45	6.7	14.2	77	$89.6+j19.3$	1.34
24.94	7.2	30.6	76	$77.0+j 0.3$	1.03
28.0	7.7	14.5	75	$65.9-j54.2$	2.15
28.5	7.5	22.8	77	$75.4-j 0.3$	1.01
29	7.3	37.1	78	$87.1+j50.1$	1.87

Table 7-2. 2 KC6T Quads Stacked 24' Apart in Free Space

Note: Z1 (upper entry) = lower quad; Z2 (lower entry) = upper quad. Since both quads are fed on the lower element, some differentials in values are normal.

Frequency Mhz	Free-Space Gain dBi	Front-to-Back Ratio dB	Beamwidth Degrees	Feed Z R +/- jX	75-Ohm SWR
14.0	9.0	11.3	70	64.6-j18.9 66.7-j20.4	1.36 1.30
14.175	8.8	20.4	73	120.8+j23.2 117.2+j13.5	1.70 1.60
14.35	8.3	12.4	75	164.8+j14.3 154.2+j12.3	2.22 2.07
18.118	9.5	21.5	73	86.8+j 3.6 85.9+j 4.1	1.17 1.16
21.0	10.1	12.9	72	56.3-j29.9 56.1-j29.6	1.71 1.71
21.225	9.9	22.3	75	81.3+j 1.3 81.1+j 1.8	1.09 1.09
21.45	9.5	13.3	77	104.1+j14.6 104.2+j15.2	1.44 1.45
24.94	10.2	23.1	77	84.1-j 5.0 84.6-j 4.9	1.14 1.15
28.0	10.8	15.1	75	70.0-j57.0 70.2-j56.7	2.16 2.15
28.5	10.7	23.5	77	79.7-j 2.2 79.9-j 2.0	1.07 1.07
29	10.5	26.8	78	92.5+j48.6 92.7+j48.9	1.84 1.85

Table 7-3. Stacking Gain Averaged by Bands

Band	20	17	15	12	10	Meters
Stacking Gain	1.6	2.2	2.6	3.0	3.2	dB

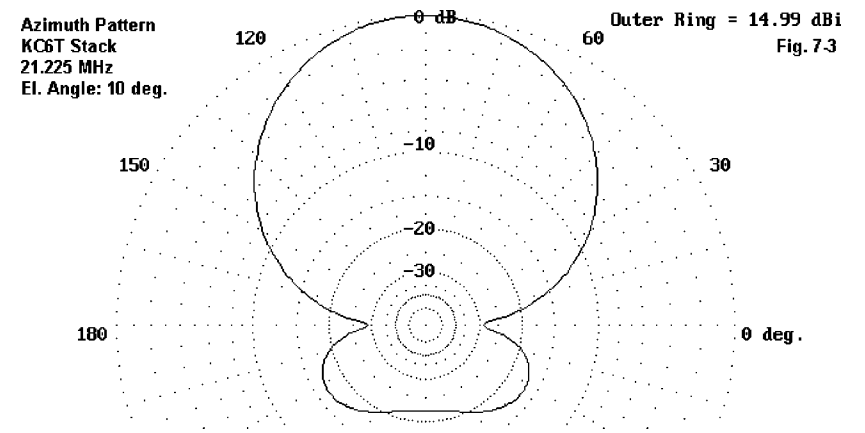
Table 7-4. 2 KC6T Quads Stacked 24' Apart at 50' and 74'

Note: Model uses average ground; Z1 (upper entry) = lower quad; Z2 (lower entry) = upper quad. Since both quads are fed on the lower element, some differentials in values are normal.

Frequency Mhz	Free-Space Gain dBi	Front-to-Back Ratio dB	B/W Deg.	Feed Z R +/- jX	75-Ohm SWR	TO Deg.
14.0	13.6	11.7	71	64.2-j19.1 66.6-j20.0	1.37 1.36	15
14.175	13.4	20.5	74	117.0+j19.6 120.1+j18.5	1.63 1.66	14
14.35	13.0	12.1	76	156.4+j20.5 162.8+j 8.5	2.13 2.18	14

18.118	14.4	21.6	74	87.7+j 4.5 85.3+j 3.5	1.18 1.15	11
21.0	15.1	13.1	72	56.7-j29.8 55.8-j29.7	1.70 1.72	10
21.225	15.0	22.0	75	82.3+j 1.1 80.5+j 2.1	1.10 1.08	10
21.45	14.6	13.1	78	105.1+j13.4 103.8+j16.3	1.45 1.45	10
24.94	15.4	22.1	77	82.7-j 5.8 86.2-j 5.5'	1.13 1.17	8
28.0	15.9	14.9	75	69.1-j56.1 69.3-j57.5	2.15 2.18	8
28.5	15.8	22.9	77	79.3-j 0.9 78.7-j 1.9	1.06 1.06	7
29	15.7	26.5	79	92.7+j50.2 91.8+j49.6	1.87 1.86	7

For reference, **Fig. 7-3** shows the azimuth pattern at mid-band in 15 meters for the stacked array over ground.



As is clearly evident, the particular quad design explored here does not suffer from being placed over ground at 50' for the center of the bottom array and at 74' for the center of the top array. The front-to-back and impedance values hold closely to their free-space values--sufficiently so that I could not think of a design change to recommend. In addition, stacking appears to shift the operating parameters to provide operating bandwidth in the stack that is superior to that of the single array. Assuming that an in-phase feedline harness can be devised, the coax run should bring virtually all SWR values un-

der 2:1 at the shack. For the stacks, they are all well within rig-tuner range without excessive loss.

A 0.174 λ Spaced Spider Quad

In any investigation, one sample is not sufficient for developing even tentative conclusions. In fact, I have run the exercise just shown for several 5-band, 2-element quads, with similar results. Perhaps a single further example, using a divergent multi-band quad design, will show what is typical for these runs.

The following data apply to a stack of 2 spider-construction 2-element, 5-band quads, spaced 24' center-to-center. The element spacing of this model is 0.174 wavelength. The spacing is wider than most commercial spider quads, which range from about 0.11 to 0.13 wavelength. An outline appears in **Fig. 7-4**. Clear in the sketch are the reflector loads, similar to those used on the KC6T model. See Chapter 5 for the details of this array.

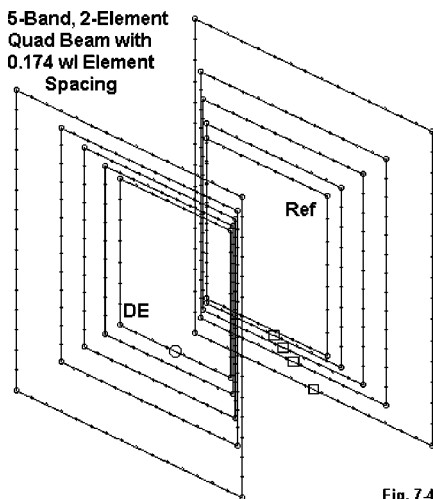


Fig. 7-4

Stack of 2 5-Band
2-Element Quads
24' Center-to-Center

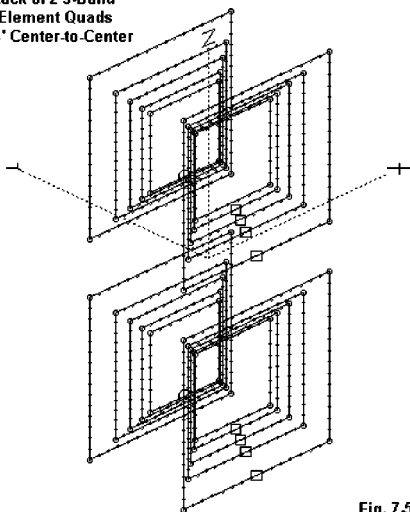


Fig. 7-5

We shall follow the same plan as we used with the KC6T planar quad model. The series of tables begin with data for a single array in free space, followed by a stack of 2 in free space. The last table places the antennas at 50' and 74', respectively, above good soil. **Fig. 7-5** shows the outline of the pair of spider quads in their stack.

As with the KC6T planar quad model, the tabulated data for the spider quad consist of the gain in dBi, the take-off angle (where relevant), the front-to-back ratio in dB,

the half-power (or -3 dB) beamwidth, the feedpoint impedances (as $R \pm jX$ Ohms), and the 75-Ohm SWR (for which the original array had been set). The data are for the band-edge and mid-band frequencies of the wider ham bands (20, 15, and 10 meters) and for the mid-point of the narrower bands (17 and 12 meters). Together, these data provide a fairly inclusive view of the performance of the antenna array when it consists of either a single beam or a pair of them in a stack.

Table 7-5. A Single 0.174 λ Spider Quad in Free Space

Frequency Mhz	Free-Space Gain dBi	Front-to-Back Ratio dB	Beamwidth Degrees	Feed Z $R \pm jX$	75-Ohm SWR
14.0	7.6	9.2	71	76.6-j22.8	1.35
14.175	7.1	23.4	75	117.3-j 2.1	1.57
14.35	6.3	11.8	79	129.7-j 1.7	1.73
18.118	7.1	25.3	76	92.8+j 8.7	1.27
21.0	7.6	12.0	73	53.1-j13.5	1.50
21.225	7.1	29.1	77	79.7+j20.2	1.31
21.45	6.5	14.3	80	105.8+j36.5	1.70
24.94	7.0	29.8	76	69.3+j 2.2	1.09
28.0	7.4	20.4	77	48.5-j39.8	2.17
28.5	7.2	32.1	79	58.5+j16.7	1.42
29	6.9	18.1	81	70.5+j70.1	2.54

Table 7-6. 2 0.174 λ Spider Quads Stacked 24' Apart in Free Space

Note: Z1 (upper entry) = lower quad; Z2 (lower entry) = upper quad. Since both quads are fed on the lower element, some differentials in values are normal.

Frequency Mhz	Free-Space Gain dBi	Front-to-Back Ratio dB	Beamwidth Degrees	Feed Z $R \pm jX$	75-Ohm SWR
14.0	8.9	11.4	72	131.1-j 1.3 136.4-j14.9	1.83 1.85
14.175	8.7	26.4	75	196.0-j 4.7 170.9-j 9.5	2.61 2.29
14.35	8.2	16.4	78	196.9-j32.2 180.6-j18.0	2.71 2.44
18.118	9.4	26.4	76	119.5+j10.0 117.9+j11.0	1.61 1.59
21.0	10.0	12.3	73	62.5-j10.7 62.2-j10.5	1.27 1.27
21.225	9.8	30.3	77	93.6+j24.4 93.1+j24.7	1.44 1.44
21.45	9.3	14.3	80	126.9+j35.9	1.89

				126.5+j36.6	1.89
24.94	10.1	33.1	78	76.3+j 1.4	1.03
				76.7+j 1.6	1.03
28.0	10.5	20.2	77	49.9-j39.5	2.11
				50.1-j39.3	2.10
28.5	10.3	26.4	79	60.1+j18.5	1.42
				60.2+j18.7	1.42
29	10.1	17.9	81	73.2+j73.7	2.61
				73.3+j74.1	2.62

Table 7-7. Stacking Gain Averaged by Bands

Band	20	17	15	12	10	Meters
Stacking Gain	1.6	2.2	2.7	3.0	3.3	dB

Table 7-8. 2 0.174 λ Spider Quads Stacked 24' Apart at 50' and 74'

Note: Model uses average ground; Z1 (upper entry) = lower quad; Z2 (lower entry) = upper quad. Since both quads are fed on the lower element, some differentials in values are normal.

Frequency Mhz	Free-Space Gain dBi	Front-to-Back Ratio dB	B/W Deg.	Feed Z R +/- jX	75-Ohm SWR	TO Deg.
14.0	13.6	11.8	73	135.1-j 3.0	1.80	15
				137.6-j11.6	1.85	
14.175	13.4	28.7	76	183.4+j 0.3	2.45	14
				182.1-j11.4	2.44	
14.35	12.9	15.8	79	197.1-j16.3	2.65	14
				182.9-j29.1	2.51	
18.118	14.3	28.1	76	121.3+j11.0	1.64	12
				116.6+j10.3	1.56	
21.0	15.0	12.6	74	62.9-j10.4	1.26	10
				61.8-j10.6	1.28	
21.225	14.9	29.6	77	94.9+j24.4	1.45	10
				92.1+j25.0	1.44	
21.45	14.4	14.0	80	18.5+j34.6	1.89	10
				125.7+j38.2	1.90	
24.94	15.3	29.8	78	75.5+j 0.2	1.01	9
				78.0+j 1.7	1.05	
28.0	15.7	19.9	77	49.1-j38.9	2.12	8
				49.4-j39.8	2.14	
28.5	15.5	25.5	79	59.6+j19.5	1.49	7
				59.3+j18.8	1.44	
29	15.4	17.5	81	73.2+j75.0	2.65	7
				72.7+j74.6	2.64	

The main line of the numbers for the spider quad are similar to those of the planar quad. However, certain deviations are worth noting. First, the spider quad impedance values for the upper and lower antennas vary somewhat more than comparable figures for the planar model. It would appear that especially the lower bands (17 and most radically 20 meters) are susceptible to changes. Second, the 20-meter--and to a lesser extent, the 10-meter--antennas alter impedance values when placed into the stack--enough to require retuning of these portions of the arrays. The spider construction gives the impression that either it leaves the individual band elements more exposed to external influence or that the planar quad is more immune to external influence--perhaps two ways of saying the same thing. The bottom line remains that spider construction quads are likely to need more than a little reformulation when placed in a closely spaced stack.

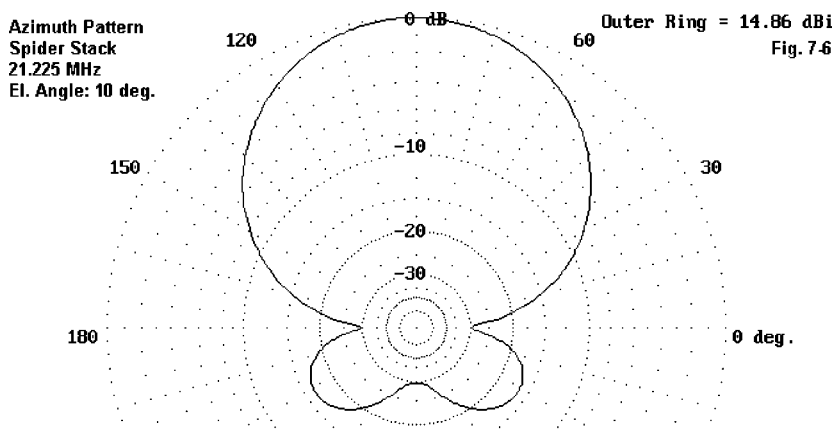


Fig. 7-6 shows the 15-meter azimuth pattern at mid-band over ground for reference.

A 0.125 λ Spaced Spider Quad

The following data apply to a stack of 2 spider-construction 2-element, 5-band quads, spaced 24' center-to-center. The element spacing of this model is 0.125 wavelength, narrower than the preceding spider quad and closer to commercial implementations of the design, which range from about 0.11 to 0.13 wavelength. An outline appearing in **Fig. 7-4** is close enough to the present design not to need a new sketch, although this design uses exactly pruned reflectors with no loading. See Chapter 5 for details of the array.

As with the other models, the series of tables begin with data for a single

array in free space, followed by a stack of 2 in free space. The last table places the antennas at 50' and 74', respectively, above good soil.

The data consist of gain in dBi, TO angle (where relevant), F-B, beamwidth, and feed Z(s). Due to the variability of the feedpoint impedances, an SWR column would be meaningless and has been omitted.

Table 7-9. A Single 0.125 λ Spider Quad in Free Space

Frequency Mhz	Free-Space Gain dBi	Front-to-Back Ratio dB	Beamwidth Degrees	Feed Z R +/- jX
14.0	7.6	7.6	69	40.6-j45.1
14.175	7.2	28.9	73	84.2-j 0.1
14.35	6.4	12.8	76	117.7+j 5.6
18.118	7.2	32.4	73	60.9-j 0.5
21.0	7.6	12.0	71	31.5-j38.6
21.225	7.2	24.7	74	52.9+j 0.2
21.45	6.6	12.3	77	76.4+j24.5
24.94	7.3	25.8	74	41.5+j 0.1
28.0	7.8	13.7	72	30.9-j61.1
28.5	7.5	20.3	74	40.0-j 0.3
29	7.2	15.6	76	50.4+j54.7

Table 7-10. 2 0.125 λ Spider Quads Stacked 24' Apart in Free Space

Note: Z1 (upper entry) = lower quad; Z2 (lower entry) = upper quad. Since both quads are fed on the lower element, some differentials in values are normal.

Frequency Mhz	Free-Space Gain dBi	Front-to-Back Ratio dB	Beamwidth Degrees	Feed Z R +/- jX
14.0	8.9	9.6	70	72.1-j18.4 73.2-j20.7
14.175	8.8	22.2	73	130.0+j24.9 126.5+j13.3
14.35	8.3	14.8	76	180.0+j13.6 163.1-j 9.3
18.118	9.4	21.1	73	74.3+j 5.3 73.5+j 5.0
21.0	10.0	11.8	71	36.8-j37.4 36.7-j37.4
21.225	9.8	19.3	74	60.3+j 3.0 60.0+j 3.0
21.45	9.4	11.7	77	88.7+j25.7 88.2+j26.0

24.94	10.3	21.1	74	45.4-j 0.8 45.3-j 0.7
28.0	10.8	13.8	72	32.1-j62.4 32.3-j62.3
28.5	10.6	18.1	74	41.5-j 0.9 41.6-j 0.7
29	10.4	14.1	76	52.6+j54.5 52.7+j54.7

Table 7-11. Stacking Gain Averaged by Bands

Band	20	17	15	12	10	Meters
Stacking Gain	1.6	2.2	2.6	3.0	3.1	dB

Table 7-12. 2 0.125 λ Spider Quads Stacked 24' Apart at 50' and 74'

Note: Model uses average ground; Z1 (upper entry) = lower quad; Z2 (lower entry) = upper quad.

Frequency Mhz	Free-Space Gain dBi	Front-to-Back Ratio dB	B/W Deg.	Feed Z R +/- jX	TO Deg.
14.0	13.6	9.8	70	71.6-j18.7 73.1-j20.0	14
14.175	13.5	23.0	74	125.2+j21.4 130.6+j18.3	14
14.35	13.0	14.3	76	170.4+j21.6 172.2+j 4.0	14
18.118	14.4	21.3	74	74.8+j 6.3 73.2+j 4.2	11
21.0	15.0	11.9	71	37.0-j37.2 36.6-j37.4	10
21.225	14.9	19.0	75	61.0+j 3.2 59.5+j 3.0	10
21.45	14.5	11.5	77	90.0+j25.2 87.4+j26.7	10
24.94	15.4	20.9	74	45.1-j 1.5 9 46.0-j 0.5	
28.0	15.9	13.7	72	31.8-j62.0 31.9-j62.6	8
28.5	15.7	17.8	74	41.3-j 0.2 7 40.9-j 0.8	
29	15.6	14.0	76	52.6+j55.4 52.1+j55.1	7

The narrower spacing of the 0.125 λ spider design results in a narrower operating bandwidth, which shows up most clearly in the front-to-back curves

that one can infer from the data. As well, when stacked, the sharp peak of the front-to-back curve does not need to be displaced much to appear as a significantly lower mid-band value, as in the charts for stacked versions of the design.

One disadvantage of the more closely spaced spider design is that equal excursions of reactance across any given band--relative to the wider-spaced spider--will result in steeper SWR curves, due to the lower initial resistive component of the feedpoint impedance. As a result, the problem of obtaining a good match for all portions of all five bands may become a major challenge.

Wider Stack Spacing

Experimental modeling with larger quad arrays in stacks suggests that wider spacing may effect greater isolation between bays. The initial 24' spacing is between 5/8 and 2/3 wavelength on 20 meters--and proportionally greater on the other bands. Hence, the major effect of modest increases in spacing from one array center to the other would be primarily on 20 and 17 meters.

Therefore, I reran the 0.125-wavelength spider array with a spacing of 30' or about 5/6 wavelength on 20 meters. I will provide the entire data set, including the single array free space information, to ease the process of making internal comparisons within the data. However, comparisons with the preceding data set are also very relevant to deciding what spacing may be best for this type of quad array.

Table 7-13. A Single 0.125 λ Spider Quad in Free Space

Frequency Mhz	Free-Space Gain dBi	Front-to-Back Ratio dB	Beamwidth Degrees	Feed Z R +/- jX
14.0	7.6	7.6	69	40.6-j45.1
14.175	7.2	28.9	73	84.2-j 0.1
14.35	6.4	12.8	76	117.7+j 5.6
18.118	7.2	32.4	73	60.9-j 0.5
21.0	7.6	12.0	71	31.5-j38.6
21.225	7.2	24.7	74	52.9+j 0.2
21.45	6.6	12.3	77	76.4+j24.5
24.94	7.3	25.8	74	41.5+j 0.1
28.0	7.8	13.7	72	30.9-j61.1
28.5	7.5	20.3	74	40.0-j 0.3
29	7.2	15.6	76	50.4+j54.7

Table 7-14. 2 0.125 λ Spider Quads Stacked 30' Apart in Free Space

Note: Z1 (upper entry) = lower quad; Z2 (lower entry) = upper quad. Since both quads are fed on the lower element, some differentials in values are normal.

Frequency Mhz	Free-Space Gain dBi	Front-to-Back Ratio dB	Beamwidth Degrees	Feed Z R +/- jX
14.0	9.3	7.7	69	57.2-j39.2 56.8-j39.7
14.175	9.4	18.5	73	109.5+j 6.9 106.9+j 6.5
14.35	8.9	14.5	76	156.0-j 0.1 153.3+j 3.1
18.118	10.1	19.8	74	71.3-j 0.7 71.1-j 0.4
21.0	10.6	12.6	71	34.9-j39.9 34.9-j40.0
21.225	10.4	17.8	75	59.6-j 1.7 59.6-j 1.6
21.45	9.9	10.5	77	85.7+j17.4 85.7+j17.5
24.94	10.7	23.0	74	43.5-j 2.6 43.5-j 2.6
28.0	11.1	15.0	72	31.4-j62.3 31.4-j62.4
28.5	10.9	18.4	75	41.7-j 1.8 41.7-j 1.8
29	10.7	13.3	76	53.2+j51.9 53.3+j51.9

Table 7-15. Stacking Gain Averaged by Bands

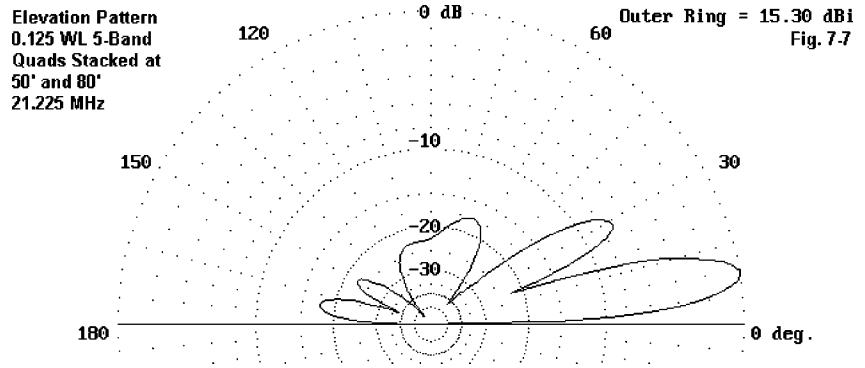
Band	20	17	15	12	10	Meters
Stacking Gain	2.1	2.8	3.2	3.3	3.4	dB

Table 7-16. 2 0.125 λ Spider Quads Stacked 30' Apart at 50' and 80'

Note: Model uses average ground; Z1 (upper entry) = lower quad; Z2 (lower entry) = upper quad. Since both quads are fed on the lower element, some differentials in values are normal.

Frequency Mhz	Free-Space Gain dBi	Front-to-Back Ratio dB	B/W Deg.	Feed Z R +/- jX	TO Deg.
14.0	13.9	8.0	70	56.8-j39.4 57.1-j39.3	14
14.175	14.0	19.2	73	106.7+j 6.5 109.1+j 7.1	14
14.35	13.5	14.0	76	153.1+j 3.8 155.6+j 0.0	13

18.118	14.9	20.0	74	70.9+j 0.3 71.1-j 1.2	11
21.0	15.5	12.6	71	35.2-j39.7 34.5-j39.9	9
21.225	15.3	17.5	76	60.9-j 1.2 9 58.6-j 0.9	
21.45	14.8	10.4	78	87.7+j16.6 85.5+j19.7	9
24.94	15.7	22.6	75	42.9-j 3.4 8 44.2-j 3.4	
28.0	16.2	14.7	72	31.1-j62.0 31.0-j62.1	7
28.5	16.0	18.0	75	41.3-j 1.0 7 41.4-j 1.3	
29	15.8	13.1	77	52.2+j53.1 53.4+j52.6	7



For reference, **Fig. 7-7** shows the elevation pattern of the 30' stack at 50' and 80' above average ground for the 0.125 λ spaced 2-element, 5-band quads at 21.225 MHz.

The changes created by increasing the spacing are subtle. Increasing the height of the overall array by 6' changes the TO angle by only a fraction of a degree on any one band. If the change shows up in the chart, it is largely a function of rounding to the nearest degree. Gain is up, more on the lower bands than on the upper, but always under an average of a half dB relative to 24' spacing. The front-to-back ratio appears to be down slightly--or the peak may have shifted in frequency so that it no longer coincides with the design frequency.

The chief merit of increasing the center-to-center spacing of the arrays to 30' shows up in the impedance column. First, the impedance values are closer to those for the single array in free space. Second, the differentials between upper and lower bay impedances are reduced. The latter effect is greater on the lowest bands but is evident to some degree on all bands. The benefit of this change from the more closely spaced stack is that once you have achieved the best arrangement for matching the main feedline to the drivers for an individual array, you can rely on that arrangement to satisfy the needs of the stack.

On paper, the added 6' of stacking space may seem little. However, two consequences are notable. First, the added 6' of space doubles the separation between the upper wire of the lower array and the lower wire of the upper array. Second, the added 6' of spacing can make significant differences in bending forces on the stack mast. Whether it is wiser to shorten the stack and wrestle with the matching or to be assured of matching and increase the strength (and weight) of the mast is a stacker's decision.

Conclusion

I have been hesitant in the past to recommend stacking multi-band quads, given the fact that a quad is already a stack in itself. However, these figures suggest that--if one can handle the matching, the mechanicals, and the weather--the enterprise may prove worthy, even with relatively close spacing, as used in these models. The results--so far--suggest that planar designs may be the best behaved in a closely spaced stack in the sense of needing the least post-stacking adjustments.

There has been a predilection to overestimate the desirability (at least electrically) of the spider design because it provides each band with the same spacing in terms of wavelengths. However, as noted in Chapter 5, that intuition of benefit encompasses only part of what is going on with a 5-band 2-element quad. Element interaction plays a role in giving the planar design a degree of stability from band to band. As well, the gain is reduced as we move the elements from a single plane into a spider configuration. Indeed, there are limits to this process, and these show up in 3-element designs and in efforts to add VHF frequencies to planar quads using the existing support arms. The mechanical differences in the schemes are, of course, beyond the scope of this modeling study.

The variety of models and stacking distances used in the preliminary study

may provide some guidance. As always, differences of design may yield different stacking results. In addition, different stacking spacings also may yield performance differences. These results apply strictly only to the 5-band quads modeled, using separate or switched feeds. Common feed system stacking results have not yet been explored. Every proposed design should be thoroughly modeled before capital investment.

8. Separately Feeding Multi-Band Quads

A persistent question about multi-band quads, whether 2-element models or larger, is the proper way to feed them. There are several questions associated with this basic inquiry, but only a few have I been able so far to shed any light on through the models in my collection. But perhaps it is worth a note or two on the question to reveal how far I have gotten so far.

Common Feed

In my collection of models, I have found no way to develop a fully successful model with a single common feedpoint for all bands. I have not found a simple placement of feed position that permits all drivers to be brought to this point and still yield a set of patterns and source impedances that are satisfactory. By “satisfactory,” I mean that the resultant patterns are for all of the bands covered by the multi-band array very close to those that result from using a system of separate feeds for each driver. Common feed system—short of feeding both the top and bottom wires of each driver with phasing lines and a system for in-phase feeding as described in Chapter 6—tend to yield somewhat distorted patterns on at least 10 meters and sometimes on other bands.

The strongest interactions in 2-element multi-band quads appear to be these: 20 vs. 10 meters when 10-meters is active; 12 vs. 10 meters when 10 meters is active.

I have modeled 2-band combinations of 12 and 10 meter quads. I am not satisfied with the results, even though the source position distorts the driver loop shapes the least of all combinations. Finding dimensions that will yield good free space patterns and usable feedpoints on both bands is not easy. The 12-meter driver acts like a 10-meter reflector, but one that either surrounds the 10-meter driver or is ahead of it. The 10-meter reflector acts like a 12-meter director, in conflict with the 12-meter reflector. Although I have been able to stabilize 12-meter performance in models, 10-meters still eludes me.

I have also modeled common-feed 20-10-meter combinations. Here, the

problem appears to differ. The 10- and 20-meter drivers interact when 10 is driven, because the 20 meter driver is about 2λ long and has a low impedance--something like 200 Ohms, when the 20 meter quad is driven on 10 meters in a monoband configuration. The combination on 10 meters not only shows angular side bulges, in line with the pattern of a 2λ loop, but as well is sensitive to the loop distortions created by the common feed position between the two drivers. In free space, the patterns tilt downward by a considerable degree.

In a five-band common-feed quad, I have found no satisfactory arrangement that will yield patterns and impedances good on all bands. So far, when the patterns look reasonably clean (meaning that they are similar to the patterns of monoband quads), the impedances become unworkable, and vice versa.

These notes do not mean that there is no satisfactory arrangement. That is why I have shown no figures here. The net result simply means that I have found no such arrangement, if it exists. However, my criteria are fairly stringent. For an arrangement to be satisfactory, the quad must on all bands have a satisfactory pattern and a satisfactory source impedance. There is some allowable latitude in the impedances that might be acceptable, but the patterns must approach the standards set by quad models using separate feed points for each band. So far, I must admit failure in this quest.

Nonetheless, one or more of the common feed systems shown in Chapter 6—or variants of them—may yield results that are reasonably well matched to the operational needs of any given builder. The stringent standards used for this study are not absolute, since every decision on antenna design must be measured against a set of criteria determined by the goals of the system.

Remotely Switched Independent Feedpoints

A multi-band quad may be fed through a couple of arrangements using a remote switching system. Perhaps the most common system is to run a section of feedline from each loop to a central remote switch and relay system. **Fig. 8-1** illustrates such a system in simplified (3-band) form.

Key to this system is that the unused lines are completely open. Neither their braid nor their center conductors are connected to anything, including the box or each other. Each line, by standard design, is $1/4\lambda$ long at the operating frequency of the unused driver. Depending upon the placement of the remote switch, one may need to use either 0.66 or 0.78 VF feedline to get

the closest approximation of the right length (without coming up short).

The benefit of this system is that all relays are enclosed in a single box that can be effectively weather-proofed (while allowing drainage or evaporation of condensation). Whether this system has disadvantages, we shall examine shortly.

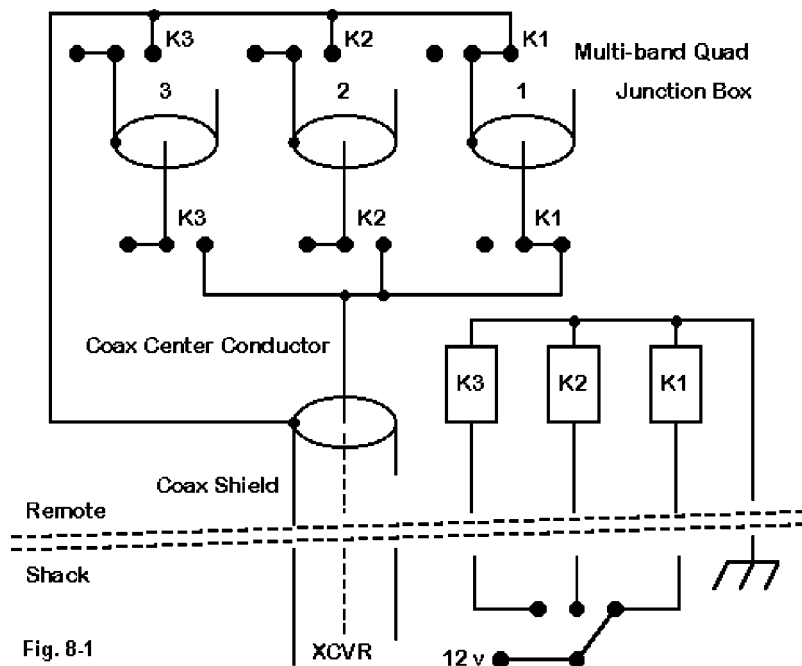


Fig. 8-1

A second system involves shorting the feedpoint of each driven loop right at the feedpoint itself, as illustrated in **Fig. 8-2**.

In this system, a weatherproofed relay is positioned at the feedpoint. The relays can be "normally closed" types so that the loops are shorted without power to the system. The only energized relay is located at the active driven element. It is opened, thus allowing the feedline to be in series with the element loop.

This system assures that the unused driver loops are closed--a condition generally considered to be more optimal for achieving good quad patterns and usable source impedances. However, the weight and exposure of the relays when placed at the sources makes this system somewhat more of a mechanical design problem than the single remote box and $1/4 \lambda$ stubs. It

entails in most designs the use of a separate feedline for each band--or a secondary switching system for the feedline.

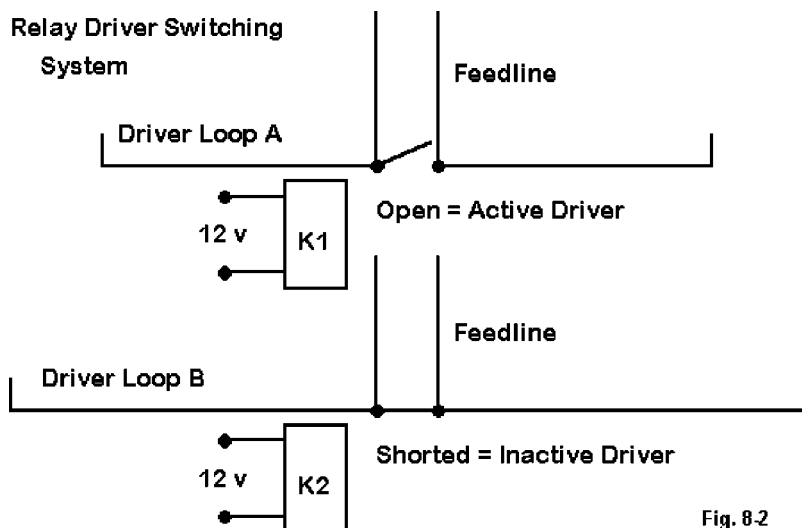


Fig. 8.2

As a consequence of this complexity, the most common design for separately feeding each band of a multi-band quad has been the central switching box and $1/4 \lambda$ stubs. However, there are still a few questions which we might pose about this system:

1. Do we need the stubs to be open-ended to create a short across the loop?

2. Since the stubs will be $1/4 \lambda$ long at the frequency for which the driver is tuned, will they effectively short the loop when the quad is operated at other frequencies?

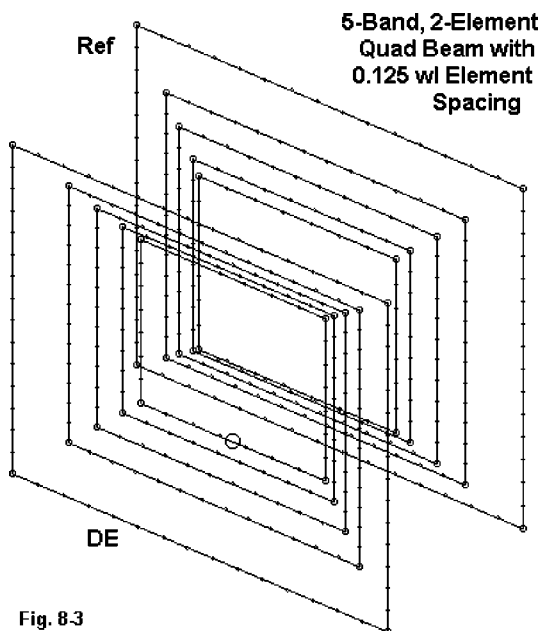


Fig. 8.3

To look into these questions together, I remodeled a couple of 2-element multi-band quads that we looked at in Chapter 5. One was the study quad that used a constant 0.125λ spacing between elements. This is a version of the spider-type quad in which elements for lower bands are both ahead and behind elements for higher bands. The second was the KC6T design that uses an 8' boom for all bands, along with capacitive reflector loading. Although 2 models might not be exhaustive as a study, the pair may give us some suggestive results.

2-Element, 5-Band Quad with 0.125λ Spacing

The 2-element, 5-band, 0.125λ spaced quad has the general appearance shown in **Fig. 8-3**. Consult Chapter 5 for the band-by-band dimensions of the model.

The data I collected from this model come in 3 parts which I shall present in tabular form. First, in **Table 8-1**, is the performance data for the model with the unused driver loops closed. The data include the free-space gain in dBi, the 180-degree front-to-back ratio in dB, and the source impedance in Ohms.

Table 8-1. Performance With Unused Loops Closed

Frequency in MHz	Gain in dBi	Front-to-Back Ratio in dB	Source Impedance (R +/- jX Ohms)
28.5	7.48	20.28	40.0 - j 0.3
24.94	7.32	25.83	41.5 + j 0.1
21.225	7.16	24.70	52.9 + j 0.2
18.118	7.23	32.38	60.9 - j 0.5
14.175	7.23	28.92	84.2 - j 0.1

We may consider this table our base-line data set against which we may compare data from modeling variations.

The first variation was to connect a $1/4 \lambda$ line to each driver. The other end of the line of the active driver element was brought to a very short wire used as the remote source point. For this exercise, the TL facility of NEC-4 was used, so the lines are handled as mathematical lines, not as physical lines that may play a desired or undesired role in far field pattern formation. Two subvariations were used. In one, each unused line was set as an open line, which uses a very remote wire and a specified very high impedance (or very low admittance) to create the open circuit. The second subvariation used a remote short, thin wire that serves as the source wire when the ele-

ment is active. Inactive lines are simply connected to their unique wires without a source. The results between the two systems varied only in the hundredths column of the model output reports, and so only one set of data will be given.

For reference, the line lengths used appear in **Table 8-2**, where the Frequency column indicates the driver element to which a given transmission line stub is connected.

Table 8-2. Stub Lengths for Unused Drivers

Frequency Band	Stub Length in feet	Stub Length in inches
10	8.628	103.54
12	9.859	118.31
15	11.585	139.02
17	13.717	164.60
20	17.347	208.16

In each case, the source impedance of the element when driven was used as the line characteristic impedance (rather than using some common figure, such as 75 Ohms). The lines use a VF of 1.0, since line loss variations cannot be determined by NEC. Actual lines would be shortened in accord with the actual velocity factor of the line used.

With the unused lines left open, the performance figures in **Table 8-3** were reported by NEC-4.

Table 8-3. Performance With Unused Lines Open

Frequency in MHz	Gain in dBi	Front-to-Back Ratio in dB	Source Impedance (R +/- jX Ohms)
28.5	7.43	20.10	39.2 + j 0.0
24.94	7.33	25.64	41.0 - j 0.0
21.225	7.17	25.02	51.6 - j 0.7
18.118	7.23	32.12	60.0 + j 0.7
14.175	7.23	28.85	85.6 - j 0.1

To the degree that NEC can model the situation, the use of $1/4 \lambda$ lines--each set to the operating frequency of the driver--that are open at the remote switch point creates virtually no change in the patterns or the source impedances of the 2-element multi-band quad on any band. For this model, at least, it does not matter that the lines are not $1/4 \lambda$ long at the frequency of current operation. They provide sufficient closure to allow standard performance on each

band.

The second variation set each unused driver line (without any other change to the line) at a remote short circuit. In principle, this would open the unused driver loops. The results reported by NEC-4 are recorded in **Table 8-4**.

Table 8-4. Performance With Unused Lines Shorted

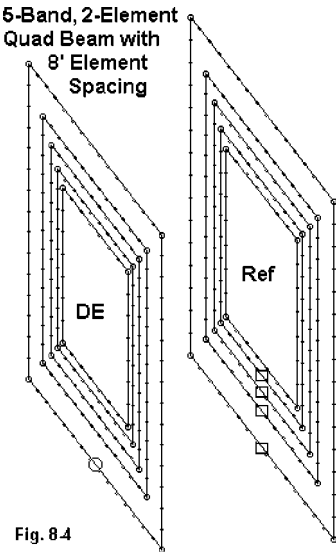
Frequency in MHz	Gain in dBi	Front-to-Back Ratio in dB	Source Impedance (R +/- jX Ohms)
28.5	7.33	19.68	54.9 + j16.9
24.94	7.17	28.95	71.0 + j 3.7
21.225	7.07	23.02	79.0 + j 1.1
18.118	7.20	37.31	78.6 - j 0.7
14.175	7.23	29.57	88.6 + j 0.7

The use of shorted $1/4 \lambda$ stubs for this concentric quad model is certainly not catastrophic. There is a slight gain loss with increasing frequency, while the changes in the front-to-back ratio are variable. These mixed results tend to indicate only a small shift in resonant frequency for the driven loops as a result of the inactive loops having shorted stubs.

The more noticeable affect is the increase in source impedance for the quad at higher frequencies relative to the impedance with shorted unused loops (or open stubs). Note that this source impedance is the value at the end of the stub for the active band, using a characteristic impedance line equal to the source impedance of the baseline value from the first table. Nonetheless, this technique bears watching in other models, since it seems at first appearance a useful result.

2-Element, 5-Band Quad with 8' Spacing

The KC6T 8'-boom 2-element, 5-band quad model was subjected to the same set of modeling trials. The array consists of 2-elements with a constant 8' separation. Consult Chapter 5 for the dimensions, load values, and other design considerations for this quad. The outline of the antenna is roughly that shown in **Fig. 8-4**. Because this planar array has performance curves somewhat dif-



ferent from the spider quad, the key question is whether the differences in element interactions would affect the performance with open and closed $1/4 \lambda$ lines to a central switching unit.

The planar 2-element quad was treated identically to the 0.125λ spaced spider quad in order to ensure that the resultant data would be comparable. For the KC6T quad, the baseline data for the array—with each driver fed independently and unused driver loops closed—appear in **Table 8-5**.

Table 8-5. Performance With Unused Loops Closed

Frequency in MHz	Gain in dBi	Front-to-Back Ratio in dB	Source Impedance (R +/- jX Ohms)
28.5	7.46	22.81	75.4 - j 0.3
24.94	7.20	30.63	76.9 + j 0.3
21.225	7.28	34.40	69.5 + j 1.7
18.118	7.30	31.71	69.5 + j 1.7
14.175	7.21	24.01	76.6 + j 1.6

As noted in Chapter 5, one of the interesting aspects of this design is the relatively constant source impedance from band to band. This factor simplifies the stub modeling. The line lengths will be the same as in the first test, but the characteristic impedances will be between 70 and 75 Ohms. For the two subvariations of an open-circuit remote stub end, the results are in **Table 8-6**.

Table 8-6. Performance With Unused Lines Open

Frequency in MHz	Gain in dBi	Front-to-Back Ratio in dB	Source Impedance (R +/- jX Ohms)
28.5	7.42	22.54	71.7 + j 0.2
24.94	7.18	31.60	74.0 + j 0.7
21.225	7.28	35.20	68.2 - j 1.2
18.118	7.30	31.72	69.0 - j 1.3
14.175	7.21	23.97	77.0 - j 1.7

As with the concentric or spider quad model, the flat-plane model shows no significant difference in any performance parameter between the baseline data set and the open unused stub set.

The only test remaining is the one in which the unused driver stubs are short circuited at their remote ends. The data for this test are in **Table 8-7**.

Table 8-7. Performance With Unused Lines Shorted

Frequency in MHz	Gain in dBi	Front-to-Back Ratio in dB	Source Impedance (R +/- jX Ohms)
28.5	-1.34	14.74	4.7 + j83.0
24.94	6.63	28.14	41.7 - j96.5
21.225	7.13	30.02	183.2 - j23.8
18.118	7.26	34.61	120.7 - j12.5
14.175	7.22	24.36	80.8 - j 1.1

The flat-plane model obviously suffers far more from the use of shorted stubs for the unused driver than does the concentric model. 12 and 10 meter operation suffers the most and requires considerable redesign before it could approach the performance of the baseline data set.

Conclusions

Any conclusions we reach must be very tentative, since only one sample of each quad type (concentric and flat plane) was used. We cannot, for example, assert with any certainty that all spider-type concentric quads would show a similar set of data relative to the model studied.

What is more assured, although by no means finalized, is the fact that unused driver loop closure is desirable for attaining good performance on all bands of a 2-element, 5-band quad. With relatively equal assurance, we can also suggest that cutting the open-ended stubs to $1/4 \lambda$ at the loop's normal operating frequency suffices to allow the array to achieve peak performance on all bands (within, of course, the design limitations inherent in each type of quad). Modeling does not seem to turn up any particular problems with the open-stub system of remote switching.

One arrangement that has not been modeled deserves note. Many remote switches use a single-throw design—that is, they switch only the center conductor of a coaxial cable. All of the stub braids would remain connected together, usually by being directly connected via coaxial fittings to a metallic switch housing. Although I am aware of no problems arising from this arrangement when the stubs are open at the switch (resulting in shorted or quasi-shortened unused driver loops), the models that we have examined cannot be used as adequate simulations of this switching scheme. Accurate modeling of this scheme would require the use of physical wires for the stubs

so that one side of the stub lines could be brought to a single junction. Unfortunately, NEC does not permit the physical modeling of small-diameter coaxial cables.

The tentative conclusions reached here are based on modeling 2-element 5-band quad arrays. They are equally applicable to larger multi-band arrays consisting of 3 or more elements per band. Most large quad arrays employ planar construction, although there are a few extended spider arrays in the marketplace. Whether the 0.125λ spider or the KC6T model would be most useful for guidance will depend on the physical arrangement of the driver loops.

This study is very incomplete, being limited to a subset of models in my collection. Nevertheless, the results seemed worth adding to this series of notes, since they do appear to allay any hesitation over using the open-stub remote switching system and to suggest that using shorted stubs may be unwise--or at least not fully predictable for any given situation.

9. Monoband Quads of More Than 2 Elements

My stock of models of quad beams having more than 2 elements is limited to a few published designs, mostly by K2OB and W6SAI. I have played a bit with the 3-element monoband quad design, but I do not claim to have optimized it fully.

Nevertheless, some of the modeled properties of published designs may be instructive in terms of setting expectations for what a modeling program is likely to say about a design. As with the remainder of the models in this book, the modeling program is NEC-4, but there are no significant differences in NEC-2 outputs for the same designs. Except where specifically noted, the designs use #14 AWG copper wire. In this chapter, all are 20-meter models, the band of choice for K2OB, whose designs make up half of those to be examined. As in past episodes, the primary operational properties that we shall graph include free space gain (in dBi), 180-degree front-to-back ratio (in dB), and SWR (referenced as relevant to a fixed value, such as 50 Ohms or 75 Ohms, or to the resonant impedance of the antenna in question).

The K2OB designs apparently have been optimized for maximum gain, which does not occur at the same frequency as maximum front-to-back ratio. The W6SAI 3-element design has intentionally reduced gain and striven for broad-band operation. My own 3-element model has striven for a balance among feedpoint impedance, gain, and front-to-back ratio.

Since comparisons with Yagi designs are inevitable, I have included a 5-element Yagi design to compare with the 5-element quads. The comparison, of course, is only at the level of modeling and cannot comment upon any perceived operational phenomena that have no correlates in modeling.

Throughout, I have discarded any references to wire-cutting formulas. In their place, I have list in tabular form the dimensions of the models themselves. As we shall discover, wire diameter does play a role in the performance curves of a quad beam. Hence, direct scaling must include wire diameter as well as loop length--or else adjustments will be required in the loop length if a certain wire size is retained. Likewise, changing wire size within any given model will require readjustment of loop sizes to return the curves to

their original positions on the graphs or performance for gain, front-to-back ratio, and swr.

3-Element Monoband Quads

The 3-element monoband quad is simply 3 quad loops so sized and arranged as to maximize gain, front-to-back ratio, or a certain feedpoint impedance--or some combination of 2 or 3 of these parameters. My stock of 3-element monoband quads for 20 meters includes a 24' boom design from K2OB, a 20' design from W6SAI, and a 24' model of my own devising. Interestingly, the loop sizes that I derived from tweaking the model turned out to be within an inch per side of those used by the W6SAI design.

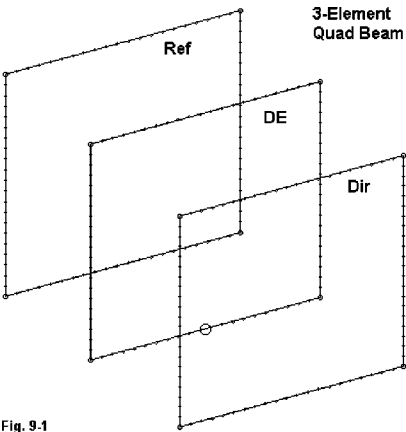


Fig. 9-1

Special note: Although “W6SAI” is conventionally used as a label for this and other designs that may appear in these notes, *Cubical Quad Antennas* is under the dual authorship of W6SAI and W2LX. Hence, dual credit should be given to any design from that book which bears the label “W6SAI” in these notes.

Fig. 9-1 provides an outline sketch of a typical monoband 3-element quad design. Essentially, only loop lengths and element spacing will change from one design to another design. **Table 9-1** supplies the dimensions used in the models of 20-meter 3-element quads that we shall compare.

Table 9-1. Dimensions of Representative 3-Element 20-Meter Quads

Model	Reflector		Driver		Director
	Side L feet	Space Re-DE	Side L feet	Space DE-Di	Side L feet
K2OB324	18.006	11	17.562	13	17.426
3LQ2024	18.12	11	17.80	13	17.20
Orr2012	18.12	10	17.80	10	17.20

Note that my own design (3LQ2024) uses the same boom length (24') and element spacing (11' and 13') as the K2OB design, but different loop

lengths. The W6SAI design uses the same loop lengths as mine, but on a shorter (20') boom with equal element spacing (10' each). The Orr design specifies #12 wire, while the other models use #14.

For reference, here are EZNEC model descriptions for each of the designs.

K2OB 3el quad 11/13=24

Frequency = 14.175 MHz.

Wire Loss: Copper -- Resistivity = 1.74E-08 ohm-m, Rel. Perm. = 1

----- WIRES -----

Wire Conn.--- End 1 (x,y,z : ft) Conn.--- End 2 (x,y,z : ft) Dia(in) Segs

1	W4E2	-9.003,	0.000,	-9.003	W2E1	9.003,	0.000,	-9.003	# 14	21
2	W1E2	9.003,	0.000,	-9.003	W3E1	9.003,	0.000,	9.003	# 14	21
3	W2E2	9.003,	0.000,	9.003	W4E1	-9.003,	0.000,	9.003	# 14	21
4	W3E2	-9.003,	0.000,	9.003	W1E1	-9.003,	0.000,	-9.003	# 14	21
5	W8E2	-8.781,	11.000,	-8.781	W6E1	8.781,	11.000,	-8.781	# 14	21
6	W5E2	8.781,	11.000,	-8.781	W7E1	8.781,	11.000,	8.781	# 14	21
7	W6E2	8.781,	11.000,	8.781	W8E1	-8.781,	11.000,	8.781	# 14	21
8	W7E2	-8.781,	11.000,	8.781	W5E1	-8.781,	11.000,	-8.781	# 14	21
9	W12E2	-8.713,	24.000,	-8.713	W10E1	8.713,	24.000,	-8.713	# 14	21
10	W9E2	8.713,	24.000,	-8.713	W11E1	8.713,	24.000,	8.713	# 14	21
11	W10E2	8.713,	24.000,	8.713	W12E1	-8.713,	24.000,	8.713	# 14	21
12	W11E2	-8.713,	24.000,	8.713	W9E1	-8.713,	24.000,	-8.713	# 14	21

----- SOURCES -----

Source	Wire Seg.	Wire #/Pct Actual	From End 1 (Specified)	Ampl.(V, A)	Phase(Deg.)	Type
--------	-----------	-------------------	------------------------	-------------	-------------	------

1	11	5 / 50.00	(5 / 50.00)	1.000	0.000	V
---	----	-----------	--------------	-------	-------	---

.....

3el quad--Yagi Spacing--20m

Frequency = 14.175 MHz.

Wire Loss: Copper -- Resistivity = 1.74E-08 ohm-m, Rel. Perm. = 1

----- WIRES -----

Wire Conn.--- End 1 (x,y,z : ft) Conn.--- End 2 (x,y,z : ft) Dia(in) Segs

1	W4E2	-9.060,	0.000,	-9.060	W2E1	9.060,	0.000,	-9.060	# 14	21
2	W1E2	9.060,	0.000,	-9.060	W3E1	9.060,	0.000,	9.060	# 14	21
3	W2E2	9.060,	0.000,	9.060	W4E1	-9.060,	0.000,	9.060	# 14	21
4	W3E2	-9.060,	0.000,	9.060	W1E1	-9.060,	0.000,	-9.060	# 14	21
5	W8E2	-8.900,	11.000,	-8.900	W6E1	8.900,	11.000,	-8.900	# 14	21
6	W5E2	8.900,	11.000,	-8.900	W7E1	8.900,	11.000,	8.900	# 14	21
7	W6E2	8.900,	11.000,	8.900	W8E1	-8.900,	11.000,	8.900	# 14	21
8	W7E2	-8.900,	11.000,	8.900	W5E1	-8.900,	11.000,	-8.900	# 14	21
9	W12E2	-8.600,	24.000,	-8.600	W10E1	8.600,	24.000,	-8.600	# 14	21
10	W9E2	8.600,	24.000,	-8.600	W11E1	8.600,	24.000,	8.600	# 14	21
11	W10E2	8.600,	24.000,	8.600	W12E1	-8.600,	24.000,	8.600	# 14	21
12	W11E2	-8.600,	24.000,	8.600	W9E1	-8.600,	24.000,	-8.600	# 14	21

----- SOURCES -----

Source	Wire Seg.	Wire #/Pct Actual	From End 1 (Specified)	Ampl.(V, A)	Phase(Deg.)	Type
1	11	5 / 50.00	(5 / 50.00)	1.000	0.000	V
.....						

Orr: 20 m: 3el Frequency = 14.175 MHz.

Wire Loss: Copper -- Resistivity = 1.74E-08 ohm-m, Rel. Perm. = 1

----- WIRES -----

Wire Conn.---		End 1 (x,y,z : ft)			Conn.--- End 2 (x,y,z : ft)			Dia(in)	Segs
1	W4E2	-9.060,	0.000,	-9.060	W2E1	9.060,	0.000,	-9.060	# 12 21
2	W1E2	9.060,	0.000,	-9.060	W3E1	9.060,	0.000,	9.060	# 12 21
3	W2E2	9.060,	0.000,	9.060	W4E1	-9.060,	0.000,	9.060	# 12 21
4	W3E2	-9.060,	0.000,	9.060	W1E1	-9.060,	0.000,	-9.060	# 12 21
5	W8E2	-8.900,	10.000,	-8.900	W6E1	8.900,	10.000,	-8.900	# 12 21
6	W5E2	8.900,	10.000,	-8.900	W7E1	8.900,	10.000,	8.900	# 12 21
7	W6E2	8.900,	10.000,	8.900	W8E1	-8.900,	10.000,	8.900	# 12 21
8	W7E2	-8.900,	10.000,	8.900	W5E1	-8.900,	10.000,	-8.900	# 12 21
9	W12E2	-8.600,	20.000,	-8.600	W10E1	8.600,	20.000,	-8.600	# 12 21
10	W9E2	8.600,	20.000,	-8.600	W11E1	8.600,	20.000,	8.600	# 12 21
11	W10E2	8.600,	20.000,	8.600	W12E1	-8.600,	20.000,	8.600	# 12 21
12	W11E2	-8.600,	20.000,	8.600	W9E1	-8.600,	20.000,	-8.600	# 12 21

----- SOURCES -----

Source	Wire Seg.	Wire #/Pct Actual	From End 1 (Specified)	Ampl.(V, A)	Phase(Deg.)	Type
1	11	5 / 50.00	(5 / 50.00)	1.000	0.000	V

The gain curves across 20 meters for all three models appear in **Fig. 9-2**. The Orr and 3LQ designs show very parallel gain curves for their identical loop lengths. Hence, the gain difference is a function of the shorter Orr boom and the different relative spacing of the elements.

The maximum gain for the K2OB model shows a peak at 14.245 MHz. The peak is roughly 0.3 dB higher than the gain of the 3LQ design at the same frequency--for the same boom length. However, the K2OB design shows a low-end fall-off. With judicious adjustment of the loop sizes, the gain curve might well be centered in the band so that it everywhere meets or exceeds the gain value of the 3LQ model on the same length boom.

The Orr quad exhibits a very smooth front-to-back ratio curve in **Fig. 9-3**. However, values never reach the 20 dB mark. The K2OB design shows a peak ratio above 25 dB, but the band-edge performance is poor, especially at

the low end of the band. In conjunction with the gain curve, it appears that the antenna has been designed for the high end of 20 meters and the overall performance can be moved downward in frequency.

3-Element 20-Meter Quads Free Space Gain

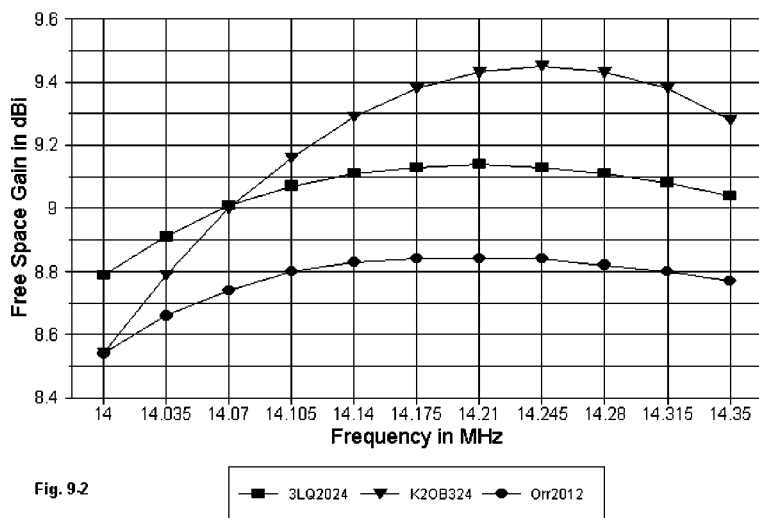
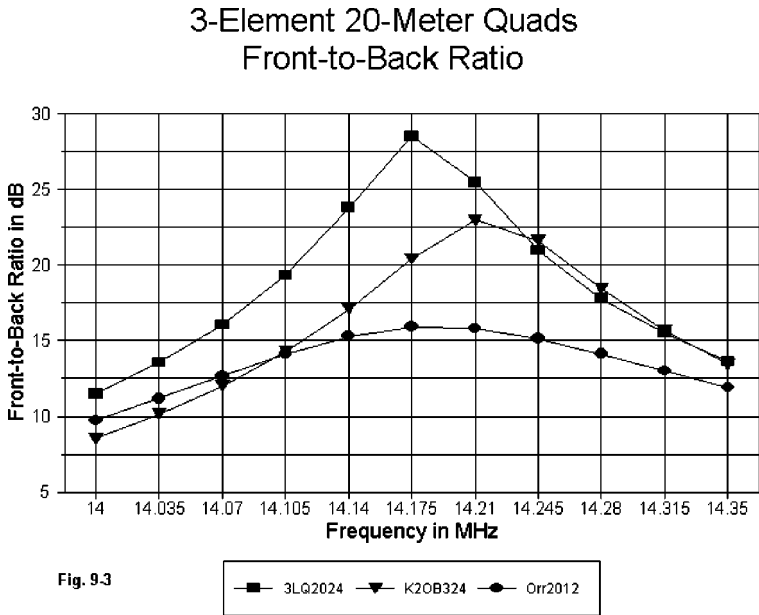


Fig. 9.2

The 3LQ design on a 24' boom shows a much higher peak front-to-back ratio and a higher average value across the band than the other two designs. Nonetheless, band-edge performance is well below 15 dB, and the range for a front-to-back ratio in excess of 20 dB is only about 150 kHz of this 350 kHz band. It would appear that considerable sacrifice in forward gain performance may be necessary to achieve a relatively smooth front-to-back performance that approaches 20 dB at the band edges.

How much gain can be sacrificed and still have a quad advantage over a Yagi of similar boom length is a difficult question to answer. In my collection of models, I have N6BV 20-meter designs for 3-element Yagis on 24' booms and 4-element Yagis on 26' booms. The 3-element Yagi shows a mid-band free space gain of about 8.1 dBi, while the 4-element design shows a gain of 8.5 dBi. The peak Orr design gain just exceeds 8.8 dBi, so there is little margin with which to play to increase its front-to-back performance. Despite seeming differences in the gain of the K2OB and the 3LQ designs, when

adjusted for a minimal front-to-back performance of 20 dB, the result would be identical designs. With the 3LQ version registering a peak gain just above 9.1 dBi, it shows about a full dB gain over the 3-element Yagi on the same length boom. It might require a reduction to about half that advantage to yield a significantly better front-to-back performance. Nonetheless, achieving a 20 dB front-to-back ratio across the 20-meter band appears to be out of the question for any modifications of the three designs.



The SWR performance of the three designs relative to a 50-Ohm standard appears in **Fig. 9-4**. All of the designs aim for an acceptable match to 50-Ohm coaxial cable (with or without a matching circuit and presumably with a common-mode current suppressing choke), although total band coverage may not be a principle goal of some designs. Neither the 3LQ nor the Orr design remains at under 2:1 SWR across 20 meters, although the Orr design comes closer to that goal. The K2OB design--intended for use with a matching circuit--shows the steepest curve of the 3 designs. In the end, none of the three designs provides full 20-meter coverage with respect to the conventional 2:1 SWR standard.

3-Element 20-Meter Quads
VSWR

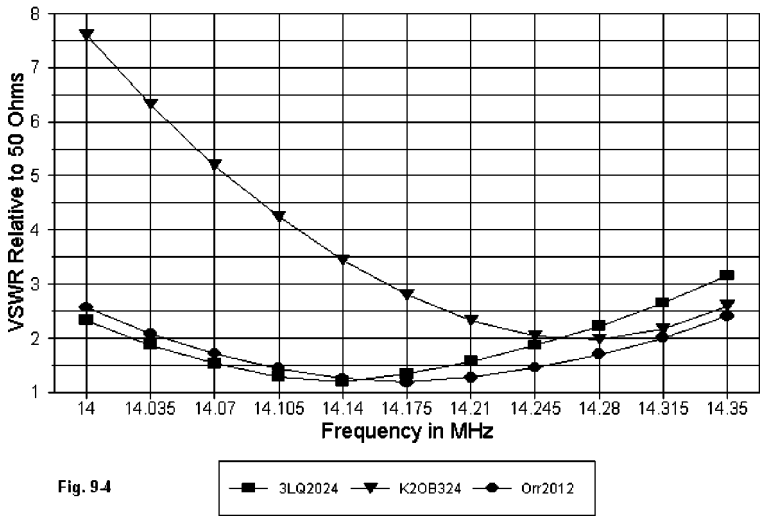


Table 9-2. Changes of Source Resistance and Reactance

Antenna	Impedance at a Specified Frequency			Delta	
	14.0	14.175	14.35	R	X
K2OB	28.4 - j80.5	25.4 - j29.3	25.4 + j25.1	3.0	105.6
3IQ	34.4 - j37.4	42.4 + j 1.4	40.2 + j39.4	8.0	76.8
Orr	36.5 - j34.8	43.2 + j11.5	45.2 + j57.5	8.7	92.3

As shown in **Table 9-2**, in all three models, the variation in the resistive component of the source impedance is small. We made a similar finding with respect to 2-element quads. Moreover, the pattern is variable, and as the 3LQ models shows, the peak resistive component may not occur at a band edge. However, the variation of reactance across the band is quite even and, comparatively speaking, very wide. Reducing this range to a more easily accommodated level is no small task indeed. At a basic design level, leaving the reduction to the masking effect of matching circuit losses or to cable losses is no solution at all, even if the process has practical advantages.

5-Element Monoband Quads (and a Yagi)

My small collection of 5-element monoband quads consist of K2OB designs for 20 meters. We shall look at two versions, one for a 40' boom, the other for an 80' boom. In both cases, the reflector is spaced 10' from the driven element. The shorter boom uses uniform 10' element spacing throughout. The spacing from the driven element to the first director and between the remaining directors in the 80' boom model is 23.3'. **Fig. 9-5** shows the outline of a 5-element monoband quad array.

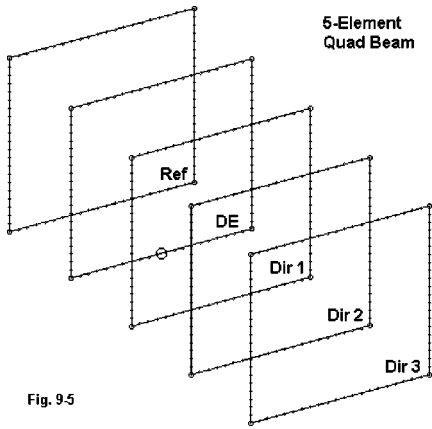


Fig. 9-5

Since K2OB specifies the same dimensions for #16 through #12 AWG wire, #14 copper is used in the models. With the spacing already specified, we need tabulate only the loops sizes, expressed in terms of the length of each side, which are used for both versions of the antenna. See **Table 9-3**.

Table 9-3. K2OB 5-Element Quad Loop Dimensions

Reflector	Driver	Director 1	Director 2	Director 3
17.786'	17.458'	17.356'	17.332'	17.332'

For reference, here is an EZNEC model description of the 80' boom model. To revise it for a 40' boom, make changes only to the Y-axis values for the directors.

```
5-el quad: K2OB 80'                                     Frequency = 14.175 MHz.

Wire Loss: Copper -- Resistivity = 1.74E-08 ohm-m, Rel. Perm. = 1

----- WIRES -----

Wire Conn.--- End 1 (x,y,z : ft)  Conn.--- End 2 (x,y,z : ft)  Dia(in) Segs

1  W4E2  -8.938,  0.000, -8.938  W2E1   8.938,  0.000, -8.938  # 14  21
2  W1E2   8.938,  0.000, -8.938  W3E1   8.938,  0.000,  8.938  # 14  21
3  W2E2   8.938,  0.000,  8.938  W4E1  -8.938,  0.000,  8.938  # 14  21
4  W3E2  -8.938,  0.000,  8.938  W1E1  -8.938,  0.000, -8.938  # 14  21
5  W8E2  -8.729, 10.000, -8.729  W6E1   8.729, 10.000, -8.729  # 14  21
6  W5E2   8.729, 10.000, -8.729  W7E1   8.729, 10.000,  8.729  # 14  21
7  W6E2   8.729, 10.000,  8.729  W8E1  -8.729, 10.000,  8.729  # 14  21
8  W7E2  -8.729, 10.000,  8.729  W5E1  -8.729, 10.000, -8.729  # 14  21
9  W12E2 -8.678, 33.300, -8.678  W10E1  8.678, 33.300, -8.678  # 14  21
```

10	W9E2	8.678, 33.300, -8.678	W11E1	8.678, 33.300, 8.678	# 14	21
11	W10E2	8.678, 33.300, 8.678	W12E1	-8.678, 33.300, 8.678	# 14	21
12	W11E2	-8.678, 33.300, 8.678	W9E1	-8.678, 33.300, -8.678	# 14	21
13	W16E2	-8.666, 56.600, -8.666	W14E1	8.666, 56.600, -8.666	# 14	21
14	W13E2	8.666, 56.600, -8.666	W15E1	8.666, 56.600, 8.666	# 14	21
15	W14E2	8.666, 56.600, 8.666	W16E1	-8.666, 56.600, 8.666	# 14	21
16	W15E2	-8.666, 56.600, 8.666	W13E1	-8.666, 56.600, -8.666	# 14	21
17	W20E2	-8.666, 79.900, -8.666	W18E1	8.666, 79.900, -8.666	# 14	21
18	W17E2	8.666, 79.900, -8.666	W19E1	8.666, 79.900, 8.666	# 14	21
19	W18E2	8.666, 79.900, 8.666	W20E1	-8.666, 79.900, 8.666	# 14	21
20	W19E2	-8.666, 79.900, 8.666	W17E1	-8.666, 79.900, -8.666	# 14	21

----- SOURCES -----

Source	Wire Seg.	Wire #/Pct Actual	From End 1 (Specified)	Ampl.(V, A)	Phase(Deg.)	Type
1	11	5 / 50.00	(5 / 50.00)	1.000	0.000	V

The 5-element quad makes a fairly large model if we use plenty of segments per side to ensure convergence. However, it runs rapidly on a current generation computer (300 MHz or higher speed CPU).

Because certain comparisons will be inevitable, we might as well take them on from the beginning. How well does a 5-element quad model do against a 5-element Yagi model? Note that I have expressed the question in terms of modeled performance, not in terms of on-the-air performance. Since we shall restrict our inquiry to what NEC-4 modeling reports, we should not pretend that the answers are perfectly general.

The Yagi selected is a 5-element 45' boom model based on a design by W6NGZ. Further modeling studies of this and other long-boom 20-meter Yagis appears in another set of notes in the collection of notes at my website (<http://www.cebik.com/5120.html>). See "Six Long-Boom Yagis." The 45' boom length is the shortest of the collection and closest to the 40' K2OB model size. For reference, here is the model description of the W6NGZ Yagi.

5L45' W6NGZ CQ 10-96 p 22

Frequency = 14.175 MHz.

Wire Loss: Aluminum -- Resistivity = 4E-08 ohm-m, Rel. Perm. = 1

----- WIRES -----

Wire Conn.---	End 1 (x,y,z : in)	Conn.---	End 2 (x,y,z : in)	Dia(in)	Segs
1	-215.60, 0.000, 0.000	W2E1	-156.00, 0.000, 0.000	6.25E-01	5
2	W1E2 -156.00, 0.000, 0.000	W3E1	-120.00, 0.000, 0.000	7.50E-01	3
3	W2E2 -120.00, 0.000, 0.000	W4E1	-72.000, 0.000, 0.000	8.75E-01	4
4	W3E2 -72.000, 0.000, 0.000	W5E1	72.000, 0.000, 0.000	1.00E+00	13
5	W4E2 72.000, 0.000, 0.000	W6E1	120.000, 0.000, 0.000	8.75E-01	4
6	W5E2 120.000, 0.000, 0.000	W7E1	156.000, 0.000, 0.000	7.50E-01	3

7	W6E2	156.000,	0.000,	0.000	215.605,	0.000,	0.000	6.25E-01	5
8		-205.95,	79.800,	0.000	W9E1	-156.00,	79.800,	0.000	6.25E-01
9	W8E2	-156.00,	79.800,	0.000	W10E1	-120.00,	79.800,	0.000	7.50E-01
10	W9E2	-120.00,	79.800,	0.000	W11E1	-72.000,	79.800,	0.000	8.75E-01
11	W10E2	-72.000,	79.800,	0.000	W12E1	72.000,	79.800,	0.000	1.00E+00
12	W11E2	72.000,	79.800,	0.000	W13E1	120.000,	79.800,	0.000	8.75E-01
13	W12E2	120.000,	79.800,	0.000	W14E1	156.000,	79.800,	0.000	7.50E-01
14	W13E2	156.000,	79.800,	0.000		205.950,	79.800,	0.000	6.25E-01
15		-198.21,	155.160,	0.000	W16E1	-156.00,	155.160,	0.000	6.25E-01
16	W15E2	-156.00,	155.160,	0.000	W17E1	-120.00,	155.160,	0.000	7.50E-01
17	W16E2	-120.00,	155.160,	0.000	W18E1	-72.000,	155.160,	0.000	8.75E-01
18	W17E2	-72.000,	155.160,	0.000	W19E1	72.000,	155.160,	0.000	1.00E+00
19	W18E2	72.000,	155.160,	0.000	W20E1	120.000,	155.160,	0.000	8.75E-01
20	W19E2	120.000,	155.160,	0.000	W21E1	156.000,	155.160,	0.000	7.50E-01
21	W20E2	156.000,	155.160,	0.000		198.209,	155.160,	0.000	6.25E-01
22		-196.55,	337.920,	0.000	W23E1	-156.00,	337.920,	0.000	6.25E-01
23	W22E2	-156.00,	337.920,	0.000	W24E1	-120.00,	337.920,	0.000	7.50E-01
24	W23E2	-120.00,	337.920,	0.000	W25E1	-72.000,	337.920,	0.000	8.75E-01
25	W24E2	-72.000,	337.920,	0.000	W26E1	72.000,	337.920,	0.000	1.00E+00
26	W25E2	72.000,	337.920,	0.000	W27E1	120.000,	337.920,	0.000	8.75E-01
27	W26E2	120.000,	337.920,	0.000	W28E1	156.000,	337.920,	0.000	7.50E-01
28	W27E2	156.000,	337.920,	0.000		196.548,	337.920,	0.000	6.25E-01
29		-189.90,	530.400,	0.000	W30E1	-156.00,	530.400,	0.000	6.25E-01
30	W29E2	-156.00,	530.400,	0.000	W31E1	-120.00,	530.400,	0.000	7.50E-01
31	W30E2	-120.00,	530.400,	0.000	W32E1	-72.000,	530.400,	0.000	8.75E-01
32	W31E2	-72.000,	530.400,	0.000	W33E1	72.000,	530.400,	0.000	1.00E+00
33	W32E2	72.000,	530.400,	0.000	W34E1	120.000,	530.400,	0.000	8.75E-01
34	W33E2	120.000,	530.400,	0.000	W35E1	156.000,	530.400,	0.000	7.50E-01
35	W34E2	156.000,	530.400,	0.000		189.900,	530.400,	0.000	6.25E-01

----- SOURCES -----

Source	Wire Seg.	Wire #/Pct Actual	From End 1 (Specified)	Ampl.(V, A)	Phase(Deg.)	Type
1	7	11 / 50.00	(11 / 50.00)	1.000	0.000	V

The Yagi model uses an extensive element diameter taper schedule, resulting in many model wires. The segment lengths have been kept as equal as possible throughout the model. The material is aluminum in diameters ranging from 1" down to 0.625". All of the models, both quad and Yagi, are in free space, with gain values in dBi.

The gain curves in **Fig. 9-6** show different design goals for the two antenna types. The Yagi has been optimized for roughly the same gain across the 20-meter band, while the quads have been designed to achieve maximum gain. The 80' boom model shows a maximum gain of about 12 dBi peak, but falls below the Yagi level at the low end of the band. The 40' version of the antenna peaks just above the Yagi level, but falls 2 dB below the Yagi at the low end of the band.

5-Element 20-Meter Quads & Yagi
Free Space Gain

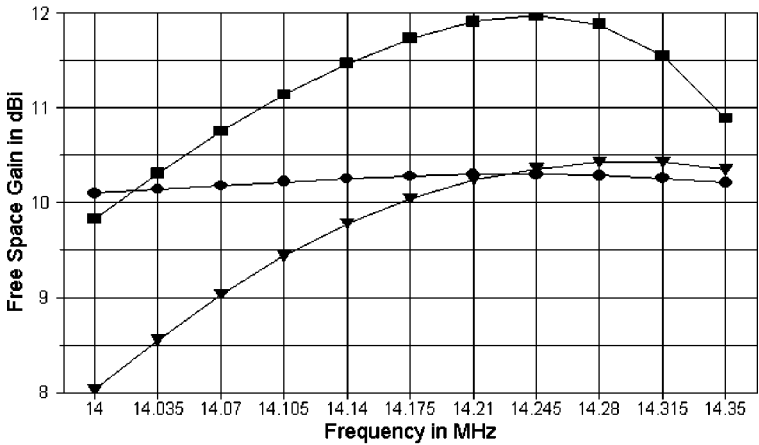


Fig. 9-6

5-Element 20-Meter Quads & Yagi
Front-to-Back Ratio

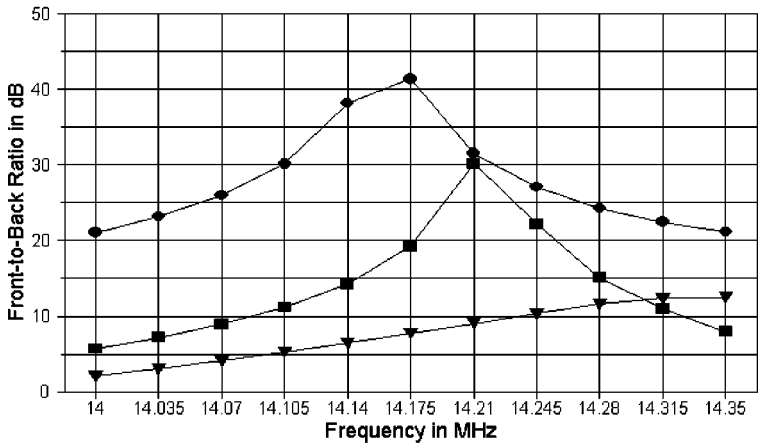
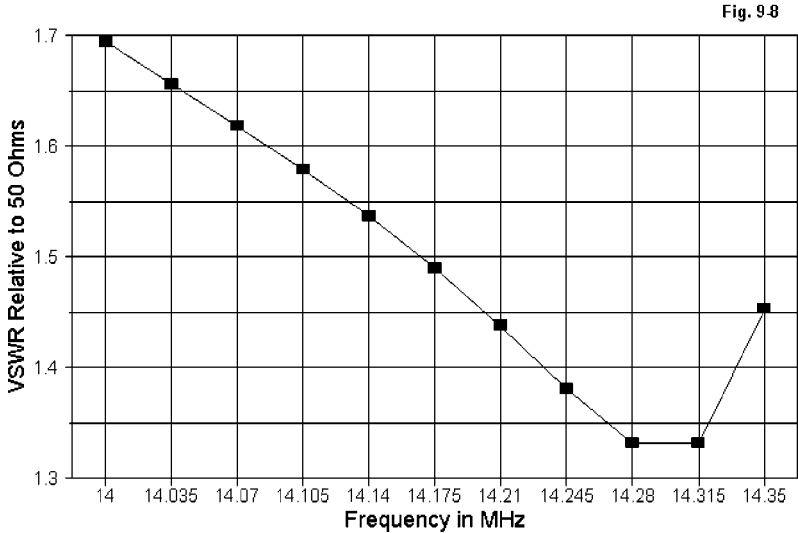


Fig. 9-7

The modeled front-to-back performance of the quads is significantly below the level achieved by the Yagi anywhere within the 20-meter band, as demonstrated in **Fig. 9-7**. Although the 80' boom model peaks at 30 dB, the

band-edge performance is below 10 dB. The low-level but rising curve of the 40' boom quad suggests that additional work needs to be done to optimize the model by bringing the front-to-back curve within the band.

5-Element 20-Meter Yagi
VSWR



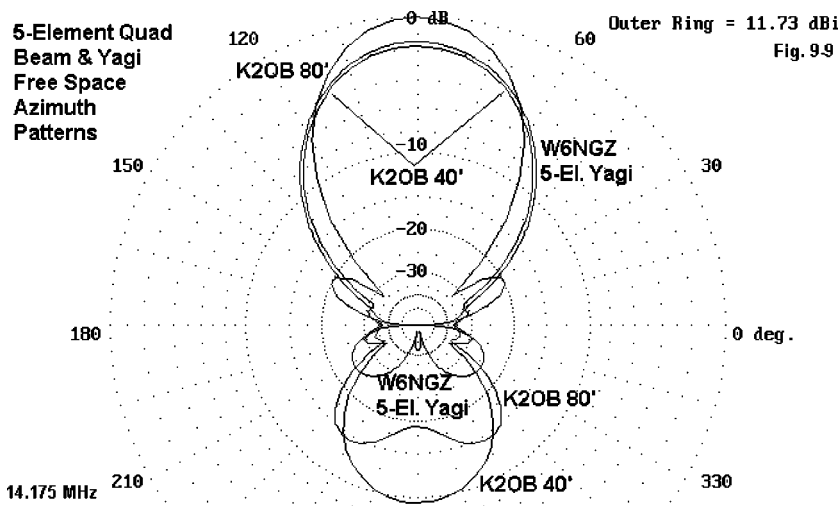
Only the 50-Ohm SWR curve for the Yagi is shown in **Fig. 9-8**. It achieves under 2:1 SWR across the entire 20-meter band. However, some of the other Yagi modeled in the long-boom collection achieve even better figures.

The quad-model source impedances are not amenable to graphing because of their wide variation, especially of the reactive component. **Table 9-4** demonstrates the difficulty.

Table 9-4. SWR Data for 2 5-Element Quads and 1 5-Element Yagi					
Antenna	Impedance at a Specified Frequency			Delta	Delta
	14.0	14.175	14.35	R	X
80' quad	31.9 - j99.6	25.5 - j47.3	15.6 + j26.6	16.3	126.2
40' quad	25.6 - j98.0	35.2 - j52.7	26.6 - j20.0	9.6	78.0
45' Yagi	32.0 - j11.4	33.7 - j 2.3	35.9 - j 7.4	3.9	9.1

The ranges of both the resistive and reactive components of the Yagi source impedance are very small indeed, leading to a very stable matching situation. Likewise, the resistive components of the quad source impedances

are also quite manageable. However, the 5-element quads exhibit (like their 3-element kin) wide swings of reactance across the 20-meter band, leading to very steep SWR curves, whatever the reference impedance value.



The relative performance at mid-band for the three antennas can be represented partially by overlaying free-space azimuth patterns, as done in **Fig. 9-9**. The superior gain of the 80' boom quad is clearly apparent, as is the relatively insignificant difference in gain and horizontal beamwidth of the shorter quad and the Yagi. The Yagi's superior front-to-back performance is also clear.

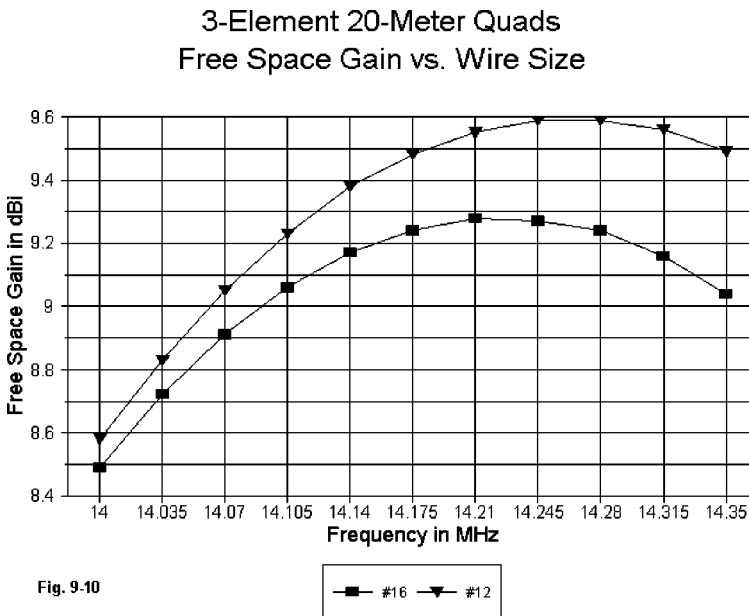
One question bound to arise is why the quads do not exceed the Yagi by much greater margins, since they have been designed for maximum gain. Orr and Cowan, for example, give the quad loop a 1.4 dB advantage over a dipole—an advantage that should be reflected in the models, but is not. The answer to “why” is “wire.”

Quad Element Diameter

Although quad enthusiasts are fond of providing loop length formulas that disregard wire size, we should not be too hasty in doing so. NEC takes the effects of the wire diameter into account in calculating the operating parameters of an antenna. Let's return to the 3-element K2OB design examined earlier in this chapter, just because it shows such pronounced peaks in performance. We may run the very same model (with no alteration in any loop

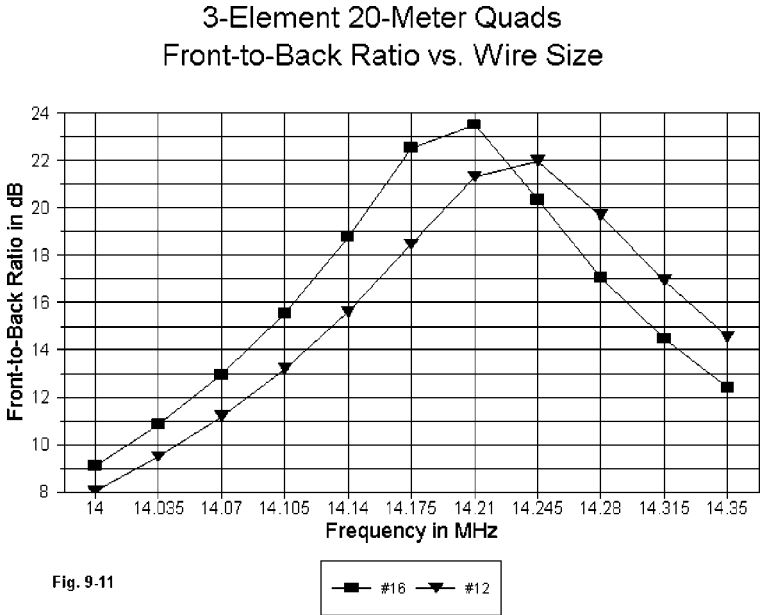
dimension or element spacing) using #16 AWG wire at one extreme and #12 AWG wire at the other, both copper. #16 AWG wire is 0.0508" in diameter; #12 is 0.0808" in diameter; and the #14 used in most of the models is 0.0641" in diameter. The diameter ratio of #12 to #16 is about 1.6:1.

Fig. 9-10 shows the free space gain of the same model using two different wire diameters. Of first note is the differential in the peak gain frequency: about 70 kHz, with the thinner wire showing the lower peak frequency. W4MB makes note in his book (*The Quad Antenna*) of the fact that for closed geometries, increasing the wire diameter also increases the resonant frequency of a loop. This fact is easily confirmed with models of resonant single wire loops. Indeed, the principle also applies to nearly closed geometries in which element end coupling plays a significant role in the design—for example, the folded X-beam. Increasing the wire diameter also raises the frequency of peak gain for a multi-element quad. (We shall look into the gain differential in a moment.)



As **Fig. 9-11** reveals, increasing the loop wire diameter also increases the frequency of peak front-to-back performance, in this case by about 35 kHz. In short, the operating center design frequency of the entire antenna is increased with each incremental increase in wire diameter.

Not only does the antenna operating frequency change with wire diameter, but as well the gain changes. More correctly expressed, the losses increase noticeably with a decrease in wire diameter. Whenever wire diameter makes a significant difference in performance parameters, we must also look at the difference made by the selection of materials for the elements, since the loss differential between, say, copper and aluminum may also make a difference in antenna performance.



To get a feel for what is involved in the differences between wire loops and linear elements, let's make a series of comparisons. The first comparison will be between 10-meter dipoles of radically different diameters: #14 AWG (0.0641") and 1" diameter tubing. Despite the large difference in diameter, both size materials are used for different types of antennas on this band. The test frequency is 28.5 MHz. We shall examine the length (vs. the diameter), the free-space gain in dBi (using various common antenna materials), and the source (feedpoint) impedance ($R \pm jX$ in Ohms). **Table 9-5** provides the results of modeling these antennas.

Table 9-5. Resonant 28.5 MHz Dipoles

Diameter inches	Length feet	Material	Free Space Gain dBi	Source Impedance R +/- jX Ohms
1	16.32	Zero-loss	2.13	71.7 - j 0.6
		Copper	2.13	71.7 - j 0.5
		Aluminum	2.13	71.7 - j 0.5
0.0641	16.67	Zero-loss	2.14	71.9 - j 1.1
		Copper	2.09	72.6 - j 0.4
		Aluminum	2.05	73.0 - j 0.1

Operationally, the differences are not significant. However, here we want to notice trends. Once the wire diameter reaches a certain region--and 1" is within that region--the difference in efficiency among materials becomes insignificant. However, when the diameter is smaller, differences in material losses can become more readily apparent, as in the case of the #14 10-meter dipole. Not only does the gain vary, but as well the source impedance varies to reflect the added losses in less conductive materials.

Typically, HF quads are constructed of wire, which has a small diameter that shows the effects of material losses. **Table 9-6** provides the same data for a single 10-meter quad loop for the three materials using #14 AWG wire.

Table 9-6. Resonant 28.5 MHz Quad Loop

Diameter inches	Length feet	Material	Free Space Gain dBi	Source Impedance R +/- jX Ohms
0.0641	9.13	Zero-loss	3.30	125.3 - j 0.7
		Copper	3.24	127.0 + j 0.8
		Aluminum	3.22	127.8 + j 1.5

For equal diameters and materials, the gain difference between a square quad loop and a dipole, when both are resonant, is about 1.15 dB in NEC model reckoning. However, the wire loop loses another increment of gain advantage when it competes with a 1" diameter dipole, even if the quad wire is copper and the dipole is aluminum. In multi-element arrays, these small increments add up quickly.

Let's make another comparison, this time between models of a 3-element quad beam and a 3-element Yagi. The quad is #14 AWG copper wire, while the Yagi is 1" aluminum. The models for which data appear in **Table 9-7** happen to be 14.175 MHz versions.

Table 9-7. Wire Quad vs. Tubular Yagi Performance

Antenna	Material	'Free Space	F-B	Source Impedance
		Gain dBi	dB	R +/- jX Ohms
3-el. Yagi	Zero-loss	8.14	27.5	25.6 - j 1.1
	Copper	8.12	27.4	25.7 - j 1.0
	Aluminum	8.11	27.3	25.7 - j 0.9
3-el. Quad	Zero-loss	9.49	25.3	40.3 + j 9.3
	Copper	9.13	28.5	43.2 + j11.5
	Aluminum	8.95	30.3	44.6 + j12.6

The gain change for the wire quad throughout the span of materials from lossless wire to aluminum is 18 times that of the 1" Yagi. Likewise, the other performance parameters in the wire quad change by significantly greater amounts as the materials are changed.

The upshot of these modeling comparisons is very basic: as long as quads (or other arrays) use thin wire with real losses, their performance will not achieve the theoretical maximum possible for any given design. In contrast, antennas using elements of appreciable diameter will tend to more closely approach theoretically achievable results, even with materials as lossy as aluminum. The differences between thin and fat wire versions of the same antenna can be significant.

Consider the 3-element quad array designated 3LQ2024, a 20-meter 3-element quad using #14 AWG copper wire. Now let's increase only the diameter of the driven element to 0.5" while leaving it copper. This effective diameter might be simulated by using a double wire driver with a spacing between wires of 5 to 10 inches. To reresonate the antenna requires an increase in the driver length per side of about 0.1 foot. For reference, here is the model description.

```
3el quad--Yagi Spacing--20m                               Frequency = 14.175  MHz.

Wire Loss: Copper -- Resistivity = 1.74E-08 ohm-m, Rel. Perm. = 1

----- WIRES -----

Wire Conn.--- End 1 (x,y,z : ft)  Conn.--- End 2 (x,y,z : ft)  Dia(in) Segs

1  W4E2  -9.060,  0.000, -9.060  W2E1   9.060,  0.000, -9.060   # 14  21
2  W1E2   9.060,  0.000, -9.060  W3E1   9.060,  0.000,  9.060   # 14  21
3  W2E2   9.060,  0.000,  9.060  W4E1  -9.060,  0.000,  9.060   # 14  21
4  W3E2  -9.060,  0.000,  9.060  W1E1  -9.060,  0.000, -9.060   # 14  21
5  W8E2  -8.950, 11.000, -8.950  W6E1   8.950, 11.000, -8.950  5.00E-01 21
6  W5E2   8.950, 11.000, -8.950  W7E1   8.950, 11.000,  8.950  5.00E-01 21
7  W6E2   8.950, 11.000,  8.950  W8E1  -8.950, 11.000,  8.950  5.00E-01 21
```

8	W7E2	-8.950, 11.000,	8.950	W5E1	-8.950, 11.000,	-8.950	5.00E-01	21
9	W12E2	-8.600, 24.000,	-8.600	W10E1	8.600, 24.000,	-8.600	# 14	21
10	W9E2	8.600, 24.000,	-8.600	W11E1	8.600, 24.000,	8.600	# 14	21
11	W10E2	8.600, 24.000,	8.600	W12E1	-8.600, 24.000,	8.600	# 14	21
12	W11E2	-8.600, 24.000,	8.600	W9E1	-8.600, 24.000,	-8.600	# 14	21

----- SOURCES -----

Source	Wire Seg.	Wire #/Pct Actual	From End 1 (Specified)	Ampl.(V, A)	Phase(Deg.)	Type
1	11	5 / 50.00	(5 / 50.00)	1.000	0.000	V

Let's see how the models compare. The #14 wire model is designated 3LQ2024 (and is specified in a model description earlier in this chapter), while the hybrid model that uses a 0.5" diameter driven element is labeled 3LQ20245. (Note: some models may show a voltage source, while others show a current source. For the antenna configurations explored in these notes, the different source type will make no difference in reported performance.)

3-Element 20-Meter Quads
Free Space Gain: #14 vs. 0.5" DE

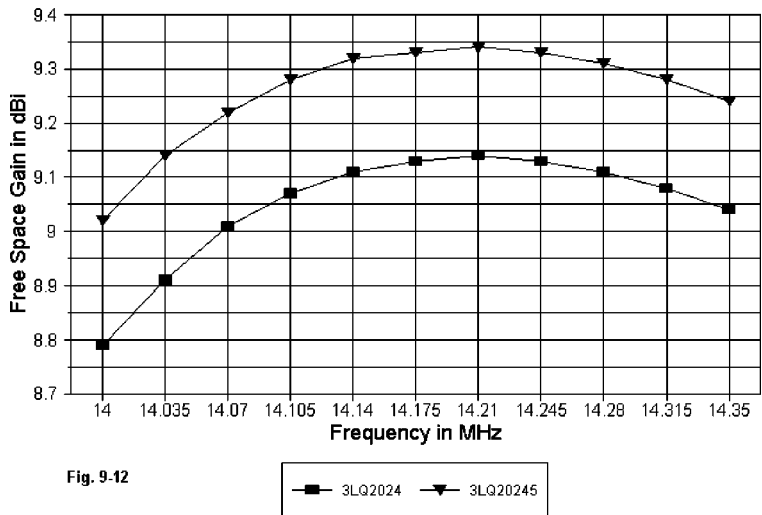
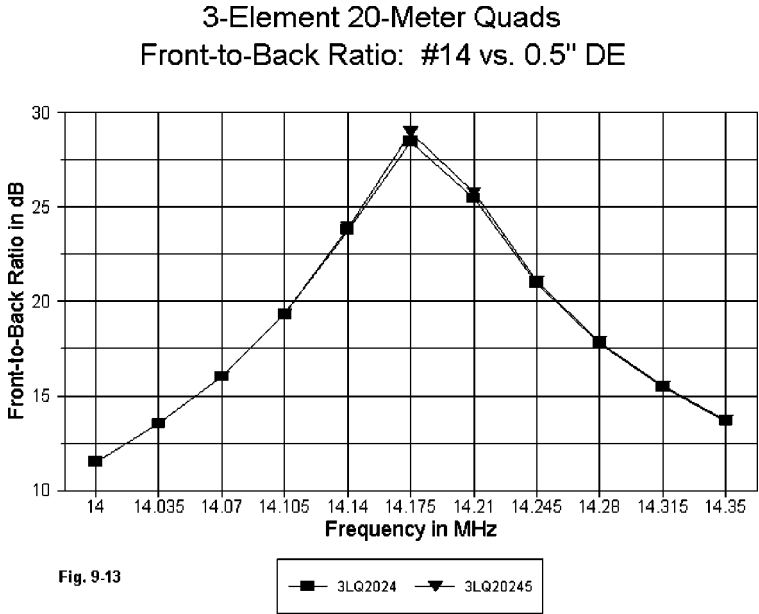


Fig. 9-12

Fig. 9-12 compares the gain curves for the two models, which are identical except for the driver wire diameter and the small adjustment in the length of the driver loop in order to recenter the performance curves. The gain difference between the two models is about 0.25 dB, favoring the model with the larger diameter driven element. This amount of gain advantage may not

be operationally significant, but it is illustrative of the advantage of larger diameter elements, especially larger diameter driven elements.

In **Fig. 9-13**, we see that the front-to-back performance of the antennas does not change with the change in driver diameter. However, if the reflector and the director on this model were also increased in diameter, then all of the elements would have to be reoptimized to place the performance curves in the same relative positions in the 20-meter band. Not only would the element sizes have changed, but as well, the spacing would have required alteration to replicate the degree of inter-element coupling. To date, there has appeared no reliable guidance on how to determine that such a condition exists, since quad design remains a “spot” rather than a systematic affair.



The 50-Ohm SWR curves in **Fig. 9-14** show a further advantage of the large diameter driven element. The SWR curve for the 0.5" driver model is flatter by far than that of the thin-wire model. Although the curve does not cover all of 20 meters with an SWR below 2:1, the improvement over the thin-wire version of the antenna is apparent, despite the fact that the fat driver shows a lower resonant source impedance (about 41 Ohms).

Reoptimizing quads with larger elements might well choose any number of parameters as a baseline for the work. However, it is likely that practical

systematic development of scaled quad dimensions would require a combination of parameters to form a complex baseline.

3-Element 20-Meter Quads
VSWR: #14 vs. 0.5" DE

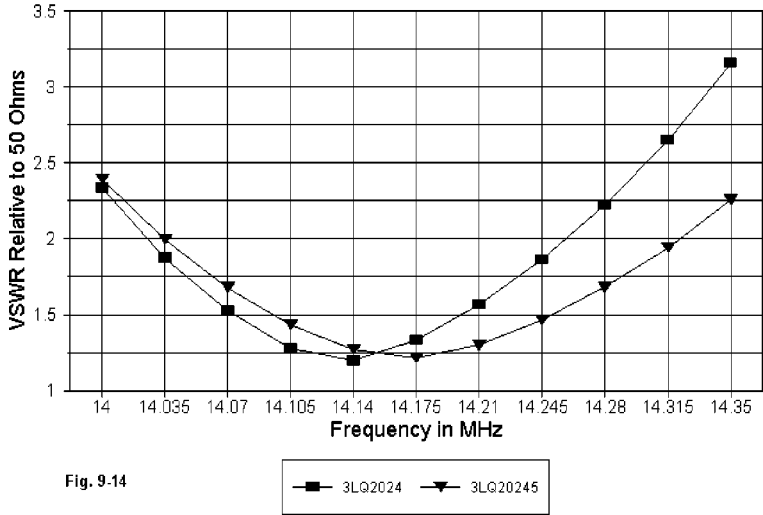


Fig. 9-14

The purpose of these comparisons is not to promote any changes in quad construction. Rather, the goal is to explain to what degree wire diameter and material play a role in quad design and performance potential. Understanding what factors limit the performance of an antenna type may be as important as understanding what makes it work as well as it does.

This foray into larger monoband quad models is necessarily incomplete. Our samples show only a few of the many design biases one might use in developing a large quad array. Nevertheless, the exercise may be accounted useful if we have acquired an appreciation for both the potentials and the limitations of this class of large parasitic antenna.

10. Special Notes on 3-Element Quads

In Chapter 8, in our discussion of multi-element monoband quads, we examined 3 different (and hopefully, representative) models of 3-element quad beams. The basic outline of a typical 3-element quad array appears in **Fig. 10-1**.

The main differences among the quad designs were the boom length and the element spacing. For a refresher, **Table 10-1** provides the dimensions of the quad models that we examined. Note the close similarity of the loop side dimensions, especially between the latter two models.

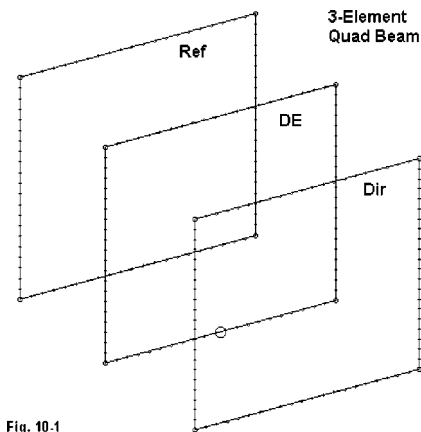


Fig. 10-1

Table 10-1. 3-Element Quad Beam Dimensions

Model	Reflector		Driver		Director
	Side L feet	Space Re-DE	Side L feet	Space DE-Di	Side L feet
K2OB324	18.006	11	17.562	13	17.426
3LQ2024	18.12	11	17.80	13	17.20
Orr2012	18.12	10	17.80	10	17.20

Detailed model descriptions appear in Chapter 9. Note that my own design (3LQ2024) uses the same boom length (24') and element spacing (11' and 13') as the K2OB design, but different loop lengths. The W6SAI design uses the same loop lengths as mine, but on a shorter (20') boom with equal element spacing (10' each). The Orr design specifies #12 AWG wire, while the other models use #14 AWG.

The Orr design exhibited the lowest gain on its short boom, while the K2OB design showed the highest peak gain--but only over a small operating bandwidth. Only the Orr design showed a feedpoint impedance close to 50

Ohms: the other two designs showed much lower impedances ranging from 25 to 40 Ohms. Interestingly, as the performance extracted from the quad increased at the design frequency, the operating and SWR bandwidths decreased.

There are some indicators of quad performance within these models that are worth pursuing a little further. So after we look at a 3-element Yagi as a comparator, we shall examine a 3-element quad that has been optimized beyond the limits set in the initial discussion in the last chapter.

A 3-Element Yagi

In the course of discussing the 3 models, I referred to an K6STI-designed Yagi for 20 meters with a free-space gain of just over 8.1 dBi at the design frequency (14.175 MHz). Perhaps we can better grasp a set of reasonable expectations by taking a longer look at a model of this design. The antenna uses 1" uniform-diameter aluminum elements. The dimensions appear in **Table 10-2**, with the model description immediately following.

Table 10-2. 3-Element Yagi Dimensions

Element	Length inches	Spacing from Reflector inches
Reflector	414.72	—
Driver	396.00	124.68
Director	372.48	270.54

```
3 el Yagi 1" elements                      Frequency = 14.175  MHz.

Wire Loss: Aluminum -- Resistivity = 4E-08 ohm-m, Rel. Perm. = 1

----- WIRES -----

Wire Conn. --- End 1 (x,y,z : in)  Conn. --- End 2 (x,y,z : in)  Dia(in) Segs
1      -207.36,  0.000,  0.000      207.360,  0.000,  0.000  1.00E+00  21
2      -198.00,125.460,  0.000      198.000,125.460,  0.000  1.00E+00  21
3      -186.30,270.528,  0.000      186.300,270.528,  0.000  1.00E+00  21

----- SOURCES -----

Source   Wire      Wire #/Pct  From End 1  Ampl.(V, A)  Phase(Deg.)  Type
      Seg.      Actual      (Specified)
1         11      2 / 50.00  ( 2 / 50.00)    1.000        0.000        V
Ground type is Free Space
```


In relationship to our upcoming quad examination, the SWR curve of the beam (relative to its design frequency resonant feedpoint impedance of 26.26 Ohms) is especially interesting. As shown in **Fig. 10-2**, the Yagi can be matched so as to operate over the entire 20-meter ham band with less than a 2:1 SWR ratio. How we arrive at this condition is revealed partially by **Fig. 10-3**.

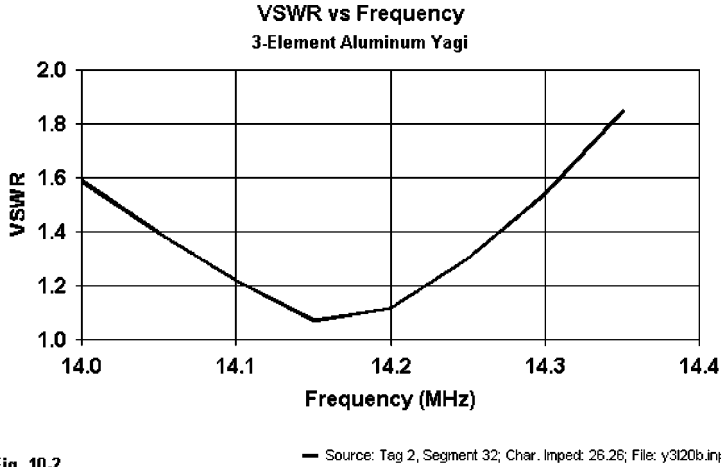


Fig. 10.2

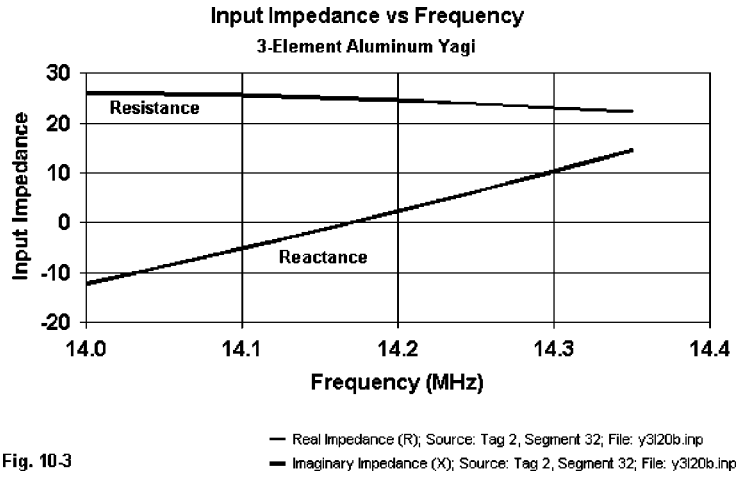


Fig. 10.3

The total difference across the band in the resistive component of the feedpoint impedance is just over 4 Ohms. The reactance passes through a

range of 26.3 Ohms. These are fairly small numbers when it comes to a bandwidth of nearly 2.5% of the center frequency. As a result of these small excursions of resistance and reactance at the array feedpoint, common matching methods, such as the beta or gamma match—or even a simple $1/4 \lambda$ section of transmission line—will provide a satisfactory 50-Ohm VSWR for the entirety of the 20-meter band.

The Yagi free-space gain shows a steady (nearly linear) increase across the band from 7.95 dBi at 14.0 MHz to 8.36 dBi at 14.35 MHz. The design maximizes the front-to-back ratio near the 14.175 MHz design frequency. The actual peak is about 28.2 dB just below the design frequency. At the risk of operating bandwidth, the resonant frequency and the front-to-back peak frequencies can be moved to other points within the passband for the antenna.

Although this Yagi-Uda design should be classified as a high-performance 3-element Yagi for its 22.5' boom and the number of elements, the general properties of the antenna are similar to those of other 3-element designs. They have come to form—rightly or not—the sorts of expectations we have of 3-element parasitic beams of all sorts, including quads.

Setting Up a Better 3-Element Quad Design

In trying to optimize a 3-element quad for the same design frequency, several considerations from the discussion in Chapter 9 came to mind. Foremost is the relative inefficiency of quad construction methods. The small diameter wire used in most quads (#12-#14 AWG) limits the efficiency of the antenna due to the small surface area available on each element. Therefore, the new design would use larger elements. 1" diameter elements seemed an appropriate size for comparison with the Yagi just described. However, such large elements are not usually realistic for practical quad construction.

On one level, we might argue that since only a model of a quad is at stake, the element size need not be realistic. We need not resort to such an argument, since this element diameter can be simulated with pairs of wires for each element spaced a distance that yields for each of the loops the same overall resonant length. Most monoband quad frames can easily support 2 wires per spoke. In test models, there is negligible difference between the 2-wire simulation and the single fat element in terms of performance and efficiency. The numbers will not be absolutely identical, since the surface area of the two wires still does not equal the surface area of the single fat element. However, gain, front-to-back, and impedance numbers generally

coincide to the first decimal place, as does the operating bandwidth of the resulting beam. Hence, the use of 1" elements in the design exercise is, in fact, practical--even if rarely used in actual quad building.

A second factor in the new design involves element spacing. Quad designs have long languished under two influences which have limited their performance. One is the desire for a near-50-Ohm feedpoint impedance. Effective design dictates that we let go of that goal and see what feedpoint impedance emerges if we optimize the other performance characteristics. Obviously, we can design so as to let the feedpoint impedance get too low. However, if a usable front-to-back ratio of about 20 dB is part of the design parameter set, then early indications are that a value in the mid-20s will emerge. This value, in fact, parallels the feedpoint impedance of good Yagi designs that also include a 20-dB front-to-back ratio requirement.

The other limiting factor is the traditional but non-rational urge to use a short boom and equal spacing between all elements. Although these design features have yielded quads with a convenient feedpoint impedance, the designs have not lived up to the so-called theoretical gain advantage of a quad over a similar Yagi of about 1.4 dB.

In redesigning the 3-element quad, one might start with new spacings at random and hope that some optimization program might catch a pair of magic distances. However, we need not resort to such measures, since we already have a large collection of parasitic beams with well-established element spacings for good performance. In fact, I took the Yagi we just described as the baseline for a fat-element quad. In the end, I enlarged the reflector-to-driver spacing by an inch and the overall boom length by 30 inches. This occurred in the process of determining the optimum loop circumference for each element in the beam.

A Somewhat Better 3-Element Quad

The redesign of the 3-element quad with 1" (or 1"-equivalent) elements resulted in the model whose dimensions appear in Table 10-3, with the model description immediately following.

Table 10-3. 3-element Quad Dimensions

Reflector		Driver		Director
Side L	Space	Side L	Space	Side L
feet	Re-DE	feet	DE-Di	feet
18.006	11	17.562	13	17.426

```
3el quad--Yagi Spacing--20m                      Frequency = 14.175  MHz.

Wire Loss: Copper -- Resistivity = 1.74E-08 ohm-m, Rel. Perm. = 1

----- WIRES -----

Wire Conn. --- End 1 (x,y,z : in)  Conn. --- End 2 (x,y,z : in)  Dia(in) Segs
1      W4E2 -110.65,  0.000,-110.65  W2E1 110.650,  0.000,-110.65  1.00E+00  21
2      W1E2 110.650,  0.000,-110.65  W3E1 110.650,  0.000,110.650  1.00E+00  21
3      W2E2 110.650,  0.000,110.650  W4E1 -110.65,  0.000,110.650  1.00E+00  21
4      W3E2 -110.65,  0.000,110.650  W1E1 -110.65,  0.000,-110.65  1.00E+00  21
5      W8E2 -107.33,125.720,-107.33  W6E1 107.330,125.720,-107.33  1.00E+00  21
6      W5E2 107.330,125.720,-107.33  W7E1 107.330,125.720,107.330  1.00E+00  21
7      W6E2 107.330,125.720,107.330  W8E1 -107.33,125.720,107.330  1.00E+00  21
8      W7E2 -107.33,125.720,107.330  W5E1 -107.33,125.720,-107.33  1.00E+00  21
9      W12E2 -104.54,299.190,-104.54  W10E1 104.540,299.190,-104.54  1.00E+00  21
10     W9E2 104.540,299.190,-104.54  W11E1 104.540,299.190,104.540  1.00E+00  21
11     W10E2 104.540,299.190,104.540  W12E1 -104.54,299.190,104.540  1.00E+00  21
12     W11E2 -104.54,299.190,104.540  W9E1 -104.54,299.190,-104.54  1.00E+00  21

----- SOURCES -----

Source      Wire      Wire #/Pct From End 1      Ampl.(V, A)  Phase(Deg.)  Type
            Seg.      Actual      (Specified)
1           11      5 / 50.00  ( 5 / 50.00)      1.000        0.000        V
Ground type is Free Space
```

Given that the design is potentially more than just an exercise in modeling, but as well a potentially buildable design, only one question remains. What did I obtain for my pains.

At the design frequency of 14.175 MHz, the free-space gain is 9.98 dBi. This represents a gain of 1.84 dB over the Yagi. However, remember that the Yagi is 30" shorter than the 25' long quad. Yagi efficiency is about 99.5%, while the use of fat elements has raised to quad efficiency to 98.8%. The remaining difference in efficiency owes to the fact that the quad elements are twice as long as those of the Yagi, and each increment of that extra length as a certain resistivity.

The 180-degree front-to-back ratio of the quad is just over 24 dB at the design frequency, with the quartering rear lobes yielding a worst-case value of 21.5 dB. The feedpoint impedance is just over 26 Ohms.

Despite these promising results, there are limitations to the design. Whoever first called a quad beam a wide-band device must have had only low-gain versions in mind. As we saw in the K2OB designs, a quad optimized so far as possible to achieve its theoretic advantage over a Yagi has a narrower oper-

ating bandwidth, both in terms of SWR and in terms of performance specifications.

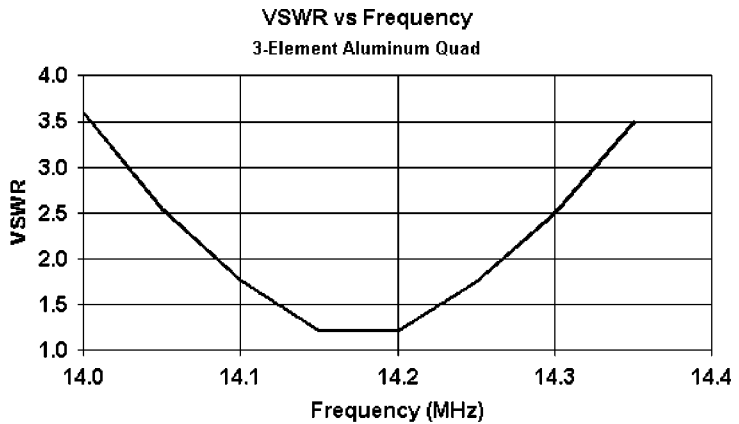


Fig. 10-4 — Source: Tag 5, Segment 50; Char. Imped: 26.26; File: q3l20c.inp

The present design is no exception. The VSWR curve, centered on the resonant impedance at the design frequency of 14.175 MHz, appears in **Fig. 10-4**.

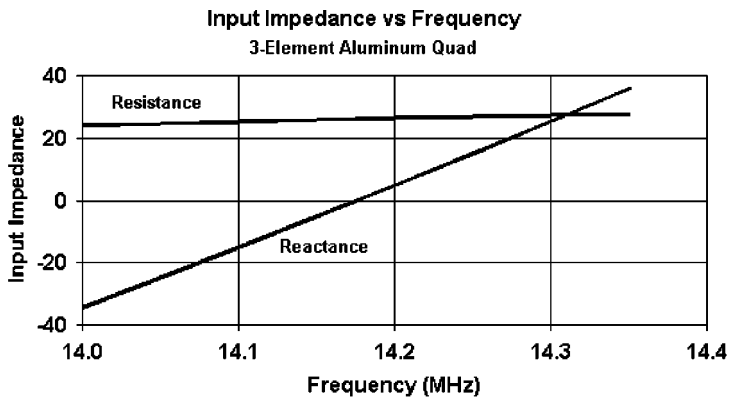


Fig. 10-5 — Real Impedance (R); Source: Tag 5, Segment 50; File: q3l20c.inp
— Imaginary Impedance (X); Source: Tag 5, Segment 50; File: q3l20c.inp

Why the curve is so steep becomes evident when we look at the resistance and reactance curves, shown in **Fig. 10-5**. Although the resistive component varies by only 3.9 Ohms (similar to the Yagi variation of 4 Ohms), the reactance varies by over 70 Ohms (in contrast to the 26-Ohm variation of the Yagi). The result is a 2:1 VSWR bandwidth of only about 175 kHz within the 20-meter band. There is little that most matching systems can do to widen the operating bandwidth without introducing a set of losses. This design, at least (but in common with the K2OB design), suggests that a high gain quad may indeed be inherently more narrow-banded than a comparable Yagi design of similar proportions.

Both the Yagi and the quad have well-behaved azimuth patterns, as shown in the overlay of **Fig. 10-6**. By “well-behaved,” I mean that neither design shows any incipient or real forward lobes other than the main lobe. Many high-gain VHF and interlaced HF Yagi designs show secondary forward lobes on each side of the main lobe, but these are absent in these two designs. Moreover the rear quadrants show only the usual set of three lobes.

The quad quartering rear lobes are larger than those of the Yagi. The feature appears to be endemic to quad arrays, although the rear lobes can usually be reduced to levels showing a 20 dB or more ratio to the forward lobe of the beam. They likely result in part from remnant radiation from the vertical portions of the quad loops.

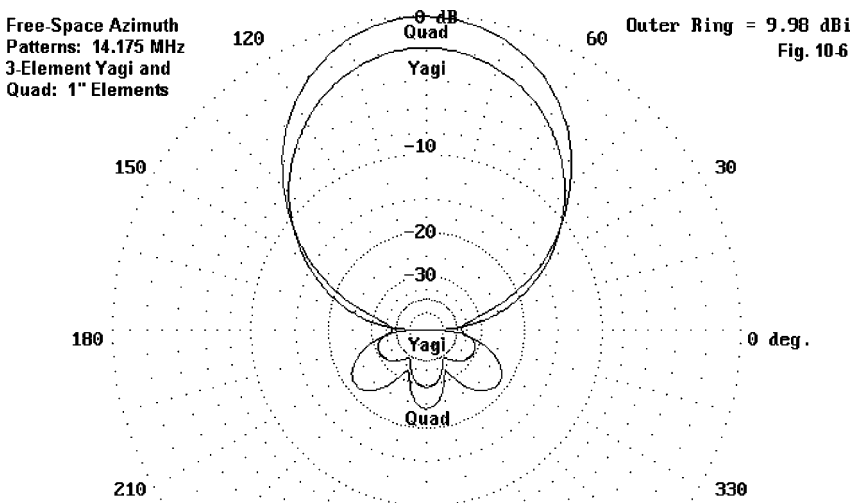
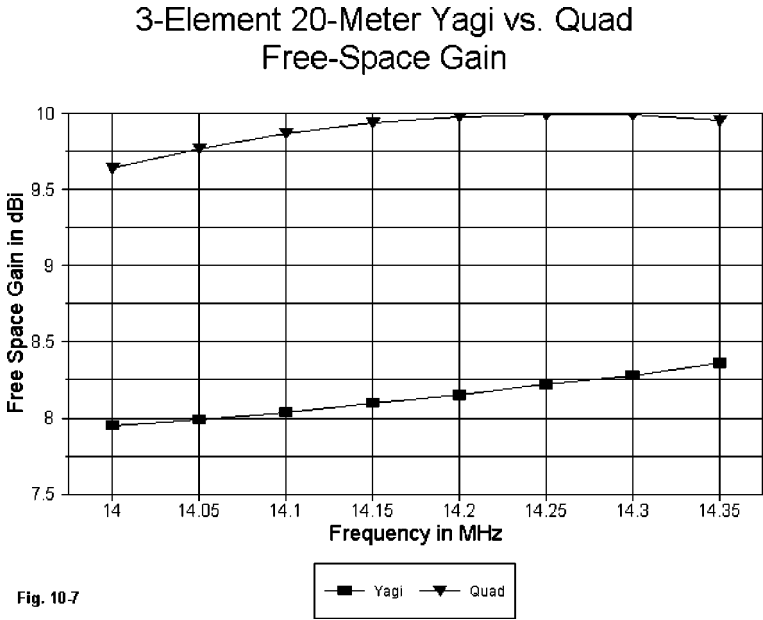


Fig. 10-7 compares the gain curves of the Yagi and the quad beams. As we noted earlier, the gain figures for the Yagi continues to increase nearly linearly across the band, with the free-space gain ranging from about 7.95 dBi to about 8.35 dBi. For most high-gain 3-element Yagis, the peak gain will fall outside the operating passband, being somewhat higher in frequency. Wide-band Yagis, such as OWA (optimized wide-band antenna) designs, are often able to place the array peak gain within the operating passband, with the benefit of having a smaller overall change of gain.

The quad shows a distinct gain peak between 14.25 and 14.30 MHz. What might have been a wide excursion of gain values across the band is held to under 0.3 dB (9.7 dBi to about 10.0 dBi). Quad design for maximum gain appears to make the in-band gain peak a more normal feature of a 3-element quad beam. The designs in preceding chapters might well be reviewed for this feature to obtain a sense of to what degree it is the norm for multi-element quad arrays.



In **Fig. 10-8**, we can observe the 180-degree front-to-back curves for the two antenna types. The Yagi front-to-back peak occurs just below the design frequency. However, the quad peak is just above the design frequency. We have some freedom to move the front-to-back peak, but not unlimited freedom. If we move it too close to one or the other of the band edges, the

operating bandwidth for either or both the gain and the feedpoint impedance can become very narrow--or we lose a significant part of the gain. (There are other antenna types--for example, the Moxon Rectangle--where the SWR and the front-to-back curves are quite non-symmetrical, changing more rapidly on one side of the design frequency than the other. In such cases, we may intentionally choose a design frequency that will tend to provide as close as possible to equal values at the band edges instead of optimizing for a band-center frequency.)

3-Element 20-Meter Yagi vs. Quad 180-Degree Front-to-Back Ratio

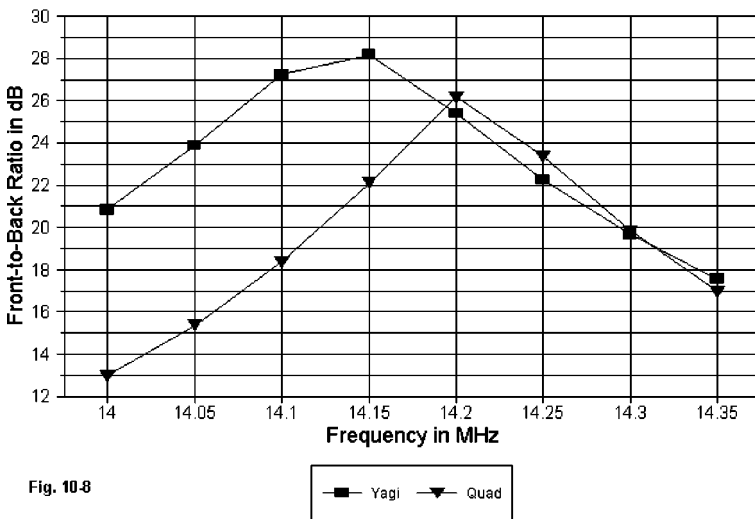


Fig. 10-8

Although the gain of the 3-element quad design is quite consistent across the band, the front-to-back values do not follow suit. The Yagi hits a low of 17.5 dB, while the quad shows a low of about 13 dB--at opposite ends of the band. In this connection, also note that the Yagi shows a decrease of feedpoint resistance with increasing frequency, but the quad shows an increase of feedpoint resistance as the frequency increases.

Conclusions (Tentative)

As a narrow-band beam, then, the 3-element quad approaches more closely than other designs I have so far seen the theoretical advantage over a comparable Yagi. (The Yagi still has better wide-band characteristics--and the Yagi design shown here is usually classified as a high-gain, narrow-band

design.) The use of fat elements--real or simulated by multiple wires per element--and more typical parasitic element spacing produced a beam with higher efficiency and more gain, while retaining within its limited passband a good front-to-back ratio and a matchable feedpoint impedance.

However, the quad beam also revealed some ways in which its behavior is unlike that of a Yagi. The gain and resistance curves show distinctly non-Yagi behaviors, especially in the wide span of reactance values that appear at the feedpoint. Moreover, designing a quad on the basis of Yagi parasitic element spacing yields an inherently narrow-band design.

It remains an open question whether or not it is possible to optimize a 3-element quad so that it exhibits high gain (for an antenna of its type) and broad bandwidth, while retaining the usual standard of a good front-to-back ratio (20 dB) and a usable feedpoint impedance (25 Ohms or more). Unless someone already has such a design in his/her pocket, it is likely that we shall not know until the 3-element quad has been run through optimizing routines as many times as Yagis have.

At most this note is a step in that direction. If it has done anything useful, then perhaps it is to have elicited some of the further properties of 3-element quads that may play a role in the "ultimate" design.

The standards applied in this note perhaps deserve an additional comment. The standards applicable in a high-performance monoband array for the amateur bands do not necessarily correspond to standards applicable to other services. AM broadcast stations can employ very narrow-band antennas and arrays since they operate at single assigned frequencies. Many governmental and military stations require operating bandwidths far greater than the amateur service. Short-wave services may use many different frequencies and have options for using separate antennas for each or an array capable of being set at all of them, even if not simultaneously.

Yagi-Uda arrays have for the last decade pretty much set the standards for performance excellence on the HF amateur bands. Full-band coverage is often defined as the 20-meter band or the first MHz of 10 meters. All of 10 meters is far wider, while 6 meters is wider still. However, for the very wide bands, most amateurs accept restricted portions of the bands as constituting "full" coverage. There are, of course, exceptions to these generalizations.

A long-boom 3-element Yagi can provide about 8 dBi free-space gain within the "full-coverage" range, while a 5-element Yagi can provide better

than 10 dBi free-space gain. The standard—not always met—for front-to-back ratio is 20 dB. It is desirable for the array to show this value not only for the 180E front-to-back ratio, but as well for the average of the entire rear area and as a worst-case value as well.

The Yagi should also have a feedpoint impedance that is capable of matching—or being matched to, via a network—one of the standard feedlines used in the amateur service across the operating passband. 50-Ohm line is the most common standard, but 75-Ohm line is also widely used.

There is no question that quad arrays can be designed to exceed Yagi gain values, as we have seen in this exercise, although the amount of gain advantage is open to design improvement. However, the major challenges facing the design of quads with 3 or more elements involve achieving the operating bandwidth standards for front-to-back ratio and matched VSWR.

11. Larger Multi-Band Quads

My collection of larger (more than 2 elements) multi-band quads is fairly small, consisting of about 3.5 models. However, since one of them is of a 3.5 element 5-band quad, perhaps the score is even. Let's see how this works out.

First, I have modeled one of the multi-band quads from recent editions of the *ARRL Antenna Book* (page 2-12 in the 17th Edition). The antenna is a 4-element 3-band quad on a 40' boom. I count it as 1.5 models, since I have modeled it in both #14 and #12 AWG copper wire. The results, especially in light of my notes on wire size in monoband quads, are interesting.

Next, ON7NQ has shared a number of models with me in his efforts to improve the performance of a commercial 3-element 5-band quad on an 18' boom. One model of note simply adjusts the sizes of virtually all of the loops. A second model adds 2 new elements--new drivers for 10 and 12 meters--making approximately a 3.5 element quad--all on the same 18' boom.

In looking at these models, we should note a number of things. First and most obvious is the standard set of performance parameters that we have surveyed for all of the quads: free space gain in dBi, 180-degree front-to-back ratio in dB, and VSWR to some specified resistive impedance value. In addition to these matters, we may also wish to note how 3- and 4-element quads are similar to and differ from 2-element multi-band quads in various characteristics. Finally, we may also wish to record some factors related to boom length--at least so far as this small sample of models might suggest about the question.

As in all other cases, modeling has been done on NEC-4. The conventions of segmentation used in earlier multi-band quads are repeated here. For each side of a given quad loop, there are 7 segments on 10 meters, 9 segments on 12, 11 segments on 15, 13 segments on 17, and 15 segments on 20. Within practical limits, this scheme approaches the goal of having equal-length segments throughout the model. Nonetheless, at least one model will have 724 segment distributed on 68 wires. Although NEC-2 will provide results as accurate as NEC-4 for these models, some implementations are

limited to 500 segments and may prove less than fully adequate for the modeling task. MININEC results are also accurate if care is taken to ensure element length segment tapering at each corner of each loop. Without the use of symmetry or core enlargement, however, some of these models may be too large for some available versions of MININEC to handle.

As with past multi-band quads, only 20, 15, and 10 meters will undergo frequency sweeps. The 2 WARC bands (17 and 12) are so narrow that antenna performance characteristics do not significantly vary from their mid-band values. Each wide band will be divided into 10 equal segments. On 20, each segment is 0.35 MHz wide, on 15 each is 0.45 MHz wide, and on 10 each is 0.1 MHz wide. Hence, the graphs cover all of 20 and 10 meters and the first MHz of 10 meters.

4-Element 3-Band Quads

In recent editions of the *ARRL Antenna Book*, there is a 3-band, 4-element planar quad design attributed to W0AIW. It uses a 40' boom, with all elements (20, 15, and 10 meters) equally spaced at 10' intervals. **Fig. 11-1** provides an outline sketch of the antenna.

Table 11-1 lists the element lengths per loop side and the element spacing for each of the three bands. Dimensions are in feet.

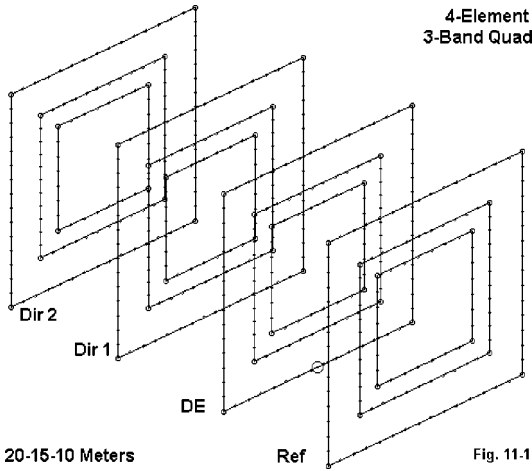


Table 11-1. Dimensions of a 4-element 3-Band Quad

Band	Reflector		Driver		Dir. 1		Dir. 2
	Side L	Space	Side L	Space	Side L	Space	Side L
	feet	Re-DE	feet	DE-D1	feet	D1-D2	feet
20	18.104	10	17.604	10	17.271	10	17.271
15	12.167	10	11.833	10	11.583	10	11.583
10	8.927	10	8.677	10	8.401	10	8.401

These loop lengths are very close to those used in one commercial quad

using a shorter boom for a 3-element version. The change from band-to-band appears to be a matter of simple loop length scaling. The elements are shorter than the monoband loop lengths recommended in Orr and Cowan for 3-and 4-element quads. For reference, here is a model description.

arrl #14

Frequency = 14.175 MHz.

Wire Loss: Copper -- Resistivity = 1.74E-08 ohm-m, Rel. Perm. = 1

----- WIRES -----

Wire Conn.--- End 1 (x,y,z : ft) Conn.--- End 2 (x,y,z : ft) Dia(in) Segs

1	W4E2	-4.200, 20.000, -4.200	W2E1	4.200, 20.000, -4.200	# 14	7
2	W1E2	4.200, 20.000, -4.200	W3E1	4.200, 20.000, 4.200	# 14	7
3	W2E2	4.200, 20.000, 4.200	W4E1	-4.200, 20.000, 4.200	# 14	7
4	W3E2	-4.200, 20.000, 4.200	W1E1	-4.200, 20.000, -4.200	# 14	7
5	W8E2	-4.200, 10.000, -4.200	W6E1	4.200, 10.000, -4.200	# 14	7
6	W5E2	4.200, 10.000, -4.200	W7E1	4.200, 10.000, 4.200	# 14	7
7	W6E2	4.200, 10.000, 4.200	W8E1	-4.200, 10.000, 4.200	# 14	7
8	W7E2	-4.200, 10.000, 4.200	W5E1	-4.200, 10.000, -4.200	# 14	7
9	W12E2	-4.339, 0.000, -4.339	W10E1	4.339, 0.000, -4.339	# 14	7
10	W9E2	4.339, 0.000, -4.339	W11E1	4.339, 0.000, 4.339	# 14	7
11	W10E2	4.339, 0.000, 4.339	W12E1	-4.339, 0.000, 4.339	# 14	7
12	W11E2	-4.339, 0.000, 4.339	W9E1	-4.339, 0.000, -4.339	# 14	7
13	W16E2	-4.464, -10.000, -4.464	W14E1	4.464, -10.000, -4.464	# 14	7
14	W13E2	4.464, -10.000, -4.464	W15E1	4.464, -10.000, 4.464	# 14	7
15	W14E2	4.464, -10.000, 4.464	W16E1	-4.464, -10.000, 4.464	# 14	7
16	W15E2	-4.464, -10.000, 4.464	W13E1	-4.464, -10.000, -4.464	# 14	7
17	W20E2	-5.792, 20.000, -5.792	W18E1	5.792, 20.000, -5.792	# 14	11
18	W17E2	5.792, 20.000, -5.792	W19E1	5.792, 20.000, 5.792	# 14	11
19	W18E2	5.792, 20.000, 5.792	W20E1	-5.792, 20.000, 5.792	# 14	11
20	W19E2	-5.792, 20.000, 5.792	W17E1	-5.792, 20.000, -5.792	# 14	11
21	W24E2	-5.792, 10.000, -5.792	W22E1	5.792, 10.000, -5.792	# 14	11
22	W21E2	5.792, 10.000, -5.792	W23E1	5.792, 10.000, 5.792	# 14	11
23	W22E2	5.792, 10.000, 5.792	W24E1	-5.792, 10.000, 5.792	# 14	11
24	W23E2	-5.792, 10.000, 5.792	W21E1	-5.792, 10.000, -5.792	# 14	11
25	W28E2	-5.917, 0.000, -5.917	W26E1	5.917, 0.000, -5.917	# 14	11
26	W25E2	5.917, 0.000, -5.917	W27E1	5.917, 0.000, 5.917	# 14	11
27	W26E2	5.917, 0.000, 5.917	W28E1	-5.917, 0.000, 5.917	# 14	11
28	W27E2	-5.917, 0.000, 5.917	W25E1	-5.917, 0.000, -5.917	# 14	11
29	W32E2	-6.083, -10.000, -6.083	W30E1	6.083, -10.000, -6.083	# 14	11
30	W29E2	6.083, -10.000, -6.083	W31E1	6.083, -10.000, 6.083	# 14	11
31	W30E2	6.083, -10.000, 6.083	W32E1	-6.083, -10.000, 6.083	# 14	11
32	W31E2	-6.083, -10.000, 6.083	W29E1	-6.083, -10.000, -6.083	# 14	11
33	W36E2	-8.635, 20.000, -8.635	W34E1	8.635, 20.000, -8.635	# 14	15
34	W33E2	8.635, 20.000, -8.635	W35E1	8.635, 20.000, 8.635	# 14	15
35	W34E2	8.635, 20.000, 8.635	W36E1	-8.635, 20.000, 8.635	# 14	15
36	W35E2	-8.635, 20.000, 8.635	W33E1	-8.635, 20.000, -8.635	# 14	15
37	W40E2	-8.635, 10.000, -8.635	W38E1	8.635, 10.000, -8.635	# 14	15
38	W37E2	8.635, 10.000, -8.635	W39E1	8.635, 10.000, 8.635	# 14	15
39	W38E2	8.635, 10.000, 8.635	W40E1	-8.635, 10.000, 8.635	# 14	15
40	W39E2	-8.635, 10.000, 8.635	W37E1	-8.635, 10.000, -8.635	# 14	15
41	W44E2	-8.802, 0.000, -8.802	W42E1	8.802, 0.000, -8.802	# 14	15
42	W41E2	8.802, 0.000, -8.802	W43E1	8.802, 0.000, 8.802	# 14	15
43	W42E2	8.802, 0.000, 8.802	W44E1	-8.802, 0.000, 8.802	# 14	15
44	W43E2	-8.802, 0.000, 8.802	W41E1	-8.802, 0.000, -8.802	# 14	15

45	W48E2	-9.052,-10.000,	-9.052	W46E1	9.052,-10.000,	-9.052	# 14	15
46	W45E2	9.052,-10.000,	-9.052	W47E1	9.052,-10.000,	9.052	# 14	15
47	W46E2	9.052,-10.000,	9.052	W48E1	-9.052,-10.000,	9.052	# 14	15
48	W47E2	-9.052,-10.000,	9.052	W45E1	-9.052,-10.000,	-9.052	# 14	15

----- SOURCES -----

Source	Wire Seg.	Wire #/Pct Actual	From End 1 (Specified)	Ampl.(V, A)	Phase(Deg.)	Type
1	8	41 / 50.00	(41 / 50.00)	1.000	0.000	V

The model has 48 wires and 528 segments. However, modeling time can be reduced by judicious use of the copy function for identical loops and by symbolic coordinate entries, if available. The source wires for each band are as follows: 20m = wire 41; 15m = wire 25; and 10m = wire 9. Source placement is at the wire center.

Because small changes in wire size resulted in noticeable differences in the antenna performance across the bands in question with monoband quads, I modeled this antenna using both #14 and #12 AWG copper wire. Only the #14 model is shown, since wire size is the only difference between the models.

As a handy reference, **Table 11-2** lists the mid-band performance for each band of each version of the antenna. Gain is free-space gain.

Table 11-2. 4-Element, 3-Band Quad Performance

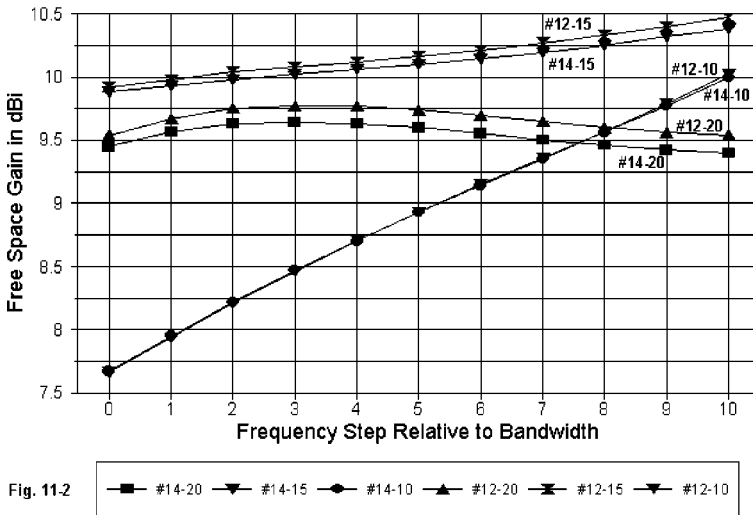
Wire-Band	Freq. MHz	Gain dBi	F-B dB	Impedance R +/- jX Ohms
#14-20	14.175	9.60	20.8	40.8 + j 3.6
#12-20		9.74	22.0	38.0 + j 1.7
#14-15	21.225	10.10	16.8	87.6 + j 4.4
#12-15		10.16	15.9	85.3 + j 3.9
#14-10	28.5	8.93	8.3	105.0 - j35.0
#12-10		8.93	8.0	103.0 - j35.8

The differences in performance figures between the two wire sizes are almost completely insignificant. This fact suggests that element interaction among loops for the various bands may play a stronger role than modest changes in wire size in determining performance characteristics in this 3-band model. The closest loop set to an uninfluenced set is for 20 meters, and the differences in mid-band performance are greatest on that band. The performance curves across the bands bear out this suggestion.

The gain curves in **Fig. 11-2** show the virtual identity of the 10-meter gain for the two wire sizes. 15-meter gain does almost as well, and only 20-meter gain shows something interesting. The low-end increase in gain toward the peak value is slightly more rapid for the fatter wire than for the thinner wire.

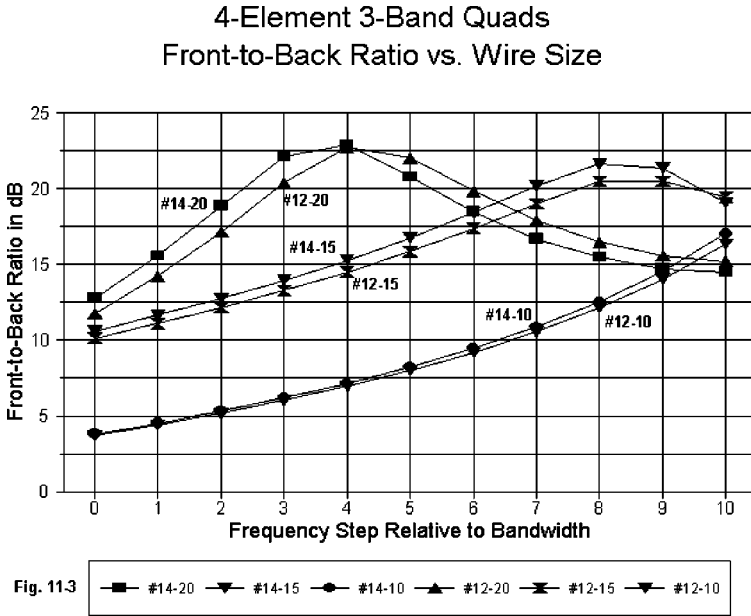
A rising gain curve across the band is natural for virtually any parasitic beam having a director and is the opposite trend from that shown by 2-element reflector-driver designs. However, the 10-meter curve strongly suggests that the performance for this band has not been optimized. The dimensions for 10-meters suggest that the design technique used to arrive at the dimension was simple scaling of the loop length from 20 and 15 meter. The result is, according to the model, relatively mediocre performance at the low end of 10 meters for a long-boom 4-element array. In addition, the spacing of the elements is arbitrary, and for 10 meters may not allow the achievement of a gain level rivaling that of 15 meters, whatever adjustments may be made to the size of the 10-meter loops. The planar design may have limits when applied to more than 2 elements.

4-Element 3-Band Quads Gain vs. Wire Size



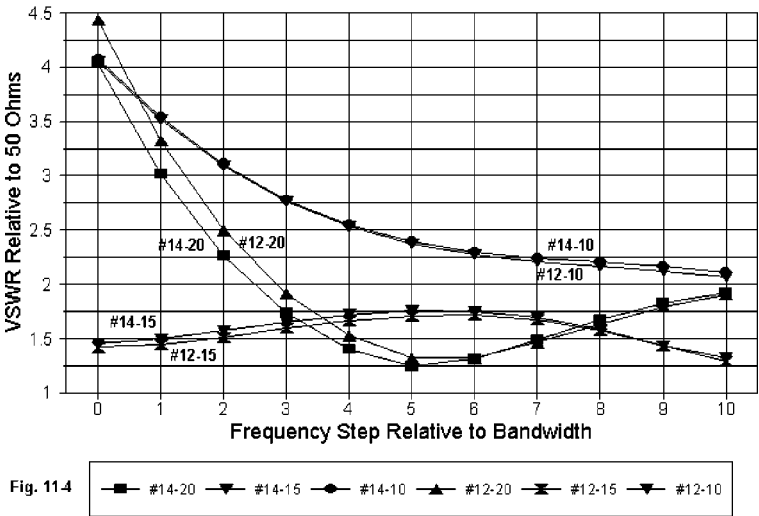
The front-to-back ratio curves in **Fig. 11-3** tend to confirm that--if the model is reasonably accurate--inadequate attention has been paid to 10 meter dimensions, including loop size and spacing. The front-to-back ratio on that band only rises above 10 dB at about 28.6 MHz and continues to climb to-

ward the 29.0 MHz mark, where the scan ceased. In contrast, the front-to-back peaks for both 20 and 15 meters occur within the passband under study. In accord with the suggestion that the 20 meter loops are least affected by the other loops in the array--in other words, act most like a monoband array--the 20-meter front-to-back curves for the two wire sizes show a frequency displacement that is missing from the 15- and 10-meter curves.



The VSWR curves in Fig. 11-4 are also revelatory. The 20-meter mid-band values suggested that the array might have a low SWR relative to 50 Ohms across that band. However, the curves show that SWR climbs precipitously below mid-band, as the resistive component of the source impedance approaches 20 Ohms. Although the mid-band impedance given for 15 meters suggests a better match to 75-Ohm line, the 50-Ohm SWR remains below 2:1 across that band. On 10 meters, the SWR only approaches 2:1 at 29 MHz. However, if the dimensions of all the 10 meter loops were changed to bring the performance reports within the passband, it is likely that the 10-meter SWR would also decrease to a more acceptable set of values relative to 50 Ohms.

4-Element 3-Band Quads
VSWR vs. Wire Size



For reference, **Table 11-3** lists the source impedance values for each band, using the #14 model, recorded for the low, middle, and high points of each band.

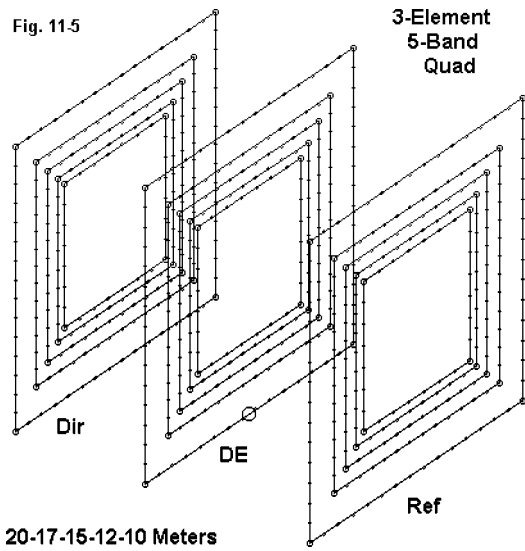
Table 11-3. Source Impedance Values for #14 AWG 4-Element Quad

Band	Impedance at a Specified Frequency			Delta	Delta
20 m	14.0	14.175	14.35	R	X
	24.2 - j45.8	40.8 + j 3.6	67.7 + j34.5	43.5	80.3
15 m	21.0	21.225	21.45		
	69.6 - j10.2	87.6 + j 4.4	60.7 + j11.3	26.9	21.5
10 m	28.0	28.5	29.0		
	92.6 - j94.6	105.0- j35.0	104.9+ j 6.7	12.4	101.3

Above 29 MHz, the 10-meter impedance descends once more. It is likely that judicious loop alteration can bring the source impedance within a 2:1 50-Ohm SWR curve that occupies most of the first MHz of 10. Likewise, adjustment to the 20 meter driver length could also move its 2:1 SWR curve lower in the band. There is no reason to touch anything on 15, except perhaps to draw the front-to-back curve more symmetrically within the band.

A 3-Element 5-Band 18'-Boom Quad Array

Correspondence with ON7NQ brought to light his efforts to improve the performance of a commercial 3-element 5-band quad he had purchased. The initial dimensions--with allowance for adding 17 and 12 meters and for dropping one element--were similar to those in the 4-element quad just studied. Improvements to 20 meter low-end performance and overall 10-meter performance were the goals of the revisions. Although ON7NQ modeled with a MININEC product, my cross checks with his numbers via NEC-4 showed a very close correlation. The results of one direction of the work yielded the 3-element array sketched in Fig. 11-5.



Since the sketch gives no hint of the final dimensions of this model (only one of several we discussed), Table 11-4 may help.

Table 11-4. 3-Element, 5-Band Quad Dimensions

Band	Reflector		Driver		Dir. 1
	Side L feet	Space Re-DE	Side L feet	Space DE-D1	
20	18.166	10	17.812	8	17.166
17	14.134	10	13.874	8	13.458
15	12.066	10	11.834	8	11.500
12	10.334	10	10.062	8	9.834
10	9.100	10	8.800	8	8.684

Compared to the dimensions given for the 3-band quad, 15 meters changes scarcely at all. In the case of both 20 and 10 meters, the loops have been enlarged, with the exception of the 20-meter director, which was decreased. The model for this 60-wire, 660 segment model follows.

ON7NQ 3 el 5 band #14

Frequency = 14.175 MHz.

Wire Loss: Copper -- Resistivity = 1.74E-08 ohm-m, Rel. Perm. = 1

----- WIRES -----

Wire Conn.--- End 1 (x,y,z : in) Conn.--- End 2 (x,y,z : in) Dia(in) Segs

1	W4E2	-52.100, 96.000,-52.100	W2E1	52.100, 96.000,-52.100	# 14	7
2	W1E2	52.100, 96.000,-52.100	W3E1	52.100, 96.000, 52.100	# 14	7
3	W2E2	52.100, 96.000, 52.100	W4E1	-52.100, 96.000, 52.100	# 14	7
4	W3E2	-52.100, 96.000, 52.100	W1E1	-52.100, 96.000,-52.100	# 14	7
5	W8E2	-52.800, 0.000,-52.800	W6E1	52.800, 0.000,-52.800	# 14	7
6	W5E2	52.800, 0.000,-52.800	W7E1	52.800, 0.000, 52.800	# 14	7
7	W6E2	52.800, 0.000, 52.800	W8E1	-52.800, 0.000, 52.800	# 14	7
8	W7E2	-52.800, 0.000, 52.800	W5E1	-52.800, 0.000,-52.800	# 14	7
9	W12E2	-54.600,-120.00,-54.600	W10E1	54.600,-120.00,-54.600	# 14	7
10	W9E2	54.600,-120.00,-54.600	W11E1	54.600,-120.00, 54.600	# 14	7
11	W10E2	54.600,-120.00, 54.600	W12E1	-54.600,-120.00, 54.600	# 14	7
12	W11E2	-54.600,-120.00, 54.600	W9E1	-54.600,-120.00,-54.600	# 14	7
13	W16E2	-59.000, 96.000,-59.000	W14E1	59.000, 96.000,-59.000	# 14	9
14	W13E2	59.000, 96.000,-59.000	W15E1	59.000, 96.000, 59.000	# 14	9
15	W14E2	59.000, 96.000, 59.000	W16E1	-59.000, 96.000, 59.000	# 14	9
16	W15E2	-59.000, 96.000, 59.000	W13E1	-59.000, 96.000,-59.000	# 14	9
17	W20E2	-60.375, 0.000,-60.375	W18E1	60.375, 0.000,-60.375	# 14	9
18	W17E2	60.375, 0.000,-60.375	W19E1	60.375, 0.000, 60.375	# 14	9
19	W18E2	60.375, 0.000, 60.375	W20E1	-60.375, 0.000, 60.375	# 14	9
20	W19E2	-60.375, 0.000, 60.375	W17E1	-60.375, 0.000,-60.375	# 14	9
21	W24E2	-62.000,-120.00,-62.000	W22E1	62.000,-120.00,-62.000	# 14	9
22	W21E2	62.000,-120.00,-62.000	W23E1	62.000,-120.00, 62.000	# 14	9
23	W22E2	62.000,-120.00, 62.000	W24E1	-62.000,-120.00, 62.000	# 14	9
24	W23E2	-62.000,-120.00, 62.000	W21E1	-62.000,-120.00,-62.000	# 14	9
25	W28E2	-69.000, 96.000,-69.000	W26E1	69.000, 96.000,-69.000	# 14	11
26	W25E2	69.000, 96.000,-69.000	W27E1	69.000, 96.000, 69.000	# 14	11
27	W26E2	69.000, 96.000, 69.000	W28E1	-69.000, 96.000, 69.000	# 14	11
28	W27E2	-69.000, 96.000, 69.000	W25E1	-69.000, 96.000,-69.000	# 14	11
29	W32E2	-71.000, 0.000,-71.000	W30E1	71.000, 0.000,-71.000	# 14	11
30	W29E2	71.000, 0.000,-71.000	W31E1	71.000, 0.000, 71.000	# 14	11
31	W30E2	71.000, 0.000, 71.000	W32E1	-71.000, 0.000, 71.000	# 14	11
32	W31E2	-71.000, 0.000, 71.000	W29E1	-71.000, 0.000,-71.000	# 14	11
33	W36E2	-72.400,-120.00,-72.400	W34E1	72.400,-120.00,-72.400	# 14	11
34	W33E2	72.400,-120.00,-72.400	W35E1	72.400,-120.00, 72.400	# 14	11
35	W34E2	72.400,-120.00, 72.400	W36E1	-72.400,-120.00, 72.400	# 14	11
36	W35E2	-72.400,-120.00, 72.400	W33E1	-72.400,-120.00,-72.400	# 14	11
37	W40E2	-80.750, 96.000,-80.750	W38E1	80.750, 96.000,-80.750	# 14	13
38	W37E2	80.750, 96.000,-80.750	W39E1	80.750, 96.000, 80.750	# 14	13
39	W38E2	80.750, 96.000, 80.750	W40E1	-80.750, 96.000, 80.750	# 14	13
40	W39E2	-80.750, 96.000, 80.750	W37E1	-80.750, 96.000,-80.750	# 14	13
41	W44E2	-83.250, 0.000,-83.250	W42E1	83.250, 0.000,-83.250	# 14	13
42	W41E2	83.250, 0.000,-83.250	W43E1	83.250, 0.000, 83.250	# 14	13
43	W42E2	83.250, 0.000, 83.250	W44E1	-83.250, 0.000, 83.250	# 14	13
44	W43E2	-83.250, 0.000, 83.250	W41E1	-83.250, 0.000,-83.250	# 14	13
45	W48E2	-84.805,-120.00,-84.805	W46E1	84.805,-120.00,-84.805	# 14	13
46	W45E2	84.805,-120.00,-84.805	W47E1	84.805,-120.00, 84.805	# 14	13
47	W46E2	84.805,-120.00, 84.805	W48E1	-84.805,-120.00, 84.805	# 14	13
48	W47E2	-84.805,-120.00, 84.805	W45E1	-84.805,-120.00,-84.805	# 14	13
49	W52E2	-103.00, 96.000,-103.00	W50E1	103.00, 96.000,-103.00	# 14	15
50	W49E2	103.00, 96.000,-103.00	W51E1	103.00, 96.000, 103.00	# 14	15
51	W50E2	103.00, 96.000, 103.00	W52E1	-103.00, 96.000, 103.00	# 14	15
52	W51E2	-103.00, 96.000, 103.00	W49E1	-103.00, 96.000,-103.00	# 14	15

53	W56E2	-106.87,	0.000,-106.87	W54E1	106.870,	0.000,-106.87	# 14	15
54	W53E2	106.870,	0.000,-106.87	W55E1	106.870,	0.000,106.870	# 14	15
55	W54E2	106.870,	0.000,106.870	W56E1	-106.87,	0.000,106.870	# 14	15
56	W55E2	-106.87,	0.000,106.870	W53E1	-106.87,	0.000,-106.87	# 14	15
57	W60E2	-109.00,-120.00,-109.00		W58E1	109.000,-120.00,-109.00		# 14	15
58	W57E2	109.000,-120.00,-109.00		W59E1	109.000,-120.00,109.000		# 14	15
59	W58E2	109.000,-120.00,109.000		W60E1	-109.00,-120.00,109.000		# 14	15
60	W59E2	-109.00,-120.00,109.000		W57E1	-109.00,-120.00,-109.00		# 14	15

----- SOURCES -----

Source	Wire Seg.	Wire #/Pct Actual	From End 1 (Specified)	Ampl.(V, A)	Phase(Deg.)	Type
1	8	53 / 50.00	(53 / 50.00)	1.000	0.000	V

This model happens to begin with the 10-meter wires, from director to reflector, and end with the 20-meter wires. The source wires are 20m = wire 53, 12m = wire 41, 15m = wire 29, 17m = wire 17, and 10m = wire 5. Dimensions are in inches in the model description. The wire size is #14 AWG copper.

The midband performance values reported by NEC-4 for this model are as follows in **Table 11-5**.

Table 11-5. 3-Element, 5-Band Quad Performance

Wire-Band	Freq. MHz	Gain dBi	F-B dB	Impedance R +/- jX Ohms
20	14.175	8.08	11.3	43.6 + j 3.2
17	18.118	8.32	15.2	39.6 + j 3.5
15	21.225	8.51	21.4	45.5 + j 6.2
12	24.94	8.52	15.9	47.7 + j 8.9
10	28.5	9.33	11.3	45.0 + j14.9

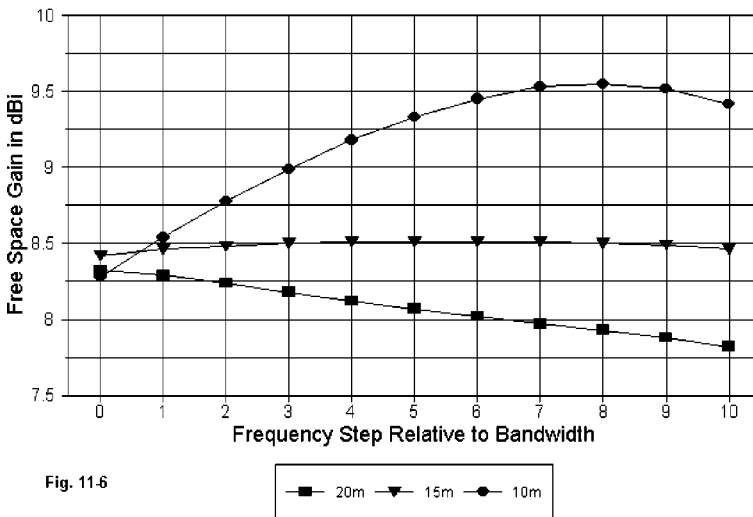
Relative to the 40' boom 4-element array, gains are down, but each band shows a good match at center to a 50-Ohm feed system. A closer look at each parameter across the wide bands may be useful in understanding the design goals of this model.

As shown in **Fig. 11-6**, the gain across 15 meters is virtually flat. The gain across 20 meters descends, but only moderately, with design emphasis upon performance at the lower end of the band. Although the 10-meter gain curve still ascends, its peak occurs within the passband. As we discovered with 2-element multi-band quad arrays, element interaction provides 10-meters with higher gain than might otherwise be obtained in a monoband 18' boom quad, since the elements are very widely spaced for that band. 20 meters

seems to “suffer” (in terms of gain) from its relative independence, with 15 meters showing a “balance” of influence.

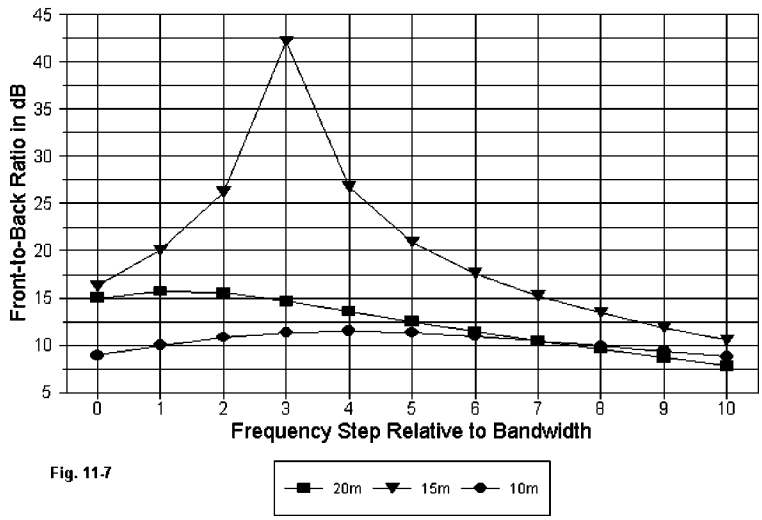
At present, terms like “suffer,” “independence,” “balance of influence” have no strict quantification and should be treated as suggestive rather than as indicating a definite property. Mutual coupling between elements in monoband quad arrays has hardly begun to be explored, and the situation is considerably worse for multi-band arrays. In such arrays, we must consider not only the coupling of elements within a band, but as well, coupling with elements for adjacent bands as well. Models show that such coupling does exist in terms of currents on inactive elements. However, the degree of coupling and its effects on array gain are yet to be developed.

3-Element 5-Band Quad Gain vs. Band (20/15/10)

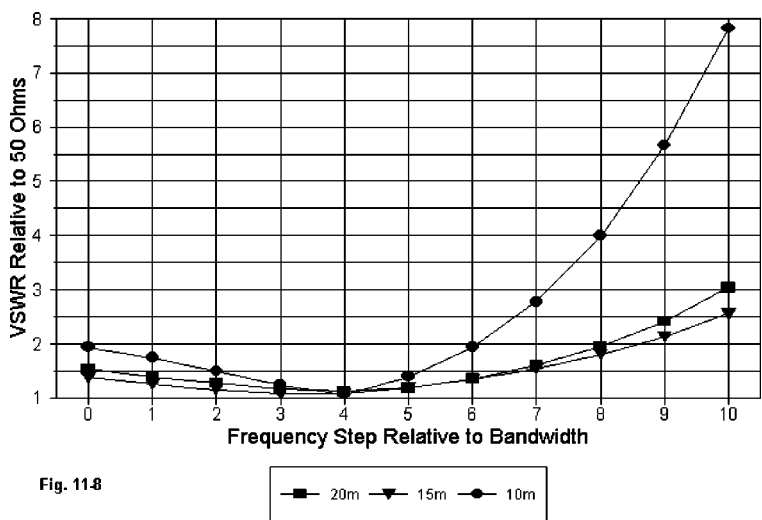


The front-to-back curves (**Fig. 11-7**) tell us that the antenna was largely designed for gain, with the source impedance the most important second factor. Front-to-back ratio was largely accepted for what it turned out to be. On 15 meters, where gain performance is exceptionally stable, the front-to-back peak can easily be moved within the passband. 20 and 10 are harder nuts to crack, and their numbers are relatively poor, except for the low end of 20 meters, where they approach being adequate. On 10 meters, the front-to-back performance across the band is similar to a 2-element reflector-driver Yagi.

3-Element 5-Band Quad
Front-to-Back vs. Band (20/15/10)



3-Element 5-Band Quad
VSWR vs. Band (20/15/10)



The 50-Ohm SWR performance of the antennas in the ON7NQ array has also been optimized for the low ends of the bands, as is readily apparent in

Fig. 11-8. On 20 and 10, the SWR is below 2:1 for at least 80% of the passbands. That figure might be raised to close to full band coverage with a slight adjustment of the minimum SWR frequency. However, the <2:1 SWR figure goes down to a 60% coverage for the first MHz of 10 meters.

For reference, **Table 11-6** gives the standard figures across each of the wide bands. Optimizing gain within the passband for each of the wide bands has resulted in an expansion of the range of reactance across the bands. Like most 3-element parasitical arrays, the lowest impedance is at the upper end of the band.

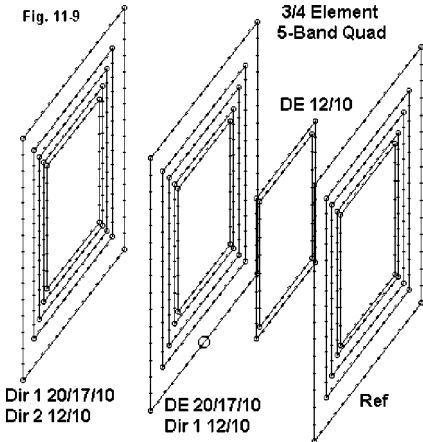
Table 11-6. Source Impedance Values for #14 AWG 4-Element Quad

Band	Impedance at a Specified Frequency			Delta	Delta
20 m	14.0	14.175	14.35	R	X
	45.3 - j19.9	43.3 + j 4.0	32.0 + j43.2	13.3	63.1
15 m	21.0	21.225	21.45		
	48.1 - j15.6	45.4 + j 6.8	35.4 + j38.3	12.7	53.9
10 m	28.0	28.5	29.0		
	76.9 - j32.2	45.0 + j14.9	27.0 + j86.7	49.9	118.9

20- and 15-meter performance are not likely to be improved by more than a small amount due to the limitations of the boom length on those bands. The boom length is short for 20 meters and about right for 15 meters, relative to maximizing gain for three elements. Improving 10 meter performance seems the only further development possible, since the boom is long for 3 elements on that band. The 10' reflector-driver spacing seems especially long.

**A 3/4-Element 5-Band
18'-Boom Quad Array**

ON7NQ added a new spreader midway between the old reflector and driver spreaders. To this, he attached what became driver loops for 10 and 12 meters, with the old drivers becoming first directors. The result is a hybrid 3- and 4-element quad, where the element spacing on the highest two bands more closely resembles that used with comparable Yagis. The



overall 18' boom length was retained. The result looks something the sketch in **Fig. 11-9**.

Table 11-7 lists the side lengths for the elements in this hybrid array.

Table 11-4. 3-/4-Element, 5-Band Quad Dimensions

Band	Reflector		Driver		Dir 1		Dir 2
	Side L	Space	Side L	Space	Side L	Space	SideL
	feet	Re-DE	feet	DE-D1	feet	D1-D2	feet
20	18.084	10	17.808	8	17.084		
17	14.042	10	13.858	8	13.316		
15	12.066	10	11.834	8	11.500		
12	10.200	5	9.932	5	9.850	8	9.892
10	9.224	5	8.816	5	8.716	8	8.666

Due to the difference in element spacing on 12 and 10 in terms of fractions of a wavelength, the forward-most director on 12 is actually larger than the first director. Many of the loop size changes are small on the lower bands, and the 15 meter dimensions did not change at all. Here is the model description for this 68-wire, 724-segment model.

ON7NQ 3/4 el 5 band #12

Frequency = 14.175 MHz.

Wire Loss: Copper -- Resistivity = 1.74E-08 ohm-m, Rel. Perm. = 1

----- WIRES -----

Wire Conn.---	End 1 (x,y,z : in)	Conn.---	End 2 (x,y,z : in)	Dia(in)	Segs
1	W4E2 -108.50, 0.000,-108.50	W2E1	108.500, 0.000,-108.50	# 12	15
2	W1E2 108.500, 0.000,-108.50	W3E1	108.500, 0.000,108.500	# 12	15
3	W2E2 108.500, 0.000,108.500	W4E1	-108.50, 0.000,108.500	# 12	15
4	W3E2 -108.50, 0.000,108.500	W1E1	-108.50, 0.000,-108.50	# 12	15
5	W8E2 -106.85,120.000,-106.85	W6E1	106.850,120.000,-106.85	# 12	15
6	W5E2 106.850,120.000,-106.85	W7E1	106.850,120.000,106.850	# 12	15
7	W6E2 106.850,120.000,106.850	W8E1	-106.85,120.000,106.850	# 12	15
8	W7E2 -106.85,120.000,106.850	W5E1	-106.85,120.000,-106.85	# 12	15
9	W12E2 -102.50,216.000,-102.50	W10E1	102.500,216.000,-102.50	# 12	15
10	W9E2 102.500,216.000,-102.50	W11E1	102.500,216.000,102.500	# 12	15
11	W10E2 102.500,216.000,102.500	W12E1	-102.50,216.000,102.500	# 12	15
12	W11E2 -102.50,216.000,102.500	W9E1	-102.50,216.000,-102.50	# 12	15
13	W16E2 -84.250, 0.000,-84.250	W14E1	84.250, 0.000,-84.250	# 12	13
14	W13E2 84.250, 0.000,-84.250	W15E1	84.250, 0.000, 84.250	# 12	13
15	W14E2 84.250, 0.000, 84.250	W16E1	-84.250, 0.000, 84.250	# 12	13
16	W15E2 -84.250, 0.000, 84.250	W13E1	-84.250, 0.000,-84.250	# 12	13
17	W20E2 -83.150,120.000,-83.150	W18E1	83.150,120.000,-83.150	# 12	13
18	W17E2 83.150,120.000,-83.150	W19E1	83.150,120.000, 83.150	# 12	13
19	W18E2 83.150,120.000, 83.150	W20E1	-83.150,120.000, 83.150	# 12	13
20	W19E2 -83.150,120.000, 83.150	W17E1	-83.150,120.000,-83.150	# 12	13
21	W24E2 -79.900,216.000,-79.900	W22E1	79.900,216.000,-79.900	# 12	13
22	W21E2 79.900,216.000,-79.900	W23E1	79.900,216.000, 79.900	# 12	13
23	W22E2 79.900,216.000, 79.900	W24E1	-79.900,216.000, 79.900	# 12	13

24	W23E2	-79.900,216.000,	79.900	W21E1	-79.900,216.000,-79.900	# 12	13
25	W28E2	-72.400, 0.000,-72.400		W26E1	72.400, 0.000,-72.400	# 12	11
26	W25E2	72.400, 0.000,-72.400		W27E1	72.400, 0.000, 72.400	# 12	11
27	W26E2	72.400, 0.000, 72.400		W28E1	-72.400, 0.000, 72.400	# 12	11
28	W27E2	-72.400, 0.000, 72.400		W25E1	-72.400, 0.000,-72.400	# 12	11
29	W32E2	-71.000,120.000,-71.000		W30E1	71.000,120.000,-71.000	# 12	11
30	W29E2	71.000,120.000,-71.000		W31E1	71.000,120.000, 71.000	# 12	11
31	W30E2	71.000,120.000, 71.000		W32E1	-71.000,120.000, 71.000	# 12	11
32	W31E2	-71.000,120.000, 71.000		W29E1	-71.000,120.000,-71.000	# 12	11
33	W36E2	-69.000,216.000,-69.000		W34E1	69.000,216.000,-69.000	# 12	11
34	W33E2	69.000,216.000,-69.000		W35E1	69.000,216.000, 69.000	# 12	11
35	W34E2	69.000,216.000, 69.000		W36E1	-69.000,216.000, 69.000	# 12	11
36	W35E2	-69.000,216.000, 69.000		W33E1	-69.000,216.000,-69.000	# 12	11
37	W40E2	-61.200, 0.000,-61.200		W38E1	61.200, 0.000,-61.200	# 12	9
38	W37E2	61.200, 0.000,-61.200		W39E1	61.200, 0.000, 61.200	# 12	9
39	W38E2	61.200, 0.000, 61.200		W40E1	-61.200, 0.000, 61.200	# 12	9
40	W39E2	-61.200, 0.000, 61.200		W37E1	-61.200, 0.000,-61.200	# 12	9
41	W44E2	-59.950, 60.000,-59.950		W42E1	59.950, 60.000,-59.950	# 12	9
42	W41E2	59.950, 60.000,-59.950		W43E1	59.950, 60.000, 59.950	# 12	9
43	W42E2	59.950, 60.000, 59.950		W44E1	-59.950, 60.000, 59.950	# 12	9
44	W43E2	-59.950, 60.000, 59.950		W41E1	-59.950, 60.000,-59.950	# 12	9
45	W48E2	-59.100,120.000,-59.100		W46E1	59.100,120.000,-59.100	# 12	9
46	W45E2	59.100,120.000,-59.100		W47E1	59.100,120.000, 59.100	# 12	9
47	W46E2	59.100,120.000, 59.100		W48E1	-59.100,120.000, 59.100	# 12	9
48	W47E2	-59.100,120.000, 59.100		W45E1	-59.100,120.000,-59.100	# 12	9
49	W52E2	-59.350,216.000,-59.350		W50E1	59.350,216.000,-59.350	# 12	9
50	W49E2	59.350,216.000,-59.350		W51E1	59.350,216.000, 59.350	# 12	9
51	W50E2	59.350,216.000, 59.350		W52E1	-59.350,216.000, 59.350	# 12	9
52	W51E2	-59.350,216.000, 59.350		W49E1	-59.350,216.000,-59.350	# 12	9
53	W56E2	-55.340, 0.000,-55.340		W54E1	55.340, 0.000,-55.340	# 12	7
54	W53E2	55.340, 0.000,-55.340		W55E1	55.340, 0.000, 55.340	# 12	7
55	W54E2	55.340, 0.000, 55.340		W56E1	-55.340, 0.000, 55.340	# 12	7
56	W55E2	-55.340, 0.000, 55.340		W53E1	-55.340, 0.000,-55.340	# 12	7
57	W60E2	-52.900, 60.000,-52.900		W58E1	52.900, 60.000,-52.900	# 12	7
58	W57E2	52.900, 60.000,-52.900		W59E1	52.900, 60.000, 52.900	# 12	7
59	W58E2	52.900, 60.000, 52.900		W60E1	-52.900, 60.000, 52.900	# 12	7
60	W59E2	-52.900, 60.000, 52.900		W57E1	-52.900, 60.000,-52.900	# 12	7
61	W64E2	-52.300,120.000,-52.300		W62E1	52.300,120.000,-52.300	# 12	7
62	W61E2	52.300,120.000,-52.300		W63E1	52.300,120.000, 52.300	# 12	7
63	W62E2	52.300,120.000, 52.300		W64E1	-52.300,120.000, 52.300	# 12	7
64	W63E2	-52.300,120.000, 52.300		W61E1	-52.300,120.000,-52.300	# 12	7
65	W68E2	-51.995,216.000,-51.995		W66E1	51.995,216.000,-51.995	# 12	7
66	W65E2	51.995,216.000,-51.995		W67E1	51.995,216.000, 51.995	# 12	7
67	W66E2	51.995,216.000, 51.995		W68E1	-51.995,216.000, 51.995	# 12	7
68	W67E2	-51.995,216.000, 51.995		W65E1	-51.995,216.000,-51.995	# 12	7

----- SOURCES -----

Source	Wire Seg.	Wire #/Pct Actual	From End 1 (Specified)	Ampl.(V, A)	Phase(Deg.)	Type
1	8	5 / 50.00	(5 / 50.00)	1.000	0.000	V

This model is listed by bands from 20 through 10 meters, with wires within a band given from the reflector forward. Consequently, the source wires are 20m = wire 5, 17m = wire 17, 15m = wire 29, 12m = wire 41, and 10m = wire 57. Dimensions are in inches, and the wire size is #12 AWG copper.

To see what basic improvements the addition of the two new drivers has made, **Table 11-8** provides a look at the midband performance reports from the model.

Table 11-8. 3-/4-Element, 5-Band Quad Performance

Wire-Band	Freq. MHz	Gain dBi	F-B dB	Impedance R +/- jX Ohms
20	14.175	8.30	15.2	44.4 + j 3.6
17	18.118	8.42	25.5	43.5 + j 0.1
15	21.225	8.52	21.6	46.6 + j 0.6
12	24.94	9.22	18.5	42.2 + j 2.9
10	28.5	9.74	27.9	56.1 + j11.3

Overall, gain and front-to-back ratios are up across the board, although only marginally on the lowest bands. Mid-band gain and front-to-back ratio are better on 10 meters especially. 15-meters remains virtually unchanged.

In the gain curves in **Fig. 11-10**, we may note that 15 remains unchanged in its flat curve, while the decrease in gain at the upper end of 20 meters has decreased. The gain curve for 10 meters remains at about 9 dBi or better for 90% of the passband, before taking a nose dive.

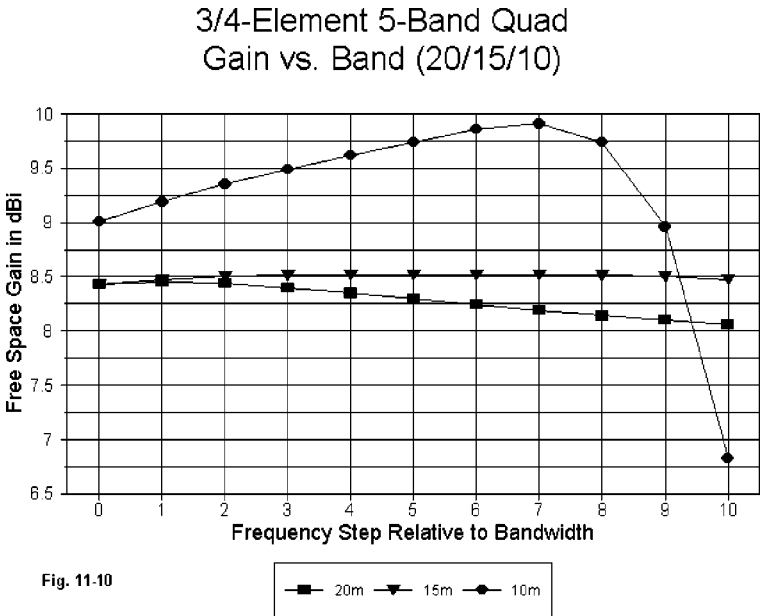
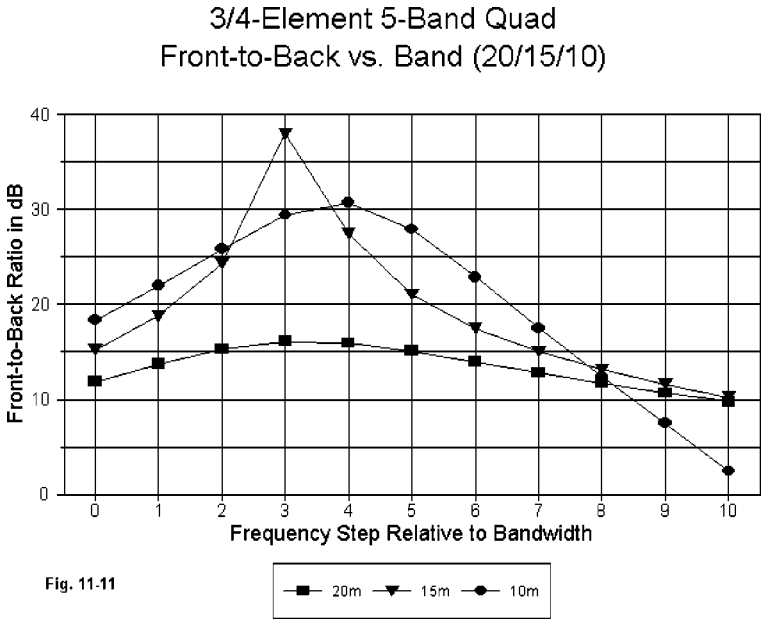


Fig. 11-10

In **Fig. 11-11**, we can see the unchanged 15-meter front-to-back curve, which serves as a back drop for the other curves. 20 meters shows a movement of the curve to better center it within the band and give better upper band-edge performance. The biggest improvement occurs on 10 meters, where the front-to-back value is at least 15 dB for more than 3/4 of the pass-band. As with the gain, we get a steep slope downward as the frequency approaches 29 MHz.



The small adjustments to the lower bands yield 50-Ohm SWR curves (**Fig. 11-12**) that are below 2:1 for 90% of 20 and 15 meters. The 10-meter 2:1 curve has been extended to over 80% of the passband and is consistent with the patterning of the gain and front-to-back figures. 28.8 to 29 MHz has been sacrificed for optimized performance at the low and middle regions of the passband. You may compare this figure with **Fig. 11-8** to more clearly see the improvement in the 50-Ohm SWR category.

It is also noteworthy to compare the performance figures of the 3/4-element 5-band quad with those of the traditional design in **Fig. 11-2** through **Fig. 11-4**. Although the 4-element, 40' boom design provides more gain on 15 and 10 meters, the 18' boom 3/4-element design is superior in all other categories, except perhaps 20-meter front-to-back ratio--which was obtained

in the 4-element model at the cost of a relatively low gain figure over most of the band. The 18' 3/4-element design is also a better match on every band.

3-Element 5-Band Quad
VSWR vs. Band (20/15/10)

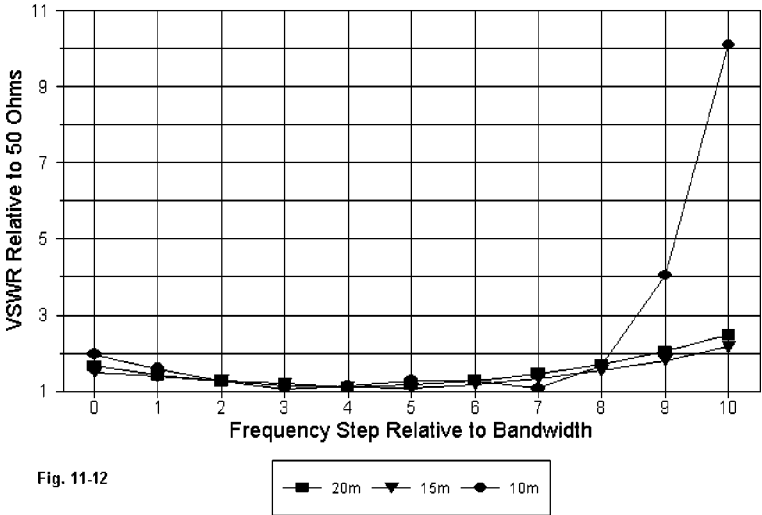


Fig. 11-12

The results of looking at these models are a few suggestions rather than judgments. First, element interaction in a multi-band quad array remains a strong candidate for being the source of some of its performance. The fact that the current ON7NQ model achieves the performance it does with a boom less than 50% the length of the more traditional models suggests that some of the element interactions can be beneficial.

The achievements of the short boom quad also suggest that those interested in quad design may wish to rethink some of presumptions underlying traditional designs. Element spacing taken in terms of fractions of a wavelength plays a role in optimizing performance, although not necessarily in a simple way. Simply adding element collections at somewhat arbitrary points along the boom may be less effective than optimizing the spacing for each major band and then working out whatever compromises may be needed. A 40' boom may be both useful and necessary for higher gain on 20 and 17, but without intermediate elements somewhere along the line, the boom length may be wasted for 10- and 12-meter performance.

Even within the realm of these design suggestions, it appears that a quad can be designed for a relatively uniform source impedance for all of the bands covered. Although this feature may not improve absolute performance, it can ease the task of installation, band-switching, and other functions of a more practical nature in constructing and using a large quad array. It also appears possible to better center the SWR curve within both the 20-and 15-meter bands.

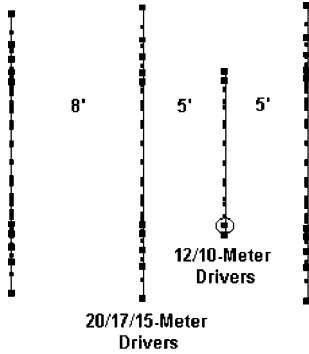
There may in fact be designs available that achieve all these goals. My small sample of models can make no claim to being exhaustive. However, if those designs are not available at present, then multi-band quad designers have a fertile field of endeavor for some time to come. If someone is going to erect something of the mechanical complexity of a many-element, many-band quad, he deserves to have the optimal performance to be gained from the array--and from the investment he has made in it and in its supporting structure.

Stacking the 3/4-Element 5-Band 18'-Boom Quad Array

The ON7NQ 3/4 element quad on an 18' boom has attracted a bit of attention, along with questions about stacking a pair of them. Stacking quads is not quite the same as stacking Yagis. For identical monoband Yagis, the best stacking distance tends to increase with individual array gain. Once you find--via models--the best distance apart for maximum gain, then the next hunt is for the distance that gives adequate front-to-back ratio--unless one wishes to redesign the antennas in the array. The higher the gain of the individual Yagis, the more likely one is to be able to find a distance that maximizes front-to-back ratio while only robbing about 0.1 dB from the maximum gain.

For quads, we have a different ball game. Although array gain does play a role in the determination of the best stacking distance, this criterion tends to be overridden by considerations of array isolation. By isolation, I mean a stacking distance that allows each array on all bands covered to show the least changes in feedpoint impedance on each band relative to a single array. Planar arrays tend to show more isolation at close spacings ($5/8$ to $2/3$ wavelength on 20 meters, or about 24') than spider designs. 2-element 5-band spiders tend to achieve satisfactory isolation with a center-to-center spacing of about 30'--at least in the models explored so far. (Remember that all of this work is exploratory.)

The ON7NQ array is planar in design, but has more gain than the 2-element planar designs examined so far. Hence, it was likely that the best stacking distance might be more than 24'. In fact, a 30' spacing produced adequate isolation (and convergence of the feedpoint impedances with the single array values). However, 36' proved to be a bit far apart, as the lower-band front-to-back ratio began to decrease--or shift off of the design frequency. Therefore, the following preliminary figures for the single array and the stack in free space use a 30' stack spacing, as measured from the hub of one array to the hub of the other. **Fig. 11-13** shows a profile of the stack.



Profile of Stacked ON7NQ Quads

The data in **Table 11-9** through **Table 11-12** consist of the gain in dBi, take-off angle (where relevant), 180E front-to-back ratio in dB, half-power beamwidth, feed impedances given as series resistance and reactance, and the 50-Ohm SWR (for which the original array had been set). Since the array was designed for 28.0 to 28.8 MHz coverage on 10 meters, the values for that band follow the designer's plan.

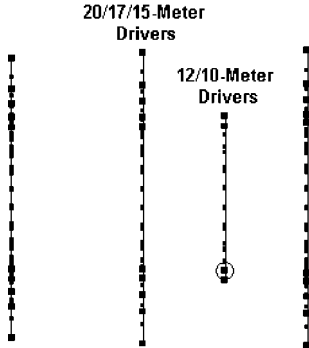


Fig. 11-13

Table 11-9. A Single ON7NQ 3-/4-Element Quad in Free Space

Frequency Mhz	Free-Space Gain dBi	Front-to-Back Ratio dB	Beamwidth Degrees	Feed Z R +/- jX	50-Ohm VSWR
14.0	8.4	11.8	66	37.5-j18.4	1.66
14.175	8.3	15.1	67	44.3+j 4.3	1.16
14.35	8.1	9.8	67	34.8+j36.2	2.48
18.118	8.4	25.5	68	43.5-j 0.3	1.15
21.0	8.4	15.2	69	49.6-j20.2	1.50
21.225	8.5	21.0	68	46.4-j 0.0	1.08
21.45	8.5	10.3	65	36.2+j30.7	2.17
24.94	9.2	19.0	59	40.9+j 2.2	1.23
28.0	9.0	18.4	65	43.8-j31.7	1.97

28.4	9.6	30.7	59	51.3+j 6.7	1.14
28.8	9.7	12.4	52	31.2+j 8.0	1.67

Table 11-10. 2 ON7NQ Quads Stacked 30' Apart in Free Space

Note: Z1 (upper entry) = lower quad; Z2 (lower entry) = upper quad. Since both quads are fed on the lower element, some differentials in values are normal.

Frequency Mhz	Free-Space Gain dBi	Front-to-Back Ratio dB	Beamwidth Degrees	Feed Z R +/- jX	50-Ohm VSWR
14.0	10.2	13.5	65	38.7-j20.9	1.71
				38.4-j20.5	1.70
14.175	10.2	14.7	65	42.5+j 9.3	1.30
				42.2+j 9.4	1.30
14.35	9.9	9.4	64	36.9+j45.7	2.88
				36.3+j45.7	2.92
18.118	10.9	23.3	67	43.9+j 1.5	1.14
				43.9+j 1.5	1.14
21.0	11.2	14.6	68	49.8-j19.7	1.48
				49.8-j19.7	1.48
21.225	11.3	21.3	67	49.4+j 2.3	1.05
				49.4+j 2.3	1.05
21.45	11.1	10.1	64	41.5+j32.1	2.04
				41.5+j32.2	2.04
24.94	12.0	17.4	59	44.7-j 0.9	1.12
				44.8-j 0.9	1.12
28.0	12.1	18.9	65	46.0-j31.9	1.93
				46.0-j31.9	1.93
28.4	12.6	25.1	59	53.2+j 5.1	1.12
				53.3+j 5.1	1.12
28.8	12.6	12.2	52	31.9+j 8.4	1.64
				31.9+j 8.4	1.64

Table 11-11. Stacking Gain Averaged by Bands

20	17	15	12	10	Meters
1.8	2.4	2.7	2.9	3.0	dB

Table 11-12. 2 ON7NQ Quads Stacked 30' Apart at 50' and 80'

Note: Model uses average ground; Z1 (upper entry) = lower quad; Z2 (lower entry) = upper quad. Since both quads are fed on the lower element, some differentials in values are normal.

Freq. Mhz	Free-Space Gain dBi	F-to-B Ratio dB	Beamwidth Degrees	Feed Z R +/- jX	50-Ohm TO VSWR	TO Deg
14.0	14.7	13.5	65	38.7-j20.6 38.4-j20.7	1.70 1.71	14
14.175	14.7	14.5	65	42.5+j 9.5 42.1+j 9.2	1.30 1.30	13
14.35	14.4	9.3	65	40.0+j45.7 36.2+j45.6	2.88 2.92	13
18.118	15.7	22.7	67	44.1+j 1.4 43.8+j 1.5	1.14 1.15	11
21.0	16.1	14.7	68	49.8-j19.9 50.0-j19.6	1.49 1.48	9
21.225	16.2	20.9	67	49.3+j 2.2 49.6+j 2.3	1.05 1.05	9
21.45	16.0	10.0	64	41.6+j32.2 41.5+j32.2	2.04 2.04	9
24.94	17.0	16.5	58	44.8-j 1.3 45.1-j 0.9	1.12 1.11	8
28.0	17.1	19.0	65	45.8-j32.1 46.0-j32.1	1.94 1.94	7
28.5	17.6	24.7	59	52.9+j 5.0 53.2+j 5.1	1.12 1.12	7
29	17.6	12.2	52	31.6+j 8.8 31.7+j 8.5	1.66 1.65	7

The two quad arrays show good isolation with a 30' spacing in free space, shifting the feedpoint impedance by only a very few Ohms on 20 and much less as the frequency goes up. Front-to-back figures remain roughly centered on the design frequencies. The stacking gain shows a relatively standard progression. Consequently, the stacking process may in some cases--considering mast stresses, mechanical complexity, and weather effects--be a worthwhile project. Greater spacing will show increased array isolation on 20 meters, but greater skewing of the performance curves. Less spacing shows decreased isolation between arrays and higher differentials between feedpoint impedance values for the two feedpoints. For reference, the forward gain of a 5-6 element Yagi on a 0.7 wavelength boom (48' on 20 meters, 24' on 10 meters) is about 10.1 dBi in free space.

Above ground, as we might expect, the values of impedance diverge more than in free space (where Z1 is the lower quad and Z2 is the upper and both quads are fed on the bottom wires of their respective drivers). There is, of course, no reason why one might not feed the upper quad on its lower wire and lower quad on its upper wire. With 30' spacing, the values--even on the lowest bands--do not diverge enough to materially affect a junction. 75-Ohm quarter-wavelength sections might be used on each band and join at a Tee prior to connection to a single remote band switch installed on the mast. If connection length is a problem, the lower quad might be fed on its top wire. As well, 75-Ohm 3/4-wavelength sections are also usable, although with greater losses. Alternatively, but with some complexities of switching, 75-Ohm parallel line can be used to transform the 50-Ohm individual feed impedances to the 100 Ohms needed at each Tee-junction for the stack common feedline.

The stacking exercise is shown only as a representative example of possibilities and to illustrate the importance of independence or isolation in quad stacking.

The design examples that we have explored, while representing a fair sampling of the available designs, only scratch the surface of what may be possible by way of improved long-boom multi-band quad arrays. Examining the weaknesses and strengths of these designs may prove productive for better big quads in the future.

12. Where Do We Go From Here?

In one sense, we have covered a lot of ground in our exploration of existing quad designs—far too much ground to summarize effectively. In another sense, we have only set the stage for more and different kinds of work on the cubical quad array.

In our survey of extant quad designs, we started with the simplest quad beam, the 2-element driver-reflector type. We then shrunk them, only to later enlarge them into 5-band 2-element designs. We have explored ways to feed multi-band quads, as well as examining the potential for stacking them to improve gain across many ham bands. We looked at larger quad arrays, both monoband types and attempts at multi-band versions.

Along the way, I hope that the data has produced some very practical information, useful to those who wish to build their own quads. More generally, I hope the data have given you a good sense of the possibilities and the limitations of quad arrays.

The exercises have had a second purpose as well: to provide antenna modelers with some sound guidance that will yield the most useful and adequate models possible for quads. The quad array—except for some coaxial-cable stub-switching issues—is eminently able to be modeled well within the limitations of NEC software. Therefore, the more individuals who actively model quads, either as exercises in analysis or as steps in design, the better quads we shall see in the future.

Our third goal deserves a bit more attention. Although we looked at “spot” designs throughout our exploratory studies, certain patterns have emerged. These patterns, while certainly not absolutely conclusive, are vivid enough to stir some rethinking about quads. Here are some salient points drawn from various chapters.

1. Although quad arrays—especially 2-element quad beams—often have very wide bandwidths with respect to meeting a 2:1 VSWR limit, other properties of quads are rather narrow-banded. For many designs, the rate of gain change within a given ham band is quite high. As well, the front-to-back ratio

exceeds 20 dB for only a small portion of an amateur band. In short, contrary to their past reputation, quads are not “low-Q” antennas, but instead, very high-Q as soon as we add operating characteristics other than SWR to our list of concerns. How to achieve a truly wide-band quad remains a significant challenge.

2. The typical quad array is a wire affair, and wire has a very small diameter relative to the length of an RF wave. If the typical 20-meter Yagi-Uda array uses elements that average 1" in diameter, the typical #14 AWG copper wire quad uses an element under 6.5% as large. Element diameter does make a difference in quad design and performance, a sizable difference. What remains to be developed is just how large a difference element diameter does make and whether that difference is sporadic or systematic.

3. When we compare seemingly similar parasitical beam designs for Yagis and quads, both of which have been optimized to the degree possible, the quad almost inevitably winds up with a longer boom length than the Yagi for the same number of elements. This fact suggests that there is a significant difference between the inter-element coupling for quad loop elements and for linear Yagi elements. The fact also is suggestive about the practice of striving for short-boom quad designs when working with more than two elements. What ramifications these outcomes may have for quad design remains to be seen.

4. If we add together all of the questions so far raised, how do they combine to yield more adequate quad designs? In the combination there may be further surprises not revealed by the individual factors, and they remain to be discovered.

So, if the exploration of existing quad designs has yielded useful information to quad designers and builders, it nevertheless leaves behind many “remains” (in the sense of work that remains to be done). Some of that work will be the subject of Volume 2, “Rethinking the Quad Beam.”

Other Publications

We hope you've enjoyed **Volume 1** of the ***Cubical Quad Notes ~ A Review of Existing Designs!*** Don't miss the **Volume 2, Cubical Quad Notes ~ Rethinking the Quad Beams**, coming soon to the ***antenneX Online Magazine BookShelf***. There, you will find other fine publications of the author, L.B. Cebik, W4RNL.

***A Publication of
antenneX Online Magazine***
<http://www.antennex.com/>
POB 72022
Corpus Christi, Texas 78472 USA

Copyright © 2000 by **L. B. Cebik** jointly with ***antenneX Online Magazine***. All rights reserved. No part of this book may be reproduced or transmitted in any form, by any means (electronic, photocopying, recording, or otherwise) without the prior written permission of the author and publisher jointly.

ISBN 1-877992-01-1
